Université Paris Sud XI

Départment des Sciences de la Terre
Hydrogéologie, hydrogéophysique
Interactions et Dynamique des Environnements Sédimentaires (IDES)
UMR 8148 UPS/CNRS

Ecole doctorale MIPEGE 534
Modélisation et Instrumentation en Physique, Energies, Géosciences et
Environnement

Cotutelle de thèse; l'Université Paris Sud and le Comenius
Université à Bratislava

Détermination d'un modèle lithosphérique en Europe centrale: modélisation géophysique intégrée

présenté par:
M.Sc. GRINC Michal

Directeur de thèse: Prof. ZEYEN Hermann (France)
Co-directeur de thèse: Prof. BIELIK Miroslav (Slovaquie)

soutenue le 24 Octobre 2013 à Bratislava devant le jury composé de:

Le président du jury:	RNDr. Peter Vajda, PhD. (Slovaquie)
examinateur:	Prof. Piotr Tucholka, PhD. (France)
examinateur:	Prof. RNDr. Michal Kováč, DrSc. (Slovaquie)
examinateur:	Doc. RNDr. Roman Pašteka, PhD. (Slovaquie)
rapporteur:	Prof. Yanni Gunnell (France)
rapporteur:	Prof. Manel Fernàndez (Espagne)
rapporteur:	Prof. Frank Horváth (Hongrie)

University of Paris-Sud XI

Department of Earth Sciences
Hydrogeology, hydrogeophysics
Interactions et Dynamique des Environnements Sédimentaires (IDES)
UMR 8148 UPS/CNRS

Ecole doctorale MIPEGE 534
Modélisation et Instrumentation en Physique, Energies, Géosciences et
Environnement

The joint supervision of thesis; University of Paris-Sud XI and
Comenius University in Bratislava

Lithospheric structure in Central Europe: integrated geophysical modelling

presented by:
M.Sc. GRINC Michal

Supervisor: Prof. ZEYEN Hermann (France)
Co-supervisor: Prof. BIELIK Miroslav (Slovakia)

defended October 24th 2013 in Bratislava in front of jury composed of:

president of jury:	RNDr. Peter Vajda, PhD. (Slovakia)
examiner:	Prof. Piotr Tucholka, PhD. (France)
examiner:	Prof. RNDr. Michal Kováč, DrSc. (Slovakia)
examiner:	Doc. RNDr. Roman Pašteka, PhD. (Slovakia)
reviewer:	Prof. Yanni Gunnell (France)
reviewer:	Prof. Manel Fernàndez (Spain)
reviewer:	Prof. Frank Horváth (Hungary)

ACKNOWLEDGEMENT

RÉSUMÉ

L'objectif principal de cette thèse est d'acquérir de nouvelles connaissances sur la structure tectonique et la lithosphérique de la région des Carpates et du bassin pannonien. Nous avons appliqué trois méthodes différentes: modélisation 1D, modélisation 2D géophysique intégrée et inversion 3D pour atteindre cet objectif. Ces méthodes sont similaires concernant les bases de données utilisées, mais diffèrent par le traitement et l'interprétation de données. Au début, nous avons appliqué la modélisation automatique 1D pour obtenir un premier aperçu de la région étudiée. Deuxièmement, nous avons appliqué la modélisation 2D intégré de la lithosphère qui combine l'interprétation du flux de chaleur, du géoïde, de la gravité et des données topographiques de la région des Carpates et du bassin pannonien et des régions avoisinantes. Cette approche est capable de contraindre des structures lithosphériques compliquées de la région étudiée mieux que l'interprétation de chaque donnée indépendamment. Nous présentons quatre modèles intégrés 2D de la lithosphère dans la région des Carpates et du bassin pannonienet des régions avoisinantes. Enfin, sur la base de l'algorithme d'inversion 3D, nous présentons les modèles géophysiques de la lithosphère dans la région des Carpates et du bassin pannonien. L'algorithme calcule la structure de la densité lithosphèriquepar l'inversion conjointe de la gravité, géoïde et données topographiques basé sur une approche bayésienne. Les modèles sont basés sur différents ensembles de données d'entrée et ils sontcontraints par différentes données *a priori*. Sur la base de notre modélisation, nous ne pouvons pas confirmer l'amincissement extrême (moins de 70 km) de la lithosphère du bassin pannonienproposé par d'autres auteurs. D'autre part, les résultats montrent la tendance à l'augmentation de l'épaisseur lithosphérique de Carpates d'occidentales vers de Carpates de l'estce que confirme les théories antérieures sur la propagation du processus de subduction. Nous avons obtenu des résultats controversés dans la région des Carpates du sud. Les résultats basés sur l'inversion 3D montrent une lithosphère extrêmement mince dans ce domainmais les résultats basés sur la modélisation 2D intégrée ne supportent pas cetamincissement. Cependant, les deux méthodes indiquent qu'il est plausible que la plateforme Moésienne soit courbée et chevauchée sous les Carpates du sud. Dans le modèle 3D, le bord sud-est du bassin pannonien montre une lithosphère inattendue et étonnamment mince. Puisque la zone est assez grande, nous pouvons exclure un effet de flexion, par conséquent, cette région pourrait être potentiellement intéressante pour une rechercheplus approfondie.

ABSTRAKT

Hlavnou myšlienkou tejto práce bolo rozšírenie poznatkov o štruktúre a tektonike karpatsko–panónskej oblasti. Na výskum študovanej oblasti sme použili tri rôzne metódy, 1D automatické modelovanie, 2D integrované geofyzikálne modelovanie a 3D inverziu. Tieto metódy sú podobné v zmysle použitých vstupných databáz, ale líšia sa spôsobom spracovania a interpretácie. Ako prvé sme aplikovali 1D automatické modelovanie, ktoré slúžilo ako prvý náhľad na študované územie. Ako druhé sme použili 2D integrované geofyzikálne modelovanie litosféry, ktoré kombinuje interpretáciu povrchového toku, geoidu, tiažových anomálií a topografie v karpatsko–panónskej oblasti a okolitých tektonických jednotkách. Tento prístup k interpretácii je schopný vymedziť komplikované štrúktúry v litosfére lepšie, ako interpretácia každého jedného geofyzikálneho poľa samostatne. V tejto práci predstavíme štyri 2D integrované modely litosféry v karpatsko–panónskej oblasti a okolitých jednotiek. Ako posledné, predstavíme geofyzikálne modely litosféry študovanej oblasti na základe modelovania použitím 3D inverzie. Algoritmus je schopný vypočítať hustotnú distribúciu v litosfére na základe Bayesianského prístupu zo spoločnej inverzie tiažovej anomálie na voľný vzduch, geoidu a topografie. Tieto modely sú vypočítavané na základe rôznych vstupných datových setov a *a priori* informácií. Na základe nášho modelovania nemôžeme potvrdiť extrémne stenčenie (menej ako *70 km*) litosféry panónskej panvy. Na druhej strane naše výsledky poukazujú na narastajúci trend litosférického hrubnutia Karpatského oblúka od Západných Karpát smerom do Východných, čo potvrdzuje predchádzajúce teórie o postupnom procese subdukcie. V oblasti Južných Karpát sme dosiahli protichodné výsledky. Výsledky získané na základe 3D inverzie poukazujú na extrémne stenčenú litosféru na druhej strane 2D integrované modelovania takéto extrémne stenčenie v danej oblasti nepodporuje. Napriek tomu je pravdepodobnejšie, že moezíjska platforma je ohnutá a podsunutá pod Južné Karpaty. Ďalšia zaujímavá vec sa ukazuje v juhovýchodnej oblasti panónskej panvy, kde výsledky 3D inverzie odhaľujú taktiež výrazné stenčenie litosféry. Táto oblasť môže byť potenciálne zaujímavá a bolo by vhodné ďalej pokračovať vo výskume danej oblasti.

Kľúčové slová: Integrované geofyzikálne modelovanie, karpatsko–panónsky region, 1D, 2D, 3D inverzia, , geoid, tiaž, topografia, geotermika

ABSTRACT

The main aim of this thesis is to gain new knowledge about the lithospherical structure and tectonics of the Carpathian–Pannonian Basin region. We applied three different methods: 1D automatic modelling, 2D integrated geophysical modelling and 3D inversion to achieve this goal. These methods are similar concerning the used databases but differ by used processing and interpretation. At first we apply 1D automatic modelling to get a very first overview of the studied region. Secondly, we apply 2D integrated modelling of the lithosphere which combines the interpretation of surface heat flow, geoid, gravity, and topography data in the Carpathian–Pannonian Basin region and surrounding areas. This approach is able to constrain the complicated lithospheric structures of the studied region better than interpreting each data set on its own. We present four 2D integrated models of the lithosphere in the Carpathian–Pannonian Basin region and surrounding areas. Finally, based on the 3D Inversion algorithm, we present the geophysical models of the lithosphere in the Carpathian–Pannonian region. The algorithm returns the density structure of the lithosphere from joint inversion of free air gravity, geoid and topography data based on a Bayesian approach. The models are based on different input data sets and constrained by different *a priori* data. Based on our modelling we cannot confirm the extreme thinning (less than *70 km*) of the Pannonian Basin lithosphere proposed by other authors. On the other hand, the results show the increasing trend of the lithospherical thickness of the Carpathian Arc from the Western Carpathians toward the Eastern Carpathians which confirms the previous theories about the propagation of subduction process. We got some controversial results in the area of the Southern Carpathians. The results based on 3D inversion show extremely thin lithosphere in the area; on the other hand, the results based on 2D integrated modelling do not support such thinning. However both methods indicate that it is probable that the Moesian Platform is bend and underthrusted underneath the Southern Carpathians. The south-eastern edge of the Pannonian Basin based on 3D inversion shows unexpected and surprisingly thin lithosphere. Since the area is quite large, we could exclude an effect of flexure, therefore this area might be potentially interesting for further investigation.

Key words: Integrated geophysical modelling, Carpathian–Pannonian Basin region, 1D, 2D, 3D inversion, geoid, gravity, topography, geothermics

PREFACE

During my master´s degree I was trying to understand from the geophysical and tectonical point of view a very small a part of the Western Carpathians: The Turčianská Kotlina Basin. I carried out 2D density modelling to create two density transects along the seismic transects which are crossing the Turčianská Kotlina Basin. During the studies, I found that the gravimetry as geophysical discipline can contribute significantly to the expansion of knowledge about the continental lithosphere structure. I realized the complexity of the measured gravity field interpretation and also the importance of the appropriate interpretative procedure choice which is dependent on the known and assumed density changes in the study area, also from its geological structure and geometry. Naturally, the study of the lithosphere cannot be based only on gravimetry, but it is also necessary to pay attention to the results obtained by other geophysical methods such as seismic refraction and reflection profiling, seismology, geothermics, magnetometrics, paleomagnetism and many others. It is also inevitable to take into account the results of geological, geographical and geodetic surveys. However, it should be noted that different geophysical methods have limitations resulting partly from their physical nature, and partly from the lack of available geophysical information. Results based only on independent geophysical field interpretations are sometimes quite inaccurate and can lead to wrong understanding or interpretation.

After I finished the degree I felt, as I have written before, that the density modelling on its own has to be well constrained with *a priori* information otherwise the uncertainty of the results might be very significant and might cast a shadow of doubt over the acquired knowledge. During the year after the degree I was working in the private companies in Australia, Czech Republic and Slovakia. After that prof. RNDr. Miroslav Bielik, DrSc offered me a possibility to work on the lithospherical scale modelling using a new method of research: the geophysical integrated modelling. This method is able to constrain the complicated lithospheric structures of the studied region better than interpreting each data set on its own. It combines the interpretation of surface heat flow, geoid, gravity, and topography. Since I was interested in the lithospheric structure I have chosen the bulk of these methods as useful tools for my PhD. study. Since I comprehended that this approach is based on the interpretation of several geophysical fields at the same time, so it could constrain the lithospherical structures better than interpreting each data set on its own and therefore, this approach should decrease the uncertainty. There was also a

possibility to gain some additional knowledge and skills at the University Paris–Sud XI under the guidance of prof. Hermann Zeyen. So I embraced the opportunity. Moreover it was also the possibility to study the Carpathian–Pannonian Basin region in a wider scale and to comprehend the big tectonics and geodynamics that has been creating our environment.

Very soon after my PhD had started the stay at the University Paris–Sud XI came true. After a year and some financial support problems I registered as PhD student also at the University Paris–Sud XI. Both Universities signed the bilateral agreement and I entered the bilateral PhD. programme under the guidance of two supervisors. It was prof. Hermann Zeyen in France and prof. RNDr. Miroslav Bielik, DrSc. in Slovakia. I have spent more than one year in France and bring valuable geophysical knowledge and skills. I am sure that it was a very good experience not only from the scientific point of view. Since I was in France with my wife, it gave us not only a perfect opportunity to live in a foreign country but also to show us a different way of life.

The thesis focuses on the application of integrated modelling of the lithosphere in the Carpathian - Pannonian Basin region to study and clarify the tectonic evolution and lithospheric structure. The work is also focused on the relation between the studied region and its surrounding tectonic units. The aim of the thesis is to create several 2D integrated lithospherical scale models of the Carpathian–Pannonian Basin region. This should serve for better understanding of the relation of the region with its surrounding units and also to extend current knowledge. Another part of the thesis was to create 3D integrated models of the lithosphere in order to clarify the structure and tectonic evolution.

From the scientific point of view, this cooperation brings some interesting results but also raise new questions about the lithosphere in Carpathian–Pannonian Basin region. It is clear that the scientific work must continue also in the future and the white spots on the map need to be filled with the knowledge. We published a scientific paper about the lithosphere in the Carpathian–Pannonian Basin region based on 2D integrated modelling in the A rank Journal of Geodynamics (Grinč *et al.*, 2013) and also presented our results in many scientific conferences from which the most known is the EGU 2013 in Vienna. Here, I try to present also the other results, findings or problems that I encountered during the four years of my PhD. I was a member of the international team who contributed to the improvement of the Windows version of the 3D programme LitMod3D, since the original programme has been compiled for a variety of Linux distributions (Ubuntu, Suse, etc. for

either 32 bit or 64 bit architectures) (Fullea and Afonso, 2010). This software package was used in the process of the 3D lithospherical modelling. We used also 1D algorithm (Fullea *et al.*, 2006) to get very first view of the studied lithosphere and to use it as starting model for the 3D inversion. In the last step we used 3D inversion to get Mohorovičić discontinuity (Moho) and Lithosphere–Astenosphere Boundary (LAB). The inversion process was repeated many time with different settings in order to get a satisfying fit of the data. Moreover we used different available input databases.

Besides this cooperation I was a member in the other projects concerning my previous research of the Turčianska Kotlina Basin. I published in cooperation another scientific paper as a first author in the journal Contribution to Geophysics and Geodesy (Grinč *et al.*, 2010), another one as a side author in the same journal (Csicsay *et al.*, 2012) and in the A rank journal the Geologica Carpathica (Bielik *et al.*, 2013).

During my PhD. I encountered some problems and most of them I was able to resolve. But there is still one which stays unresolved; I was not able to finish the 3D integrated geophysical modelling. The problem is still opened and I hope that I will have an opportunity to finish it afterwards. This different approach is based on trial and error methodology so the interpreter has more options to "play" with the resulting model and have more liberty to consider the importance of explanation the dataset than it is in 3D inversion case.

TABLE OF CONTENTS

1 INTRODUCTION

Geophysical survey is an integral, although very often unrecognized part of geological survey. A clear advantage is its non–invasive nature, effectiveness and efficiency, whether in shallow or in deep exploration. Its critics point to the contrary, the lack of *a priori* data and often controversial correlation of geophysical data with geological reality. Gradual and thorough study of geophysical fields and phenomena with the contribution of the development of computers, a suitable combination of several geophysical methods, this criticism becomes unjustified or at least attenuated. Geophysics proves a unique place especially in the analysis and research of deep structures, tectonic setting, but it can be also very useful for solving problems of the geodynamic evolution of the studied areas and regions. However, its advantages can defend well in shallow geological survey for the needs of hydrogeology, engineering geology and environmental geology.

The Carpathian–Pannonian Basin region is an interesting place that gives us an opportunity to study tectonics, geodynamical processes, but also the subduction that recently ends in the eastern part of the region. The attractivity of the region from a geological and geophysical point of view can be confirmed by the amount of the previous investigations. Most attention has drawn the Vrancea Zone where the last stadium of the subduction process can still be observed. The Western Carpathians and the central part of the Pannonian Basin were also well studied (e.g. Ádám, 1976; Babuška *et al.*, 1987; Šefara *et al.*, 1987; Praus *et al.*, 1990; Horváth, 1993; Szafián *et al.*, 1997; Bielik *et al.*, 2004; Posgay *et al.*, 1995;. Tomek *et al.*, 1987; 1989; Lillie, 1991; Lillie *et al.*, 1994; Zeyen *et al.*, 2002; Alasonati Tašárová *et al.*, 2009; Janik *et al.*, 2011) by different geophysical approaches. The main interest in this area was caused by the very high heat flow which was interpreted as expression of thin crust and thin whole lithosphere. Also the Transylvanian Basin has drawn attention due to its low heat flow and also somehow higher topography comparing with the neighbouring Pannonian Basin. But there are still some enigmatic places in the map of this region and some detailed survey should be done. I also realized the fact that the strict interpretation of the Carpathian–Pannonian Basin region is insufficient, so it needs to be extended to the surrounding tectonic units, which in my case are the Bohemian Massif, the European Platform, the Black Sea, the Moesian Platform, the

Balkanides, the Rhodopes, the Aegean Sea, the Dinarides, the Adriatic Sea and the Eastern Alps.

Since we used three different approaches of the investigation based on the integrated geophysical modelling I believe that the results give new knowledge about tectonics and geodynamics of the Carpathian–Pannonian Basin region. The thesis work plan is following:

- A general overview of current knowledge and research in the field, which used a different methodology of study and research, and their confrontation with the results achieved in this dissertation

- The creation of four regional integrated 2D models of the lithosphere by applying the 2D algorithm (Cages) (Zeyen and Fernandez, 1994), cross different tectonic units in Central and Southern Europe

- The creation of an integrated 3D model of the lithosphere in the focused area by using the 3D inversion programme (Motavalli-Anbaran *et al.*, 2013)

- The creation of an integrated model of the lithosphere in the Transylvanian Basin by using LitMod3D (Fullea *et al.*, 2009)

The work is divided into a few logical chapters. In the first I describe the basic geology of the area and summarize the results of the previous geophysical surveys. The second part is devoted to simple principles, methodology and data processing of 2D and 3D integrated geophysical modelling (3D inversion and LitMod3D). The third unit is devoted to the results achieved. Work was performed sequentially at two sites, because the study is designed as a double doctorate under management. Part of the study was headed by prof.RNDr.Miroslav Bielik, DrSc. at the Department of Applied and Environmental Geophysics at the Comenius University in Bratislava, and the second part by prof. Hermann Zeyen from the IDES laboratory at the University Paris-Sud XI.

2 GEOLOGY

The study area includes a series of very different lithospheric blocks that have been amalgamated during the major European orogeneses from the Cadomian to the Alpine ones (Fig. 1). The northern part of the study area is formed by the North European Platform, which is separated by the Trans–European Suture Zone (e.g. Pharaoh, 1999) into the Precambrian East European Platform in the E and the Paleozoic West European Platform in the W. The West European Platform consists of a collage of Gondwana related Precambrian and/or Cadomian terranes amalgamated during pre–Variscan tectonic events and then covered by thick sedimentary deposits. In the area described, these terranes also include the Małopolska Massif and the Bohemian Massif surrounding the German–Polish Caledonides.

During the Alpine orogeny, the terranes of Alcapa and Tisza–Dacia docked to the older ones, forming the immense East Alpine–Carpathian Arc. S–wards, the Carpathian Arc turns around the Moesian Platform and continues into the orogenic zones of the Balkanides. The southern branch of the Alpine orogen includes the Southern Alps that are linked to the Dinarides, the Albanides and the Hellenides towards the SE. All these Alpine mountain belts are wrapping around the large Pannonian Basin rimmed by volcanic chains, which were formed by back-arc extension during the Neogene (Csontos *et al.*, 1992). This type of volcanism was preceded by the regional extension-related silicic and andesitic volcanism (Kováč, 2000; Konečný *et al.*, 2002). As a whole, the Alpidic orogenic system of the area shows a very complex structure and evolution, consisting of numerous units and blocks with intricate relationships in space and time (see e.g. Csontos and Vörös, 2004; Schmid *et al.*, 2008; Ustaszewski *et al.*, 2008).

2.1 *Western Carpathians and Pannonian Basin*

The Western Carpathian Mountains form the western and the northern parts of the Carpathian arc, which is characterized by strong zonal arrangement with a strong fold structure and migrating orogenic system from the S to the N. On the basis of lithology and age of the rocks, the Western Carpathians can be divided into two parts, the Outer and the Inner Western Carpathians (Kováč, 2000), or the Internides and the Externides. These two parts are separated from each other by the Pieniny Klippen Belt. The Inner Western

Carpathians folding was finished before the Cretaceous (about *65 Ma* ago), while the Outer Western Carpathians were folded during the Tertiary (*30–12 Ma*). The Inner Western Carpathians contain also elements of older Hercynian tectonogenesis which has been transformed and incorporated into Alpine units. Morphological and tectonic settings of the Western Carpathians, however, were strongly influenced by Tertiary (Neoalpine) tectonics.
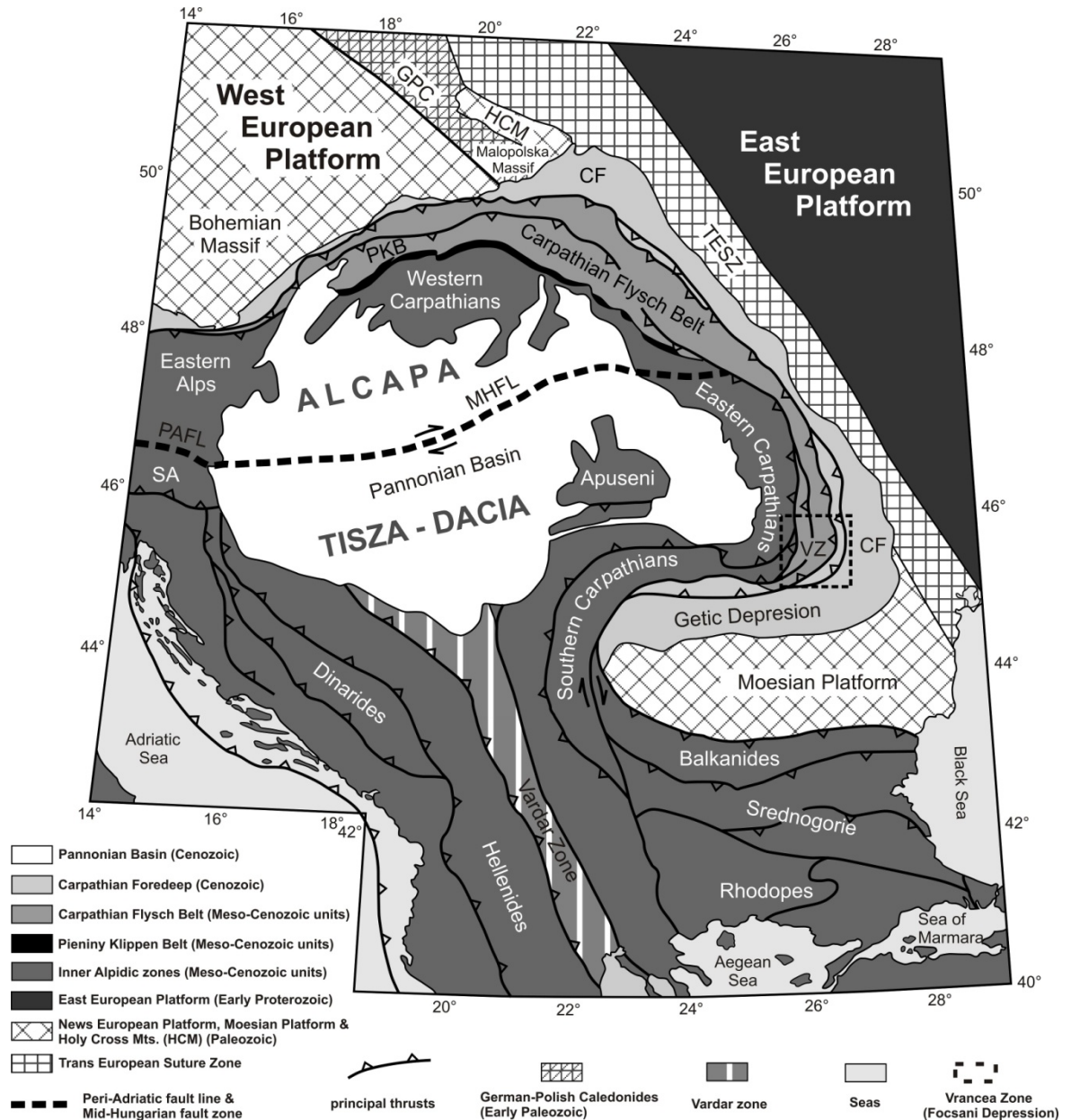
Fig. 1   Simplified tectonic map of the Central Europe (modified after Mahel', 1973; Artemieva *et al.*, 2006). Keys: HCM, Holy Cross Mts.; GPC, German-Polish Caledonides; SA, Southern Alps, VZ, Vrancea zone; PAFL, Periadriatic fault line; MHFL, Mid-Hungarian fault line; CF, Carpathian Foredeep

The Tertiary accretionary prism of the Outer Western Carpathians is a tectonic feature, which is typical for the whole Alpine–Carpathian region. In this area there are

several nappe units which were thrusted onto the folded European Platform. The final process of forming an accretionary wedge was associated with the margin flexure of the Platform on which the foredeep was formed (Konečný et al., 2002; Minár et al., 2011) (Fig. 2).

The Western Carpathian foredeep is filled with Middle Miocene, mostly marine sediments (Oszczypko, 1998). Further S, these are overridden by the frontal nappes of the Carpathian Flysch Belt, which is the Tertiary accretionary complex with a typical fold–and–thrust structure and wedge–shaped geometry (e.g. Oszczypko, 2006). Numerous thrust sheets are composed of flysch–dominated sediments that were scraped off presumably oceanic lithosphere attached to the southern passive margin of the North European Platform. The backstop of this wedge is formed by a few km wide subvertical zones with intricate inner structure, which is called the Pieniny Klippen Belt.

Further SE, the Central Western Carpathians contains a pile of basement and cover nappes that originated during the mid–Cretaceous orogenic movements (Froitzheim et al., 2008; Plašienka et al., 1997 and references therein). The southernmost Western Carpathian zones are characterised by the presence of allochthonous relics of ophiolite–bearing Triassic/Jurassic melanges and blueschist–facies metamorphosed complexes attributed to the Meliatic Unit, a possible remnant of the Neotethyan (Meliata Ocean) suture. The Western Carpathians form the eastern part of the Alcapa (Alps–Carpathians–Pannonia) Megaunit, which represents a wedge–shaped megablock strongly squeezed in its Eastern Alpine part between the Adriatic indenter and the southern spur of the Bohemian Massif during the Tertiary collision.

The Western Carpathian part of Alcapa was extruded during this collision towards the unconstrained eastern area occupied by an oceanic lithosphere underlying complexes of the present Carpathian Flysch Belt (e.g. Ratschbacher et al., 1991). The southern boundary of the escaping block is formed by the Periadriatic fault line, which continues ENE–ward through the wide Mid–Hungarian fault line (Csontos and Nagymarosy, 1998; Palotai and Csontos, 2010). This zone provides the contact to another large Tertiary crustal block known as the Tisza–Dacia Megaunit, or Tiszia, which occupies a central position within the Carpathian arc (e.g. the Apuseni Mountains), and is mostly covered by thick Neogene and Quaternary sediments and volcanics of the Pannonian Basin.

In the S, the Tisza–Dacia block is obducted by Tethyan ophiolites of the Transylvanides (Mures Zone–Ionescu *et al.*, 2009 and/or Eastern Vardar Ophiolite Unit–Schmid *et al.*, 2008).

The Pannonian Basin began as the back–arc basin system, which was a consequence of a lithospheric extension and of the upwelling of the mantle material on the inner side of the Carpathian arc (Csontos *et al.*, 1992; Horváth, 1993; Royden, 1993; Kováč, 2000). Along the margins of microplates were created normal and listric faults, but also large strike slip faults during the formation of this basin system. The system is filled by Tertiary and Neogene sediments that are locally up to *7 km* thick (Bielik, 1988; Kilényi and Šefara, 1989; Vakarcs *et al.*, 1994; Bielik *et al.*, 2005; Csato *et al.*, 2007). The Pannonian Basin is filled with Neogene and Quaternary sediments and volcanics. Locally preserved Lower Miocene marine deposits and felsic volcaniclastics predated the main rifting phase of the back–arc Pannonian Basin during the Badenian. Middle Miocene syn-rift, still marine deposits are followed by the Upper Miocene and Pliocene brakish to freshwater, post–rift sediments of the "Pannonian Lake". This strong later thermal subsidence is ascribed to thermal thinning of the mantle lithosphere due to asthenosphere upwelling (Plašienka, 2012).
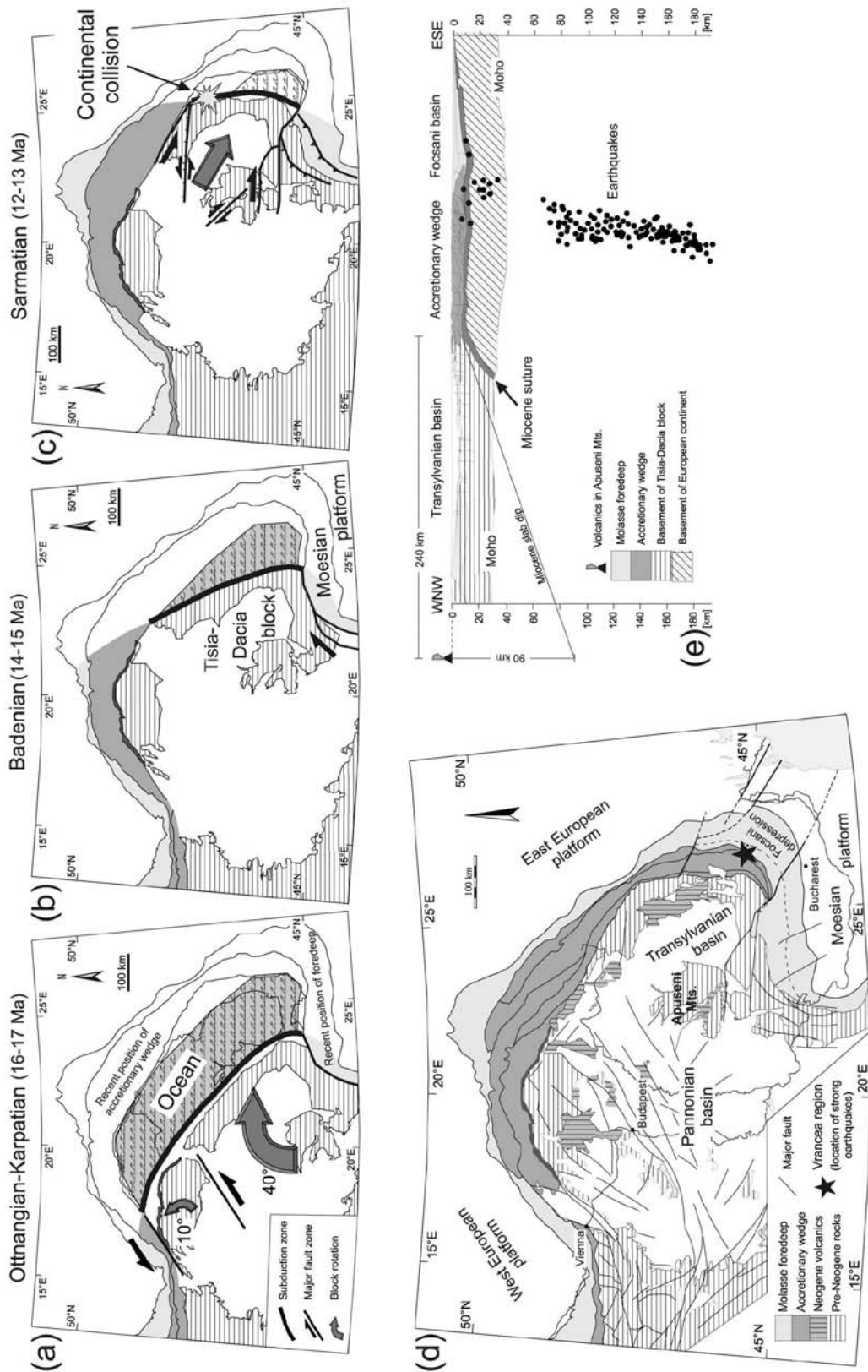
Fig. 2   (a), (b), (c) - Miocene geodynamic evolution of the Carpathian–Pannonian Basin region; (d) - Tectonic map of the Carpathian–Pannonian Basin region (Sperner *et al.*, 2005); (e). Transect through the Vrancea Zone (modified after Radulescu *et al.*, 1976 and Stefanescu *et al.*, 1985)

2.2   *Transylvanian Basin, Eastern Carpathians and Apuseni Mountains*

The Eastern Carpathians are formed by the E–ward thrusting nappe sheets of the Median and the Outer Dacides and the Moldavides (Fig. 3) (Săndulescu, 1994) that were stacked during the mid–Cretaceous "Austrian" phase. The Median Dacides (the Central East Carpathians) involve basement/cover units attributed to several nappe systems– the Bucovinian, Sub–Bucovinian and Infra–Bucovinian (this corresponds to the Getic unit of the Southern Carpathians – their pre-Alpine basement is composed of various, high- to low-grade metamorphic series; the cover includes Permian red–beds, Triassic carbonates, Lower Jurassic Gresten–type clastics, later Jurassic and Lower Cretaceous pelagic facies and pre–Albian synorogenic flysch sediments. The Bucovinian nappe stack is sealed by an Albian–Cenomanian post–tectonic cover, but their final thrusting over the more external Outer Dacides was post-Albian in age (Plašienka, 2012).

The Outer Dacides are already elements of the Carpathian Flysch Belt and are composed of several fold-and-thrust, thin–skinned units. The innermost Black Flysch Nappe contains Jurassic basalts and deep–water sediments. The underlying Ceahlău Nappe was derived from the Severin–Ceahlău oceanic domain and contains Jurassic radiolarites and basalts and Tithonian–Lower Cretaceous calcareous flysch overstepped by Albian conglomerates. Still more external are the Moldavides– a frontal Carpathian fold–and–thrust system overriding the Neogene foredeep and Phanerozoic cover of the East European Platform. The Moldavides consist of numerous fold–and–thrust units composed mostly of Cretaceous flysch in the inner subunits (Convolute Flysch, Macla, Audia). The outer nappes (Tarcău, Marginal Folds) are dominated by Palaeogene sandy flysch deposits. The Subcarpathian Nappe occurs in the outermost position, being composed of detached Oligocene and Lower Miocene sediments. The foredeep includes sediments of Upper Miocene to Quaternary age (Plašienka, 2012).

The Outer East Carpathian flysch nappes partially overthrust the Palaeozoic Trans-European Suture Zone followed by reactivation of faults of the Teisseyre–Tornquist Zone. In the area concerned, the Trans–European Suture Zone is hidden and the Carpathian frontal nappes override the margins of the East European Precambrian Platform and the northern tip of the Scythian Platform, the latter affected by Palaeozoic deformation and covered by thick Devonian to Jurassic sediments. SE–wards, the Trans-European Suture

Zone involves also the Cimmerian (Jurassic) North Dobrogea orogen that fixes a contact between the Moesia Platform and the North European Platform. In this way, the Moesian Platform in the E and the southern Bohemian Massif edge in the W provided two fixed lateral boundaries that had to be passed by the E–ward translating and rotating megablocks Alcapa, Tisia and Dacia during the Miocene (Plašienka, 2012).

The Transylvanian Basin is a large, nearly circular depression *150–200 km* in diameter that spreads between the Apuseni Mountains and the Eastern Carpathians. The basin has a polygenic fill with unconformities between the Upper Cretaceous, Palaeogene and Miocene sediments. The Miocene volcaniclastic, terrigenous and evaporitic sediments are partly related to the Pannonian Basin and can reach thicknesses in excess of *4 km* (Sanders *et al.*, 2002).

The Transylvanian Basin represents a post–Cenomanian sedimentary basin developed on top of the Middle Cretaceous basement nappes (internal Carpathians). The nappes form the hinterland of the Carpathians 'backstop' of the foreland folded belt further to the E (Krézsek and Bally, 2006). The Middle to Late Miocene Transylvanian Basin (similarly as the Vienna Basin) is not considered as a part of the Pannonian Basin system and do not belong to the back–arc basin area. (e.g. Royden, 1985; Tari and Horváth, 1995; Kováč and Bada, 1999; Fodor *et al.*, 1999, Krézsek and Filipescu, 2005; Tilită *et al.*, 2006). It shows a moderate fault pattern, except for superficial extension related to salt tectonics (e.g. De Broucker *et al.*, 1998; Krézsek and Filipescu, 2005) and it is characterised by low regional surface heat flow (e.g. Demetrescu *et al.*, 2001). High subsidence rates are documented during the Middle to Late Miocene (e.g. Crânganu and Deming, 1996). The driving mechanism of the subsidence is one of the major unresolved questions of the geology of the Transylvanian Basin (Huismans *et al.*, 1997). One of the most important factors influencing the late stage of the Transylvanian Basin is related to the Late Miocene uplift of the Carpathians (e.g. Sanders, 1999) and associated gravitational spreading (Schultz-Ela, 2001) of the post-salt overburden strata (Krézsek, 2004).
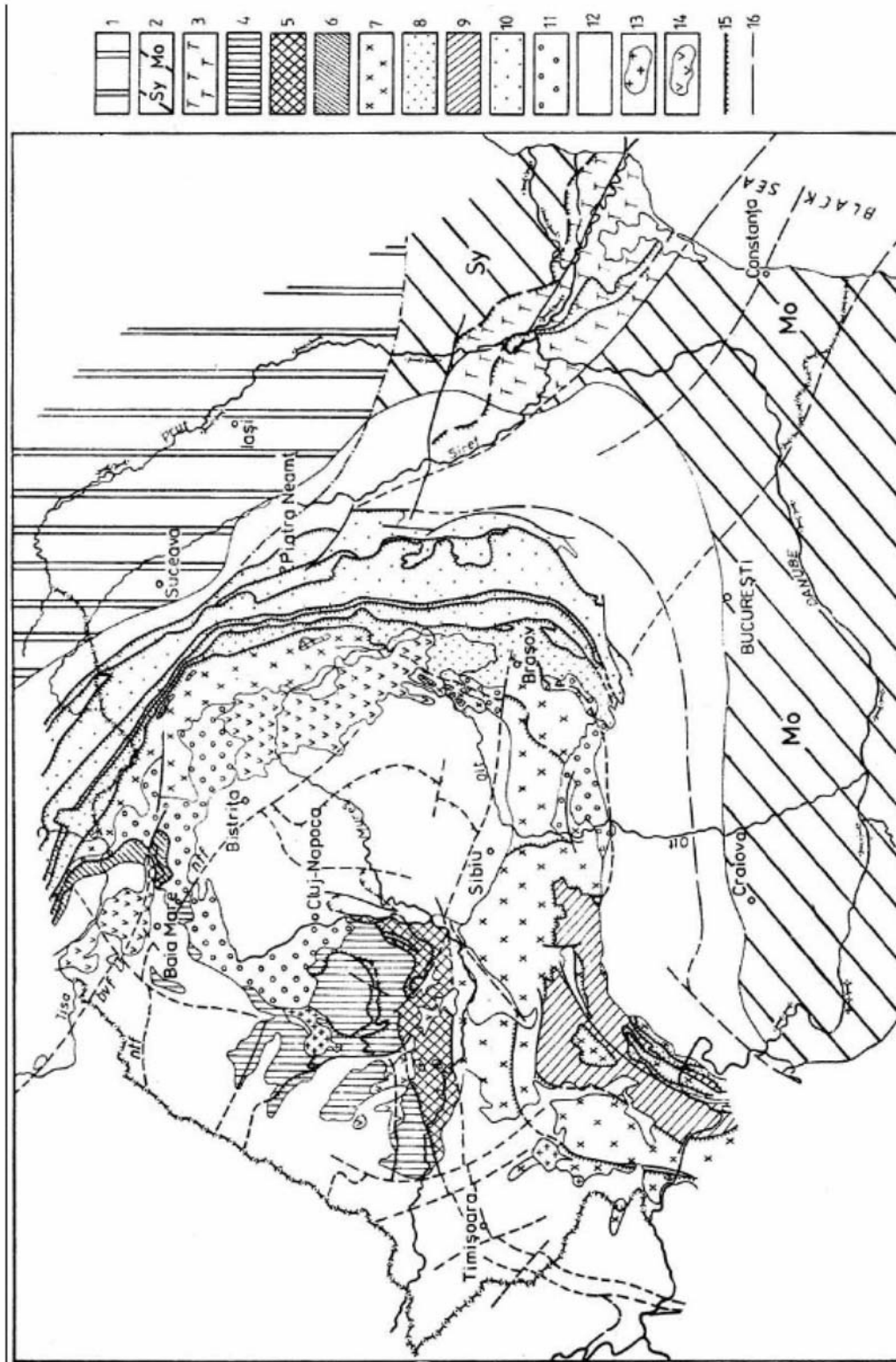
Fig. 3   Tectonic sketch of Romania, Carpathian Foreland (Săndulescu, 1994): 1. East European Platform; 2. Scythian (Sy) and Moesian (Mo) Platforms; 3. North Dobrogea Orogen; 4. Inner Dacides; 5. Transylvanides; 6. Pienides; 7. Median Dacides; 8. Outer Dacides; 9. Marginal Dacides; 10. Moldavides; 11. Post tectogenetic covers; 12. Neogene Molasse Depression and Foredeep; 13. Upper Cretaceous – Paleocene magmatic arcs; 14. Neogene magmatic arcs; 15. thrust-sheets; 16. Faults.

Basement of the Transylvanian Basin centre is composed of the supra–subduction ophiolite and volcanic island arc complexes of the Transylvanides. Comparable oceanic crust rocks are found also in the Southern Apuseni Mountains. These rocks are considered as remnants of a marginal or back-arc basin, in which a volcanic arc developed. (Ionescu *et al.*, 2009). However, position of Transylvanides is not fully understood yet – they either represent the "Main Tethyan Suture Zone" located between the Tisia and Dacia terranes and connect, via the Pienides of the Poiana Botizei Klippen Zone, with the Alpine–Western Carpathian Penninic sutures NW–ward (Săndulescu, 1994), or alternatively, they belong to the obducted, fully allochthonous Eastern Vardar ophiolitic unit overlying the Median Dacides (Bucovinian, Supragetic and Biharia; Schmid *et al.*, 2008).

The Apuseni Mountains are an example of an orogen in the interference zone between two subduction systems. They form an internal mountain belt with respect to the present–day Carpathian and Dinaridic–Hellenic Belts and are situated at the transition between the Tisza, East Vardar and Dacia tectonic units (Merten *et al.*, 2011). The East Vardar Ocean was probably obducted onto parts of Dacia during Late Jurassic times (Schmid *et al.*, 2008), followed by late Early Cretaceous obduction and continental collision between the Tisza and the Dacia continental blocks (Săndulescu, 1988; Csontos and Vörös, 2004). The latter is responsible for the E–ward emplacement of a large sheet of Transylvanides (ophiolites) over the Dacia basement, which are recognized as far East as the East Carpathians (e.g. Săndulescu and Visarion, 1978; Ionescu *et al.*, 2009). In the Apuseni Mountains, thrusting was followed by intra–Turonian W–ward back–vergent thrusting, creating the retro–vergent side of the orogen in a series of four main nappe units (Mecsek, Bihor, Codru and Biharia) (e.g. Săndulescu, 1984; Balintoni, 1994; Haas and Pero, 2004; Schmid *et al.*, 2008)

The Apuseni Mountains in western Romania are built of numerous, N–ward verging thrust sheets emplaced during the mid–Cretaceous period (Inner Dacides in terminology of Săndulescu, 1994). The Bihor "autochthon" in the Northern Apuseni Mountains is composed of Pre–Alpine basement and its Permian to Cretaceous sedimentary cover and is overridden by the Codru basement/cover nappe system and the Biharia basement–dominated thrust units. In the Southern Apuseni Mountains (Munţii Metaliferi, Mureş Zone), the latter underlay obducted sheets of the Transylvanides – Tethyan ophiolite and island-arc magmatites with related Lower Cretaceous flysch and olistostrome complexes. The post-tectonic formations include the Senonian, Gosau–type

shallow-marine terrigenous deposits (e.g. Schuller *et al.*, 2009) and Upper Cretaceous–Palaeogene calc-alkaline magmatites, so–called "banatites". Intramontane grabens are filled with Miocene deposits and acid volcanic rocks (Plašienka, 2012).

2.3   *Southern Carpathians, Moesian Platform, Rhodope*

The Southern Carpathians (Fig. 1) are predominantly built up of pre–Alpine polymetamorphic, low– to high–grade crystalline basement complexes creating several south-verging thick-skinned thrust sheets (Median Dacides–Sandulescu, 1994). Their basement is made up of high-grade Proterozoic rocks showing Variscan reworking and cooling (Dallmeyer *et al.*, 1998; Iancu *et al.*, 2005). The scarce sedimentary cover includes Permian and Scythian clastics, Middle Triassic carbonates, and variegated Jurassic to Lower Cretaceous strata.

The Getic Depression (Fig. 1) that rims the Southern Carpathians from the S was formed by Early Miocene dextral transtension and is filled with Neogene terrigenous, molasse-type sediments more than 5 km thick. The external zones of the Getic Depression continue laterally E–wards into the Focsani foredeep of the southern Eastern Carpathians. S–wards, the Moesian Platform is located; it is a large crustal block forming the foreland of the Carpathian–Balkan arcuate mountain belt that wraps it from the N, the W and the S. It extends over a large area of Bulgaria, S of the Southern Carpathians and N of the Balcanides. The metamorphic bedrock is covered by a more than 6 km thick layer of sediments from Early Paleozoic to Recent and volcanic rocks as well (Carboniferous–Permian, Triassic and Miocene) (Tari *et al.*, 1997; Sandulescu, 1994). The deeper substratum of the Moesian Platform is formed by the Precambrian basement affected by Neoproterozoic orogenesis (Seghedi *et al.*, 2005).

The Balkanides (Fig. 1) represent a thrust system overriding the southern margin of the Moesian Platform. They include Lower Palaeozoic low–grade volcano–sedimentary complexes, some Variscan granitoids and thick Upper Palaeozoic to Middle Eocene carbonates and deep–water clastic deposits. Deformation occurred during two principal phases–in the late Early Cretaceous and in the Eocene. The Srednogorie is composed of high–grade metamorphic basement (probably Precambrian) and Paleozoic metasedimentary complexes intruded by Variscan granitoids. Cover successions include variegated Upper Carboniferous to Lower Cretaceous sediments intensely folded in mid– and end– Cretaceous times. The Rhodope metamorphic complex (Ricou *et al.*, 1998;

Schmid *et al.*, 2008) forms a large, dome–like tectonic window. It consists of basement-dominated complexes and involves several allochthonous units differing considerably in their tectonometamorphic histories (Janák *et al.*, 2011).

The system of mountain ranges in the SE Europe serves as a type locality of general concepts of the mountain tectonics, orogenic collapse and subduction dynamics. Between the Carpathian and Balkan orogenic system is the Moesian Platform, considered as a part of the stable European Platform (Fig. 4). Therefore, it is often used as a fixed point for interpretation and kinematic reconstruction of the SE European plate movements during the Cenozoic (e.g. Linzer, 1996; Morley, 1996; Linzer *et al.*, 1998; Ricou *et al.*, 1998; Schmid *et al.*, 1998; Zweigel *et al.*,1998; Van Hinsbergen *et al.*, 2008).

However, tectonic stability of the block during the evolution of the Carpathians, the Balkans and the Aegean region is still controversial and poorly defined by reliable paleomagnetic studies of the vertical axis rotation. The adjacent regions of the Moesian Platform (Fig. 1) were determined by extensive paleomagnetic rotation about a vertical axis, which allowed to define and quantify the Mesozoic kinematics (Horner and Freeman, 1983; Balla, 1987; Kissel and Laj, 1988, Morris, 1995; Speranza *et al.*, 1995; Kissel *et al.*, 2003; Csontos and Voros, 2004; Van Hinsbergen *et al.*, 2005; 2008) In the N, in the Carpathian region, *~80°* of clockwise rotations in the large Tisza Block since the Oligocene are generally interpreted as reflection of its wholesale motion around the NW corner of the Moesian Platform during E–ward roll–back of the subducted Carpathian slab (Patrascu *et al.*, 1994; Panaiotu, 1998; Schmid *et al.*, 1998). In the S, the whole domain consists of the western Aegean and Albanian regions rotated about *~50°* clockwise (away from the northern Rhodope and the Moesian Platform) during the period *15* to *8 Ma*. This was interpreted as a combination of the effect of African plate S–ward roll-back and the W–ward extrusion of Anatolia (Kissel and Laj, 1988; Kissel *et al.*, 2003; Van Hinsbergen *et al.*, 2005). However, these interpretations are based on the assumption that the Moesian Platform itself did not rotate during rotation of the domain. Although paleomagnetic data from the Moesian Platforms are very rare, they indicate some Mesozoic rotation (Dolapchieva, 1994) or some local rotations (Fig. 4) may have occurred during Eocene compression (Van Hinsbergen *et al.*, 2008)
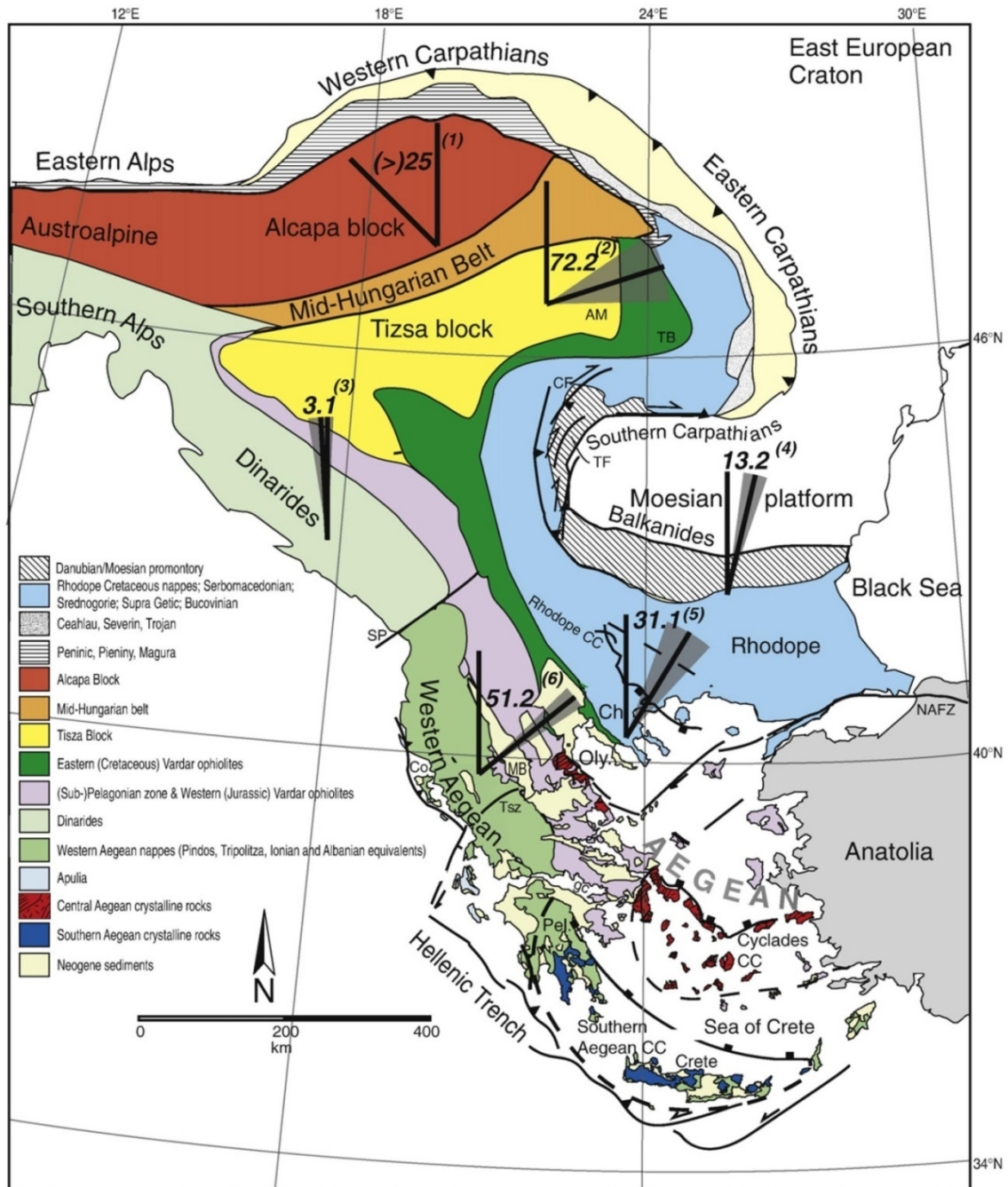
Fig. 4   Schematic geological map with the main tectonostratigraphic units of the SE Europe, with the paleomagnetic declinations obtained from Eo-Oligocene rocks of the main blocks of the region (Van Hinsbergen *et al.*, 2008).

Present-day knowledge indicates ~*15°* clockwise rotation of contractile tectonics and re-magnetization during the middle Eocene (Jordan *et al.*, 2001). Along the northern edge of the Moesian Platform foredeep sediments of the Southern Carpathians, recorded ~*30°* rotation in a clockwise direction at a time between *13* and *6 Ma* (Dupont–Nivet *et al.*, 2005).

This phase of rotation is interpreted as a dextral movement associated with the E–ward heading of the Tisza block provided that the Moesian Platform did not rotate. However, an alternative interpretation presents another solution, namely that the Tisza block and Southern Carpathians rotated clockwise together with the Moesian Platform from *13* to *6 Ma*. Based on the fact that the rotation takes place simultaneously with the rotation of the western Aegean region, it can be expected that the Tisza block and the western Aegean region partially rotated together. This could have important implications for motion (extension), the location of the Aegean region and the Carpathian block rotation (i.e. the west–Aegean rotations might be partly accommodated in the Carpathian back–arc) (Van Hinsbergen *et al.*, 2008).

On the southern margin of the Moesian Platform, the Alpine deformation processes are associated with N–ward heading emplacement of the Balkanides and the Srednogorie nappes in a back-thrust system. This was also accompanied by N–ward subduction during African–European convergence (Boccaletti *et al.*, 1974; Ricou *et al.*, 1998; Van Hinsbergen *et al.*, 2005) which caused the upper Cretaceous to Paleogene sedimentation cover of the Platform (Tari *et al.*, 1997). During the middle Eocene, the contraction ended almost on the entire length of the southern platform margin, with a few exceptions that were still active in the Eocene (Sinclair *et al.*, 1997). The Rhodope Mountains form a complex structure involving exhumed high–grade metamorphic rocks, which were buried and uncovered during the Creataceous to Paleogene (Ricou *et al.*, 1998; Brun and Sokoutis, 2007) overlain by Oligocene to Eocene sedimentary basins and volcanic fields (Lilov *et al.*, 1987; Yanev and Pecskay, 1997; Yanev *et al.*, 1998). Significant contraction south of the Moesian Platform ended in the Eocene (Ricou *et al.*, 1998). After this the deformation moved further S in the form of accretion (Van Hinsbergen *et al.*, 2005). By this time the Rhodope accretion was stuck on the Moesian Platform as indicated by the absence of major post–Eocene structures, which in itself could carry traces of significant movements between blocks. The post middle–Eocene exhumation of a wide metamorphic dome in the southern Bulgarian Rhodopes core complex was widely conceived as a tectonic denudation as a result of large-scale extension (Dinter and Royden, 1993; Ricou *et al.*, 1998; Krohe and Mposkos, 2002; Brun and Sokoutis, 2007). This extensional history has created a series of post middle-Eocene graben and half–graben in the southern Rhodope Mountains, which cross–cut pre-Eocene nappes (Tzankov *et al.*, 1996; Nakov, 2001; Burchfiel *et al.*, 2003).

Along the northern margins of the platform, late Cretaceous nappes are followed by significant post–Eocene deformation. Although contractile deformation along the southern edge of the Moesian Platform ended in the Eocene, western and northern margins were subjected to overthrusting and right–lateral wrenching associated with the N–ward and E–ward propagation of the Carpathian fold–and–thrust belt around the Moesian Platform from Eocene to Pliocene (Schmid *et al.*, 1998; Bertotti *et al.*, 2003; Matenco *et al.*, 2003; Dupont–Nivet *et al.*, 2005; Vasiliev *et al.*, 2005).

2.4   *Surrounding tectonic units*

As we can divide the Western Carpathians, we can sectionalize also the Eastern Alps. Based on the age of tectonic units, rock lithology and lithostratigraphic contents in the Eastern Alps, one recognizes several zones: molasse zone, flysch zone, Northern Limestone Alps and the Central Eastern Alps (Kováč, 2000). The Bohemian Massif forms the eastern part of the Variscan orogen and is composed primarily of metamorphic rocks, granites and Paleozoic sedimentary rocks with plenty of fossils (Matte, 1991). European Platform includes the Precambrian East European Platform in the NE and a younger Paleozoic platform in the SW. These two units are separated from each other by the Trans-European Suture Zone, which locally reaches a width up to *200 km* and passes through Europe from the N of the North Sea to the Black Sea in the S. The north–easternmost boundary of the fault zone is in Poland, called Teisseyre–Tornquist Zone (Dadlez *et al.*, 2005). The Trans–European Suture Zone contains several interesting studied areas, which were stuck on the SW border of the East European Platform during the Paleozoic (Winchester, 2002). In eastern Poland they are known as the Bruno–Silesian (or Upper Silesia), Małopolska and Lysogory blocks, while the last two have been uncovered in the Holy Cross Mountains and separated from each other by the Holy Cross fault. The Adriatic Sea is made of a stable intra–orogenic, Gondwana–derived terrane–the Adriatic (Apulian) microplate. It creates a submerged foreland for both the Apennine thrust belt approaching from the SW and for the frontal Dinaridic units thrust from the NE. The part of the Aegean Sea as a part of the studied region is built of basement belonging to the Dacia–Balkan Belts (Schmid *et al.*, 2008).

2.5   *Tertiary evolution of the Carpathian arc and the Pannonian Basin*

The Carpathian-Pannonian domain is located in an embayment of the European Platform. Its NW corner has a border with the Bohemian massif and the SE edge with the Moesian Platform (Dérerová *et al.*, 2006). Part of the Carpathian flysch zone is located in the outer Western Carpathians, which is lying either on pre-Oligocene oceanic crust (Tari *et al.*, 1993) and / or on thinned continental crust (Winkler and Slaczka, 1992; Sperner *et al.*, 2002). Outside the Western Carpathian flysch zone is situated the foredeep on the bent platform.

Tertiary evolution of the Alpine–Carpathian orogen is characterized by the influence of the W to SW directed subduction (Fig. 5) (Sperner *et al.*, 2001). Originally, this was an active subduction along the Alpine–Carpathian arc. But after the continental collision in the Eocene in the Alps, the subduction resumed only in the Carpathians, where the passive European continental margins provided space for further subduction. (Dérerová *et al.*, 2006).

The Tertiary evolution of the Carpathians and the Pannonian back–arc basin was interpreted by Konečný *et al.* (2002) in terms of Alpine subduction and orogenic evolution of the compression zone. This resulted in a lateral intrusion of the Alcapa lithosphere along transform faults during the Alpine collision and Carpathian gravitative subduction of the oceanic or highly thinned continental lithosphere, where the flysch basin is located. Back–arc basin extension was associated with the diapiric upwelling of the asthenospheric mantle.
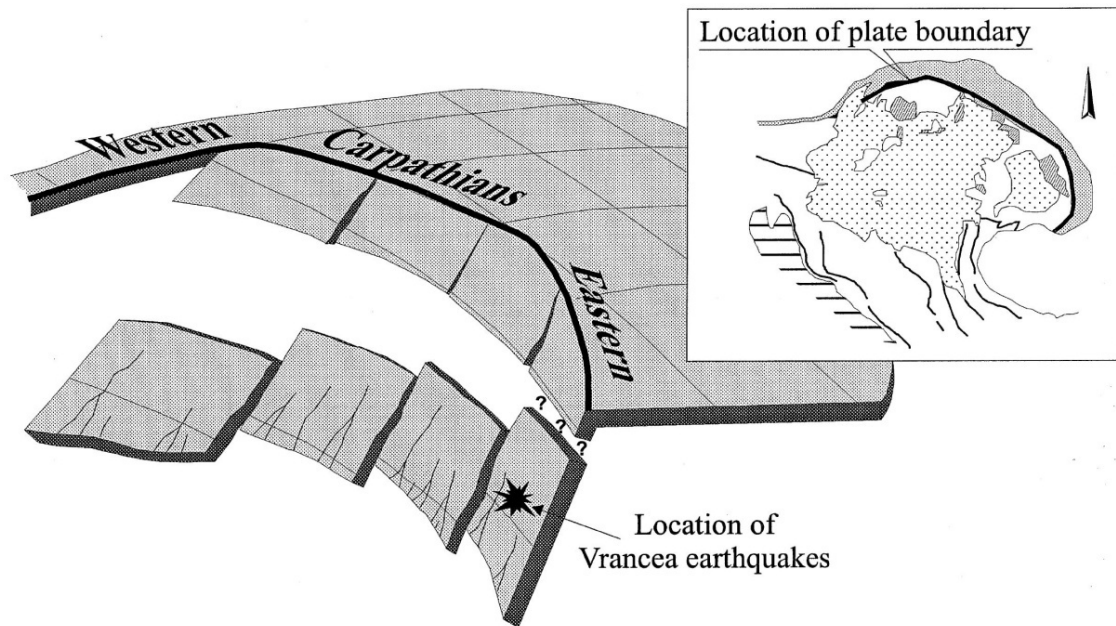
Fig. 5   Model for slab break-off beneath the Carpathian arc (Sperner, 1996). The slab segments in the northern parts are already detached; the south-easternmost segment is still mechanically coupled with the European plate (Sperner *et al.*, 2001).

The subduction was always parallel within any segment of the Carpathian orogene and it was not finished at the same time throughout the whole arc. Numbers of observations suggest that the propagation of the subduction process was conducted from the W to the E or to SE during the Neogene (Royden and Horváth, 1988; Rumpál and Horváth, 1988; Ratschbacher *et al.*, 1991a, 1991b; Csontos *et al.*, 1992; Horváth, 1993; Tomek and Hall, 1993; Linzer, 1996; Kováč *et al.*, 1998; Kováč, 2000; Konečný *et al.*, 2002; Van Hinsbergen *et al.*, 2008).

The back–arc extension indicates a middle Miocene slab retreat (Royden,1988), which is considered as main mechanism of the Miocene movements for both Inner Carpathians microplates of Alcapa and Tisza-Dacia (Van Hinsbergen *et al.*, 2008) (Fig. 6). These microplates, bounded by Mesozoic geometry, were moved independently from of each other at different speeds and directions (Lankreijer *et al.*, 1999). Paleomagnetic data revealed a strong rotation of both microplates, the Tisza–Dacia block was turned clockwise by *~60°* during the Miocene (Balla, 1987; Márton and Fodor, 1995; Linzer *et al.*, 1998; Panaiotu, 1998; Wortel and Spakman, 2000; Sperner *et al.*, 2001; Dupont–Nivet *et al.*, 2005) and Alcapa by *~80°* counter clockwise (e.g. Kováč *et al.*, 1997; Márton and Fodor, 1995). After the ending of movements both lithospheric fragments were amalgamated along mid–hungarian tectonic zone (Csontos, 1995).
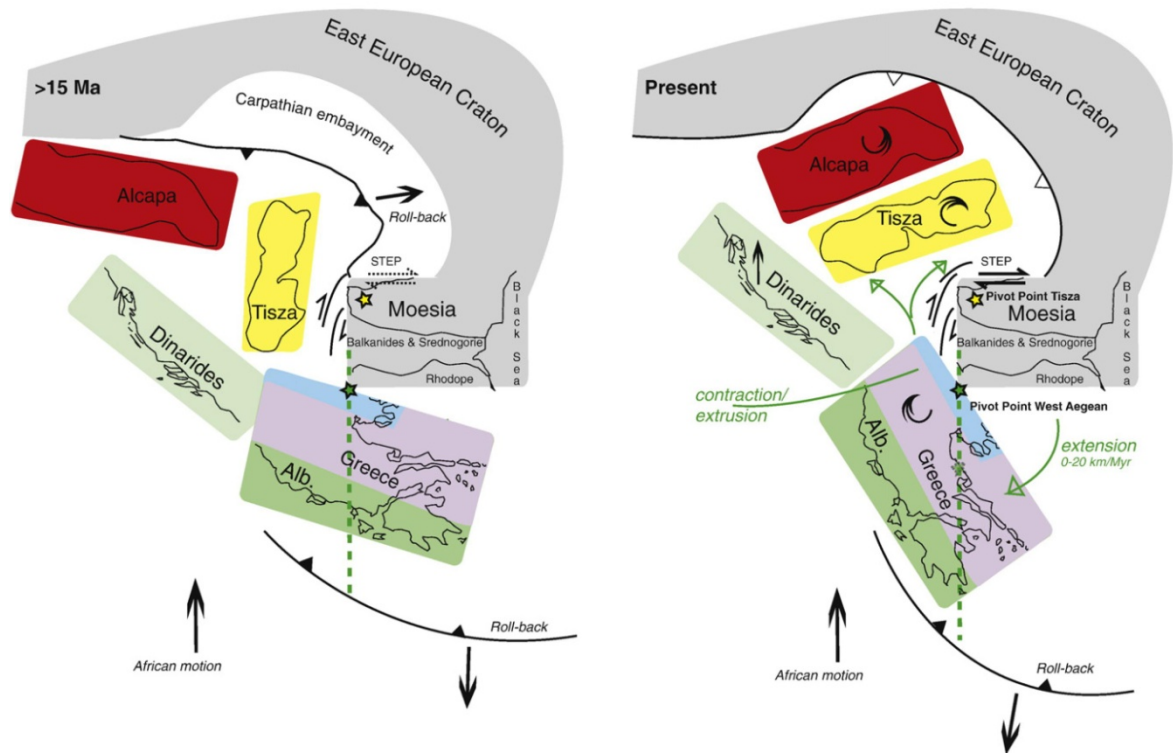
Fig. 6   Movement of the Alcapa and Tisza microplates caused by roll-back effect, extension of the basin and rotation the Tisza microplate and whole west Aegean area around a stable Moesian Platform (Van Hinsbergen *et al.*, 2008).

Neogene evolution of the Carpathian arc was influenced mainly by subduction of the lithosphere, which was located beneath the front of orogene. This development took place in three phases: 1) remnant oceanic lithosphere subduction, which was located in the North Peninic–Magura flysch zone, active from late Oligocene to early Miocene (Kováč *et al.*, 1994), 2) active subduction of the Krosno–Menilite flysch zone basement from early to late Miocene, 3) the last activity of subduction, at the southern tip of the Eastern Carpathians in Vrancea area is dated to late Miocene to Quaternary. The present subsurface contact zone between the European Platform and the Carpathians is suggested to be situated along the axis of the Carpathian gravity low (Tomek *et al.*, 1989; Tomek and Hall, 1993).

Continental collision started in the northernmost parts of the Carpathians and continued further S or/ to the SE, which led to a corresponding shift in sedimentation of the foredeep basins (Jiříček, 1979; Meulenkamp *et al.*, 1996; Kováč, 2000; Sperner *et al.*, 2001) and shifting volcanic activity (Pécskay *et al.*, 1995; Konečný *et al.*, 2002; Seghedi *et al.*, 2004).

The contrasting evolution of the accretionary prism and its subsequent folding allows identification of three segments with different subduction history, roughly corresponding with the Western Carpathians, NW part of the Eastern Carpathians and the SE part of the Eastern Carpathians (Kováč, 2000).

Temporal and spatial distribution of arc (subduction) type andesites suggests that subduction processes stopped when the subducted slab was almost in vertical position, closely followed by the detachement of the descending lithospheric plates from the continental margin. The plate detachement is manifested as lack of seismicity in intermediate depths in the northern parts of the Carpathians (Sperner *et al.*, 2001). Like the evolution of collision in the northern Carpathians, slab detachement began in the N and gradually continued to the S. Final detachment of the sinking lithospheric fragment in the Eastern Carpathians is confirmed by the results of seismic tomography (Goes *et al.*, 1999; Wortel and Spakman, 2000). The Recent lithosphere detachement process can be seen in the Eastern Carpathians in the Vrancea seismic zone (Constantinescu and Enescu, 1964; Sperner *et al.*, 2001). This zone is considered to be the last place in the Carpathians with ongoing gradual subduction, slab detachement and retreat of the tectonic plates, which is responsible for the development of back–arc system in this area (Tomek and PANCARDI Colleagues, 1996; Seghedi *et al.*, 1998; Wortel and Spakman, 2000).

In general, a short period of andesite arc-type volcanism is interpreted as an indication of the limited width of subducted lithosphere (*200* to *300 km* in the NW segment (Krosno–Moldavicum zone) and less than *200 km* in the SE segment), or as a sign of gradual detachment of the slab during the volcanic activity

Subduction beneath the flysch in the external Carpathians was from the beginning compensated by the uplift of asthenosphere and with this related to rifting in back–arc region. Temporal and spatial distribution of back–arc extension reflects segmentation of the subducting slab, as well as its final vertical tilt. This segmentation can be understood as a process driven by gravity, which makes space for astenospheric flow and accelerates the process of subduction (Dérerová *et al.*, 2006).

Thinning of the lithosphere in the Pannonian region corresponds to diapiric uplift of the asthenospheric material. Thinner lithosphere is documented by thermal modelling (e.g. Lenkey, 1999) and the spatial distribution of andesite and acid volcanism associated with regional extension (Szabó *et al.*, 1992; Kováč, 2000; Konečný *et al.*, 2002). Miocene

volcanic activity (Karpatian to Badenian) began in the W and the NW part of the Pannonian basin system area, associated with subduction in front of the Western Carpathians. The volcanic activity (Badenian to Sarmatian) continued in the NE regions of back arc basin, associated with accelerated subduction in the NW part of the Eastern Carpathians and finally the subduction and volcanic activity (Sarmatian to Pannonian) hit the northern, central and eastern regions of the Eastern Carpathians (Pécskay *et al.*, 2006). Late–phase alkali basalt volcanism shows that during the late development stage of the back–arc basin extensional conditions persisted and that diapiric uplift of the astenospheric material incorporated unmetasomatised mantle material in itself.

3 GEOPHYSICAL DATA AND MODELS

The whole studied region was subject of the many geophysical studies not only in the past but the research still continues these days. The tectonic history and unique interesting geodynamics are keeping scientists curious and challenging. From the beginning of the research, scientists have brought many different interpretations of the tectonic evolution, geodynamics, the composition and structure of the Carpathian–Pannonian Basin lithosphere. Since the amount of geophysical methods and approaches is from its beginning large and still increasing, also the amount of the results is considerable. These methods differ in the way of data acquisition, processing and interpretation which many times bring controversial results. Despite of these controversies the knowledge is wide and in most of these cases integrated together. However we cannot consider the research finished and well done. These days also, there are white spots on the map of the knowledge in the region; still a lot of questions and theories remain, so the investigation must continue in the future as well.

3.1 *Overview of the lithospheric thickness and the crust in the Carpathian–Pannonian Basin region*

In the following chapter, I try to present some of the previous lithospherical scale focused results.

The research of the lithosphere in the past was based mainly on the interpretation of seismic, seismologic, gravimetric, geothermal and magnetotelluric data (Fig. 7). One of the first models presented was the map of the Carpathian–Pannonian Basin lithosphere based on magnetotelluric measurements (Ádám, 1976; Praus *et al.*, 1990). Later, this map was reinterpretated based on different geophysical approaches (e.g. Babuška *et al.*, 1988; Horváth, 1993; Lenkey, 1999; Zeyen *et al.*, 2002; Dérerová *et al.*, 2006). The lithosphere was also investigated using geothermal modelling (Čermák, 1982; 1994; Majcin, 1994; Majcin *et al.*, 1998). More studies were done to investigate shallover, crustal structures. The density modelling studies of the area were focused mainly on the development of continental crust collision zones (Lillie, 1991; Lillie *et al.*, 1994). In the Balkan Peninsula a Moho map has been obtained on the basis of deep seismic profiling and seismological data (Boykova, 1999). In Romania, regional maps for the upper crust and the Moho have been

presented based on seismic refraction, reflection data, gravimetric and other geophysical data (Radulescu, 1988; Enescu *et al.*, 1992). Later, newer results including main crustal boundaries (upper crust, Moho and crystalline basement) and a gravity stripped map of the Romania were presented (Ioane and Ion, 2005). These geophysical models have been constructed using information derived from published crustal models based on refraction seismic and borehole data.

	Study area or transects of this theses
	Study area of the Carpathian - Pannonian region (e.g. Babuška et al., 1988; Horváth, 1993; Lenkey, 1999; Zeyen et al., 2002; Dérerová et al., 2006; Csicsay, 2010)
	Study area of Vrancea99 (Hauser et al., 2001)
	Study area of Alasonati - Tašarová et al. (2009)
	Study area of Bulgaria (Boykova, 1999)
	Study area of CELEBRATION 2000 (Janik et al., 2011)

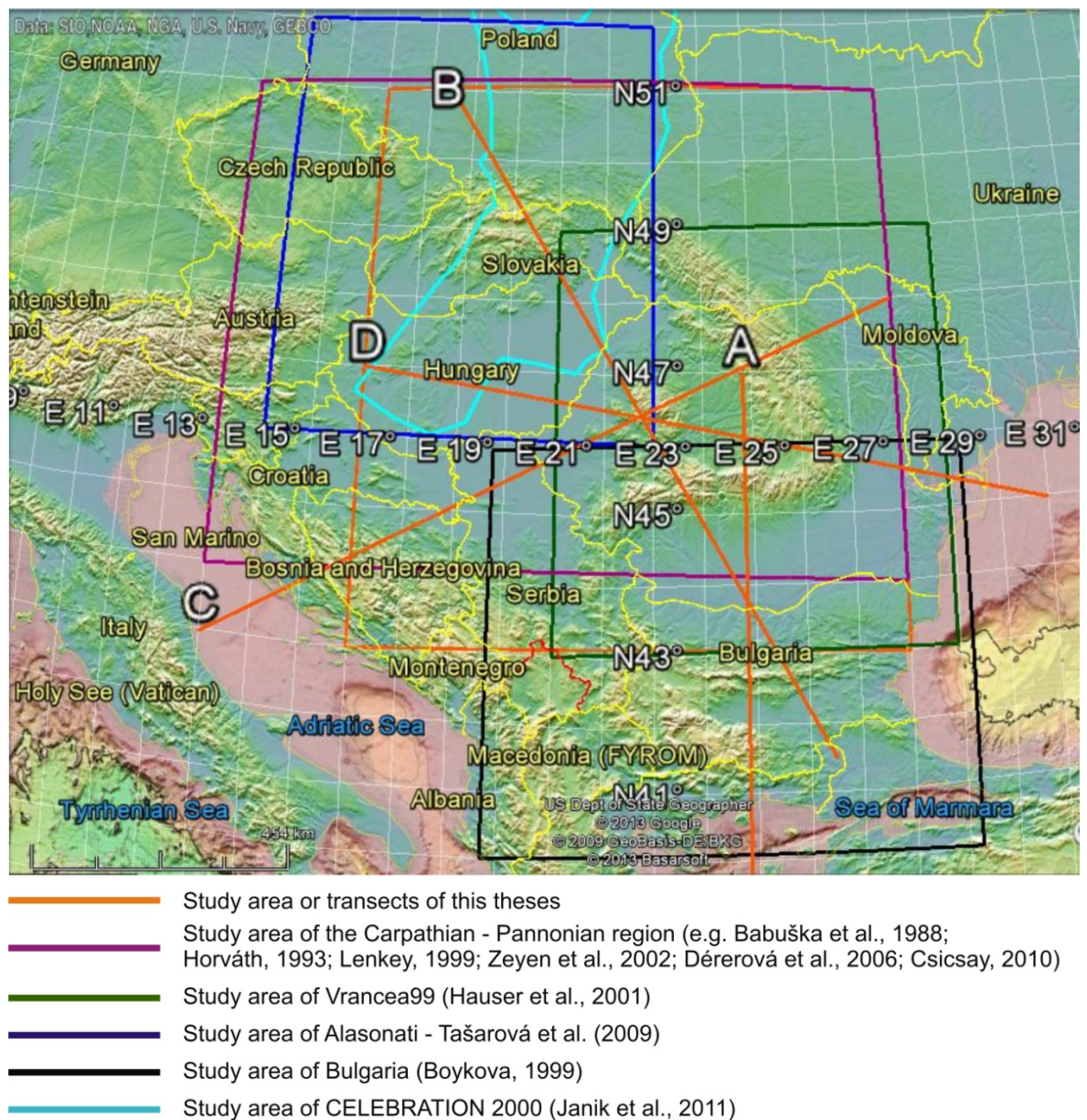Fig. 7   Topographic map of central Europe and Balkan shows the geographical location of the previous and our geophysical investigations.

One of the most important geophysical research projects was conducted in Central Europe between the years 1997 and 2003. The projects were carried out in extensive international cooperation, which included *30* institutions from *16* countries all over Europe

and North America, namely POLONAISE'97 (Polish Litospheric onsets–An International Seismic Experiment, 1997) CELEBRATION 2000 (Central European Litospheric Experiment Based on Refraction 2000), Alp 2002 (Eastern Alps and adjacent regions), SUDETES 2003 (Sudetes Mountains and adjacent regions) (Guterch *et al.*, 2003). The area was covered with a net of seismic profiles, where CELEBRATION 2000 is the most important projects for the present thesis (Fig. 8). These seismic profiles cover a large area, spreading from the Baltic to the Adriatic Sea.

The total length of all profiles is about *20 000 km* and *295* big blasts were made with an average distance of ca. *50 km*. As a result of these projects, a net of refraction seismic transects spreads from the North European Platform (eastern part of the Baltic Sea) along the Trans-European Suture Zone, over Poland and the Bohemian Massif, through the Carpathians, Sudetes and the Eastern Alps to the Pannonian Basin, Dinarides and the Adriatic Sea.

During the last decade, a big amount of work on the CELEBRATION 2000 data interpretation has been done. The results of the 2D seismic modelling for the main profiles have already been published (Janik *et al.*, 2005; 2009; Malinowski *et al.*, 2005; Hrubcová *et al.*, 2005, 2010; Hrubcová and Środa, 2008; Grad *et al.*, 2006; 2007; Środa *et al.*, 2006; Guterch *et al.*, 2007). The results of integrated seismic modelling along several profiles (CEL01, CEL04, CEL05, CEL06, CEL11, CEL12 and CEL28 seismic profiles) from the SE Poland were presented by Janik *et al.* (2009), and a geological interpretation of these results was presented by Narkiewicz *et al.* (2011).These data were incorporated together into the map of the Moho depth that covers eastern part of Slovak Republic and northern Hungary (Janik *et al.*, 2011) (Fig. 9).
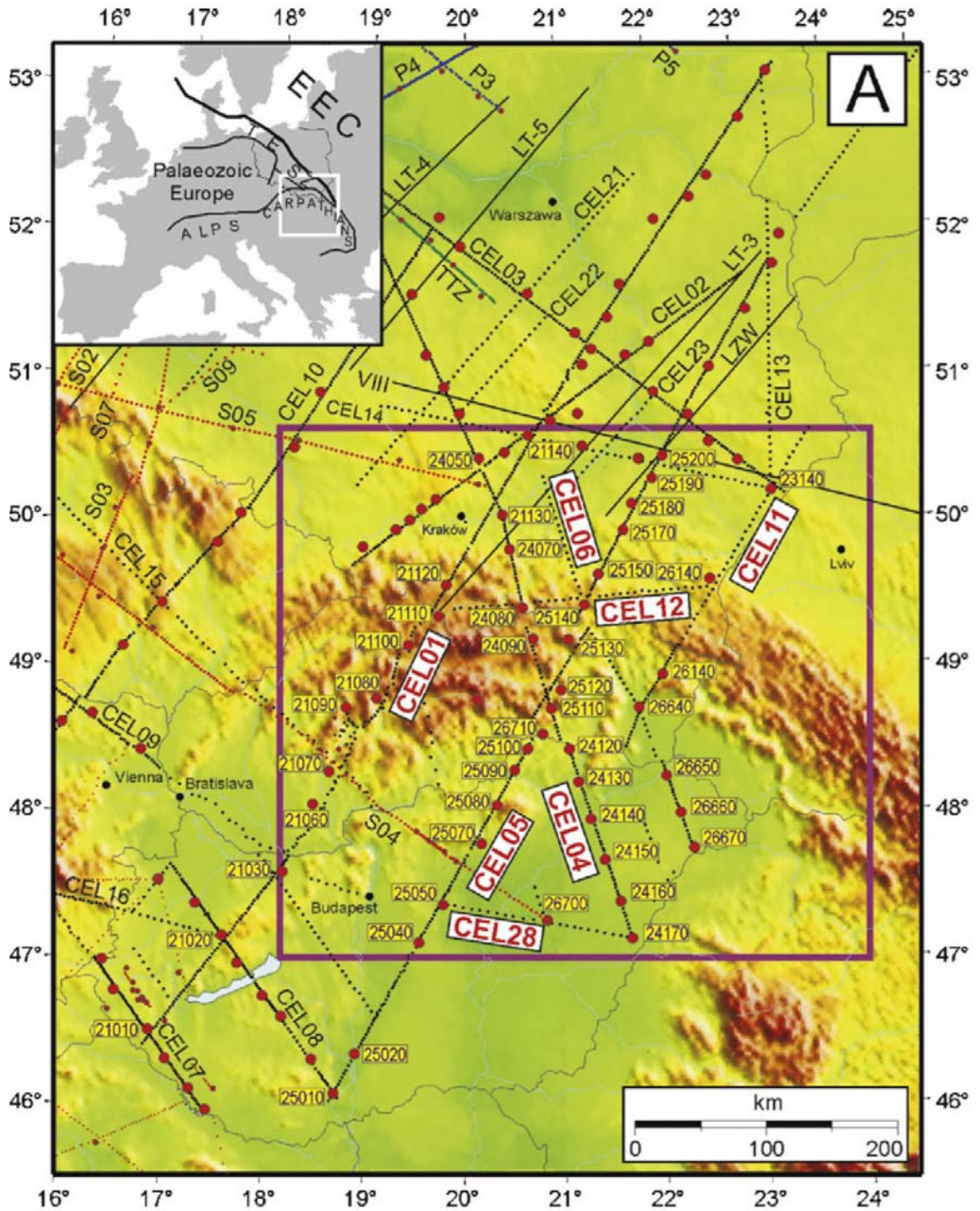
Fig. 8   Location of seismic profiles of the international project CELEBRATION 2000, with shot points (big red dots) and receiver positions (small black dots). Profiles in white boxes are the seismic profiles interpreted by Janik *et al.* (2011) (Fig. 9)The numbers in small yellow boxes refer to shot points along these profiles. The picture shows also the seismic profiles from POLONAISE'97 (P3, P4, P5), SUDETES 2003 (S02, S03, S04, S05, S09) and other experiments (TTZ, LT-4, LT-5, LT-3, LZW, VIII) (Janik *et al.*, 2011).
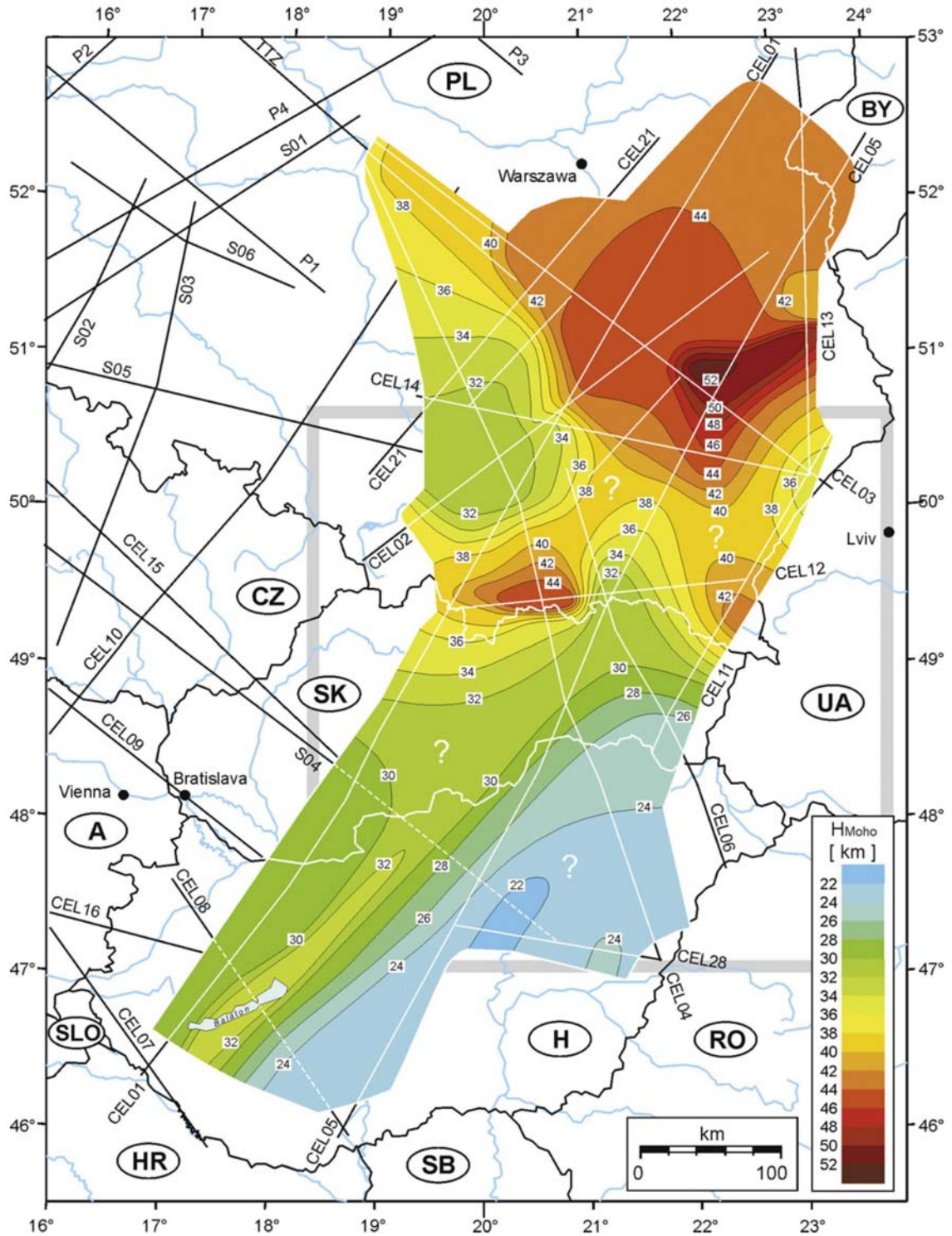
Fig. 9   Moho depth map of the study area based on the CELEBRATION 2000 data (Janik *et al.*, 2011).

Joint modelling of surface heat flow, gravity and topographic data using geological and seismic data, allowed to create a new model of lithospheric thickness of the northern part of the Carpathian–Pannonian Basin region and adjacent tectonic units (Zeyen *et al.*, 2002; Dérerová *et al.*, 2006). This lithospheric thickness model was based on the

results of the 2D integrated modelling along nine profiles (sections I, II, III, IV, V Zeyen *et al.*, 2002 and sections VI, VII, VIII and IX Dérerová *et al.*, 2006) It includes also results published earlier (Babuška *et al.*, 1988, Horváth, 1993 and Lenkey, 1999) (Fig. 10).
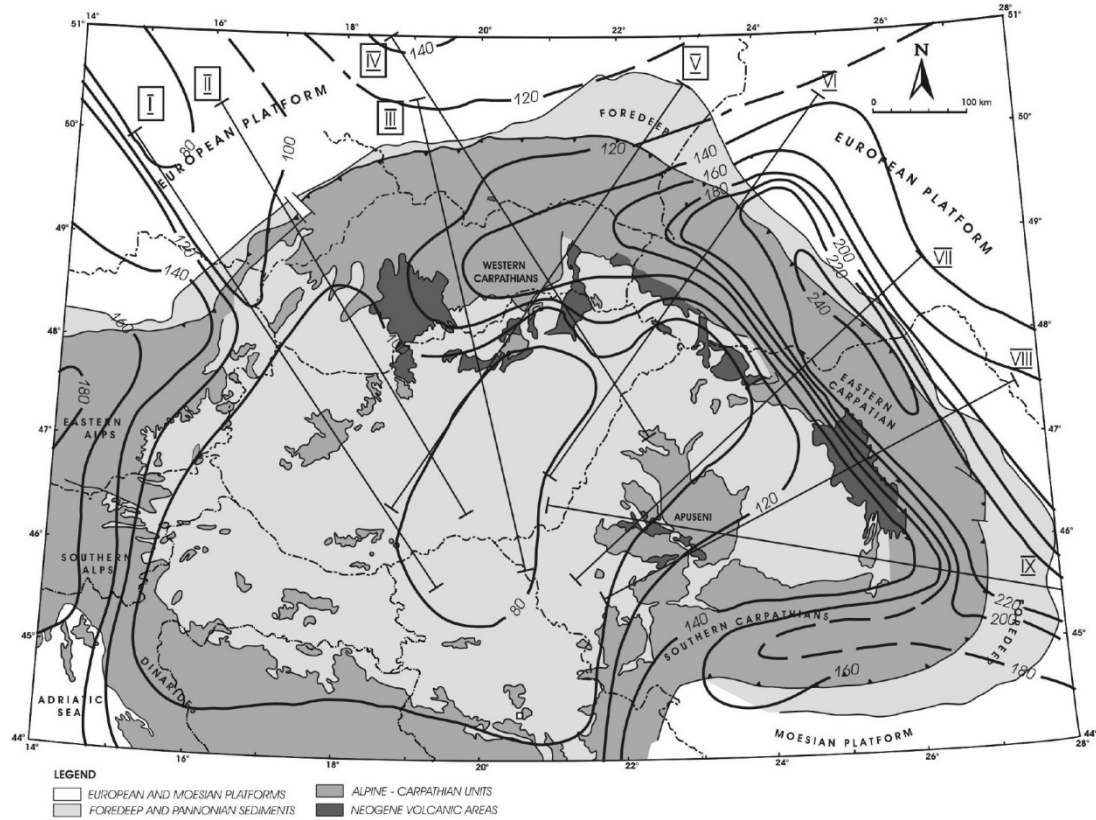
Fig. 10   Map of the lithospherical thickness of the Carpathian-Pannonian region (Dérerová *et al.*, 2006).

This map shows significant changes in the thickness of the lithosphere along the strike of the Carpathian arc. An increase of lithospheric thickness can be observed along the Carpathian Mountains from the W to the E. Under the western segment of the Western Carpathians no lithospheric thickening is observed, and values vary among *100* to *120 km*. This is in good agreement with the interpretation of the Alcapa movements against the Eastern Alps and the Bohemian Massif in the Miocene (Fodor, 1995; Linzer, 1996). They suggest that the strong Bohemian core had a root deep into the lower lithosphere. Then this core behaved as a rigid anchor that blocked the N–ward movement of the colliding Alpine region. This caused large–scale sinistral strike–slip movements in the Eastern Alps and opened the Vienna basin (Lankreijer *et al.*, 1999). The thickness of the lithosphere started to increase in the eastern segment of the Western Carpathians (*150 km*) and reached its maximum in the Eastern Carpathians and the foredeep in Ukraine and Romania (*240 km*). This thickening can be interpreted as a remnant of the tectonic plates that began to

delaminate in the Miocene (Spakman, 1990, Spakman *et al.*, 1993, Goes *et al.*, 1999, Wortel and Spakman, 2000, Dérerová *et al.*, 2006). These results suggest that the subducting plate may be detached from the European plate from the NW to the SE, its effect still being seen strongly in the SE (Vrancea area) but fading out in the Western Carpathians. A flat–lying, high–velocity anomaly at the bottom of the upper mantle has been interpreted as subducted lithosphere that sunk into the deeper mantle as a result of rollback and slab detachment along-strike of the Carpathian arc (Girbacea and Frisch, 1998; Sperner *et al.*, 2001; 2003; 2004; 2005; Landes *et al.*, 2004; Hauser *et al.*, 2001; 2005; 2007; Raileanu *et al.*, 2007). This roll–back movement could explain among other things why maximum crustal thickening is observed under the foreland. (Fig. 11) The lithospheric thickness increases from the W to the E. This supports the assumption that the detachement of the slab began in the NW and gradually spread to the SE. Vrancea seismogenic zone is considered as the last place where the progressive subduction roll–back is still active at present. These phenomena were responsible for the development of the arc (Tomek and PANCARDI Colleagues, 1996; Kázmér *et al.*, 2003; Dérerová *et al.*, 2006).

Lithosphere beneath the Pannonian Basin according to Dérerová *et al.* (2006) seems to be thicker than usually interpreted (Babuška *et al.*, 1988; Horváth, 1993; Šefara *et al.*, 1996; Lenkey, 1999; Zeyen *et al.*, 2002; Bielik *et al.*, 2004). These models do not support the thinning of the lithospheric to less than *70 km* compared proposed by other models claiming thinning to *60 km* (Babuška *et al.*, 1988; Horváth, 1993 and Lenkey 1999) or *40 km* (Ádám, 1996; Praus *et al.*, 1990; Ádám and Bielik, 1998). However, Dérerová *et al.* (2006) did not exclude a thinner lithosphere if the lower lithosphere had denser material than normal. This could explain the relatively low topography of the region.
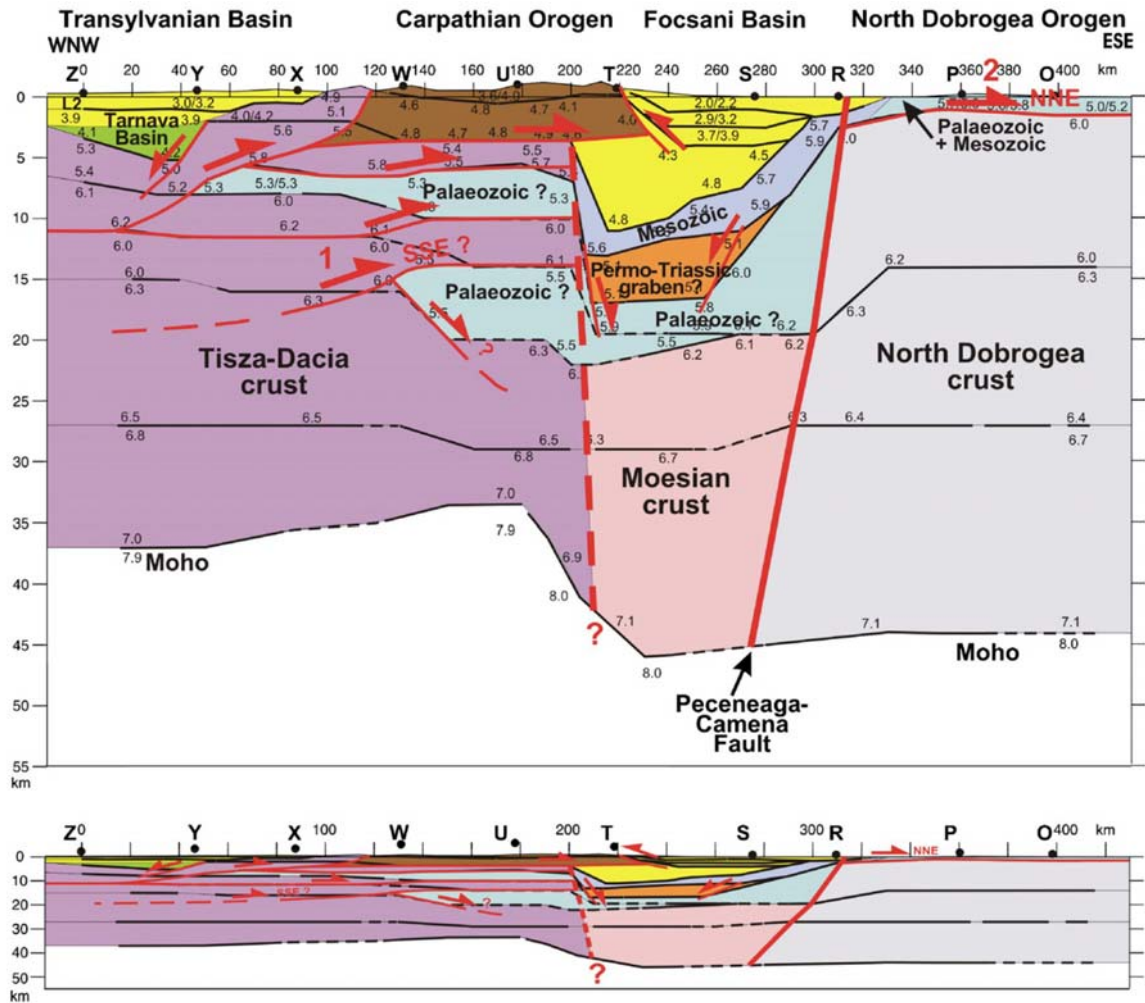
Fig. 11   Interpreted geological cross-section from the 2D seismic model along the main VRANCEA2001 seismic refraction line (Hauser *et al.*, 2007).

Recent studies about the Western Carpathian–Pannonian lithosphere have been presented by Alasonati Tašárová *et al.* (2009). They studied the region using 3D modelling of the Bouguer gravity anomaly constrained by seismic models and other geophysical data. They also show strongly thinned lithosphere, and place the boundary between asthenosphere and lithosphere (LAB) at depths from *60* to *100 km* (Fig. 12). The depth of LAB decreases W–wards (*160 km* in the eastern Alps) and N–wards (*140 km* beneath the Bohemian Massif and the Western Carpathians). This boundary reaches its maximum under the East European Platform at a depth of a little less than *200 km*.

41
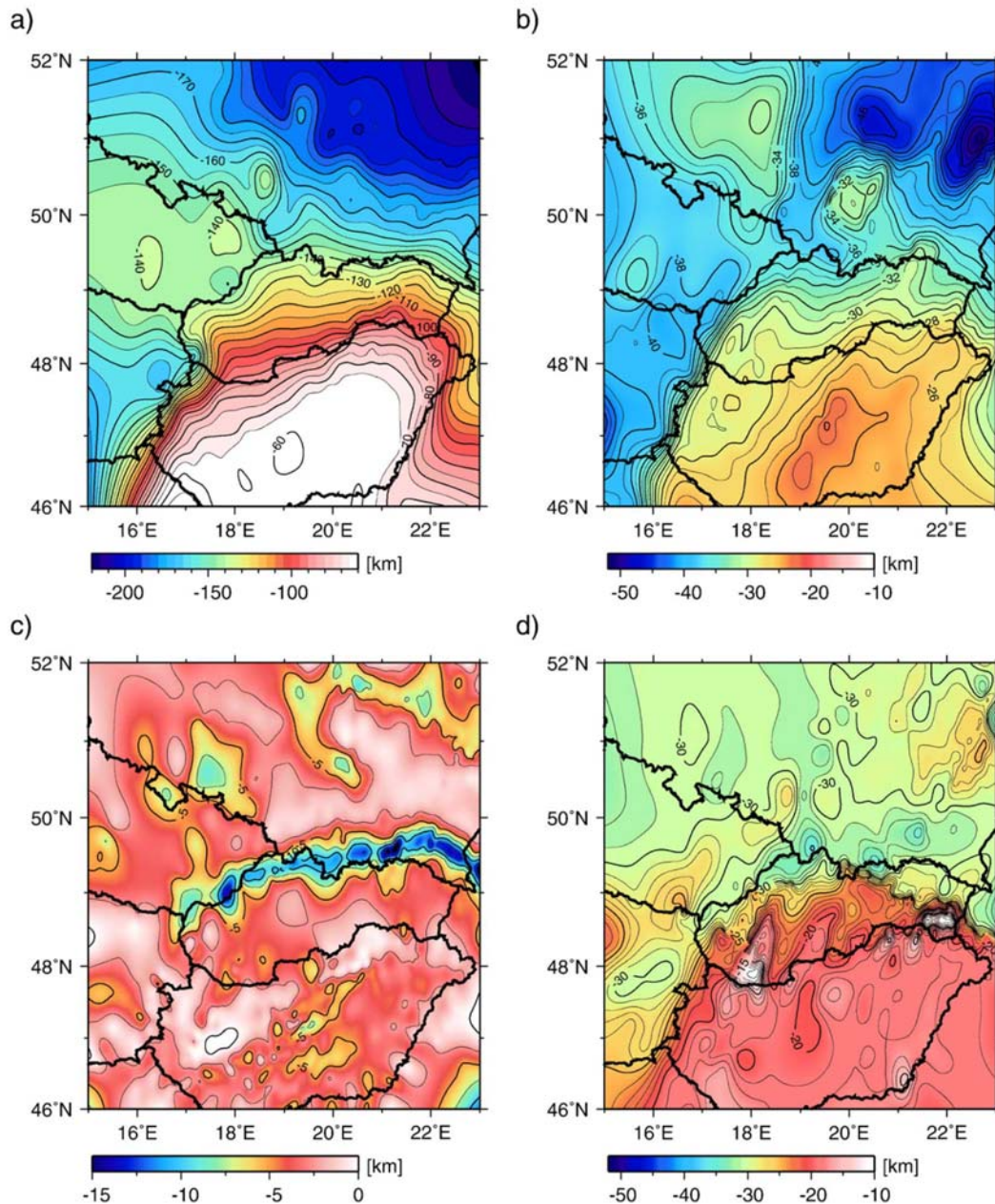
Fig. 12   The result of the 3D modelling of the Bouguer gravity anomaly constrained by seismic models and other geophysical data. Maps show depth to the major density boundaries: a) lithosphere-asthenosphere boundary (LAB), b) crust/mantle boundary (Moho), c) bottom of the sedimentary basins, and d) top of the lower crust (Alasonati Tašárová *et al.*, 2009).

The thickness of the crust varies parallel to lithospheric thickness. The thinnest crust is found under the Pannonian Basin and the thickness gradually increases towards the Alps and the East European Platform. The smallest crustal thickness was modelled along profile CEL05 (cca. *22 km*), which is consistent with estimation of Moho depth from seismic data (Grad *et al.*, 2006; Janik *et al.*, 2011). This area is located in the central part of the Pannonian Basin, where the strongest lithospheric stretching happened. However, the entire Pannonian Basin is not characterized by such a thin crust; in the East it is about *26*

km and in the W it is even a little more. On the southern edge of profile CEL01 the crustal thickness is *28 km* (Šroda *et al.*, 2006; Janik *et al.*, 2011) and *35 km* at the border of Hungary and Austria. The crust gradually thickens to values about *47 km* beneath the Eastern Alps (Behm *et al.*, 2007) and *35* to *38 km* beneath the Bohemian Massif. The Western Carpathians are characterized by intermediate crustal thicknesses, generally in the inner Western Carpathians the values are in the range of *29* to *36 km,* while in the outer Western Carpathians and the foredeep the thickness reaches from *30* to *45 km* (Alasonati Tašárová *et al.*, 2009).

The maximum values of crustal thickness were obtained in the northern part of the Carpathian Foredeep, in the region of the Trans-European Suture Zone (up to *50 km*) along the profile CEL05 (Grad *et al.*, 2006; Csicsay, 2010), similar thicknesses were obtained by other seismic interpretations (Tomek *et al.*, 1987). Thickness of sediments varies in the range from *0* to *7.8 km* in the Pannonian Basin, *0-2 km* in the inner Western Carpathians and the maximum values are found in the Flysch zone of the outer Western Carpathians, up to *21.5 km*. The Carpathian Foredeep reaches values in the range of *1-3 km*, thickness of sediments in the Polish Basin is about *5 km*, in some places up to *7 km*. The boundary between the East European Platform and the Trans-European Suture Zone is characterized by sediment thicknesses from *5* to *8 km* (Alasonati Tašárová *et al.*, 2009), which is comparable with the results of seismics (Šroda *et al.*, 2006; Guterch and Grad, 2006; Janik *et al.*, 2009; Janik *et al.*, 2011). The East European Platform is covered by a relatively thin layer of sediments, less than *3 km*.

Another approach used in the study of the crustal structure in the Carpathian Pannonian Basin region was performed by Csicsay (2010) He carried out density modelling along the same seismic profiles (CELEBRATION 2000) and performed 2D integrated gravimetric modelling, which used the seismic refraction modelling results as constraints. His models are based on relations between seismic velocity and density published by Sobolev and Babeyko (1994). The interpretation indicates clearly lithospheric structures varying significantly between the single megaunits and reflects the complicated structure of the tectonic contact between the Western Carpathians and the southern margin of the European Platform. This Moho depth map is shown in Fig. 13. The map reflects a very deep and narrow Moho depression, which is not located exactly under the highest topography (the High Tatras), but it is shifted towards the NE. In some places this map differs from the older results. Locally this difference can reach *15 km*.
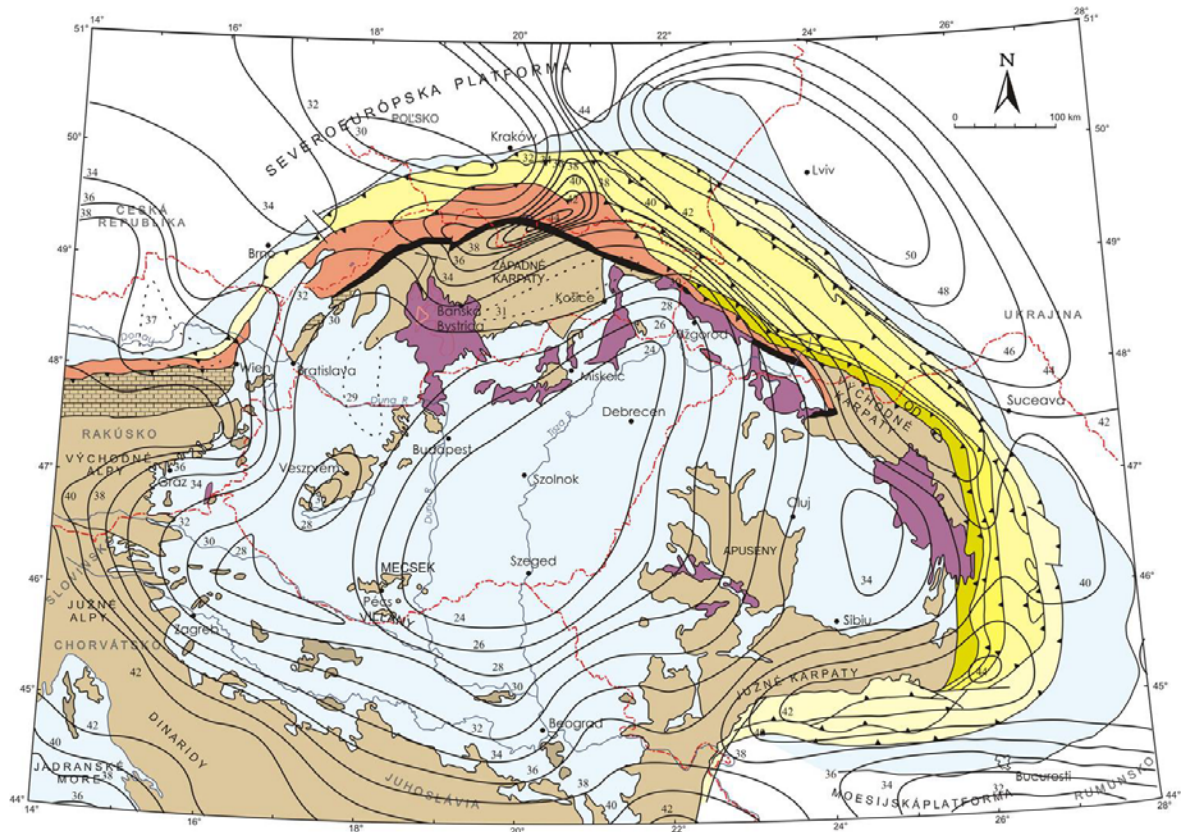
Fig. 13   The new map of the Moho boundary in the Carpathian – Pannonian Basin region (Csicsay, 2010).

Tóth *et al.* (2002) re–evaluated 20 000 measured and historical earthquake data for the entire Pannonian Basin region. In addition, a review is given of the stress data derived from *190* focal mechanism solutions for individual earthquakes. These data demonstrate a high level of seismic activity in the Dinarides and the Carpathians, the Vrancea area included. Hypocenters are mostly located in the upper parts of the crust (to *20 km*) in this area, but in Vrancea intermediate–depth mantle earthquakes occur. The majority of seismic events in the Pannonian Basin are concentrated at depths between *6-15 km* with strike-slip and thrust stress releases.

Grenerczy *et al.* (2005) presented an overview of crustal deformation structures in the Pannonian–Carpathian–Dinarides region, which were obtained from GPS campaigns and space geodesy. This work supports a scenario in which the N–ward moving Adriatic promontory squeezes out the Alpine-North Pannonian units to the East from between the Bohemian Massif and Adria, the E–ward escape being probably absorbed in the central part of the Pannonian Basin.

3.2   *Detailed geophysical studies of the Carpathian–Pannonian Basin region*

3.2.1   Pannonian Basin

In the Pannonian Basin being an integral part of the Carpathian–Pannonian Basin region, extensive geophysical investigation has been done. The formation of the Pannonian back-arc basin is generally related to the rapid Miocene rollback of a slab attached to the European continent. The newest knowledge assumes that Carpathian rollback is not the only mechanism responsible for the formation of the Pannonian Basin. The interpretation of the regional seismic lines shows that an additional middle Miocene rollback of a Dinaridic slab is required to explain the observed structures (Matenco and Radivojević, 2012). The results of a detailed tectonic analysis performed by integrated interpretation of bore–hole data and seismic reflection data argue in favour of a major clockwise rotation of the maximum and minimum horizontal stress axes during the Neogene through Quaternary, relating it to the shift of the termination of subduction along the Carpathian arc (Lörincz *et al.*, 2002). The Pannonian basin is characterised by high heat flow which can be explained by the subsidence and maturation history of the Neogene sediments (Lenkey *et al*., 2002) in general by Middle Miocene extension and thinning of the lithosphere (e.g. Royden *et al.*, 1983) (Fig. 14). The evidence for such a conclusion can be explained by the presence of thin crust (e.g. Horváth, 1993; Csicsay, 2010; Janik *et al.*, 2011), thin lithosphere (e.g. Ádám, 1976; Babuška and Plomerová, 1988; Praus *et al.*, 1990; Horváth, 1993, Dérerová *et al.*, 2006) and normal faults in the basement of Neogene sediments (e.g. Tari *et al.*, 1993). The interpretation of the heat flow is quite difficult in terms of simple conductive models because groundwater flow in porous sedimentary rocks or in fractured rocks disturb the geothermal field.
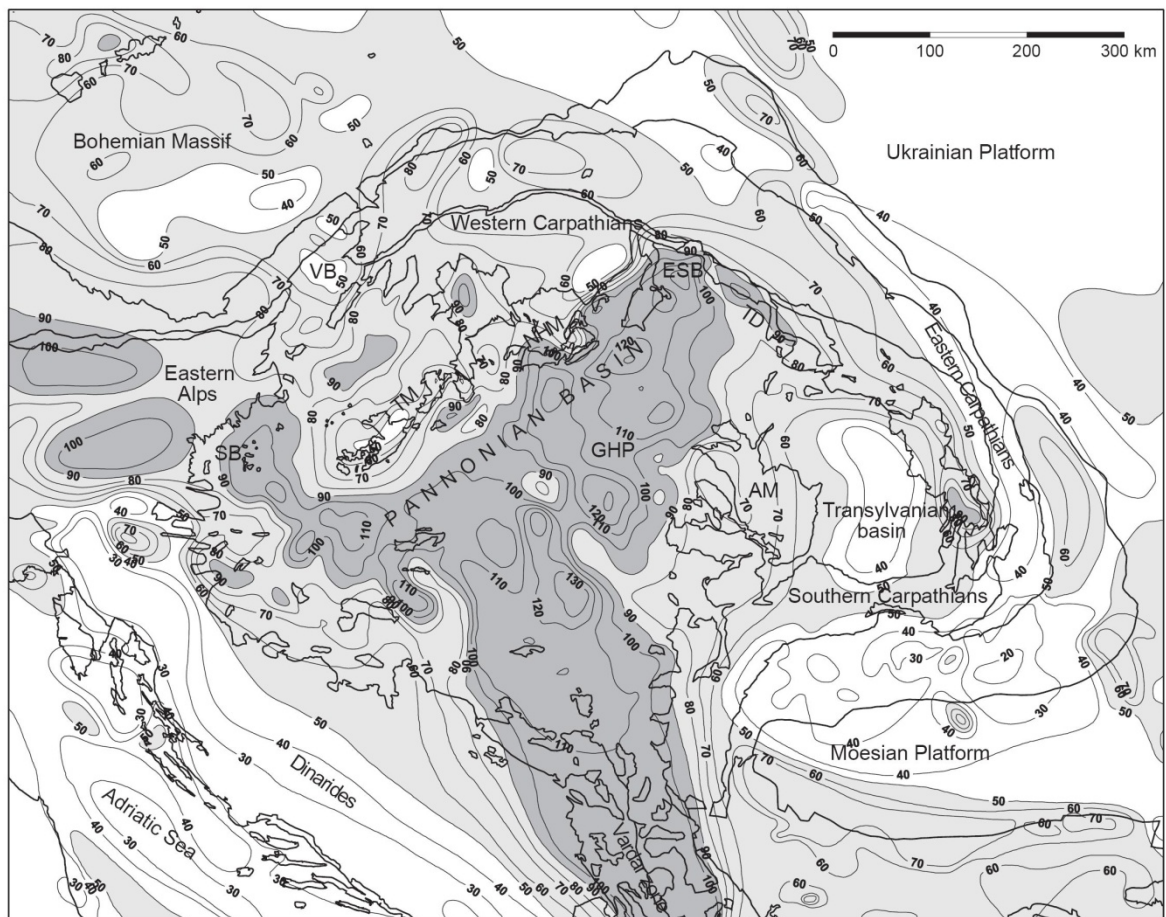
Fig. 14   Heat flow in the Pannonian basin and the surrounding areas. Inside the basin the heat flow is corrected for the Neogene sedimentation Contour interval is 10mW/m^2. Thick lines denote the boundaries of the Carpathian molasse and flysch belts, the outcrop of the pre-Neogene rocks and Neogene volcanic rocks on the surface. VB: Vienna basin, SB: Styrian basin, TM: Transdanubian Mountains, NHM: North Hungarian Mountains, GHP: Great Hungarian Plain, ESB: East Slovakian basin, TD: Transcarpathian depression, AM: Apuseni Mountains. (Lenkey *et al.,* 2002).

The results of a combined seismic and gravity modelling study along a dip–oriented transect in the Hungarian part of the Danube basin reveals significant updoming of the Moho under the Danube basin. On the other hand, the thinnest part of the lithosphere is shifted further S of the Danube basin (Szafián *et al.*, 1999). This confirms the previous theories (Horváth, 1993; Lankreijer *et al.*, 1995) that the Neogene deformation in the upper crust is decoupled from that of the lithospheric mantle lid along a rheologically weak lower crust. The seismicity of the area can be understood in terms of collision of the Adriatic microplate with Europe and differences in thermal state of the lithosphere (Lenkey *et al.*, 2002).

3.2.2   The Transylvanian Basin

Transylvanian Basin (depression) presents features that are not only special, but also in stark contrast with what is observed in the adjacent Pannonian Basin.

It is famous mainly for its methan gas (but no oil) and salt deposits. For the purpose of investigation and exploitation of these natural resources many boreholes were drilled. Besides these facts, the basin is characterised by an unusually high topography (around *600 m*), a very low surface heat flow, about *40 mW/m²* (e.g. Visarion and Veliciu, 1981), which is approximately two times less than in the Pannonian Basin, a very strong, positive, airborne geomagnetic anomaly in the centre of the basin, normal thickness of the crust or a rather thick crust (e.g. Horváth, 1993), and a basaltic layer in the basement, in the very centre of the depression (Ionescu *et al.*, 2009). Despite these unusual geological and geophysical properties, the Transylvanian Basin suffers from a considerable lack of quality data (Huismans *et al.*, 1997). Only a few models were presented to explain the tectonic evolution (e.g. Royden, 1988; Huismans *et al.*, 1997; Krézcek and Bally, 2006), unfortunately no satisfying explanation of the Neogene subsidence of this area was given. The reflection seismic profiles done in the area show the Cenozoic structures in the Transylvanian Basin and the eastern part of the Pannonian Basin (Ciulavu *et al.*, 2000). Evidence for Late Miocene transpressional strike slip faulting in both areas has also been observed.

It is hard to explain why heat flow increases from low values (*30 mW m⁻²*) in the central part towards higher values (*60 mW m⁻²*) in the margins of the Transylvanian Basin. Şerban *et al.* (2001) conclude that any of the investigated disturbing effects such as topography, topographically driven ground water flow and climatic changes cannot explain the thermal anomaly in Transylvanian Basin. Based on this assumption, it can be suggested that the reason for such a low heat flow is the very low heat production in the crust (Şerban *et al.*, 2001). This suggestion was examined by a model which includes the effects of lateral variation of heat-production rate in the crust, lateral variation of mantle heat flux, sedimentation and erosion, sediment compaction and lateral variations of the lithology and compaction parameters (Andreescu *et al.*, 2002). It shows that the anomaly requires a depletion in crustal heat-production rate in the centre of the basin corresponding to ~*15mW m⁻²*. Laterally constant low heat production of the upper crust (*0.5 μW m⁻³*) could be explained by the existence of ophiolite complexes in this area obducted on a thinner upper crust and very thin radiogenic heat producing upper crust. The increase of the surface heat flux towards the margins of the basin corresponds to an increase of the thickness of the upper crust and might be accounted for by larger values (*2.0 μW m⁻³*) of the heat–production rate in the upper crust in these areas (Andreescu *et al.*, 2002).

3.2.3 The Carpathians

The Carpathians, from a tectonic point of view, are an integral part of the Carpathian–Pannonian Basin region. Therefore, geophysical investigation has been focused on the region as a whole. However we can consider some of the surveys in a local sense.

One of the first Moho-focused investigation in the Western Carpathians were carried out by the seismic refraction method HSS (Beránek and Zátopek, 1981a;b). The reinterpretation of these results has brought some doubts, because the difference between the new and the previous results was about *5-7 km* (Šefara *et al.*, 1996). The new results of the Moho in the Western Carpathians have brought the interpretation of the CELEBRATION 2000 (Fig. 9) seismic experiment (Grad *et al.*, 2006; 2007; Janik *et al.*, 2005; 2011). The Eastern and Southern Carpathians are pushed aside of the main scientific interest because it has been focused mainly on the Vrancea area. The research here were carried particularly out to understand the geodynamics and tectonics of the whole Carpathian – Pannonian Basin region (e.g. Ádám, 1976; Babuška *et al.*, 1988; Horváth, 1993; Lenkey, 1999; Zeyen *et al.*, 2002; Dérerová *et al.*, 2006; Csicsay, 2010). These studies are usually missing data from seismics within these regions, so they use different methods to interpolate among the areas. Although the regions are on the edge of interest, they show interesting features within the lithosphere that should be studied.

More problematic from a geophysical point of view is to investigate the lithosphere–astenosphere boundary. The problem is that with increasing depth, the sensitivity of geophysical data decreases and also the different geophysical methods may display the LAB at different depths because of their investigated geophysical nature. In addition, the determination of the LAB is usually worked out for bigger areas, therefore, the previous investigations in the Carpathian–Pannonian Basin region are summarised further up in the regional scale paragraph.

3.2.4 The Vrancea zone

The Vrancea region in the South–Eastern Carpathians (Romania) is one of the few regions in the world where one can observe and study the geodynamic processes of post-collisional tearing off of an almost vertically hanging slab segment (Wenzel *et al.*, 1998). It has still attracted interest of geoscientists. Therefore, many studies were done here (regional seismic tomography, seismology, refraction studies, GPS, gravimetry,

geothermic studies and others) Very important geophysical research experiments are international and multidisciplinary projects the VRANCEA99 (Fig. 15) and VRANCEA2001 (Fig. 11) seismic refraction experiments which are part of a multidisciplinary project in Romania (Hauser *et al.*, 2001; Landes *et al.*, 2004).
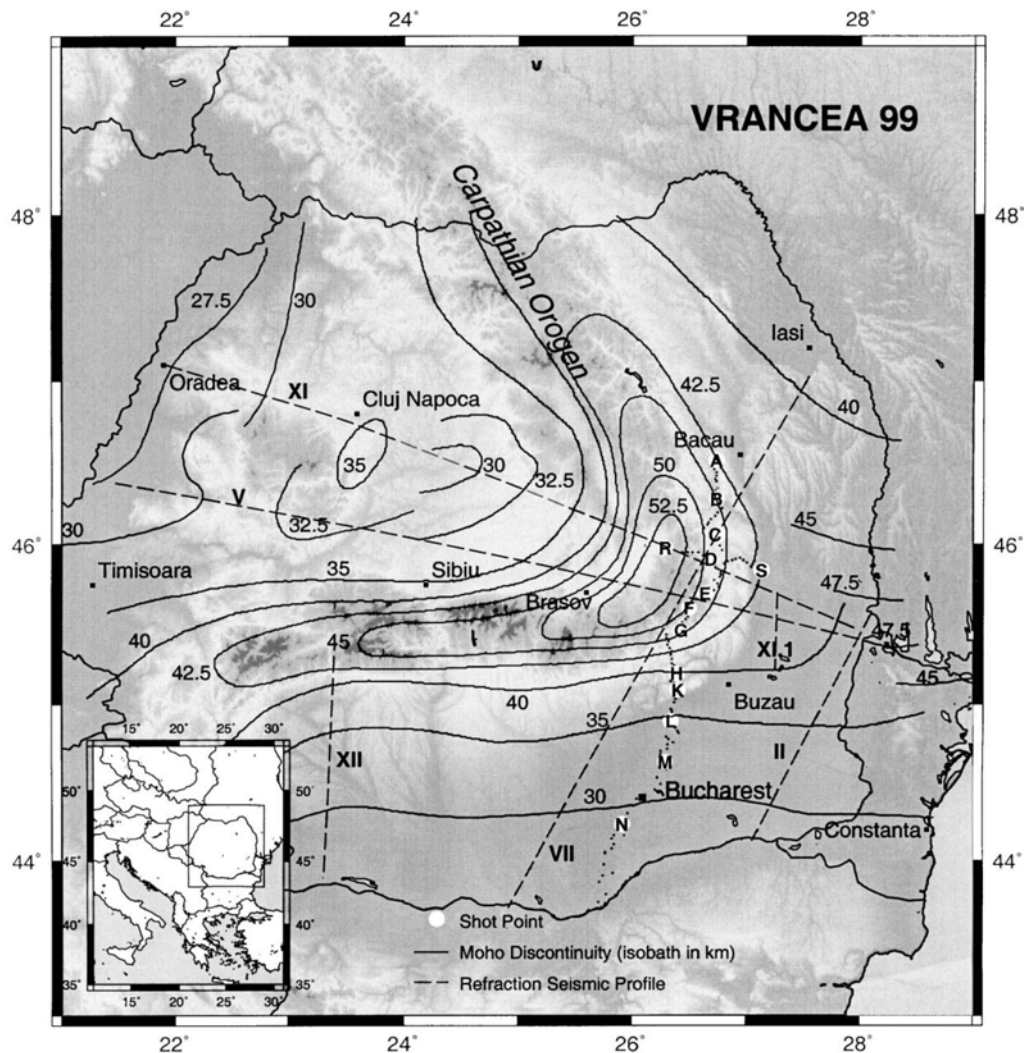
Fig. 15   Topographic map of Romania shows the geographical location of the VRANCEA99 seismic refraction lines (Hauser *et al.*, 2001). The contour lines indicate the depth to Moho (after Radulescu, 1988).

The Vrancea area is characterized by intermediate (*70-200 km*) seismic events with frequent earthquakes which are localized in a narrow (*20 km* x *50 km*) nearly vertical column (Bonjer *et al.*, 2000; Oncescu and Bonjer, 1997) having often magnitudes above *7* (Wenzel *et al.*, 1998). This suggests that the subducting slab is still hanging beneath the South–Eastern Carpathians (Linzer *et al.*, 1996; Sperner *et al.*, 2001; 2005), whereas the Miocene subduction zone extends laterally over a much larger area from the North–Western to the South–Eastern Carpathians. Oncescu (1984) suggests that the intermediate–

depth seismic events come from the zone that separates the sinking slab from its neighbouring immobile part of the lithosphere. However, the most common theory about the present days seismicity of the Vrancea zone is the detachement of the slab, there are still different kinds of detachement and delamination theories put forward (e.g. Gîrbacea and Frisch, 1998; Wortel and Spakman, 2000; Gvirtzman, 2002; Knapp *et al.*, 2005; Sperner *et al.*, 2005) (Fig. 16)
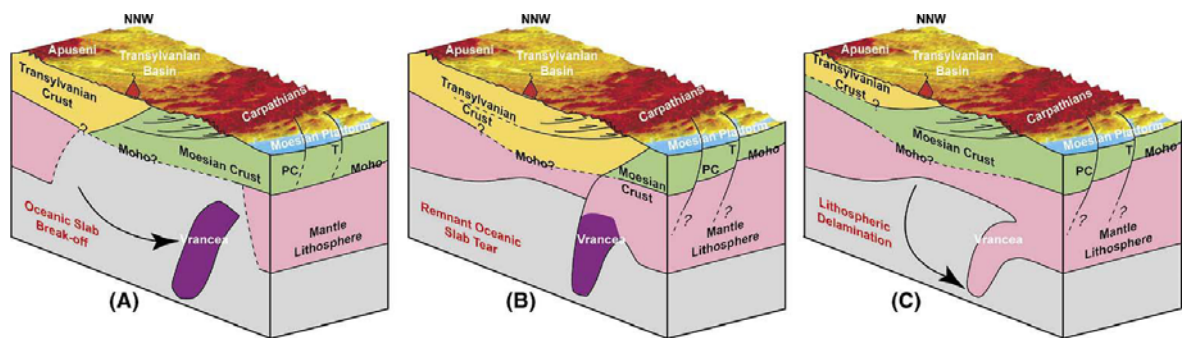
Fig. 16   3D perspective lithosphere-scale block models (view towards NNW), shows three different scenarios for the geodynamic setting of the Vrancea zone. (A) Oceanic slab subduction and break off. (B) Oceanic slab subduction and progressive lateral tear within the Carpathian foreland. (C) Continental lithospheric delamination (Knapp *et al.*, 2005).

There is still debate about the character and origin of the descending lithosphere, whether it is a continental or an oceanic slab. The theory of continental slab is supported by the lack of geological evidence concerning Miocene oceanic crust in the Carpathians. Some authors suggest that the descending lithosphere is rather thinned continental or transitional lithosphere (Pana and Erdmer, 1996; Pana and Morris, 1999). Cloetingh *et al.* (2004) argue in favour of a complex configuration of the underthrusted lithosphere and its thermo–mechanical age as primary factors in the behaviour of the descending slab after continental collision.

3.2.5   The Moesian Platform

The Moesian Platform is well known as petroleum province on the western margin of the Black Sea. It is usually considered as a Precambrian basement block that is generally regarded to belong to stable Europe. This platform was a subject of many previous investigations of the Moho. The results were based mainly on data from deep seismic profiling and seismology. Boykova (1999) unified these results and presented a new Moho map in the Bulgarian region (Fig. 17). The deep refraction seismic profiles in the area show crustal thicknesses around *35–40 km* (Radulescu, 1988), which is in good fit the seismological data of *34 km* (Enescu *et al.*, 1992). Most of the research in the Moesian

Platform was focused on the sedimentary cover (e.g. Ionesi, 1989) and fault system (e.g. Visarion *et al.*, 1988).

Fig. 17   Map of the Moho discontinuity in the central part of Balkan Peninsula. The isolines are in km from the sea-level; Solid isolines show major isolines every 3 km; Dashed lines are secondary isolines every 1.5 km (Boykova, 1999).

4 METHODOLOGY

Methodology of almost every geophysical work can be divided into two phases, the preparatory and interpretation stage itself. The internal structure of these stages is then dependent on the selected method of research. This thesis discusses research of tectonics of the Carpathian-Pannonian Basin regio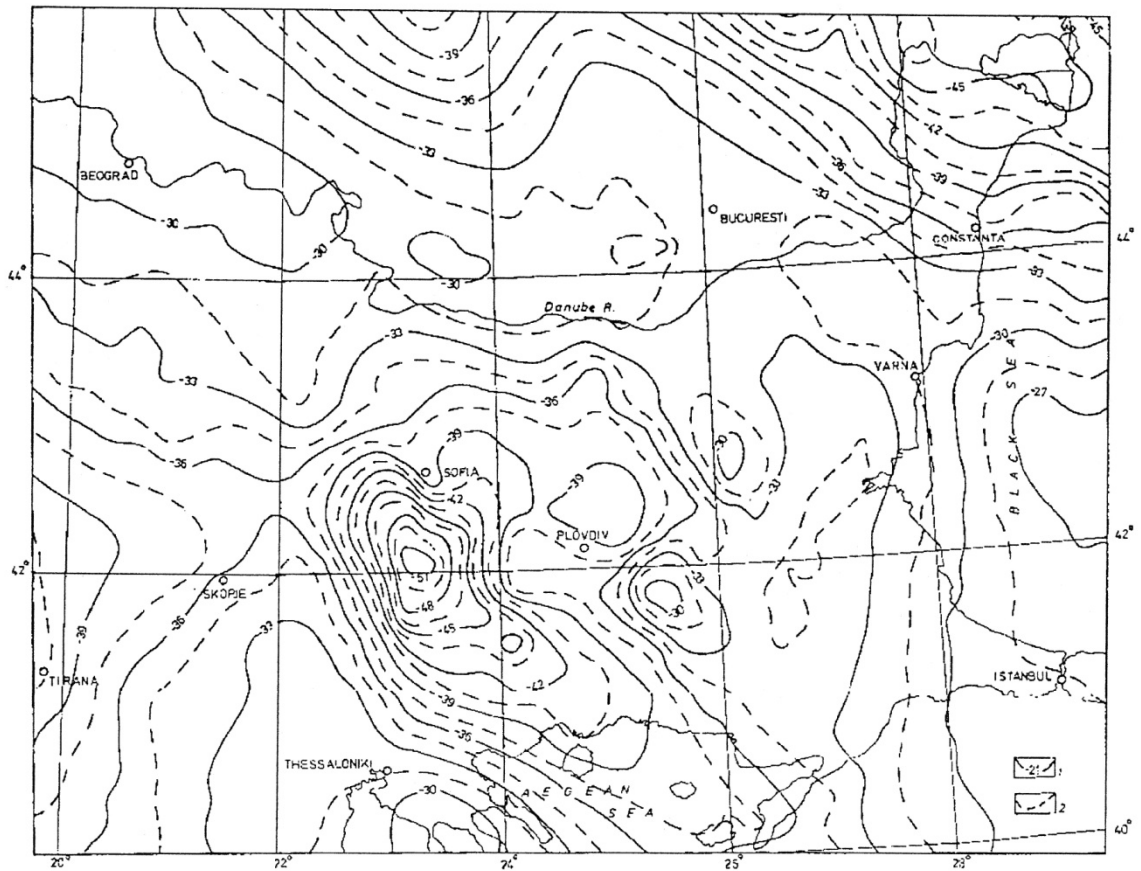n lithosphere, the chosen methods of research are 1D modelling, 2D integrated geophysical modelling and 3D Inversion. All of these approaches have their own methodology, which is in very broad terms similar.

The aim of the integrated geophysical modelling is to constrain complicated lithospheric structures by using joint interpretation of different geophysical data sets at the same time. This approach offers then an improved geophysical interpretation of lithospheric structures and has more advantages than traditional kinds of interpretation of the mentioned data sets on their own. In our case, we used 3 or 4 different data sets; potential field data (gravity–Bouguer or free air–and geoid), topography and corrected heat flow data. The quality of the interpretation may increase when these data are constrained by results of the other geophysical methods or *a priori* data (borehole data, seismics). Since we were interested in deeper lithospherical structures, the most suitable was taking into account the results of the seismic interpretation done in the study region. We used the same databases to extract all of our profiles or whole area for interpretation (it is discussed further down in the input databases paragraph).

4.1 *1D modelling*

This paragraph is worked out based on the papers of Fullea *et al.* (2006; 2007)

One dimensional modelling is a very fast method which allows to establish the very first model of the Moho and LAB and an overview of the Carpathian–Pannonian Basin lithosphere. This automatic modelling approach was presented by Fullea *et al.* (2006). From a scientific point of view, it is 1D modelling but on the other hand, when doing this 1D analysis on many vertical columns covering an area, it gives us a 3D overlook of the main boundaries that we are interested at in the studied area.

This method is based on the combination of elevation and geoid anomaly data to map crustal and lithospheric thickness. The reason for using different data sets is that each of these data sets is sensitive to different lithospherical phenomena. Topography reflects

variations of the average density within the lithospheric column, whereas geoid anomaly depends on the depth distribution of density variations and is proportional to the dipole moment of density (Turcotte and Schubert, 1982). In this case, only two layers are considered: crust and lithospheric mantle. Topography is modelled in local isostasy, based on the assumption that the lithosphere floats freely on the asthenosphere and below a certain level of compensation, z_{max}, the pressure does not vary laterally. Then, the elevation is a measure of the buoyancy of the lithospheric columns. This can be expressed as (Lachenbruch and Morgan, 1990):

$$E = \frac{\rho_a - \rho_L}{\rho_a} L - H_0, \quad E \geq 0,$$ eq. (1)

$$E = \frac{\rho_a}{\rho_a - \rho_w} \left[\frac{\rho_a - \rho_L}{\rho_a} L - H_0 \right], \quad E \leq 0,$$ eq. (2)

where E is elevation above sea level (*m*), ρ_a is density of the asthenosphere ρ_L is average density of the lithosphere (*kg.m^{-3}*), ρ_w is density of sea water (*kg.m^{-3}*), L is thickness of the lithosphere (*m*); and H_0 is depth below sea level of an unloaded asthenospheric column (*m*) Parameters ρ_a, ρ_w, and H_0 are supposed to be known and are taken from Lachenbruch and Morgan (1990). The elevation depends on two unknown parameters, ρ_l and L, therefore it is necessary to know the average density of the lithosphere or its thickness.

In a two layer model where each layer has a constant density, ρ_L can be written as:

$$\rho_L = \frac{(E + z_c) \rho_c + (z_L - z_c) \rho_m}{E + z_L},$$ eq. (3)

where z_c is the depth of the Moho, z_L is the depth of the LAB, ρ_c the mean density of the crust and ρ_m the mean density of the lithospheric mantle. The depths are positive downwards and referred to the mean sea level. However, topography is taken positive upwards. By combining eq. (1), eq. (2) and eq. (3), an equation can be obtained that relates the crustal and lithospheric depths under local isostasy:

$$z_c = \frac{\rho_a L_0 + E(\rho_c - \rho_w) + z_L(\rho_m - \rho_a)}{\rho_m - \rho_c},$$ eq. (4)

Eq. (4) is valid for points above or below sea level. If elevation is above sea level ($E > 0$), then $\rho_w = 0$; if it is below sea level, $\rho_w = 1030\ kg.m^{-3}$ is the density of sea–water. If

local isostasy holds and the wavelengths of the lateral density contrasts are big enough with respect to their depth, i.e., the 1D approximation is suitable, then the geoid anomaly (*N*), is proportional to the dipolar moment of the anomalous mass distribution (Fullea *et al.*, 2005; Haxby and Turcotte, 1978; Ockendon and Turcotte, 1977; Turcotte and Schubert, 1982):

$$N = -\frac{2\pi G}{g} \int_{LC} z \Delta\rho(z) dz,$$

eq. (5)

where *Δρ(z)* is the density contrast with respect to a given reference column, *G* is the universal gravitational constant, *g* is the Earth's surface gravitational acceleration and *LC* indicates integration along the whole model column containing the lithosphere and the asthenosphere above the compensation level. For a two–layer model with constant density for crust and lithospheric mantle we can rewrite eq. (5) as (with a positive downward coordinate system):

$$N = -\frac{\pi G}{g} \left[\rho_w E^2 + \left(z_c^2 - E^2\right)\rho_c + \left(z_L^2 - z_c^2\right)\rho_m + \left(z_{max}^2 - z_L^2\right)\rho_a \right] - N_0,$$

eq. (6)

where z_{max} is the depth of compensation and ρ_a is the density of the asthenosphere. An integration constant N_0 is used to adjust the zero level of the geoid anomalies. N_0 is determined by applying eq. (6) to a lithospheric reference column.

Eq. (4) and eq. (6) form a system of equations with five unknowns. Moho depth (z_c), depth of LAB (z_L), density of crust (ρ_c), lithospheric mantle (ρ_m) and N_0. Since there are five variables and only two constraints, here we fixed ρ_c and ρ_m as known densities and defined a reference model for N_0. N_0 is hard to determine. In our study, we used many different values for N_0, the best model fits the best with the model using Hauser *et al.* (2007) seismic interpretation crossing the Vrancea Zone. However this is not a unique solution, the inversion is stable for all points on the map. z_c and z_L are the calculated parameteres.

For the lithospheric mantle density, ρ_m, we consider a linear dependence on the temperature based on Parsons and Sclater (1977). Therefore:

$$\rho_m(z) = \rho_a \left(1 + \alpha\left[T_a - T_m(z)\right]\right),$$

eq. (7)

where α is the linear coefficient of thermal expansion (K^{-1}), T_a is the temperature at the LAB and $T_m(z)$ is the temperature at depth *z* in the lithosphere.

The temperature distribution within the crust with the boundary conditions: fixed temperature at the surface of the Earth (T_s) and fixed heath flow at the base of the crust (q_m) and constant thermal conductivity k_c is:

$$T^c(z) = T_s + \frac{q_m}{k_c}(z + E) + \frac{H_s}{2k_c}\left(E^2 - z^2 + 2z_c[z + E]\right),$$ eq. (8)

for constant crustal heat production H_S or

$$T^e(z) = T_s + \frac{q_m}{k_c}(z + E) + \frac{H_s h_r^2}{k_c}\left(1 - \exp\left(-\frac{(z + E)}{h_r}\right)\right),$$ eq. (9)

for heat production decreasing exponentially with depth.

where H_s is the crustal surface heat production, h_r is the characteristic length scale of heat production distribution, z is depth, E is the topography which is referred to the mean sea level (see Fig. 18). T^c is the temperature profile using constant decreasing heat production throughout the crust and T^e is the temperature profile using exponentially decreasing heat production throughout the crust.

The temperature at the Moho ($z=z_c$), T_{mh}, is calculated as:

$$T_{mh} = T_s + \frac{q_m}{k_c} + (z_c + E) + \frac{f}{k_c},$$ eq. (10)

where for a constant heat production $f=f_c$ and for an exponentially decreasing heat production $f=f_e$:

$$f_c = H_s \frac{(E + z_c)^2}{2},$$ eq. (11)

$$f_c = H_s h_r^2\left(1 - \exp\left(-\frac{(z_c + E)}{h_r}\right)\right),$$ eq. (12)

For the lithospheric mantle we consider a linear temperature profile (Lachenbruch and Morgan, 1990). Therefore the heat flow is constant within the lithospheric mantle and equal to:

$$q_m = k_m \frac{T_a - T_{mh}}{z_L - z_c},$$ eq. (13)

where k_m is the thermal conductivity of the lithospheric mantle. We can introduce Eq. (13) into eq. (10) to obtain the temperature at the base of the crust as a function of E, z_c, z_L and the thermal parameters:

$$T_{mh}\left(E,z_c,z_L\right) = \frac{\left(z_L - z_c\right)\theta + \delta}{z_c\Delta k + z_L k_c + Ek_m},$$

eq. (14)

where

$$\theta = \left(k_c T_s + f\right); \delta = k_m T_a\left(z_c + E\right); \Delta k = k_m - k_c$$

The average value of the lithospheric mantle density, $\bar{\rho_m}$, can be determined by integrating eq. (7) between z_c and z_L:

$$\bar{\rho_m} = \frac{1}{z_L - z_c}\int_{z_c}^{z_L} \rho_m\left(z\right)dz = \rho_a\left(1 + \frac{\alpha}{2}\left[T_a - T_{mh}\right]\right),$$

eq. (15)
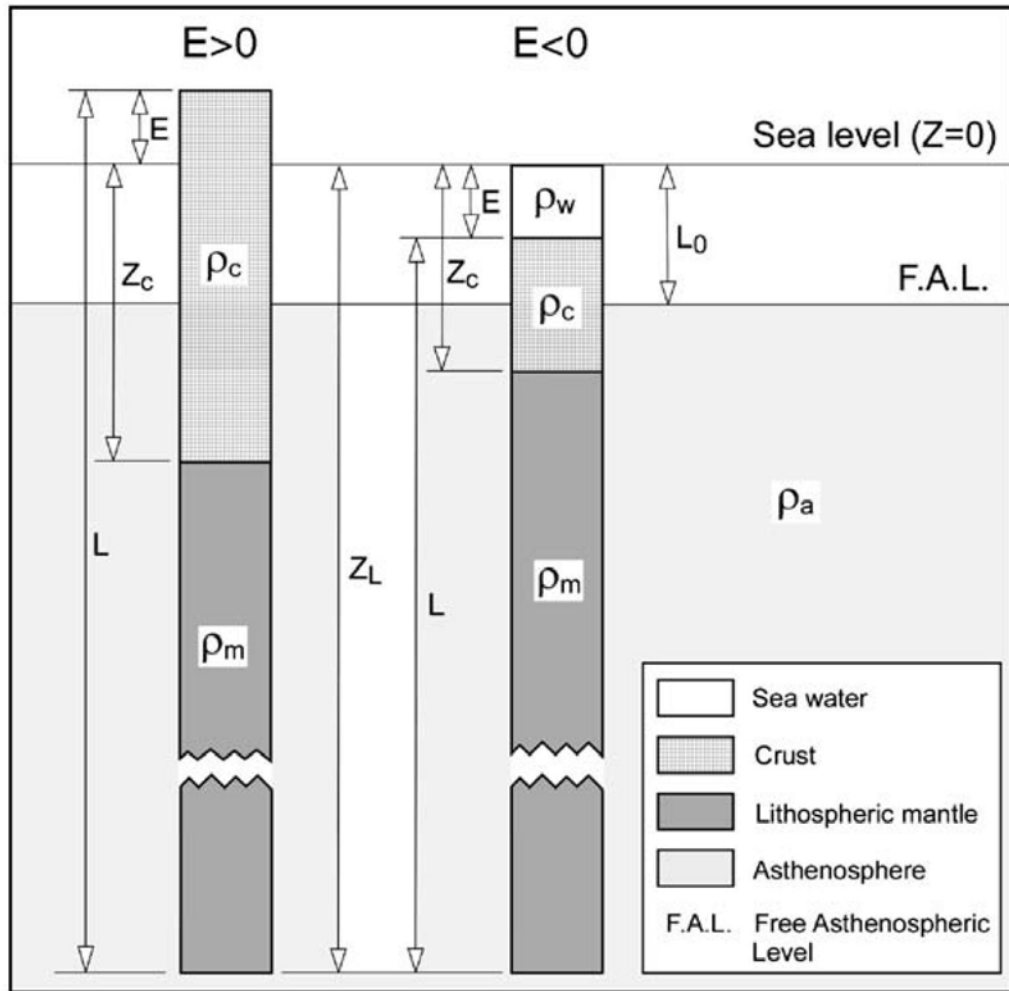
Fig. 18   The two layer model, where the density of the crust is ρ_c and ρ_m for lithospheric mantle, for sea water ρw and asthenosphere ρ_a. E is the elevation ($E>0$ topography, $E<0$ bathymetry), z_c, and z_L are the depths of the crust/mantle and lithosphere/asthenosphere boundaries, respectively, referred to the sea level. L is the total thickness of the lithosphere and L_0 is the depth of the free asthenospheric level, i.e. without any lithospheric load (Fullea *et al.*, 2007).

4.2 *2D modelling*

This paragraph is worked out based on the paper Zeyen and Fernàndez, 1994

The thermal structure and density distribution in the upper mantle is estimated using a combination of geophysical information. This approach is able to constrain the complicated lithospheric structures of the studied region better than interpreting each data set on its own. We use a two–dimensional algorithm to determine the steady state thermal structure of the lithosphere in the study area.

The program used consists of a two dimensional finite element algorithm to calculate the temperature distribution based on a user–defined lithospheric structure where each body is characterized by its density, thermal conductivity and heat production. The first step is to solve the conductive heat transport equation under the steady state temperature distribution using a finite element code:

$$\nabla\left(k\left(x,z\right)\cdot\nabla T\left(x,z\right)\right)+A\left(x,z\right)=0, \qquad\qquad \text{eq. (16)}$$

where k is the thermal conductivity, T the temperature, A the volumetric heat production and ∇ the 2D operator. The body structure is as much as possible constrained by existing seismic and geological data. The thermal boundary conditions are fixed temperatures at the upper limit (Earth's surface; *20°C*) and the lower one (lithosphere-asthenosphere boundary; *1300°C*) as well as no horizontal heat flow across the lateral, vertical boundaries. After the calculation of the temperature distribution, the body densities are modified at each node of the finite element grid taking into account the thermal expansion coefficient. With this modified density distribution, we calculate the gravity and geoid variations and the topography, after having calculated the average lithospheric density for every column of the grid. Data and model results are compared and the model is then changed interactively by trial and error until an acceptable fit is obtained.

In summary, the thermal and gravity fields and local isostatic equilibrium are coupled by the density distribution and lithospheric thickness. Surface heat flow and temperatures in the uppermost mantle depend strongly on the lithospheric thickness and may affect the Bouguer anomaly and elevation when a temperature dependent density is assumed for the lithospheric mantle. Crustal thickness and its density distribution also affect the Bouguer anomaly and surface elevation data (Zeyen *et al.*, 1994). Topography is sensitive to lateral variations of the average density above a certain compensation level.

The level is defined within the asthenosphere that is supposed to have a sufficiently small viscosity to relax shear stresses at geologically short timescales and to have a constant density. Gravity anomalies depend on distance r to density variations by r^{-2}. Therefore gravity anomalies will depend mainly on density variations within the crust. The geoid, reflecting variations of the elevation of the gravimetric isopotential surface corresponding to sea level depends on the distance to density variations by r^{-1}. The geoid is therefore also more sensitive to near-surface density variations (specifically to topography) than to deep ones. However, the decay is relatively slow, and therefore geoid anomalies reflect crustal as well as mantle density variations. The formulas used have been published by Zeyen *et al.* (2005).

Surface heat flow values and geotherms in the deeper parts of the crust and in the upper mantle may be obscured by near-surface effects like groundwater flow or paleoclimatic variations and also by the generally unknown distribution of heat–producing elements in the crust. That is the reason why the surface heat flow should be properly corrected for superficial phenomena. Such a surface heat flow is the sum of incoming heat flow from the asthenosphere and the one produced by radiogenic heat production in the lithosphere. From the modelling point of view, the asthenospheric heat flow is controlled by thickness, thermal conductivity, surface and basal temperature of the lithosphere. The majority of radiogenic heat is produced in the upper crust where it depends on lithology (Vilà *et al.,* 2010). It is much higher than in the lower crust and in the lithospheric mantle, respectively (Wollenberg and Smith, 1987; Rybach, 1988). Pollack and Chapman (1977) empirically deduced that radiogenic heat production, on average, contributes *40%* to the continental surface heat flow.

Determination of lithospheric thickness based only on surface heat flow data has large uncertainties. To reduce this uncertainty, one has to use other information. One possibility is to take into account the dependence of density on temperature through the coefficient of thermal expansion:

$$\rho(T) = \rho_0\left(1 + \alpha\left(T - T_0\right)\right), \qquad\qquad \text{eq. (17)}$$

where $\rho(T)$ is the density *(kg.m^{-3})* at a given temperature *T(°C)*, ρ_0 is the density at temperature T_0 (usually room temperature except for the mantle, where it is given at asthenospheric temperature) and α is the thermal expansion coefficient taken as *3.5 * 10^{-5} K^{-1}* (Afonso *et al.*, 2005).

The Bouguer anomaly is calculated at the top of the model when topography is above sea level, otherwise at sea level using Talwani *et al.* (1959) two–dimensional algorithm for each element (Zeyen and Fernàndez, 1994).

The calculation of the geoid anomaly was carried out by converting the triangular elements of the grid into rectangular prisms with a large lateral extension in order to simulate two-dimensional anomalies (Zeyen *et al.,* 2005).

If local isostasy is assumed, the absolute elevation of a given lithospheric column can be calculated by comparing its buoyancy force with that of a reference column. Lachenbruch and Morgan (1990) take this reference column at the mid–oceanic ridges where average elevation and lithospheric structure are well known. Surface elevation is then given by Lachenbruch and Morgan (1990) (see eq. (1) and eq. (2))

4.3   *3D inversion programme*

This paragraph is worked out based on the paper Motavalli-Anbaran *et al.* (2013)

Although, the 2D approach previously presented has some advantages, it cannot treat all the complexity of the three–dimensional structure of the Carpathian–Pannonian Basin region. A 3D approach is needed. In this work, we applied 3D inversion to obtain a 3D model of the lithosphere in the studied region. The algorithm used is a relatively fast method based on a Bayesian approach with Gaussian probability density functions. We used a 3D algorithm (GT_3D_INV) to obtain the density structure of the lithosphere from joint inversion of free air gravity, geoid and topography data. The algorithm delivers the crustal and lithospheric thicknesses and the average crustal density in vertical columns. The inversion process may be stabilised by using damping and smoothing parameter as well as use of *a priori* information like crustal thicknesses from seismic profile.

The method used is direct, linearized, iterative inversion procedure. It returns lateral variations in crustal thickness, average crustal density and lithospheric thickness. The area of interest is subdivided into rectangular columns of constant size in the N–S (Y) direction and E–W (X). In depth (*Z*), each column is subdivided into four layers: sea water (if present, with known thickness, i.e. bathymetry, and a density of *1030 kg/m^3*), crust, lithospheric mantle and asthenosphere. The programme calculates topography in one dimension. Local isostasy is assumed as a function of thickness and average density of the

lithosphere (eq. (1) and eq. (2)) along vertical columns of the model using the linear density–temperature relationship of eq. (17) (Turcotte and Schubert, 1982).

In terms of densities, the crust is treated as a single layer. There is no difference between sediments, upper and lower crust. In order to limit the effect of this disadvantage, the programme allows modelling vertical density gradients in two ways: One option is to fix the density at the Moho and the inversion algorithm returns density variations at the surface, which results in variable vertical density gradients. The second option is to fix the density contrast between surface and Moho, then the algorithm returns the average crustal density. In the present case, we fixed the density at the base of the crust at *3000 kg/m³* and inverted for surface density. In the mantle, density varies linearly with increasing temperature (eq. (17)).

Mantle temperature is estimated in a 1D approach to make the inversion procedure less time consuming. Geotherms are calculated using fixed temperatures at the surface and at the LAB (usually *10°C* and *1300°C*, respectively). Continental crust is automatically subdivided into two layers of equal thicknesses (corresponding to upper and lower crust) with different, user-defined thermal conductivity and heat production. The reason for this is to obtain more realistic thermal models. Oceanic crust is assumed automatically if bathymetry is deeper than a user–defined value (typically *2000 m*). Its properties correspond to those of the lower continental crust. In this way, we assume that density varies linearly with depth in the crustal and lithospheric mantle blocks. Analytical formulas can be used to calculate the gravity and geoid effects for such rectangular blocks. The gravity effect is calculated based on Gallardo–Delgado *et al.* (2003) formula and the geoid effect is calculated based on Fullea *et al.* (2009) formula.

The data were extracted from worldwide data sets in geographical coordinates and transformed onto a Cartesian coordinate grid with $N_{xd}*N_{yd}$ grid points. All data sets have to be defined on the same grid which is should be denser than the grid of material blocks in order to stabilize the inversion procedure. From these grids, data are stored as a vector with $3*N_d$ points, being $N_d = N_{xd}*N_{yd}$ the number of interpolated points in each one of the three data sets. The data vector has then the following form:

$$\boldsymbol{d}^T = \left[d_1, ..., d_{Nd}, d_{Nd+1}, ..., d_{2Nd}, d_{2Nd+1}, ..., d_{3Nd} \right] = \left[t_1, ..., t_{Nd}, \Delta g_1, ..., \Delta g_{Nd}, \Delta H_1, ..., \Delta H_{Nd} \right],$$

eq. (18)

Where dT is the transposed data vector, t for topography, Δg (free air) gravity anomaly and ΔH geoid anomaly.

We have also $N_b = N_{xb} * N_{yb}$ blocks for the crust and the same amount for the lithospheric mantle. Therefore a number of $N_p = 3 * N_b$ parameters has to be inverted. The parameters are also stored in a common vector having the following form:

$$\boldsymbol{p}^T = \left[p_1, ..., p_{Nb}, p_{Nb+1}, ..., p_{2Nb}, p_{2Nb+1}, ..., p_{3Nb} \right] = \left[\rho_1, ..., \rho_{Nb}, z_{c1}, ..., z_{cb}, z_{m1}, ..., z_{mp} \right], \text{ eq. (19)}$$

There are 3 parameters per column of blocks: thickness (z_c) and average density (ρ) of the crust and thickness of the lithospheric mantle (z_m). Density and thickness of the water layer are known, density of the asthenosphere is taken as constant (ρ_a) and its base is defined at a constant, arbitrary depth below the expected deepest point of the lithosphere (e.g. at a depth of *300 km*) and density of the lithospheric mantle is calculated temperature dependent using eq. (17).

There are two difficulties when potential field and topography data are inverted:

1) different uncertainties for different data sets.

2) the ill–posedness of the problem due to non–uniqueness, i.e. the impossibility to find a solution to the mathematical problem.

The first problem is solved by defining a vector of data uncertainties σ_d, which has the same length as the vector $\boldsymbol{d}$. The quality of data adjustment can then be defined in the least squares sense as the weighted norm of the differences between synthetic data $f(p)$ calculated with the parameter set $\boldsymbol{p}$ and the measured data $\boldsymbol{d}$. If these differences are defined as the following vector:

$$\varepsilon_{di} = \frac{d_i - f_i(\boldsymbol{p})}{\sigma_{di}}, \qquad\qquad\qquad \text{eq. (20)}$$

the norm is defined as

$$E_d = \boldsymbol{\varepsilon}_d^T . \boldsymbol{\varepsilon}_d = \left(\boldsymbol{d} - \boldsymbol{f}(\boldsymbol{p}) \right)^T . \boldsymbol{C}_d^{-1} . \left(\boldsymbol{d} - \boldsymbol{f}(\boldsymbol{p}) \right), \qquad\qquad \text{eq. (21)}$$

C_d is the covariance matrix of the data taken here as a diagonal matrix having the variances σ_{di}^2 on the diagonal.

The second problem (ill-posedness) is overcome by regularization. The regularization makes the inverted matrix non-singular. This gives a mathematically unique

solution, although the geological non–uniqueness is not resolved. In this case a Bayesian approach was used. For this regularization, a vector σ_p is defined having the same length as $\boldsymbol{p}$ and containing the variability of each parameter with respect to an initially defined value (the inversion process is iterative). If $\boldsymbol{p_0}$ is the initial parameter set, a second norm is defined as follows:

$$\boldsymbol{\varepsilon}_{pi} = \frac{p_i - p_{0i}}{\sigma_{pi}}, \qquad\qquad \text{eq. (22)}$$

Also here, it is important to normalize the differences of the parameters to avoid others to dominate this expression (densities typically vary by tens of kg/m^3, Moho thickness by thousands of meters and LAB depths by tens of thousands of meters). The normalization is done by dividing the differences within each parameter set by their specific σ_p. The σ values can be interpreted as a measure of the permitted variability of every parameter type. The second important use of these normalization factors is the possibility to use them as a definition of *a priori* information. If at some locations *a priori* data are known, such as Moho depth from seismic studies or near–surface densities from borehole measurements, in that case these values can be used to construct the initial model and constrain the solution at the particular locations. The corresponding σ_{pi} is then set to the uncertainty of the measured value of the specific parameter at the specific block. This value should then be smaller than the overall σ_p for the corresponding parameter type and constrain the variability of the single parameter during the inversion process. Based on these considerations, the second norm is defined as:

$$E_p = \boldsymbol{\varepsilon}_p^T . \boldsymbol{\varepsilon}_p = \left(\boldsymbol{p} - \boldsymbol{p}_0 \right)^T . \boldsymbol{C}_p^{-1} . \left(\boldsymbol{p} - \boldsymbol{p}_0 \right), \qquad\qquad \text{eq. (23)}$$

Sometimes, it is necessary to stabilize inversion to have a more or less smooth model reducing its "roughness". Although roughness can be minimized in different ways, in this case, we used the first derivative in X and Y direction for each parameter set as a definition of roughness that has to be minimized:

$$\boldsymbol{\varepsilon}_s = \sum_{i=1}^{3Nb} \left[\sum_j \left(\frac{p_i - p_j}{\sigma_{pi}} \right)^2 \right], \qquad\qquad \text{eq. (24)}$$

where j describes all blocks in the immediate neighbourhood of block i *(j>i)*. Also in this case, differences have to be normalized for the different parameter types. For this

normalization the same values of σ_{pi} as in eq. (22) are used without eventual modifications due to *a priori* information. This sum may be expressed in matrix form:

$$E_S = \boldsymbol{p}^T . \boldsymbol{C}_S . \boldsymbol{p} \, , \qquad\qquad\qquad\qquad\qquad \text{eq. (25)}$$

The matrix $\boldsymbol{C}_S$ has on its diagonal the number of direct neighbours of each block in all directions (a value of 2 for the corner blocks, 3 for the blocks along the edges and 4 for all other blocks of the model) divided by σ_{pi}^2. Off–diagonal, the positions j of row i corresponding to the blocks touching block i have a value of $-\sigma_{pi}^{-2}$.

During the inversion process, a cost function has to be minimized defined as:

$$\boldsymbol{C} = E_d + \lambda E_p + \mu E_S \, , \qquad\qquad\qquad\qquad \text{eq. (26)}$$

where the factor λ controls the overall importance of parameter variability *(E_p)* with respect to data adjustment *(E_d)* whereas μ is a factor controlling the importance of smoothing which can be different for each parameter set. If λ and μ are small, data adjustment controls the inversion process, therefore parameters may change more freely. This may introduce instability if the initial parameter set is too far–off from the optimum set. On the other hand, if λ is large, the parameters are forced to stay near their initial values at the expense of a good data fit. If μ is large, a very smooth model is obtained. In the algorithm, $\boldsymbol{p}_0$ is updated in every iteration step using the steepest descent method with the values obtained from the last iteration. In this way, the parameters are not necessarily forced to stay near the initial (*a priori* unknown) values. The exception is the case when the parameters are marked as known through a small variability. Moreover, the use of λE_p implicitly introduces damping in the inversion.

The user can chose the values of λ and μ by his own will, and is quite difficult to give optimal values. In theory, they should be as small as possible so that the inversion remains stable without excessive smoothing. A good way how to find out acceptable parameters is running the inversion with different values or reducing the values between subsequent iterations. On the other hand, if the variability of the model parameters is correctly chosen, λ and μ may be close to unity. The inversion process is iterative because the equations that should be solved are non–linear.

Minimizing eq. (26) is then achieved by calculating the following matrix equation (Menke, 1984):

$$p^{k+1} = \left(A^T * C_d^{-1} * A + \lambda * C_p^{-1} + \mu C_S \right)^{-1} * A^T * C_d^{-1} * \left(d - f\left(p^k \right) \right) + p^k , \qquad \text{eq. (27)}$$

where A is the Frechet matrix of size *($3N_d$ x N_p)* that contains on its position *(i,j)* the influence of parameter *j* on the value of data point *i*, calculated as a linearized partial derivative of data point *i* with respect to parameter *j*:

$$A_{i,j} = \frac{\partial d_i}{\partial p_j} , \qquad \text{eq. (28)}$$

These derivatives are linear for density and calculated as the effect of body j at point i divided by the actual density of the body. On the contrary the effects are strongly non–linear for the depths of the prisms. They are calculated by varying the base of each prism by a predefined value and calculating the difference of the effects on each data point. The procedure does not increase the calculation time with respect to calculation of the analytic linearized derivatives, however, it turned out to be more stable. The reason is that the slope is averaged over a certain distance (typically *1 km* for Moho depth, *10 km* for LAB depth) and the temperature effect, which is difficult to integrate into the linearized partial derivatives, is automatically taken into account. The distance over which averaging is done has little influence on the results as long as it is not too small to stay stable (>1 km for LAB depth) and not too large to become meaningless (*<20 km*). Using LAB variations *10* times larger than Moho depth variations gives generally similar effects for both, as well for gravity as for geoid effects. In order to normalize the values of matrix A and to stabilize its inversion, the derivatives for Moho depth are calculated on the base of *100 m*

$$A_{i,j} = \frac{\partial d_i}{\partial \left(\dfrac{z_{MOHO,j}}{100} \right)} , \qquad \text{eq. (29)}$$

and the derivatives for LAB depth on the base of *1000 m*

$$A_{i,j} = \frac{\partial d_i}{\partial \left(\dfrac{z_{LAB,j}}{1000} \right)} , \qquad \text{eq. (30)}$$

In this way, the variability for the model parameters σ_p should be in the order of unity and in order to obtain similar values on the diagonals of matrices C_p^{-1} and $A^T C_d^{-1} A$

The quality of the inversion result can be determined by using Bayesian inversion. There are two matrices that are used to work out such an analysis: the resolution matrix R

and the posterior covariance matrix E. In order to obtain the model parameters from the data, a system of linear equations has to be solved:

$$p^{k+1} - p^k = G\left(d - f\left(p^k\right)\right)$$
eq. (31)

where

$$G = \left(A^T C_d^{-1} A + \lambda C_p^{-1} + \mu C_S\right)^{-1}\left(A^T C_d^{-1}\right)$$
eq. (32)

The resolution matrix indicates how well every single parameter is resolved just by the existing data. It is calculated as (Menke, 1984)

$$R = GA$$
eq. (33)

If no regularization parameter or *a priori* information is used *(i.e. $\lambda=\gamma=0$), R* is the identity matrix. When the diagonal values become smaller than *1* and off–diagonal values appear, this can be interpreted as indication that only a combination of parameters can be effectively resolved from the data. The posterior parameter covariance matrix contains on its diagonal the variance of the parameters as a function of the data variance. It is calculated as (Menke, 1984)

$$E = G C_{post} G_T$$
eq. (34)

C_{post} is a squared matrix of size *$3 x N_d$*. It contains on its diagonal the *a posteriori* data variance, defined as the square of the difference between measured and calculated data *$(d_i - f_i(p))^2$*. The square root of the diagonal values of *E* is interpreted as propagated uncertainty of the data misfit onto the resulting parameters.

4.4   *LitMod3D–3D programme*

This paragraph is worked out based on the paper Fullea *et al.* (2009, 2010)

LitMod3D (*LIT*hospheric *MOD*elling in a *3D* geometry) was used in this work to create a 3D model although finally, not more than a thorough debugging of its Windows version was possible. This software has been developed by J. Fullea and J.C. Afonso to perform integrated geophysical–petrological modelling of the lithosphere. The main advantage is that it combines in a self–consistent manner concepts and data from thermodynamics, mineral physics, geochemistry, petrology, and solid–Earth geophysics.

LitMod3D is composed of two modules: A module of the forward calculation LITMOD3D_FOR and an interactive interface module LITMOD3D INTF that is used for visualization and modification of the input data. LITMOD3D_FOR calculates heat transfer, thermodynamic and rheological equations, gravitational potential and isostatic equations (local and regional isostasy) for any sublithospheric to lithospheric mantle. Outputs are temperature, surface heat flow, density, seismic velocity, geoid and gravity anomalies and topography. The program allows modelling to a depth of *410 km*, with different user–defined layers. These layers are characterized by their own thermophysical properties (e.g. density, thermal conductivity, volumetric heat production rate, etc.). (Fullea *et al.*, 2009).

The volumetric heat production rate is assumed to be constant for each element, which is mainly a function of lithology. The relative effect of temperature and pressure on the density of crustal bodies is considered by the coefficients of thermal expansion (*α*) and compressibility (*β*):

$$\rho(\mathrm{T},\mathrm{P},C) = \rho_0\left[1 - \left(T - T_0\right)\alpha_C + \left(P\beta_C\right)\right], \qquad\qquad \text{eq. (35)}$$

where *C* represents mineralogical composition, ρ_0 is reference density at the surface *(kg.m^{-3})*, *T* is temperature pressure of interest *(°C)*, T_0 is temperature at the surface *(°C)*, *P* is pressure *(Pa)*

Therefore, the density within the crustal bodies may change in both vertical and lateral direction according to the *T–P–C* field (Afonso *et al.*, 2008; Fullea *et al.* 2009).

4.4.1 Lithosphere

In absence of convection/advection, the 3D thermal steady–state thermal structure of the lithosphere is defined by the following vector equation:

$$\nabla\left(k\left(\vec{x}, T, P\right)\nabla\left(T\left(\vec{x}\right)\right)\right) = -H\left(\vec{x}\right),$$

eq. (36)

where T is temperature (°C), k is the thermal conductivity tensor ($W.m^{-1}K^{-1}$), H is the radiogenic heat production per unit volume ($W.m^{-3}$) and $\vec{x}$ is position in space.

The temperature and pressure dependence of k in the mantle is modelled as (Hofmeister, 1999).

$$k_{(T,P)} = k°\left(\frac{298}{T}\right)^a \exp\left[-\left(4\gamma + \frac{1}{3}\right)\int_{298}^{T}\alpha(T)dt\right] \times \left(1 + \frac{K_0'P}{K_T}\right) + k_{rad}(T),$$

eq. (37)

where $k°$ is the thermal conductivity at standard T–P conditions, a–fitting parameter, γ is the thermodynamic/thermal Grüneisen parameter, $\alpha(T)$ is the T–dependent coefficient of thermal expansion (in Kelvin), K_T is the isothermal bulk modulus, K'_0 its pressure derivative and k_{rad} is term describing the radiation contribution to k.

The parameter a for typical mantle phase has values in the range of *0.2* to *0.9*, while Grüneisen parameter γ varies between *1.0* and *1.45* (Hofmeister, 1999). The parameter k is also changing with the composition which is affected by changes in thermodynamic parameters, chemistry and relative proportions of the constitutive minerals.

Program LitMod3D solves eq. (36) with the finite differences technique. The boundary conditions are as follows:

(a) fixed surface temperature (T_s)

(b) fixed temperature at the lower limit of the lithosphere (T_a),

(c) no heat flow perpendicular to the vertical boundaries. These boundary conditions are widely used in thermal modelling. In general, the choice of the surface temperature T_s is simple, because usually the exact surface temperature does not have a significant impact on the resulting model. The third boundary condition is widespread and often used in thermal modelling (Fullea *et al.*, 2009).

4.4.2 Sublithospheric mantle and super-adiabatic buffer layer

The heat transfer in the sublithospheric mantle is typically dominated by convection (Schubert *et al.*, 2001) and therefore, the temperature distribution approximately follows the adiabatic temperature gradient. The lower limit of the model is always set to a depth of Z_{bot}=*400 km*, where the estimated average reference T_{bot} is *1793 K*. This estimation is based on experiments of high–pressure and high–temperature phase equilibrium in the system *(Mg, Fe)$_2$SiO$_4$* (e.g. Frost, 2003; Katsura *et al.*, 2004, Frost and Dolejš, 2007). This is also consistent with the estimates of (a) potential temperature at mid-ocean ridges *(MOR)* and (b) the global average depth discontinuity at *410 km* depth (Afonso *et al.*, 2008). The uncertainty associated with the reference temperature at the bottom boundary of the model should not be greater than ± *50 K* (Katsura *et al.*, 2004, Afonso *et al.*, 2008). However, the expected lateral changes in temperature at a depth of *400 km* could be easily larger than *100 K*. Between the lithosphere and the sublitospheric mantle is located an area with a continuous superadiabatic gradient where the heat transfer is controlled by conduction and convection. This area is modelled with a buffer layer, which is located immediately below the lithosphere. This layer causes a continuous variation of temperature between the two areas and mimics the thermal effect of rheologically active layer, which is located at the bottom of the upper thermal boundary layer in convecting mantle-like fluids (Solomatov and Moresi, 2000; Zaranek and Parmentier, 2004). The temperature in the buffer zone varies linearly from the value at the bottom of the lithosphere T_a = *1588 K* to the value T_{buffer} = *1673 K* at the bottom of this layer The thickness of the buffer layer varies automatically to maintain the heat balance (i.e. energy conservation) between the basal heat input (assumed constant), internal heat generation, and surface heat release in the system in order to be consistent with both the adiabatic temperature profile at the reference MOR column (Afonso *et al.*, 2008) and mantle convection models (Solomatov and Moresi, 2000; Zaranek and Parmentier, 2004; Afonso *et al.*, 2008).

A constant temperature at the bottom of the numerical T_{bot} domain can be defined by the user in LitMod3D or range of adiabatic sublitospheric gradients. Adiabatic temperature gradient in the sublitospheric domain is defined by:

$$\frac{dT}{dz}_{adiab} = \frac{T_{bot} - T_{buffer}}{z_{bot} - (z_L + z_{buffer})},$$
<div align="right">eq. (38)</div>

where z_L is depth to T_a (base of the lithosphere) and z_{buffer} is depth to T_{buffer}

If there is an assumption that T_{bot} is constant ($T_{bot} = 1793 K$), then the sublithospheric gradient is clearly defined and its lateral variation depends on the structure of the lithosphere. But on the other hand, if a range of possible values is defined for eq. (38), then T_{bot} will vary accordingly. The temperature gradient given by eq. (38) can vary only in the expected range of *0.35* to *0.6 K.km^{-1}*. This condition is usually reflected in a maximum lateral temperature change of *120 K*, which is in good agreement with the prediction from seismic observations of the *410 km* discontinuity (e.g. Afonso *et al.* 2008, Chambers *et al.* 2005).

4.4.3 Thermodynamic modelling and density calculation

Stable mineral assemblages in the mantle are calculated by Gibbs free energy minimization of the system *CaO–FeO–MgO–Al$_2$O$_3$–SiO$_2$ (CFMAS)* or *Na$_2$O–CaO–FeO–MgO–Al$_2$O$_3$–SiO$_2$ (NCFMAS)* (e.g. Connolly, 2005; Afonso *et al.*, 2008). Each mantle layer is thus characterized by a specific major–element composition (in *wt.%*), which translates into specific bulk properties

LitMod3D works with a thermodynamic formalism and associated databases used in free energy minimizing from Stixrude and Lithgow–Bertelloni (2005). Each mantle layer is characterized by an index number and has three associated files that contain the thermodynamic information. These files are then converted to the final format and the user can create those files for any necessary *CFMAS* or *NCFMAS* composition.

Equilibrium mineral assemblages at temperatures below *500°C* in LitMod3D is not yet included due to the absence of reliable quantitative information on the kinematic reaction and metastability at low temperatures. Thermophysical properties of the such low-temperature assemblages are therefore calculated on the basis of local temperature and pressure, but the modal proportions and phase compositions are assumed for mineral assemblages, which have a temperature of *500°C*. To calculate the bulk rock properties, this program uses the Voigt–Reuss–Hill averaging scheme. The minimization system has then the form:

$$G^T = \sum_{i=1}^{\Pi} n_i G^i ,$$

eq. (39)

where Π is the number of phases possible in the system, G^i is the Gibbs energy of a mole of the i–th phase, n^i the amount of the phase, which is subject to the physical constraint $n_i \geq 0$.

Mass balance requires:

$$n_j^t = \sum_{i=1}^{\Pi} n_i x_j^i ,$$
eq. (40)

where n_j^t is the amount of j–th component in the system, c is the number of independent components , x_j^i is the amount of the j–th component in the i–th phase.

4.4.4 Pressure

After calculating the temperature field, the pressure and density distribution in the model is solved. The density of the crustal layer is given by:

$$\rho(T,P) = \rho_0 - \rho_0 \alpha (T - T_0) + \rho_0 \beta (P - P_0) ,$$
eq. (41)

ρ_0 is reference density at T_0 and P_0, α is the coefficient of thermal expansion (K^{-1}), β is the compressibility (Pa^{-1}).

The mantle layer density is taken from the associated thermodynamic files. The density and pressure are related through a coefficient of compressibility and through the definition of lithostatic pressure $P(z)$

$$P(z) = \int_0^z \rho(z')g dz' ,$$
eq. (42)

where g is the gravitational acceleration ($mGal$). The effect of pressure in the crust is relatively small, therefore LitMod3D uses the explicit "one–iteration" formula:

$$P(z) = P(z - dz) + g dz \left\{ \rho(z - dz) \left[\left(1 + \frac{g \rho_0 \beta dz}{2} \right) - \rho_0 \alpha \left(\frac{T(z) - T(z - dz)}{2} \right) \right] \right\},$$
eq. (43)

This formula can be introduced into eq. (41) and the result is the density of the crust at any depth z provided that the pressure, density and temperature are known at the level of $(z–dz)$. However, when using this formula to calculate the density at greater depths, the accumulated error would become prohibitive. In this case, the density–pressure coupling is solved in a fully iterative scheme. Iterations will stop only when the pressure difference between two successive iterations is less than a predefined value (set by the user).

4.4.5 Elevation

The concept of local isostasy in an idealized model that assumes the Earth as an ideal flat area defined by rigid vertical columns, freely floating on a viscous fluid, so that the weight of the column acting per unit area is equal to the level of compensation (Watts *et al.*, 1993).

This is defined mathematically as follows:

$$\int_{LC} \Delta\rho(z)dz = 0 \, ,$$

eq. (44)

Δρ(z) is the density contrast between the density of a given column and a reference column, *LC* indicates integration from the compensation level to topography.

If dynamic sublitospheric load has little effect on isostatic equilibrium, then the level of compensation can be placed at any depth below the base of the deepest lithospheric column (Lachenbruch and Morgan, 1990). In LitMod3D this base is set to the depth of *400 km*. The reasons are:

a) it covers the entire depth of the potential thickness of the lithosphere

b) a unique global compensation level requires only one calibration constant (Afonso *et al.*, 2008):

$$E = L - \frac{P_{bot}}{g\rho_{bot}} - \Pi_0 \, , \, (\mathrm{E} > 0)$$

eq. (45)

$$E = \frac{P_{bot}}{\rho_{bot} - \rho_w}\left(L - \frac{P_{bot}}{g\rho_{bot}} - \Pi_0\right), \, (E < 0)$$

eq. (46)

ρ_{bot} is the average density at the bottom of the model ($z=z_{bot}$), P_{bot} is the pressure at the bottom of each column, ρ_w is the density of seawater (*1030 kg.m^{-3}*), L is the solid part of each column ($L = z_{bot} + E_{obs}$ *where* E_{obs} is the observed elevation), Π_0 is a calibration constant.

When the reference column is adopted, then a calibration parameter can be calculated. For its calculation a reference column can be used taken usually at the mid-ocean ridges (MOR). Using eq. (41) with the parameters of the reference column, the formula is as follows:

$$\Pi_0 = z_{bot} - \frac{\rho_{MOR}(z_{bot} - E_{ridge}) + \rho_w E_{ridge}}{\rho_{bot}} \, ,$$

eq. (47)

where ρ_{MOR} is the average density of the reference mid–ocean ridge column, E_{ridge} is the average bathymetry of the reference mid–ocean ridge column

If short wavelength density anomalies are present (usually *<200 km*, however it mainly depend on the effective elastic plate thickness), such as intrusion or crustal material underneath a tectonic plate, local isostasy cannot be used anymore to calculate the geometry of the topography from the lithospheric geometry (Watts *et al.*, 1993, Turcotte and Schubert, 2002). This is the reason why this program has incorporated an algorithm to calculate also regional isostasy. It uses the 2D thin elastic plate approach to calculate the vertical motions that are associated with short wavelength lithospheric loads.

Regional compensation reduces the effect of lithospheric loads, depending on the chosen values of the effective elastic thickness (*Te*). Small *Te* values filter only short wavelength effects and in the limit case *Te=0*, locally and regionally compensated elevations are identical (*100%* local compensation). On the other hand, large *Te* values filter short–wavelength and long–wavelength deformations as well. In the limit case when *Te* approaches infinity, the entire load is supported by the intrinsic rigidity of the lithosphere (*0%* local compensation).

4.4.6 Potential fields: Gravity and Geoid anomalies

Geoid and gravity anomalies are calculated in the spatial domain, which works with rectangular prisms with a flat top centred at each node of the FD (finite differences) grid. However, this approach is more complicated and time–consuming than for example. FFT (Fast Fourier Transformation), it is much more suitable to work with density gradients and discontinuities. To optimize the speed of calculation, the density of each prism is approximated by a linear function of depth. This simplification works only when the vertical change in density in any single prism is approximately linear. In the crust, the density can be constant, or may be a linear function of depth. In this case, this procedure will not introduce significant errors in the computed model of the gravity field, and therefore each top and bottom surface of each crustal layer is used to define the limits of vertical prisms. On the other hand, in the mantle, density may suddenly change even within a single layer (because of phase changes). LitMod3D in this case is able to perform three different operations:

1) one layer is defined for each mantle layer (the same as for the crust)

2) the program searches for possible phase transitions within each layer defines one prism for each stable field

3) another check is performed in order to confirm that the density at the middle of each prism is close enough to the average between the values for the upper and lower limits. If this condition is not reached, the prisms are subdivided until a satisfactory result will be reached for the third condition

Gravity anomalies and geoid surface in each point of the model are calculated by adding the effect of all individual prisms. The vertical gravitational acceleration produced by a rectangular prism whose density varies with the depth can be expressed analytically in Cartesian coordinate system (Fullea *et al.*, 2009). These equations are solved using the values of density that varies linearly with depth. However, only the relative gravity and geoid anomalies are important in this context, because the gravitational field of the reference model is subtracted from the total field. The free air anomaly is then entered directly by the reference model deducted from the gravitational acceleration effect. Bouger gravity anomaly is then obtained by correcting the free–air anomalies for gravitational attraction of topography assuming constant density reduction of *2670 kg/m^3* for the Earth's crust and *1030 kg/m^3* for water.

Columns placed at the edges of the model are extended by *10^6 km* to avoid border effects which are produced by the density contrast at the border of the model. The fit of the average calculated gravity anomalies and the observed gravity anomalies should be very similar. The geoid low–frequency (regional) components are usually present in the measured signal, which is caused by the slower decay (*1/r*) with increasing distance from the density anomaly. In addition, small deviations of the isostatic equilibrium, whether local or regional, on the model borders can produce longwave components in the calculated anomaly. These effects are removed by subtracting from the geoid a best–fit plane (least squares method) (Fullea *et al.*, 2009).

5 STUDY AREA AND DATABASES

Although there are three different geophysical modelling approaches carried out in this thesis, they differ only in the way of interpretation and the size of the grid or area they affect. Since all of them are working on similar principles, the same databases can be used for the extraction of the input data.

5.1   *1D area*

To get first ideas about the tectonics of the Carpathian–Pannonian Basin region, first of all we started our modelling process with a 1D approach. This gives us very first outlook on the studied region. The coordinates of the regions are (*17°/28°E – 43°/51°N*) so that the area includes the whole Carpathian–Pannonian Basin region including its surrounding tectonic units. In the N and E these are the North and the East European Platform, in the S the Moesian Platform and the Dinarides, and the Eastern Alps and the Bohemian Massif in the W.

5.2   *2D profiles*

The northern part of the Carpathian–Pannonian Basin region was previously investigated by the same method (Zeyen *et al.*, 2002; Dérerová *et al.*, 2006) as we recently carried out. Therefore we focused our interest on the rest of the Carpathian–Pannonian basin region and modelled four 2D integrated geophysical lithospherical models crossing the whole area and surrounding tectonic units, including for some of them parts of the existing profiles in order to integrate the new results with the older ones (Fig. 19).

Transect A (*24,5°E/47°N – 24,5°E/39,5N°*) is *830 km* long and has a N–S direction. It starts in the Transylvanian Basin, crosses the Southern Carpathians, the Moesian Platform, the Balkanides and the Rhodopes and finishes in the northern Aegean Sea.

Transect B (*18,5°E /51°N – 26,5°E /41,5°N*) is *1220 km* long and has a NW–SE direction. It starts on the North European Platform and crosses the Western Carpathians, the Pannonian Basin, the Apuseni Mountains, the Southern Carpathians, the Moesian Platform and the Balkanides.

Transect C (*14°E /43°N – 28°E /48°N*) is *1220 km* long and runs SW–NE. It starts in the Adriatic Sea and crosses the Dinarides, the Pannonian Basin, the Apuseni Mountains, the Transylvanian Basin and the Eastern Carpathians, finishing on the East European Platform.
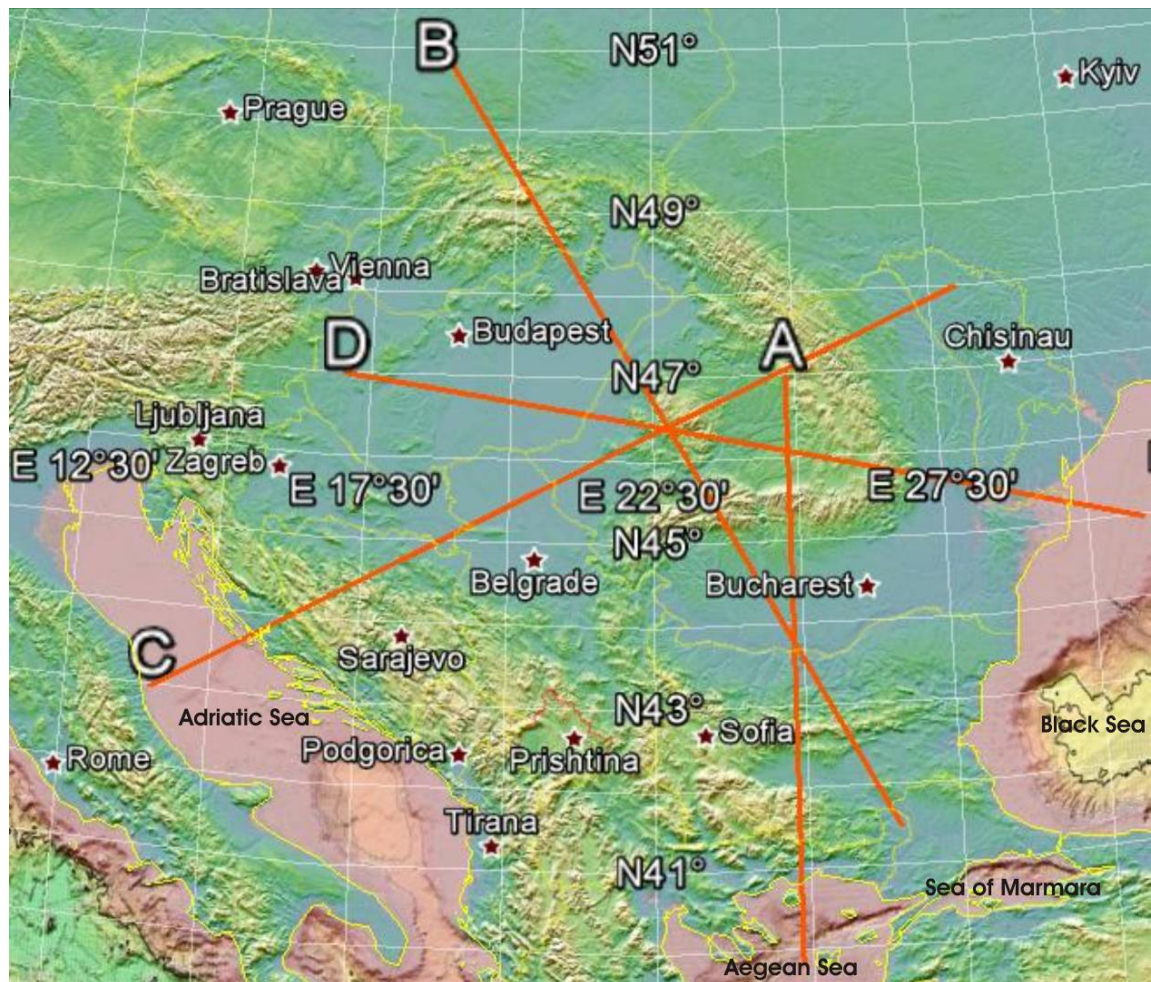
Fig. 19   Location of the presented transects A, B, C and D on Google Earth with overlain topography (SIO, NOAA, NGA, US Navy, GEBCO: SRTM30 PLUS V8.kmz).

Finally, Transect D (*17°E /47°N – 31°E /45°N*) is *1100km* long and has a WNW–ESE direction. Its starts in the western Pannonian Basin and crosses the Apuseni Mountains, the Vrancea zone and the East European Platform and finishes in the Black Sea

5.3   *3D inversion area*

The 2D modelling approach may be very easily applicable in research of structures perpendicular to the chosen transects. However, the Carpathian–Pannonian

Basin region has clear 3D structures; therefore a 3D modelling approach is necessary. Firstly, we used an inversion algorithm based on the joint interpretation of gravity, geoid and topography data (Motavalli-Anbaran *et al.*, 2012) to get an idea about studied region and its three dimensionality. This approach is able to give rapidly a simplified lithospheric model which can be subsequently used as starting model in LitMod3D.

The modelled area contains the same area as the 1D model (*17°E /43°N – 28°E /51°N*). We created three different models which differ from each other by the input *a priori* data applied to the calculation. We started the inversion process with a starting model (Fig. 25 and Fig. 27) resulting from the 1D inversion of geoid and topography data. The other two models are using *a priori* data coming from the seismic models of the Moho, however the 1D inversion was ran anyway. The first one is based on the interpretation of the Moho discontinuity from CELEBRATION 2000 (Janik *et al.*, 2011) and includes only the Western Carpathians and northern part of the Pannonian Basin. They present the results of modelling refracted and reflected waves employing 2D ray tracing for seven interlocking profiles. These profiles were jointly modelled and interpreted with the constraint that the models match at the crossing points of the profiles (Janik *et al.*, 2011). The second one is based on the integrated study of the whole area by Csicsay (2010). This study is basically a compile of the previous works and its own gravity and integrated modelling along some seismic profiles. His model is very well constrained by the recent seismic experiments such as CELEBRATION 2000 and Alp2002 on the other hand the quality of interpretation of the rest area is unknown.

5.4 *Input databases*

Topography has been taken from the GTOPO30 database (Gesch *et al.*, 1999). A map of the Carpathian–Pannonian Basin topography including the area of Southern and Eastern Europe is shown in Fig. 20. The highest topography on average of about *1800-2000 m* can be observed in the Southern Carpathians. The Western, the Eastern Carpathians and the Apuseni Mountains are characterised by an average topography of *1200 m*. In the Transylvanian basin topography is in average about *500 m*. Minimum elevations occur in the Pannonian Basin, the East European platform and the Moesian Platform (approximately *100 m*). We can observed also some negative values of the topography offshore in the Aegean, Adriatic and the Black sea, these data are taken from the ETOPO1 data set (ftp.//topex. ucsd.edu/pub).
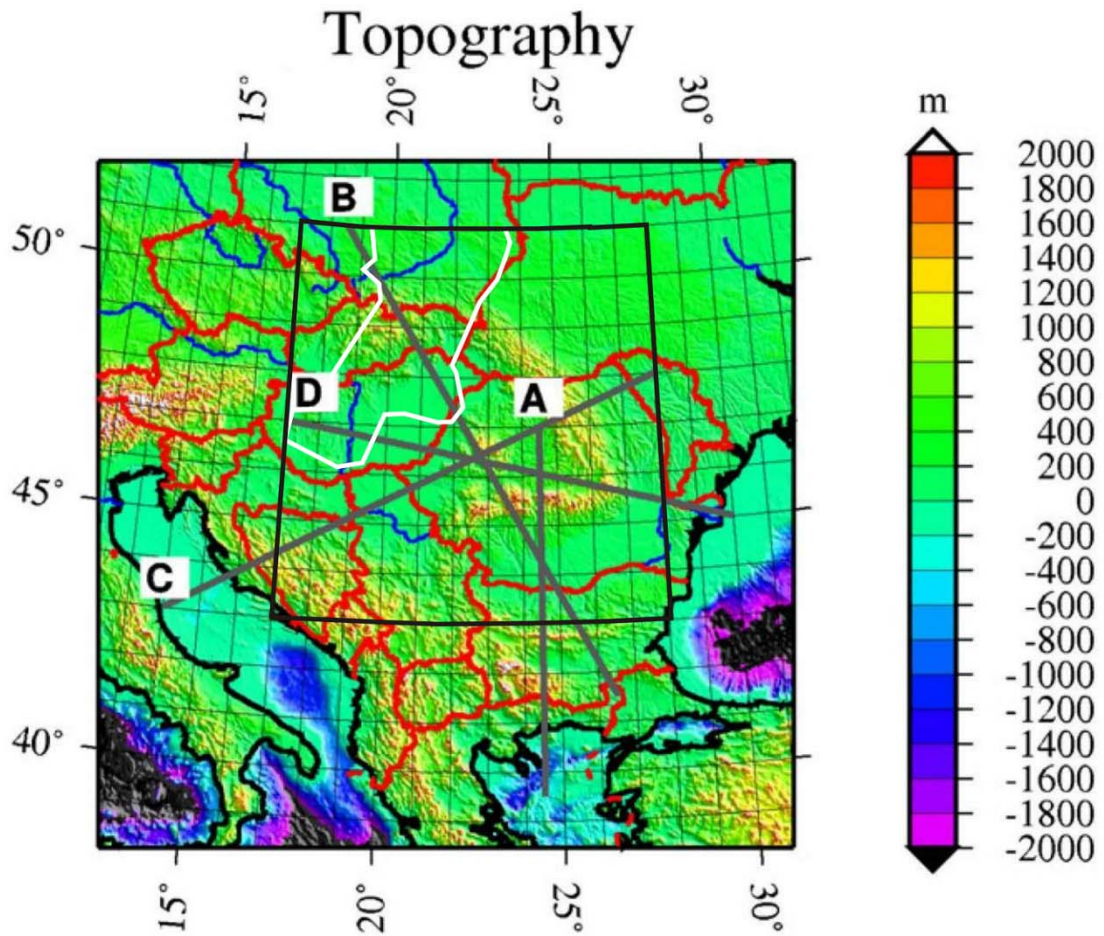
Fig. 20   Topography of the Central European region (from GTOPO30 data set, Gesch *et al.*, 1999). The gray lines show the position of the four interpreted 2D profiles, the black rectangle shows 1D, 3D interpreted area as well as input Moho based on Csicsay (2010) data. The white polygon shows the input Moho based on Janik *et al.* (2011) data.

Geoid data (Fig. 21) are taken from the EGM-2008 global model (Pavlis *et al.*, 2008). In order to avoid effects of sublithospheric density variations on the geoid, we have removed the geoid signature corresponding to the spherical harmonics developed until degree and order *10* (Bowin, 1991). In general the Carpathian−Pannonian region stands out as positive anomaly with maxima of near *14 m* in the Southern Carpathians and the Apuseni Mountains and in the average with values about *12 m*. The Eastern Carpathians have a positive signature too, whereas the northern part of the Western and Eastern Carpathian junction and the Transylvanian Basin as well as the North European Platform show intermediate values. Relative minima are located along the Carpathian foreland basin, the North European Platform and offshore.
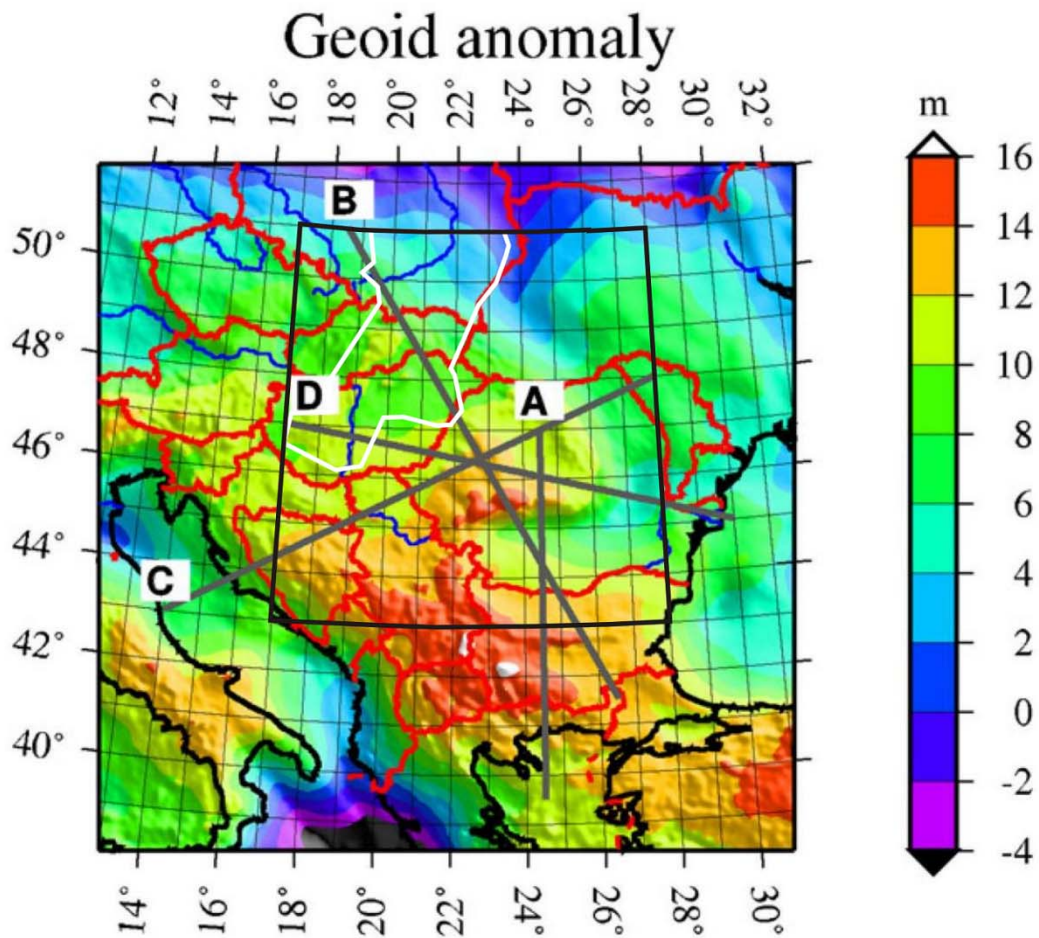
Fig. 21　Geoid anomaly map of the Central European region (from the EGM 2008 dataset (Pavlis *et al.*, 2008) after removing the spherical harmonics until degree and order 10). The gray lines show the position of the four interpreted 2D profiles, the black rectangle shows 1D, 3D interpreted area as well as input Moho based on Csicsay (2010) data. The white polygon shows the input Moho based on Janik *et al.* (2011) data.

The free air gravity anomalies (Fig. 22) were taken from the TOPEX 1−min gravity dataset (ftp.//topex. ucsd.edu/pub; Sandwell and Smith, 1997). Values between *−50* and *+150 mGal* are observed. A comparison between Fig. 20 and Fig. 22 shows that the free air anomalies reflect in general the topography variations. A series of maxima marks the Alps, the mountains of the Bohemian Massif and the higher regions of the Inner Western, the Eastern and the Southern Carpathians, the Balkanides, the Rhodopes. They are bordered by the minima of the foreland basins in Italy, Austria, Poland, Ukraine, Romania and Bulgaria as well as in the Pannonian Basin. However, a more detailed analysis shows that the anomalies in the Pannonian Basin are, in relation to the topographic elevation, less pronounced than those of the different foreland basins. In the Southern

Carpathians, to compare with the rest of the Carpathians, the higher values of the free air anomaly can be observed however the topography is very similar.
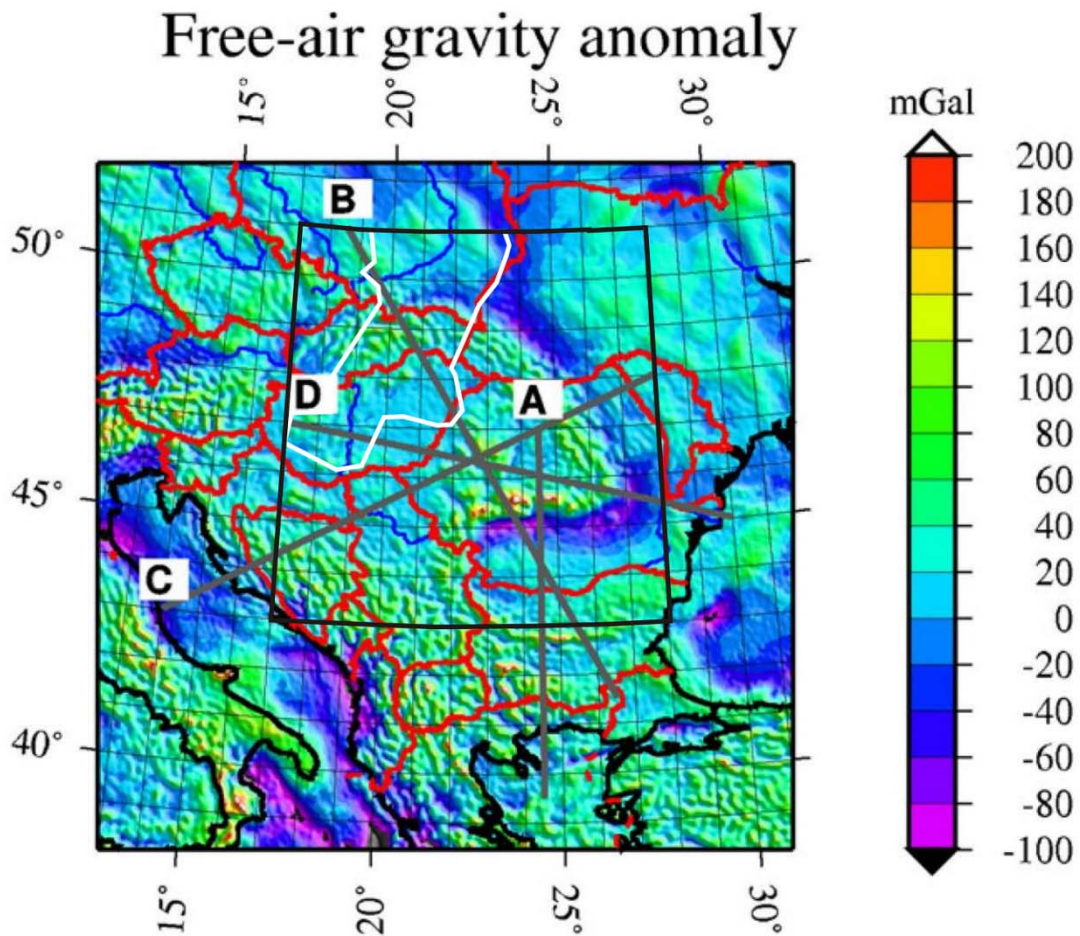
Fig. 22   Smoothed free-air gravity anomaly map of the Central European region (from TOPEX gravity data, 1 min grid, ftp.//topex.ucsd.edu/pub). The gray lines show the position of the four interpreted 2D profiles, the black rectangle shows 1D, 3D interpreted area as well as input Moho based on Csicsay (2010) data. The white polygon shows the input Moho based on Janik *et al.* (2011) data.

The heat flow density data (Fig. 23) were compiled from the worldwide dataset of Pollack *et al.* (1993). The dominant feature of the heat flow density map is a general increase from the Bohemian Massif and the Polish Platform via the Western Carpathians towards the Pannonian Basin. The heat flow in the Bohemian Massif and on the Polish Platform varies from *40* to *60 mWm^{-2}* with a minimum in the Moldanubicum (the core of the Bohemian Massif). In the Outer Western Carpathians, the average heat flow increases from *50* to *60 mWm^{-2}* in the SW to about *70 mWm^{-2}* in the NE (Čermák, 1994). Similar values are observed in the Central Western Carpathians, except of the Central Slovakia Volcanic Field with a local maximum of *100 mWm^{-2}*. The Pannonian Basin is characterised by the highest mean values of the heat flow density (*90 mWm^{-2}*), attaining

over *110 mWm^{-2}* in the East Slovakian Basin (Horváth *et al.*, 1989). Low values of the heat flow can be found in the Platform areas.
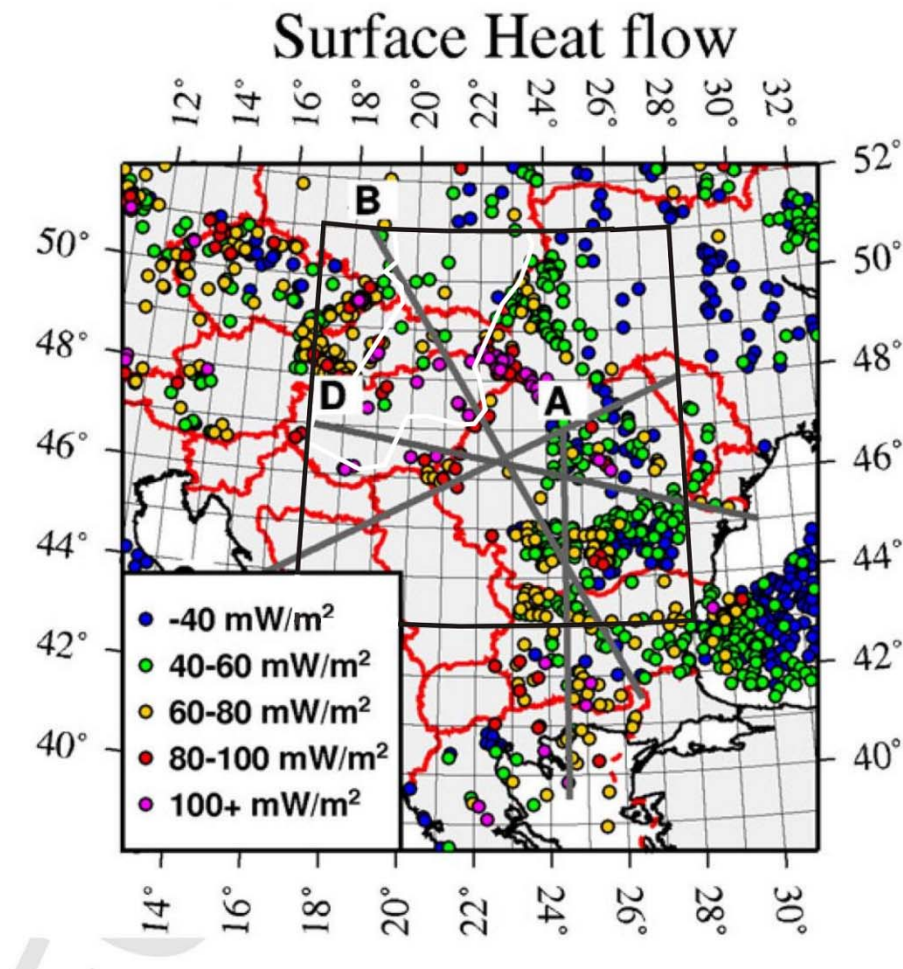
Fig. 23   Map of the surface heat flow density of the Central European region (from Pollack *et al.*, 1993). The gray lines show the position of the four interpreted 2D profiles, the black rectangle shows 1D, 3D interpreted area as well as input Moho based on Csicsay (2010) data. The white polygon shows the input Moho based on Janik *et al.* (2011) data.

The maps of the pre−Tertiary substratum relief published by Kilényi *et al.* (1989), and seismic data (Tomek *et al.*, 1989; Posgay *et al.*, 1990) provide a good knowledge about the Neogene sedimentary fill in the Pannonian Basin. The Neogene sediments are in average *2–3 km* thick, in some subbasins the thickness exceeds more than *5 km* (the East Slovakian Basin, the Békés Basin, the Makó Basin) and in the Danube Basin over *7 km* (Kilényi *et al.*, 1989). We have very good seismic data of the Transylvanian Basin, the Southern Carpathians and the Moesian platform (Mucuta *et al.*, 2006). Thickness of the Tertiary sediments in the Transylvanian Basin is about *2-3 km* and more than *9 km* on southern side of the Southern Carpathians at the contact with the Moesian Platform. Seismics shows only a relatively thin layer of Tertiary sediments on the Moesian Platform

(less than *1 km*). There are few data concerning the thickness of the Western Carpathian molasse foredeep and Flysch. Based on the results published by Tomek *et al.* (1987; 1989) and Tomek and Hall (1993), the thickness of the Molasse and the Flysch sediments seems to increase from *0* to *15 km* going from the frontal thrust towards the Klippen Belt.

For the input depth of the crust−mantle discontinuity (Moho) we used the data published by Mayerová *et al.* (1994), Šefara *et al.* (1996), Horváth (1993), Lenkey (1999), Guterch *et al.* (1986), Lazarescu *et al.* (1983), Boykova (1999), Mucuta *et al.* (2006) and Hauser *et al.* (2007). The newest maps of the Moho discontinuity were produced by Grad *et al.* (2009) and Csicsay (2010). The Carpathian Mountain belt is characterized by a thickened crust (*30-55 km*) in comparison with a thin crust (*25-30 km*) in the Pannonian Basin. The Moho depth increases to *45-50 km* underneath the Trans−European Suture Zone (e.g. CELEBRATION 2000 Working Group, 2000). The crustal thickness tends to increase from west to east along−strike of the Carpathian orogen. The Western Carpathians are characterized by crustal thicknesses of about *30-35 km*, the Eastern Carpathians by *32-42 km* and the seismogenic Vrancea zone by up to *45 km*. The Moho underneath the Southern Carpathians is at a depth of *42-50 km*. However, in general, the Carpathians are characterized by a rather thin crust and relatively low topography in comparison with other orogens, which might be a result of the "soft collision".

An initial model of the lithosphere thickness was defined from maps published by Babuška *et al.* (1988); Horváth (1993); Šefara *et al.* (1996); Mocanu and Radulescu (1994); Zeyen *et al.* (2002) and Dérerová (2006). As input data for the 3D inversion process, we projected the before−mentioned data sets as it is described in the chapter 4.3.

6 MODELLING RESULTS

6.1 *1D geophysical modelling*

The 1D modelling provides a very fast but preliminary view into the lithosphere structure. We used this method to get a first result of the Carpathian–Pannonian Basin lithosphere. We also used this 1D result as starting model in the 3D inversion. We obtained the best results (the tightest fit between observed and measured data) by using the input parameters shown in the Tab. 2. These settings also satisfy well our expectations about the Moho and the LAB in the region (Fig. 25 and Fig. 27). Since there is a problem to determine the reference geoid (N_0–see the methods chapter 4.1), we show different models with different reference geoids used (Tab. 1, Fig. 24 and Fig. 26). Depending on the value of N_0 used, the positions of maxima and minima are the same, but the absolute values change.

symbol	parameter	value A	value B	value C	value D
ρ_c	Average crustal density	2840 kg m^{-3}	2860 kg m^{-3}	2850 kg m^{-3}	2850 kg m^{-3}
z_c	Moho depth of the ref. column	28 km	28 km	27 km	29 km
ρ_a	density of the asthenosphere	3200 kg m^{-3}			
ρ_w	Density of Water	1030 kg m^{-3}			
z_{max}	The compensation level depth	300 km			

Tab. 1   Values used for the different reference geoid models (Fig. 24 and Fig. 26).

symbol	parameter	value
ρ_c	Reference average crustal density	2850 kg m^{-3}
z_c	Moho depth of the reference column	28 km
ρ_a	density of the asthenosphere	3200 kg m^{-3}
ρ_w	Density of sea water	1030 kg m^{-3}
z_{max}	The compensation level depth	300 km

Tab. 2   Parameter values that satisfy the best our expectations about the Moho and the LAB of the region (Fig. 25 and Fig. 27). Also the starting model for 3D inversion using these parameters achieve the best results.

Fig. 24   1D results for Moho depth in the Carpathian–Pannonian Basin region based on different reference geoids (see Tab. 1 for model parameters).

The Moho depth map shows significant crustal thickness variations (Fig. 25) within the studied area, what can be expected based on the many previous studies of the area (Zeyen *et al.*, 2002, Bielik *et al.*, 2004; Dérerová *et al.*, 2006; Csicsay, 2010; Janik *et al.*, 2011; Hauser *et al.*, 2001, 2007; Mocanu and Radulescu, 1994; Beránek and Zátopek, 1981; Guterch *et al.*, 1984, 1986; Čekunov *et al.*, 1988; Čekunov, 1993; Posgay *et al.*, 1995; Tomek *et al.*, 1987, 1989; Tomek and Hall, 1993; Horváth, 1993; and many others). It can be seen that the crustal thicknesses increase from the Pannonian Basin towards the E and NE but the thickness of the crust does not fit well with the previous works in some parts of the studied area. The misfit can be caused by the used local isostasy conception

and by the 1D approach. It is very likely that the whole region is still not fully compensated, some tectonic processes are still going on and therefore the local isostasy cannot fully explain the topography of the region. The thickest crust is found underneath the Carpathian arc or its immediate foredeep. Very high values are found in the Eastern Carpathians and Vrancea area (*40 km*). In defiance with the expectations, the thickest crust even in the small area is found in the Southern Carpathians (*42 km*). That area is shifted from the Vrancea zone (the zone with the thickest expected crust) towards the West. This implies that some additional research of the area might be needed to test this result. Also in the Dinarides, crust with thicknesses higher than *40 km* can be found and can reach in some parts more than *40 km*. The East European Platform is characterised by a crust with thickness about *34 km*. In the Apuseni Mountains, the depth of the Moho is about *36 km*. On the other hand, the Pannonian Basin and the Moesian Platform have thinner crust than the surrounding areas. Here we got crustal thicknesses of less than *30 km* in average. The thinnest crust can be found in the SE part of the Pannonian Basin near the contact with Southern Carpathians where it is only *26 km*. This result is surprising because the thinnest crust is expected in the central part of the Pannonian Basin (less than *25 km*) (Beránek and Zátopek, 1981; Guterch *et al.*, 1984; 1986; Čekunov *et al.*, 1988; Čekunov, 1993; Posgay *et al.*, 1995; Tomek *et al.*, 1987, 1989; Tomek and Hall, 1993; Horváth, 1993; Lenkey, 1999; Bielik *et al.*, 2004; Dérerová *et al.*, 2006; Csicsay, 2010), or even less (*22 km*) based on the interpretation of the CELEBRATION 2000 project (Janik *et al.*, 2011). This enigmatic result should be tested by one of the 2D lithospheric transects presented later.

Fig. 25   1D inversion result for Moho depth in the Carpathian–Pannonian Basin region. (see Tab. 2 for model parameters and further explanation).
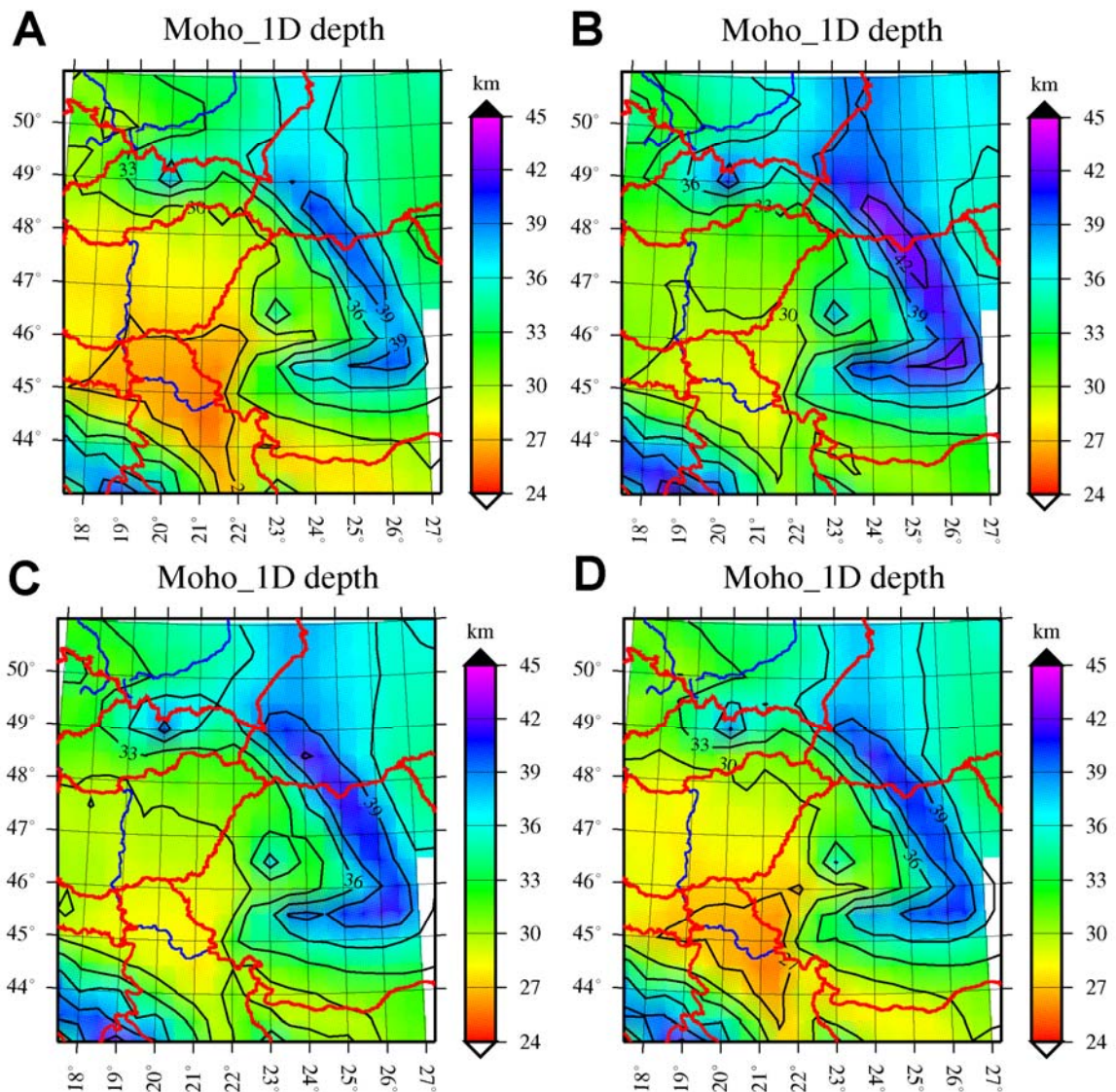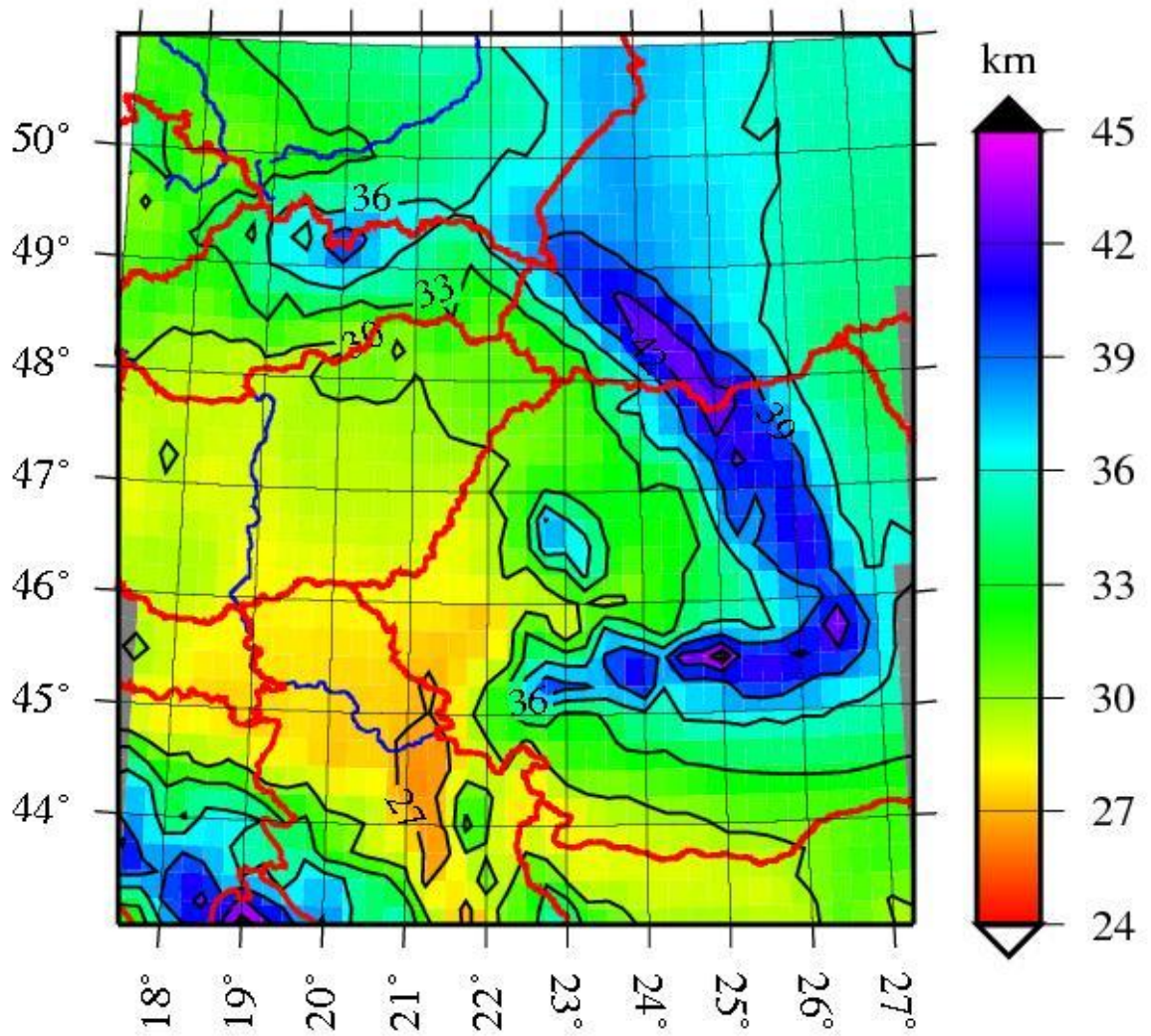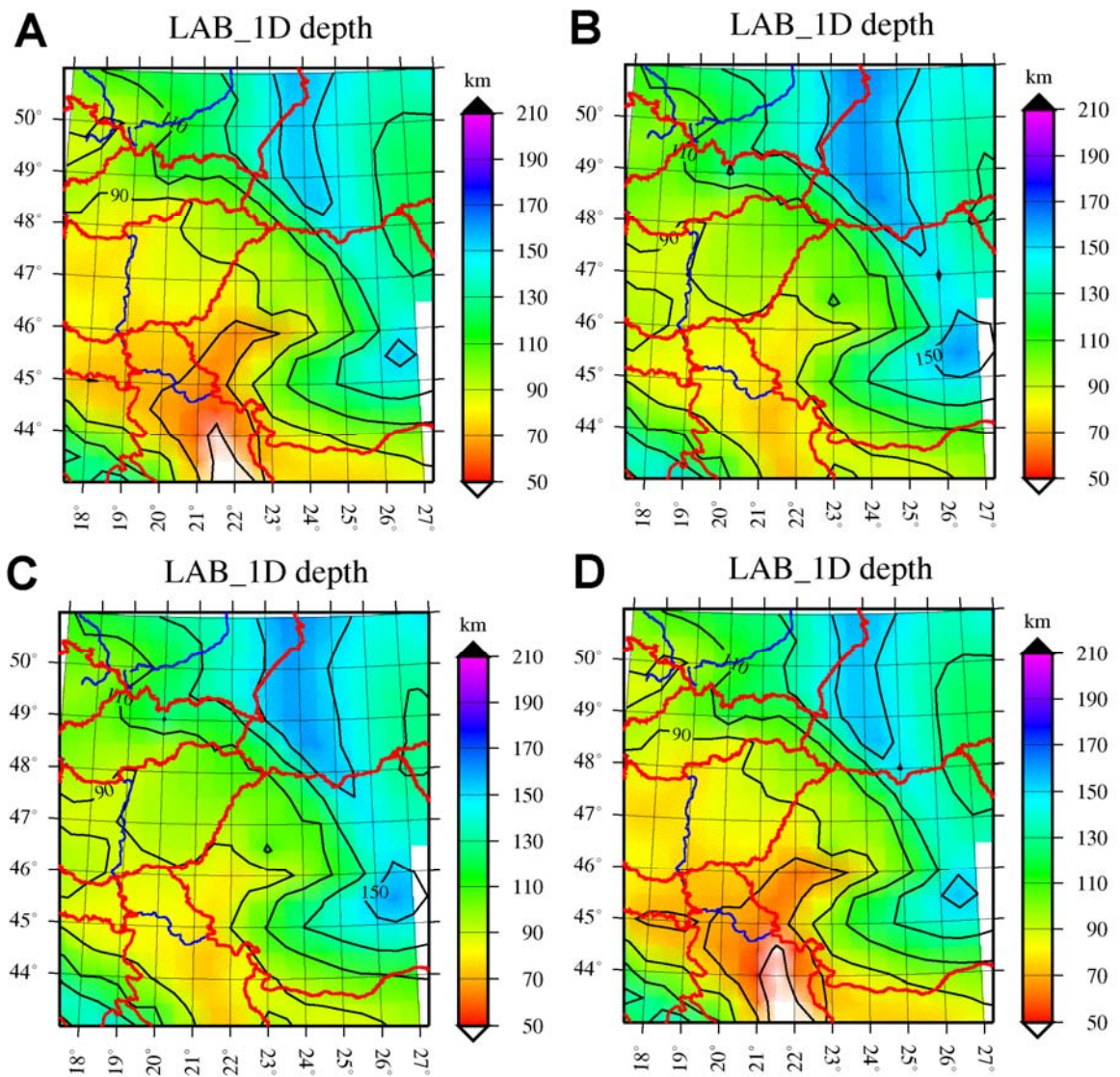
Fig. 26   1D results for the LAB in the Carpathian–Pannonian Basin region based on different reference geoids (see Tab. 1 for model parameters).

The lithospheric thickness map shows also significant variations (Fig. 27). Again here we did not reach any extreme values of thinning or on the contrary thickening of the lithosphere. The thickest lithosphere is placed in the NE part of the map where the East European Platform, Eastern Carpathians and Southern Carpathians are located. The thickness of the lithosphere of the East European Platform is on average more than *120 km* but in the northern part of this area some thicker places can be found. A strip of thicker lithosphere follows the Eastern Carpathians and its foredeep where the values reach in average *160 km*. This result is in contrast with the results obtained by Babuška *et al*., (1988); Horváth, (1993); Šefara *et al*., (1996); Lenkey, (1999); Dérerová *et al.* (2006) who published values between *160 km* and *240 km*. Especially in the Vrancea zone, a thicker lithosphere is expected. From here, the thickness of the lithosphere is decreasing towards

87

the West where the thickness is less than *110 km*. The decreasing trend continues from here also towards the South and reaches a minimum at the southern border of the Southern Carpathians and in the SE part of the Pannonian Basin. Here, it is only *60 km*. The extremely low values of lithospheric thickness in this area were not shown before. The Moesian Platform is characterised by an E-W trend of lithospheric thickness decrease. In the East, the thickness is about *110 km* and in the west it is only *80 km*. The Pannonian Basin lithospheric thickness ranges from *80* to *100 km* which is in accordance with Babuška *et al.* (1988), Horváth (1993), Šefara *et al.* (1996), Lenkey (1999), Zeyen *et al.* (2002) and Dérerová *et al.* (2006). The Dinarides in the SW part of the map show a maximum thickness of about *140 km*.

Fig. 27   1D inversion model of the lithospheric thickness in the Carpathian–Pannonian Basin region (see Tab. 2 for model parameters and further explanation).
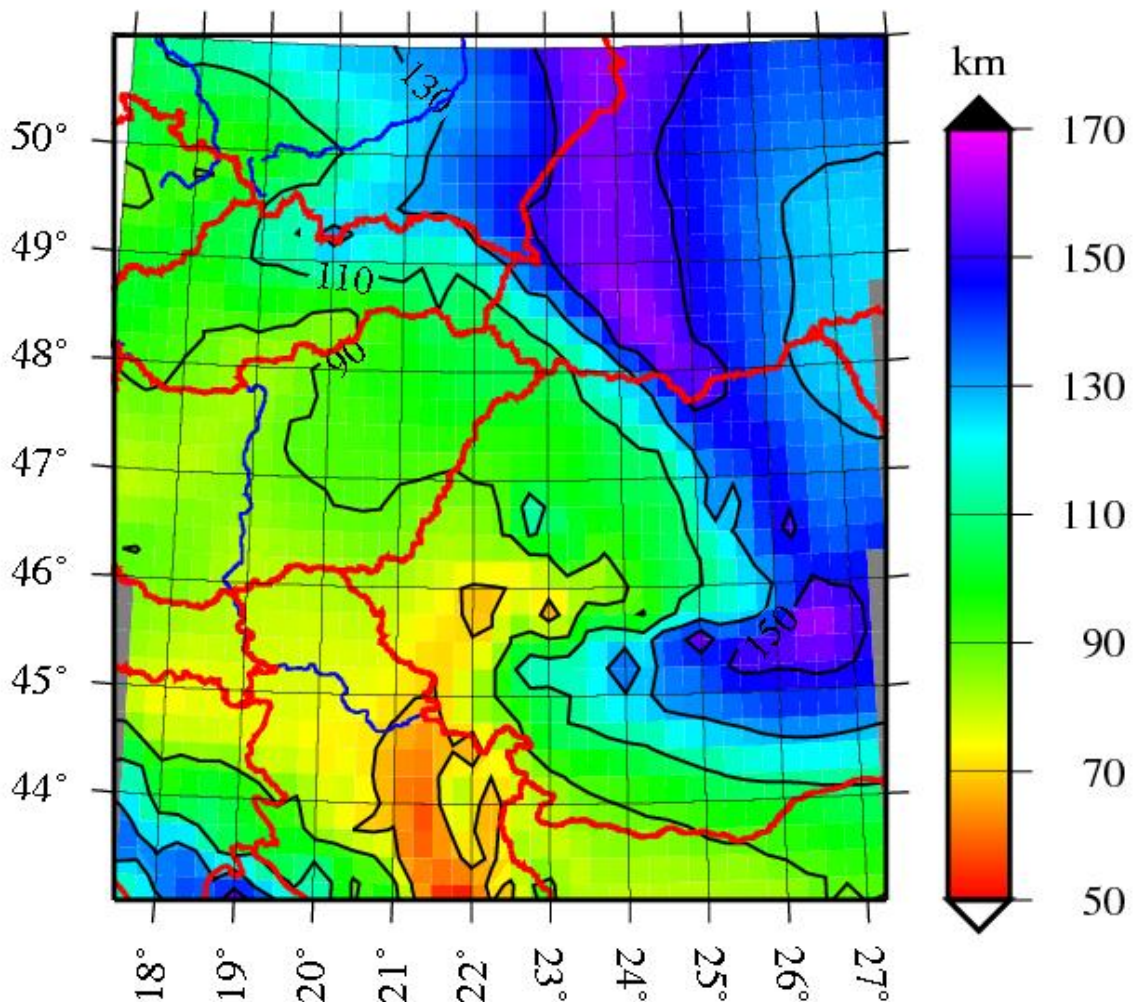
6.2   *2D integrated geophysical modelling*

This chapter is based on the paper Grinč *et al.* (2013)

Based on the before mentioned different crustal models that were constructed on the different geophysical data, we created for each transect an initial model. The density–related parameters were modified by trial and error until a reasonable fit was obtained between measured and calculated data (Fig. 28, Fig. 30, Fig. 31, Fig. 32). Densities and thermal parameters for the different bodies of the four transects are shown in Tab. 3. For densities, no pressure dependence was used, since at a given depth, density variations due to pressure variations are very small and the general density increase with depth would only alter absolute values of gravity, geoid and topography not the lateral variations. We took as reference density for the astenosphere the value of *3200 kg/m³* published by Lachenbruch and Morgan (1990). Also results based on gravity modelling in the Carpathian–Pannonian region confirm the same reference density value (Bielik *et al.*, 1990; Bucha and Blížkovský, 1994; Lillie and Bielik, 1992; Vyskočil *et al.*, 1992). The radioactive heat production for the mantle (*0.02 μW/m³*) is compatible with average estimations given by Mareschal *et al.* (2012). For the lower crustal heat production, we used average values from Rudnick and Fountain (1995) (Tab. 3). Both values have only very little influence on the results. Doubling them would change the surface heat flow by only *2–3 mW/m²* which is much less than the uncertainty estimated to be about *10 mW/m²*. The upper crust, however, has a strong influence on the resulting surface heat flow and in this layer, the concentration of radioactive elements (mainly U, Th and K) may be highly variable. Since hardly any data exist for the study area, we used a standard value for felsic upper crust of *2 μW/m³* (e.g. Vilà *et al.*, 2010). Also for the sediments, we used standard values (Vilà *et al.*, 2010). The transects are crossing each other at some places and in these crosspoints the parameters of layers are the same.

No.	Units	Density [kg/m³]	HP [μW/m³]	TC [W/m K]
1	Pannonian Basin sediments	2400	1	2
2	Western Carpathians	2670	1	2
3	Transylvanian Basin sediments	2400	1	2
4	Transylvanian Basin Mesozoic	2710	1	2
5	Apuseni Mts.	2670	1	2
6	Getic Depression sediments	2400	1	2
7	Moesian Platform Mesozoic	2700	1	2
9	Rhodopes	2650	1	2
10	Aegean sea	2400	1	2
11	Western Carpathian Flysch	2560	1	2
12	Adriatic sea	2400	1	2
13	Dinarides	2690	1	2
14	Eastern Carpathians	2690	1	2
15	Focsani Basin	2630	1	2
16a	Balkanides, Western Carpathian-Pannonian-Apuseni-Southern Carpathian, Transylvanian-Southern Carpathian, Dinaric-Pannonian-Apuseni-Transylvanian-Eastern Carpathian upper crust	2750	2	2,5
17	Moesian Platform upper crust	2770	2	2,5
18	Balkanidian-Rhodopian upper crust	2760	2	2,5
19	Aegean sea upper crust	2730	2	2,5
20	East European Platform upper crust	2770	2	2,5
21	Adriatic sea upper crust	2770	2	2,5
22	Focsani Basin-East European Platform upper crust	2790	2	2,5
23	Focsani Basin-East European Platform middle crust	2870	1	2,5
24	Focsani Basin-East European Platform lower crust	2970	0,2	2
25a	Western Carpathian-Pannonian-Apuseni-Southern Carpathian, Transylvanian-Southern Carpathian, Dinaric-Pannonian-Apuseni-Transylvanian-Eastern Carpathian lower crust	2950	0,2	2
26	Moesian Platform lower crust	2970	0,2	2
27	Balkanidian-Rhodopian lower crust	2960	0,2	2
28	Aegean sea lower crust	2930	0,2	2
29	East European Platform lower crust	2970	0,2	2
30	Adriatic sea lower crust	2970	0,2	2
31	Lower Lithosphere	3200	0,02	3,4

Tab. 3   Densities and thermal properties of the different bodies used in the models. "No" refers to body numbers in Fig. 28e, Fig. 29e, Fig. 30e, Fig. 31e and Fig. 32e.

The calculated values of gravity and geoid are generally between the maximum and minimum values of the uncertainty bars (Tab. 4). These uncertainties were calculated

for topography, geoid and gravity as the standard deviation of the data sets in a stripe of *50 km* to each side of the profiles and represent the variability of the data, and therefore implicitly of the models, in the direction perpendicular to the profiles. The short wavelengths of the discrepancies in the free air gravity are produced by shallow and small–scale crustal structures that could not be considered in these regional models. Misfits of short wavelength can be also found in the topography data where they are generally larger. They are most likely due to not locally compensated structures and cannot be reproduced by our model. These correspond to local features such as thrusting structures or underplating. The regional isostasy (elastic flexure) should be integrated in order to explain all the features. Part of the topography may be supported by elastic constraints if equivalent elastic plate thicknesses (EET) are too large. Therefore, if we could not find a model explaining all data sets together, we gave preference to a good fit of gravity and geoid data and left topography unadjusted. A few authors have analysed the effective elastic thicknesses of the different tectonic units of our region. Lankreijer *et al.* (1999) proposed very low values for the Polish platform (*5–17 km*) and the Pannonian Basin (*5–10 km*). For the wavelengths we are concerned with (*100–200 km*), the elastic effects should then be small (e.g. Turcotte and Schubert, 1982). However, locally the elastic support and deformation may be important. The strongest problems occur in the foreland basins at the contact between the Southern Carpathians and the Moesian Platform (Fig. 28 and Fig. 30) and between the Eastern Carpathians and the East European Platform (Fig. 32) where subduction–related plate bending may be the cause for a rather bad fit at wavelengths around *50 km* between modelled and measured data.

In every model, heat flow data show a large degree of scatter (Fig. 28a, Fig. 29a, Fig. 30a, Fig. 31a and Fig. 32a). In general, these variations are related to groundwater circulation or not totally corrected paleoclimatic effects (Kukkonen *et al.*, 1993; Stulc, 1998). These effects are not included in the used algorithm that is why our models result in a smooth variation with a minimum of *50 mW.m^{-2}* in the East European Platform and a maximum of more than *80 mW.m^{-2}* in the Pannonian Basin. Moreover, the heat flow data that we took into account were not well distributed and shows also a big range of different values on the short distances in the studied area. For our regional models, we interpret therefore only smooth variations and try to keep the average values with our calculated curve. The consequence for such interpretation is that the calculated field does not fit very

well with the values extracted from the map of the surface heat flow density (Pollack *et al.*, 1993).

Transect	Std.Dev.	Var.Reduction %
A		
Topography	271 m	71
Free_air	13,5 mGal	87
Geoid	0,28 m	96
B		
Topography	208 m	56
Free_air	12,3 mGal	81
Geoid	0,37 m	92
C		
Topography	181 m	80
Free_air	11,1 mGal	81
Geoid	0,21 m	99
D		
Topography	161 m	70
Free_air	9,3 mGal	84
Geoid	0,23 m	>99

Tab. 4   Misfit between observed and calculated data (topography, free air gravity anomaly and geoid) for transect A, B, C and D.

In general, the thickness of the lithosphere decreases from the older and colder Platforms to the younger and hotter Pannonian Basin with a maximum thickness under the Eastern and Southern Carpathians. The thickness of the Carpathian arc lithosphere varies between *150 km* in the N to about *300 km* in the Vrancea zone, in the Platform areas it is between *120* and *150 km* and in the Pannonian Basin, it is about *70 km*. This thickness is larger than published earlier (e.g. Horváth, 1993; Lenkey, 1999) but smaller than the results from Dérerová *et al.* (2006). Hence part of the surface heat flow may be explained as an increase in radioactive heat production in the Pannonian upper crust and sediments. Reducing the lithospheric thickness to values between *40* and *60 km* would uplift the modelled topography and make it incompatible with the observed one. The lithosphere thickness underneath the Apuseni Mountains reaches in the models a depth of about *120 km* and thickens strongly underneath the Transylvanian Basin reaching locally values of nearly *200 km*.

Our models discover some interesting features. They show that the Moesian Platform is overthrust from the North by the Southern Carpathians and from the South by

the Balkanides, which had been indicated already earlier based on geological studies (Bergerat *et al.*, 2010; Fügenschuh and Schmid, 2005; Iancu *et al.*, 2005; Rabăgia and Matenco, 1999) (Fig. 28 and Fig. 30). This overthrusting induces bending of the platform which gives a characteristic signature in the observables. To show its effect, we produced also a model with a flat Moesian Platform Moho and underthrusting of the Southern Carpathians and the Balkanides crust. This model explains also quite well geoid and free air data, but produces a topography that differs much more from observed data than our preferred model. Another result is strong lithospheric thickening underneath the Eastern Carpathians and their foreland that reaches values of more than *230 km*. For a good correlation between the observed and modelled topography and geoid anomalies this thickening is needed. The thickening can also be found in the Southern Carpathians but much smaller (about *180 km*) and underneath the Western Carpathians (about *150 km*).

Thickening of the lithosphere in the Western and the Eastern Carpathian foreland is also accompanied by crustal thickening except in Southern Carpathians. In all transects, the crustal thickening is shifted towards the areas of highest topography. The thickest crust outside the orogens is modelled under the Moesian Platform with thicknesses of about *45 km* in some parts. Models based on seismic data are contradictive in the Vrancea area. Mocanu and Radulescu (1994) indicate a crustal thickening to nearly *50 km*, whereas Hauser *et al.* (2001) and Landes *et al.* (2004) give a maximum thickness of *40–41 km*. For our interpretation, we used the model of Hauser *et al.* (2007) (maximum thickness of *47 km*) as reference, since it seems to be the best constrained. All models place the maximum thickness not underneath the highest topography but under the Focsani foreland basin. In our best fitting model we found the thinnest crust in the Pannonian Basin at about *26-27 km* which is similar to Posgay *et al.* (1995) but about *2 km* thicker than Janik *et al.* (2011).
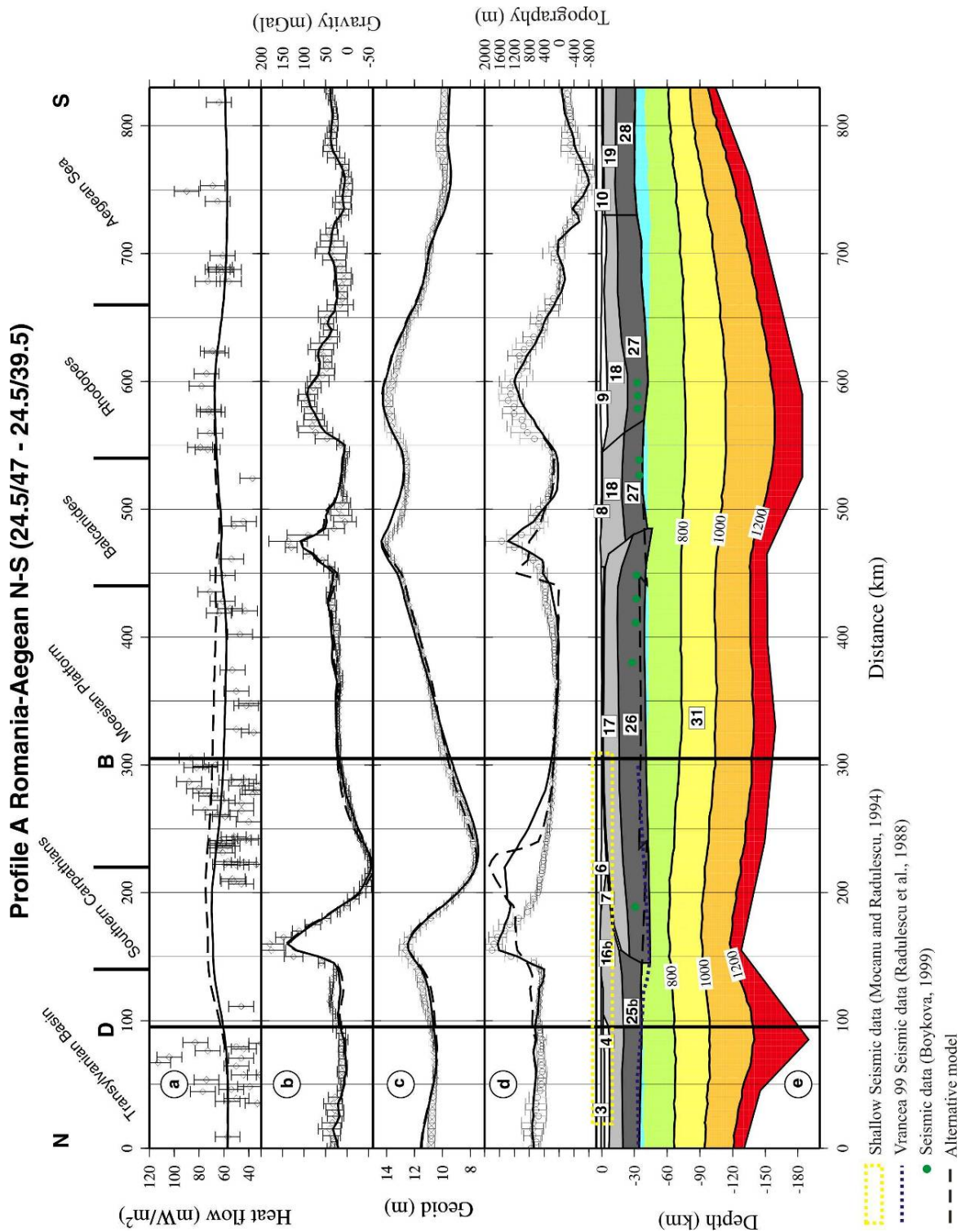
Fig. 28   Lithospheric model for transect A. (a) Surface heat flow density, (b) free-air gravity anomaly, (c) geoid, (d) topography with dots corresponding to measured data with uncertainty bars and solid lines to calculated values; (e) lithospheric structure; numbers in (e) correspond to material number in Tab. 3. In the lithospheric mantle, isotherms are drawn every 200°C. Numbers in the figure title indicate the starting and endpoint coordinates of the transects. The black dashed lines correspond to the results of a model with flat lower-upper-crustal limit and Moho underneath the Moesian Platform. Dotted lines and dots show positions of interfaces obtained from different seismic experiments. Black fat capital letters denote crossing points with the other interpreted transects.

94

Fig. 29 Alternative results (for transect A) of a model with flat lower-upper-crustal limit and Moho underneath the Moesian Platform. For further explanations, see Fig. 28.
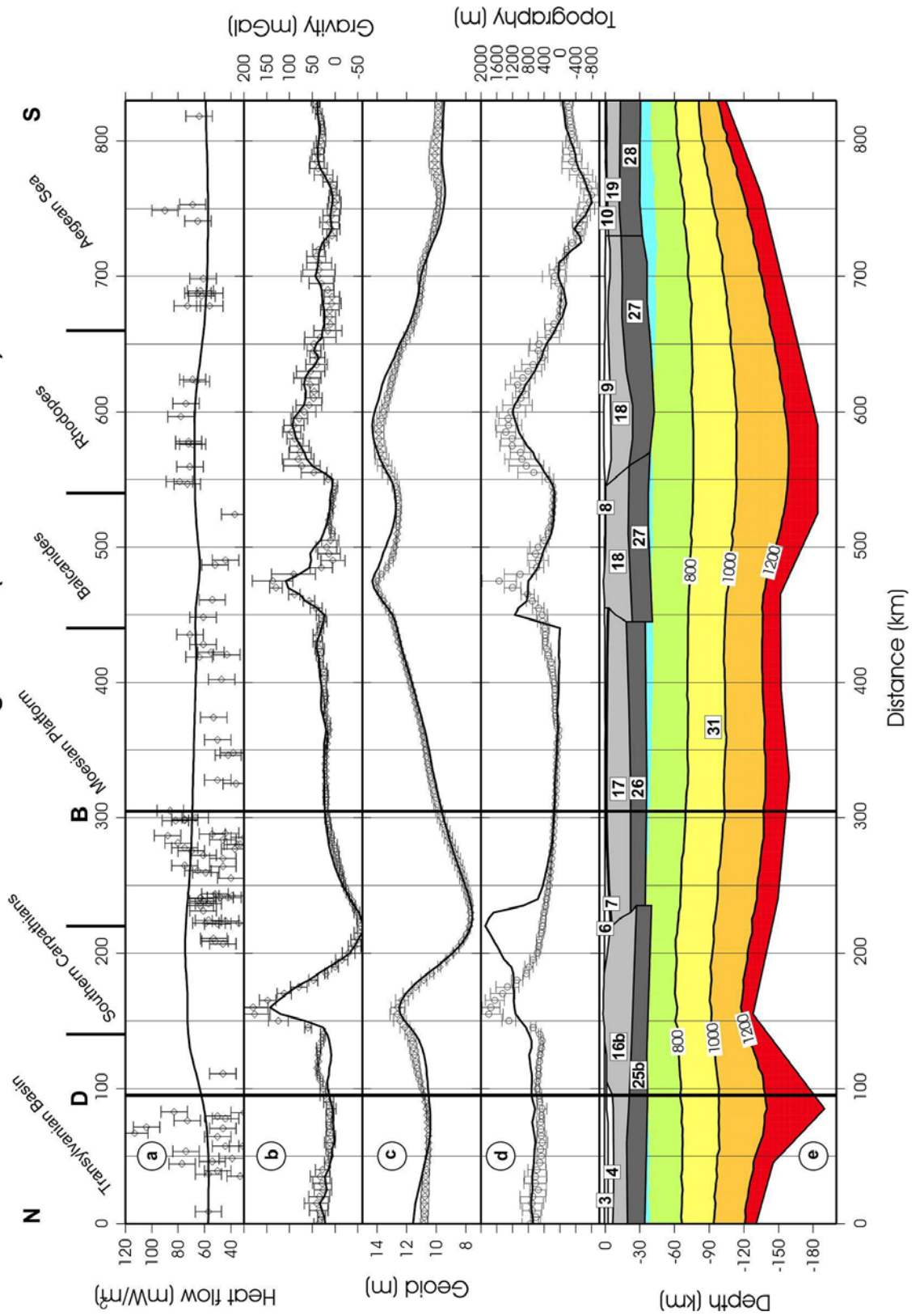
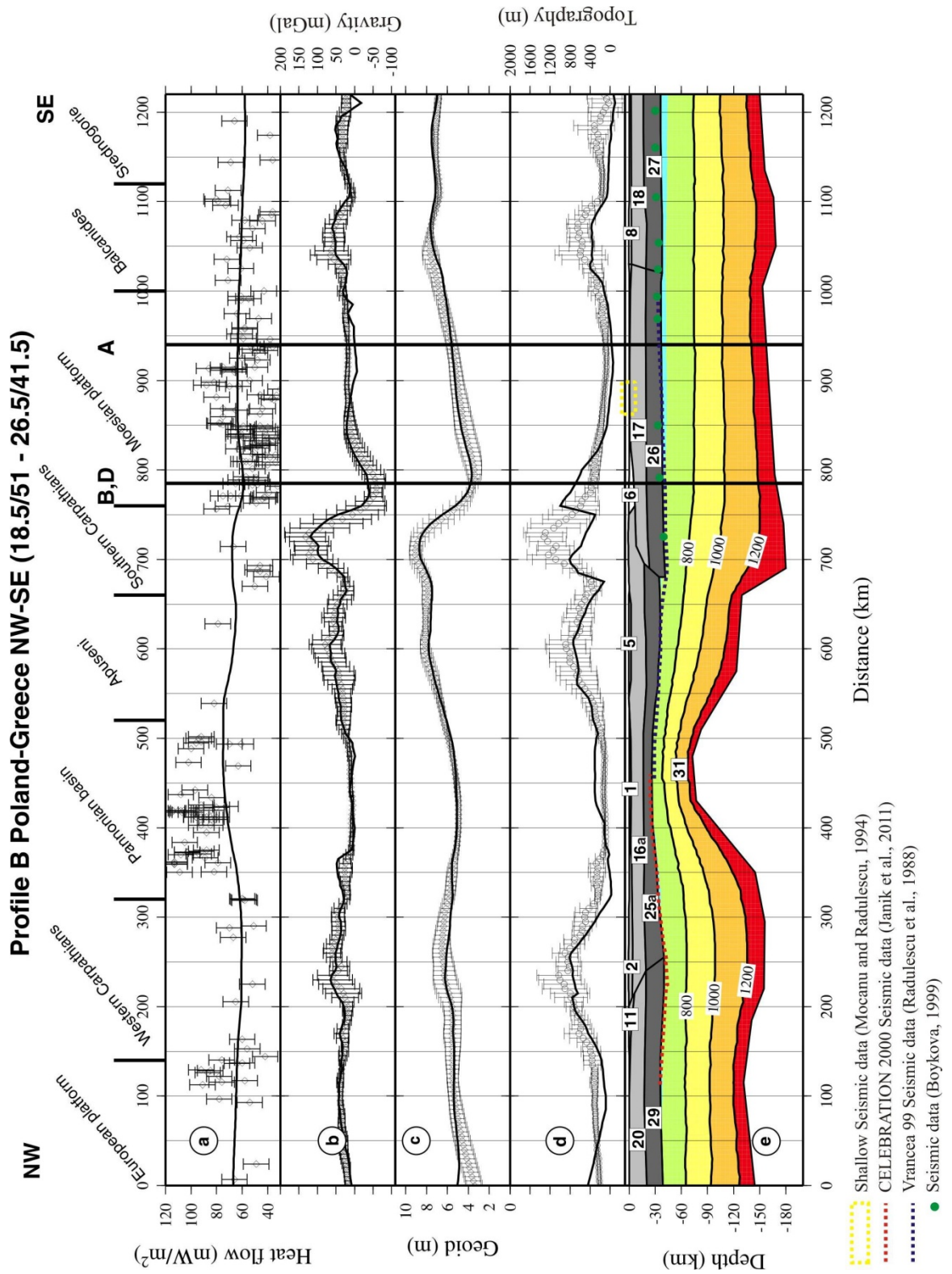Fig. 30   Lithospheric model for transect B. For further explanations, see Fig. 28.
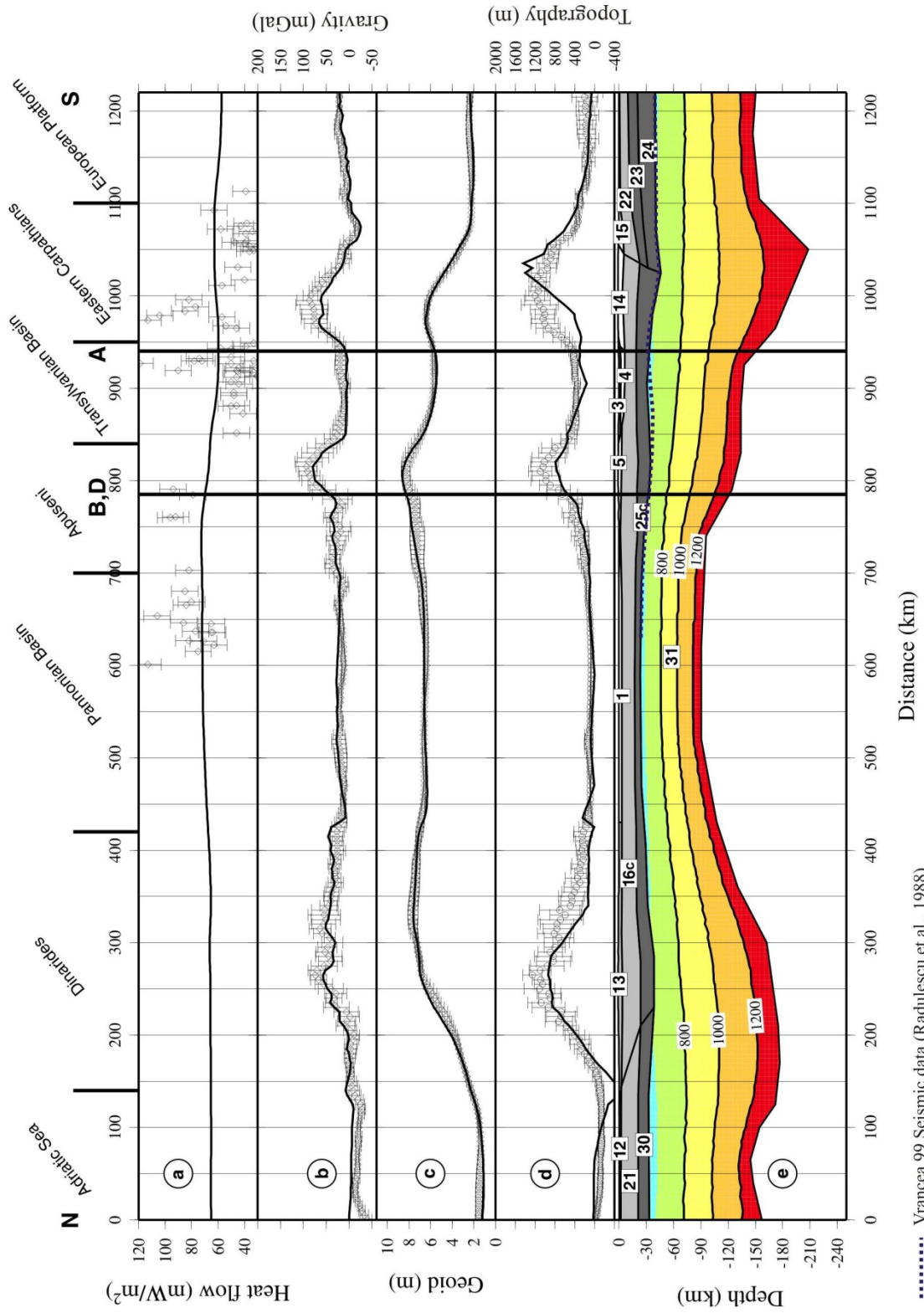
96

Fig. 31   Lithospheric model for transect C. For further explanations, see Fig. 28.
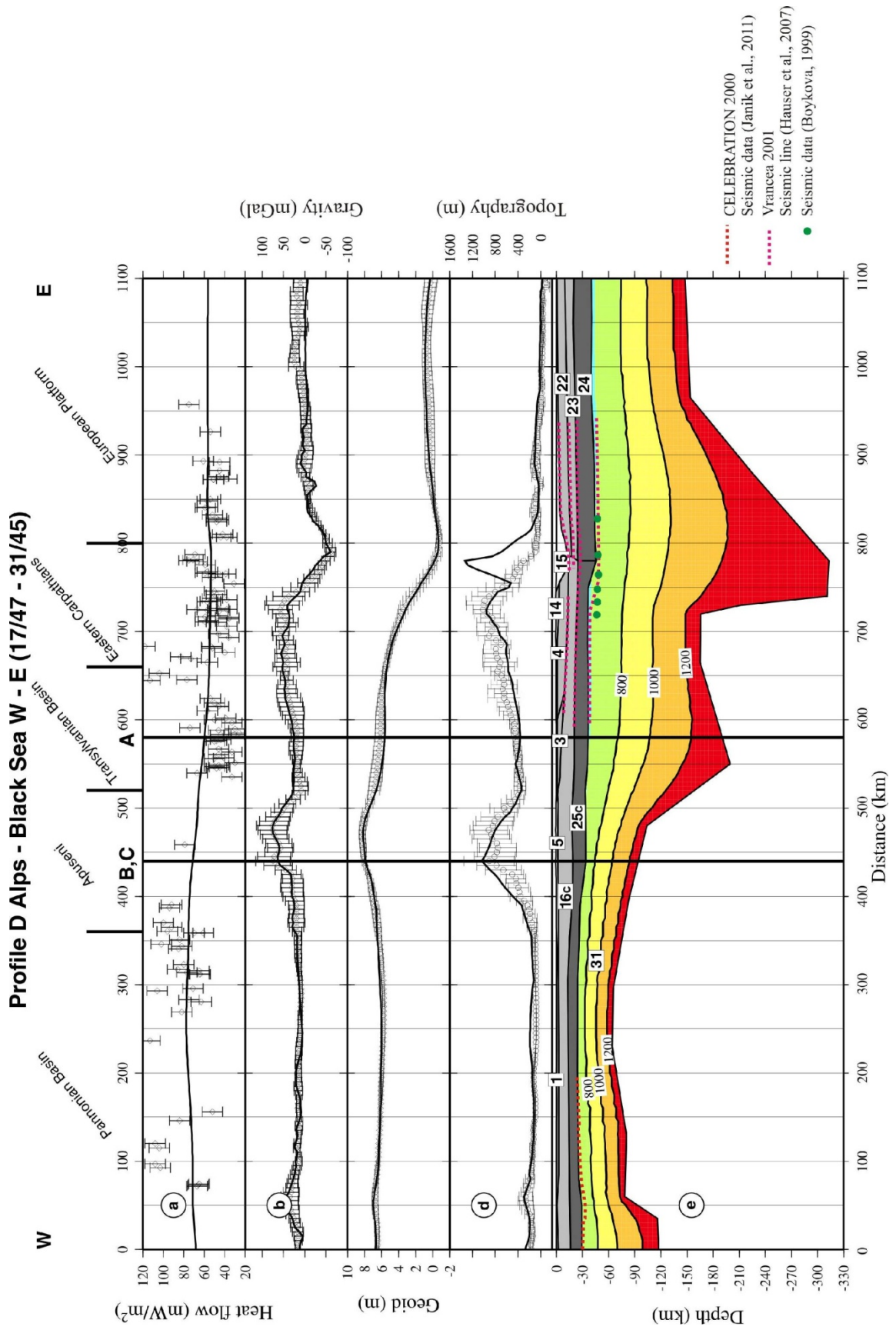
Fig. 32   Lithospheric model for transect D. For further explanations, see Fig. 28.

6.3   *3D inversion modelling*

The Carpathian–Pannonian Basin region is not very active these days. The main subduction process has finished; however, there is one place where the active underthrusting process can still be observed. It is the Vrancea zone. There are also some enigmatic places within the region, where only little research was done, the Apuseni Mountains and the Southern Carpathians. Since these regions, especially the Vrancea and the Apuseni Mountains, do clearly have 3D structures, we decided to do also three–dimensional modelling. Since we have also two different Moho data sets (Csicsay, 2010; Janik *et al.*, 2011) for the focused area, we used them as *a priori* information as well. So we produced three models, one without using *a priori* data for the Moho depth and two with different Moho models as *a priori* information.

At first, we started the inversion process without *a priori* input data, but with a more realistic starting model than flat Moho and LAB boundaries. Therefore, we started the inversion process with a starting model (Fig. 25) resulting from the 1D inversion of geoid and topography data (chapter 6.1). For this starting model we used a constant crustal density of *2850 kg/m³* based on empirical observations (the average crustal density from 2D models). For the 3D inversion, we chose a model with linear increase in density with depth. The crustal density is fixed to *3000 kg/m³* at Moho decreasing linearly upwards, the gradient being a result of the inversion procedure. This density variation with depth simulates the fact that generally, crustal density is smallest in sediments and largest in the lower crust. Numerical experiments showed that most of the gravity and geoid effect of vertical density variations can be explained by such a model (Motavalli-Anbaran *et al*, 2013). More detailed models like an exponential density distribution in the sediments add relatively little to the large–scale effects. The model is built of columns of *30x30 km* size, *28* blocks in E–W and *29* in N–S direction giving a total of *812* columns and *2436* unknowns, which are for each column Moho depth, LAB depth and surface density. In every model we use the same settings for physical properties during calculation of the thermal model (Tab. 5) (e.g. Zeyen and Fernàndez, 1994) and also the same settings for damping (Tab. 6). The parameter variability (Tab. 6) was used in order to keep the resulting model parameters near to the input *a priori* data where they exist. The variability used in the inversion process reflects how much we trust the *a priori* data. We used smoothing of parameters in the case without *a priori* data and with CELEBRATION 2000

a priori data. These parameters were used to reduce the non–uniqueness of the inversion results and increase the stability of the inversion process. They are empirical, we obtained the best results with them, which means that the differences between calculated and measured values were the smallest.

T-surface	T-LAB	Thermal.exp.coeficient Mantle
10°C	1300°C	$3.50*10^{-5} \, K^{-1}$
Conduct Upper Crust	Conduct Lower Crust	Conduct Mantle
2,50 W/(K∗m)	2,00 W/(K∗m)	3,40 W/(K∗m)
HP Upper Crust HP	HP lower Crust	HP mantle
2,00 ($\mu W/m^3$)	0,20 ($\mu W/m^3$)	0,00 ($\mu W/m^3$)

Tab. 5   Physical properties fixed during the calculation of the thermal model.

uncertainty	Gravi (mGal)	Geoid (m)	Topography (m)
	5.0	0.3	30.0
variability	Density (kg/m^3)	Moho (m)	Lithosphere (m)
	10	100	1000

Tab. 6   Used general parameters for 3D inversion. For points where Moho *a priori* data exist, the corresponding variability was reduced by a factor *10.*

6.3.1   Results for the model without *a priori* data

The model without *a priori* data obtains the best fit for all measured data among all tested models. We applied both non–smoothing and slight smoothing of the model to make it geologically more realistic, however, smoothing impedes strong lateral variations of parameters. Regarding the fit of the measured vs. calculated data, the best one was obtained in the non–smoothed model as has to be expected (Fig. 33 D, E, F). Based on the 2D modelling, we estimated densities for every tectonic unit in the area integrated in the 3D inversion. The average lithospheric densities are shown in Tab. 8. Fig. 33 A, B, C and Fig. 33 D, E, F show the final 3D models after 5 iterations with slight smoothing and without smoothing respectively. On Fig. 34 and Fig. 35 one can see the differences between measured and calculated data sets. The misfit standard deviations and variance reductions are given in the Tab. 7.

	Stand. Deviation	Var. Reduction %
Without a priori data		

and smoothing		
topography	122 (m)	83
geoid	0,18 (mGal)	100
free air	10 (m)	90
Janik et al., 2011		
topography	123 (m)	83
geoid	0,22 (m)	99
free air	11 (mGal)	88
Csicsay,2010		
topography	126 (m)	83
geoid	0,35 (m)	98
free air	15 (mGal)	77

Tab. 7   Resulting standard deviations and variance reduction of data misfits for different models.

Pannonian Basin	Transylvanian Basin	Apuseni Mountains	Western. Carpathians
2790 (kg/m^3)	2810 (kg/m^3)	2820 (kg/m^3)	2850 (kg/m^3)
Eastern Carpathians	Southern Carpathians	Moesian Platform	Platforms
2820 (kg/m^3)	2850 (kg/m^3)	2870 (kg/m^3)	2870 (kg/m^3)

Tab. 8   Average crustal density based on the 2D integrated geophysical modelling.

On both Fig. 33A, B, C and Fig. 33 D, E, F we observe very similar features. The differences between them are due to the smoothing parameter used in the model of Fig. 33 A, B, C and so the first results are smoother than the other ones.

We can observe that the Moho depth increases from the Pannonian Basin towards the NE to the East European Platform and also towards the SW to the Dinarides (Fig. 33 A, D). In the Pannonian Basin, the most shallow Moho is in the SE part where it reaches values of about *25–26 km* and in the central part about *27–28 km* in the model without smoothing. In the smooth model such a thin crust in the SE part of the Pannonian Basin cannot be observed. Here the thickness is about *28 km*. The thickness of the crust in the East European Platform reaches values about *36 km* in both models; locally, it can be about *39 km*. The deepest Moho is observed underneath the Carpathian Arc or its foredeep. A trend of increasing depth propagating from the Western Carpathians (about *37 km*) towards the Eastern Carpathians (about *43–44 km*) can be also observed. The deepest Moho is

obtained in the Vrancea area and locally in the Southern Carpathians where our models show a depth of about *45 km*. In the smoothed model a relatively shallow Moho is observed underneath the southern part of the Southern Carpathians and in the central part of the Moesian Platform (only less than *30 km*).

The LAB maps (Fig. 33 B, E) has very similar features as Moho depth maps. The depth of the LAB increases from the Pannonian Basin towards the NE to the East European Platform. In the Pannonian Basin, it is in average between *90* and *110 km* and the most shallow LAB is also in the south-eastern part of the basin with values around *70 km* in the model without smoothing. In the other one, such extrem values were not reached. In the Moesian Platform, we obtained very similar values as in central part of the Pannonian Basin. Values between *100* and *140 km* were obtained in the East European Platform. The deepest LAB is observed beneath the Carpathian Mountains and their foredeep, reaching values between *140* and *180 km*, locally in the Eastern Carpathians and the Vrancea area up to *200 km*. An interesting feature can be observed spreading from the Eastern Carpathians to the East European Platform. It is a kind of channel with relatively thick lithosphere between *160* and *180 km*. Another interesting zone can be observed spreading between the Southern Carpathians and the Apuseni Mountains. It is a zone with very low values of the LAB depth (about *60 km*).

Crustal densities Fig. 33 C, F are very similar to those we got from the 2D integrated geophysical modelling. Average crustal densities are influenced by the sedimentary cover thickness. A very good example for that is the Getic basin, where we got the lowest values of about *2770 kg/m³*. Seismic data (Mocanu and Radulescu, 1994) indicate that the thickness of the sediment cover reaches in this area values of more than *10 km*. On the other hand, areas with nearly no sediment cover, very old platform areas such as the East European Platform are characterised by very high average crustal densities (about *2890 kg/m³*). The Pannonian Basin is characterised by the quite low crustal densities of about *2810 kg/m³*.
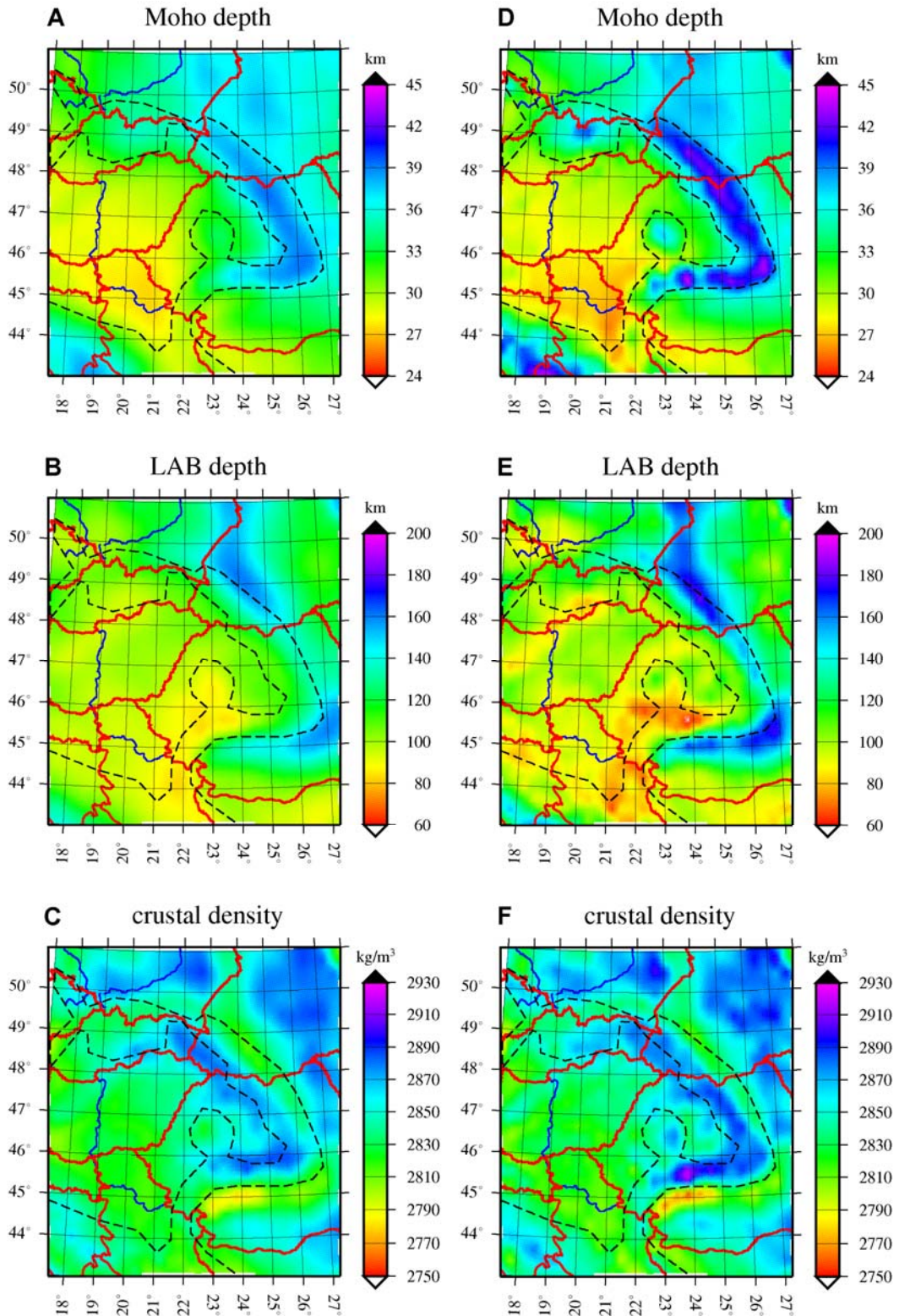
Fig. 33   Result of the 3D inversion for Carpathian Pannonian Basin region with standard parameters (Tab. 6). Figures A, B, C represent modelling with slight smoothing (smoothing factor for density and Moho: 0.1, for lithosphere: 0.3). Figures D, E, F show results for modelling without smoothing. Although the modelling algorithm returns surface densities, the densities presented here are average crustal densities. Black dashed line indicates the position of mountain topography (Carpathian arc, Apuseni Mountains and Dinarides).
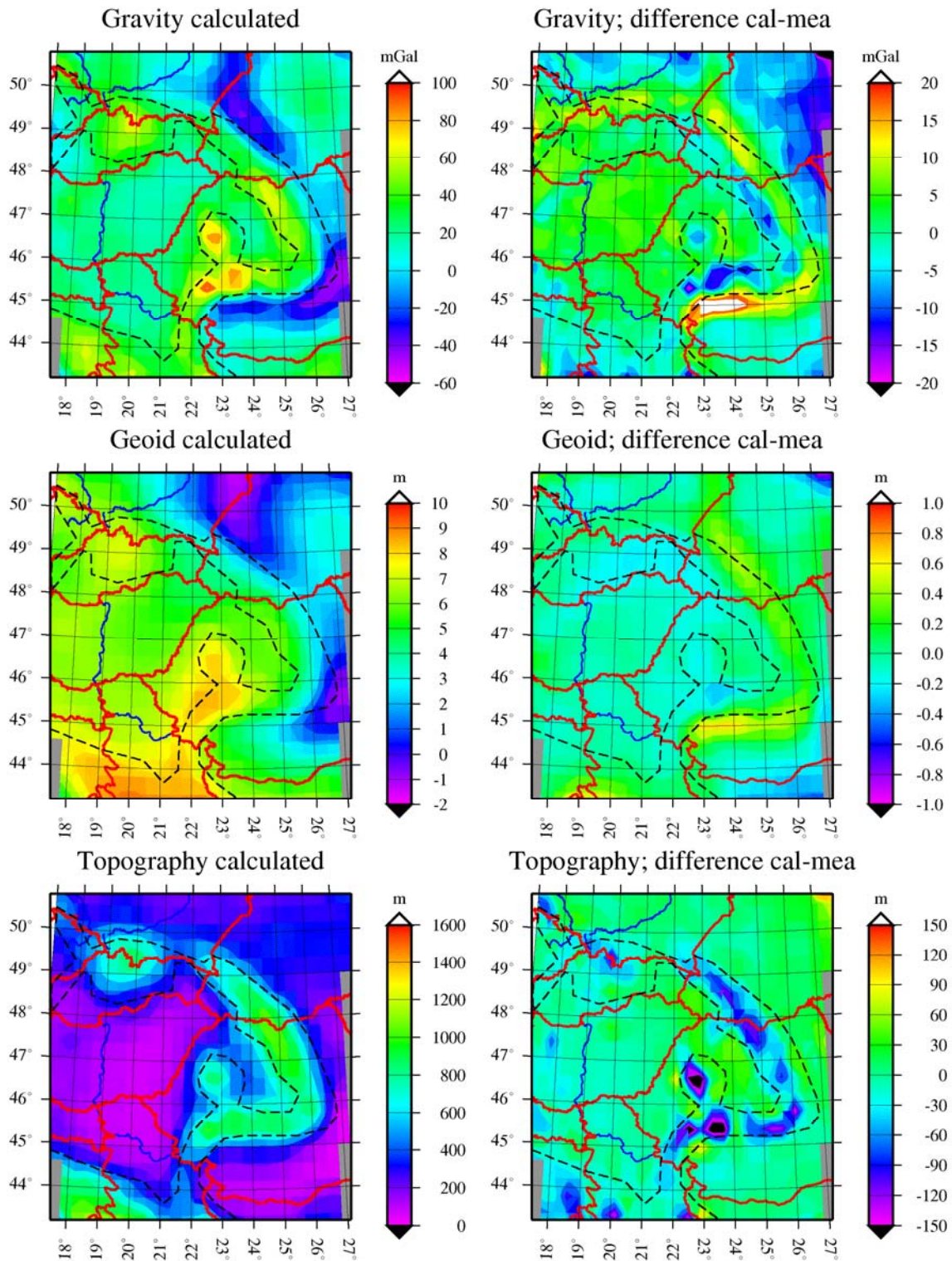
Fig. 34   Plot of calculated data (left column) and difference "calculated minus measured" data with slight smoothing. Black dashed line indicates the position of mountain topography (Carpathian arc, Apuseni Mountains and Dinarides).

Fig. 35   Plot of calculated data (left column) and difference "calculated minus measured" data without smoothing. Black dashed line indicates the position of mountain topography (Carpathian arc, Apuseni Mountains and Dinarides).

6.3.2　Results for the models with *a priori* data

We produced also models using the *a priori* data sets of Moho depth from seismics and combined seismic and gravity data. This approach is another strategy to reduce the non–uniqueness of the inversion results and increase the stability of the inve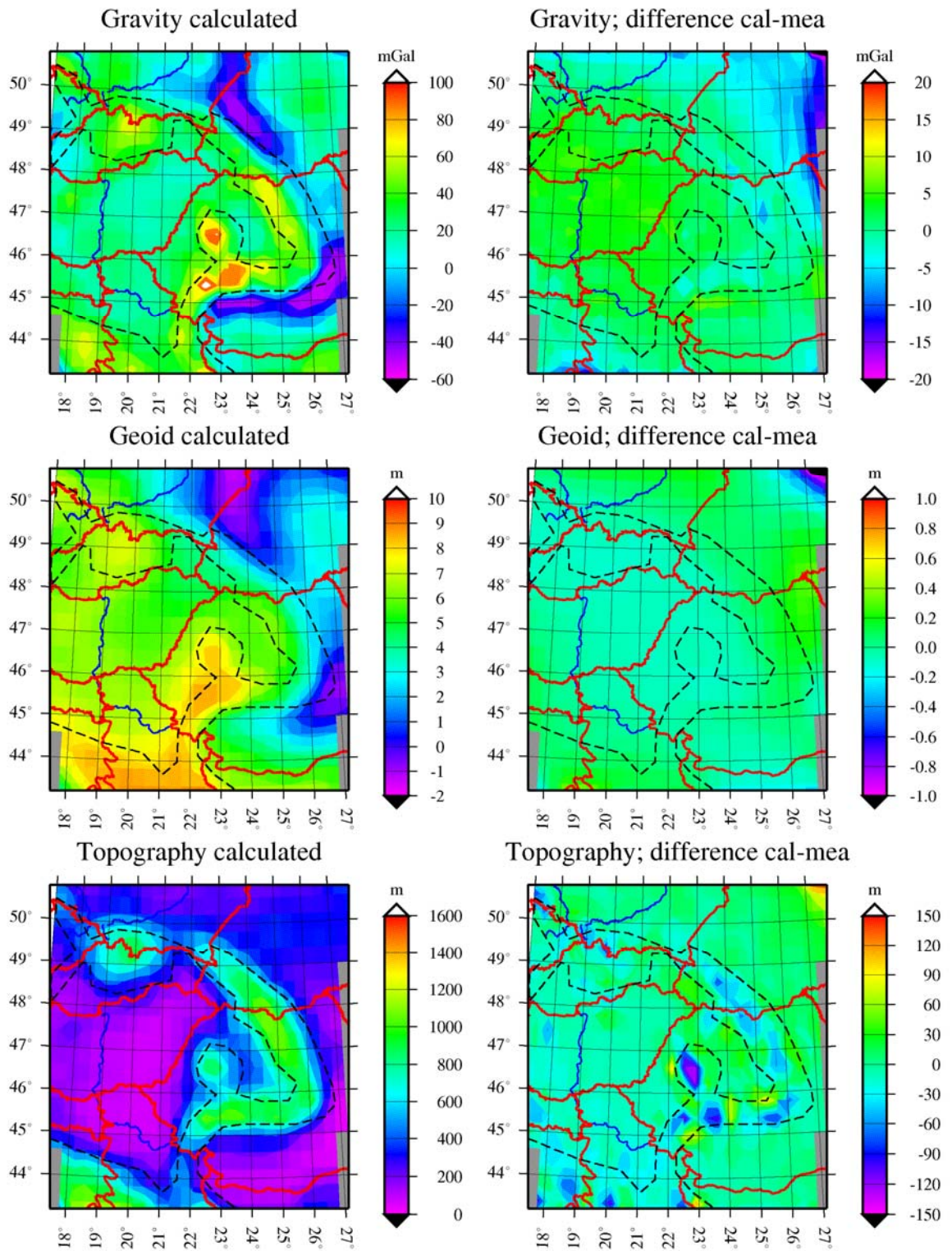rsion process. The algorithm allows to give *a priori* data for crustal density and/or Moho depth. In our case, we used only Moho depths. The first model is based on the CELEBRATION 2000 seismic interpretation (Fig. 9) (Janik *et al.*, 2011), the second one is based on the interpretation of Csicsay (2010) based on the integration of seismic and gravity data sets (Fig. 13). Based on the CELEBRATION 2000 data, we defined *552* points and *7476* points for the Csisay´s data set, which covers the whole area. We applied a slight smoothing in the models with CELEBRATION 2000 *a priori* data. It is necessary in order to avoid important jumps in Moho depth at the edges of the given information. As it was written before, smoothing impedes strong lateral variations of parameters. In the case of thick sedimentary cover and short–wavelength variations (*<100–150 km*), it affects the result of crustal densities, since the program cannot recover the sharp density variations expected between the area with sediments and the surrounding areas. We used the same parameters as in the previous chapter. Fig. 36 shows the final 3D model of the lithosphere after *5* iterations for both models with different *a priori* input data. On Fig. 37 and Fig. 38 one can see the differences between measured and calculated data.

The Moho depths of the final models in both cases are very strong influenced by the input Moho data set, they do not differ much from their original files. The only difference is that in the case of Janik *et al.* (2011) (Fig. 36 A–C) the input data does not cover the whole Carpathian–Pannonian Basin region but only a part of the Western Carpathians and northern parts of the Pannonian Basin. The rest of the area is based only on the 3D Inversion. These two models also differ from each other.

In the Janik *et al.* (2011) (Fig. 36 A–C) model one cannot see the difference in Moho depth between the Carpathian arc, its foredeep and the East European Platform. All of these tectonic units have very similar Moho depths (about *39 km*). Moho depth decreases, however, towards the Pannonian and the Transylvanian Basin and also towards the Moesian Platform. The thinnest crust is found in the Pannonian Basin (*22–23 km*) exactly where the CELEBRATION 2000 data exist. The Transylvanian Basin is characterised by higher values (about *32 km*) which decrease towards the Eastern and the Southern Carpathians (about *38 km*). A somehow strange crustal feature can be found in

the southern part of the study area. Here a belt with crustal thickness values between *27* and *30 km* spread from the southern part of the Pannonian Basin through the Moesian Platform. The thickest crust is found again in the area where the CELEBRATION 2000 data exist, it is in the Trans–European Suture zone (*51 km*).

The second model of the Moho based on Csicsay (2010) (Fig. 36 D–F) *a priori* data is strongly influenced by them. The thinnest crust is shown in the central part of the Pannonian Basin (*60 km*). The thickness increases slightly towards the Transylvanian Basin and in the central part of it reaches values about *33 km*. In the NE direction the Moho depth increases quite dramatically: underneath the Trans European Suture zone it reaches maximum values of more than *51 km*. In this model, the Pannonian Basin and the Moesian Platform are separated from each other by an area with thicker crust (about *42 km*). This area spreads westward to the Dinarides and eastward to the Southern Carpathians. A crustal thickness of about *46 km* can be found in the Vrancea zone.

For the LAB both models (Fig. 36) differ more from each other than for the Moho. The main features can still be spotted but the values are very different. As it was in the previous model, the LAB depth increases from the Pannonian Basin towards the N and NW and reaches its maximum underneath the Carpathian arc or its foredeep. Then it stabilises in the East European Platform. The Moesian Platform is also characterised by somewhat smaller values of LAB depth than would be expected and than we obtained from 2D modelling.

The LAB in the Pannonian Basin in the CELEBRATION 2000 case has values about *80 km* in the thinnest area but in the central part of the Pannonian Basin it is around *100 km*. The Transylvanian Basin is characterised by slightly higher values of the LAB depth (*110 km*) than the Apuseni Mountains (*100 km*), which is thicker than in the Pannonian Basin. The deepest LAB is located in the Eastern Carpathians and the Vrancea area (about *170 km*). Even deeper values of the LAB (*190 km*) are obtained further North in Poland in the Trans European Suture Zone. The Moesian Platform lithospheric thickness is surprisingly similar to the Pannonian Basin one; therefore, the boundary between them cannot be distinguished.
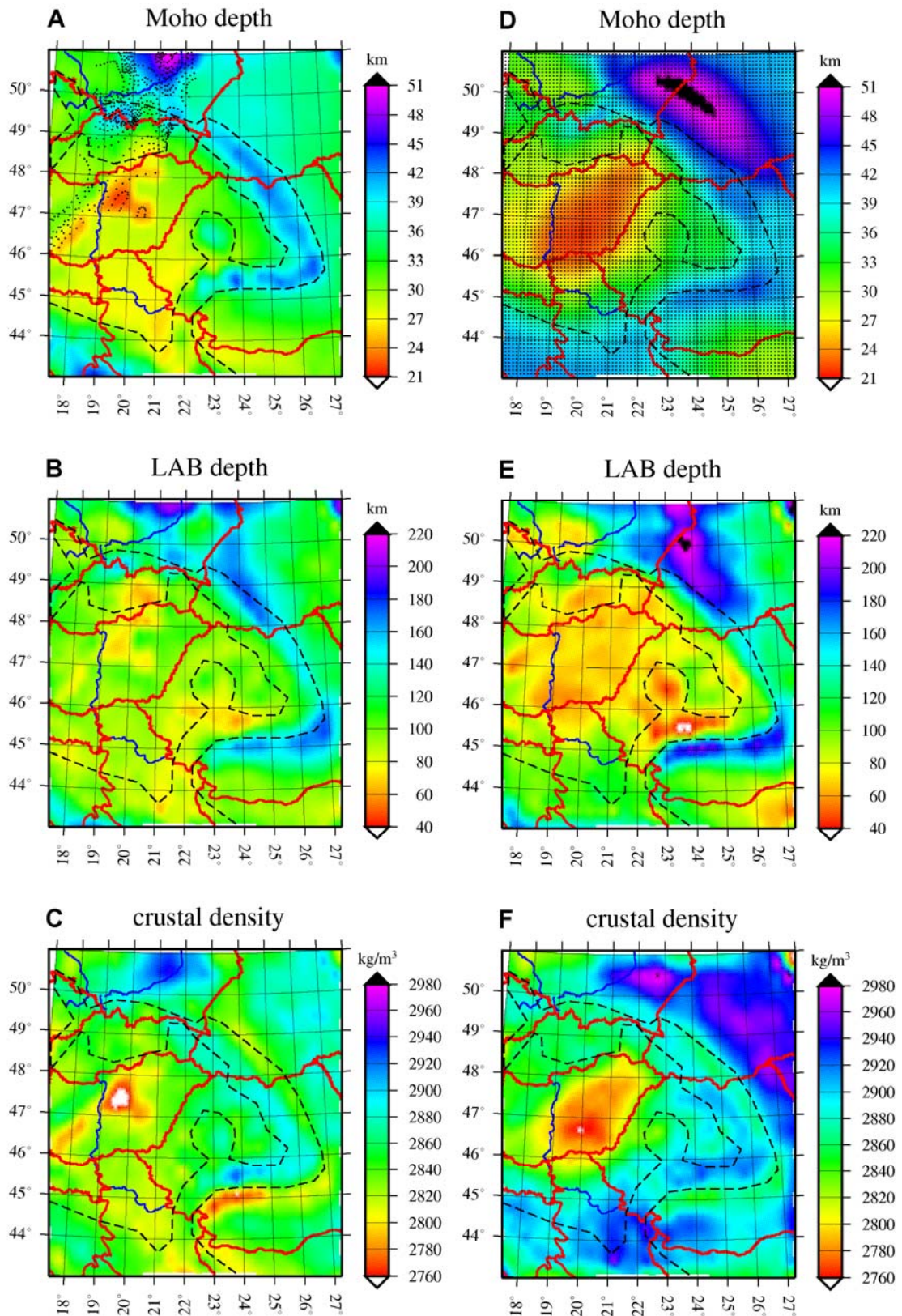
Fig. 36   Result of the 3D inversion with two different *a priori* data sets. A, B, C used as *a priori* Moho data from Janik *et al.* (2011) and D, E, F used *a priori* Moho data from Csicsay (2010). Black dots in A and D indicate the location of *a priori* data points. Black dashed line indicates the position of mountain topography (Carpathian arc, Apuseni Mountains and Dinarides).

108
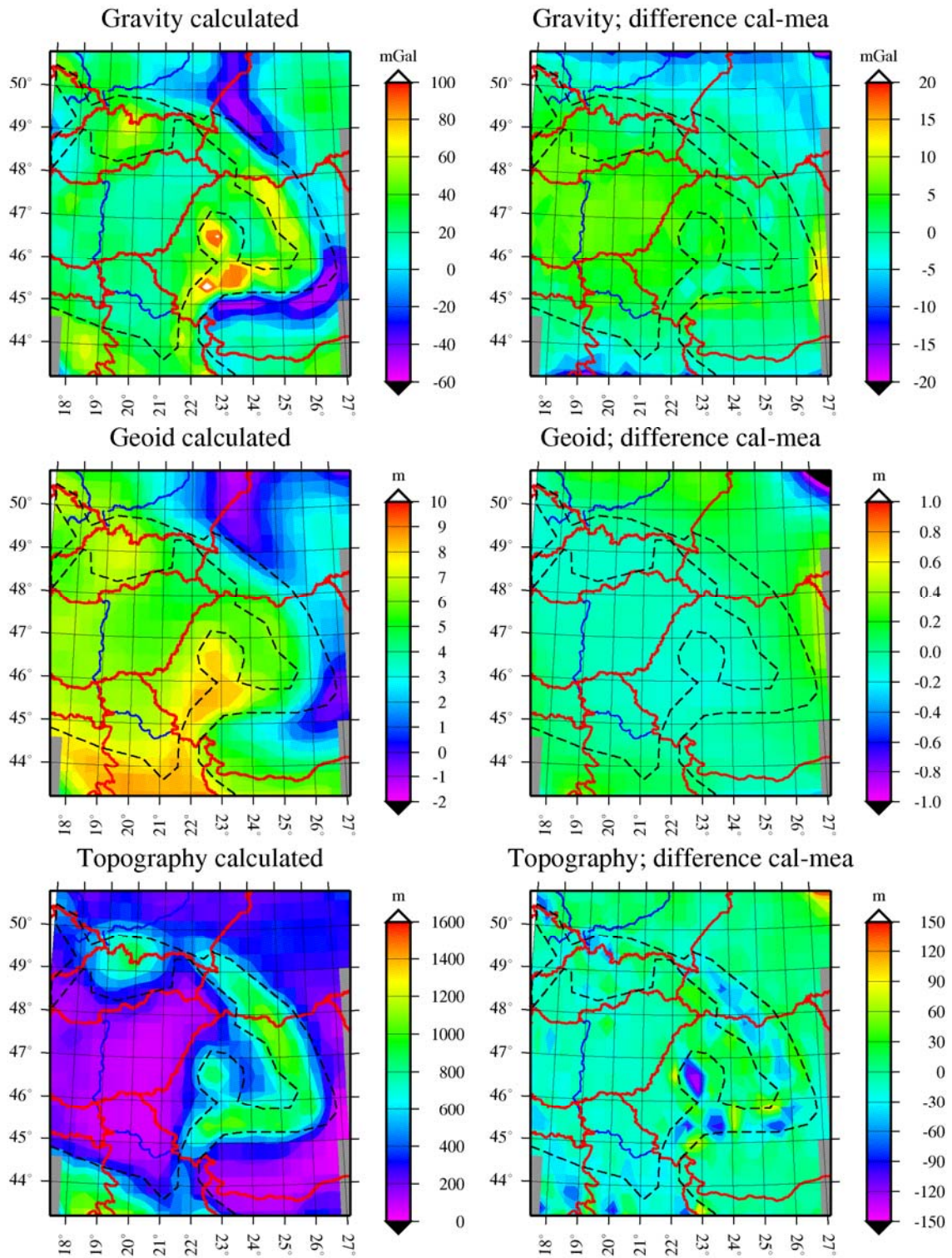
Fig. 37   Plot of difference data between calculated and measured data. Janik *et al.* (2011) Moho *a priori* data used. Black dashed line indicates the position of mountain topography (Carpathian arc, Apuseni Mountains and Dinarides).
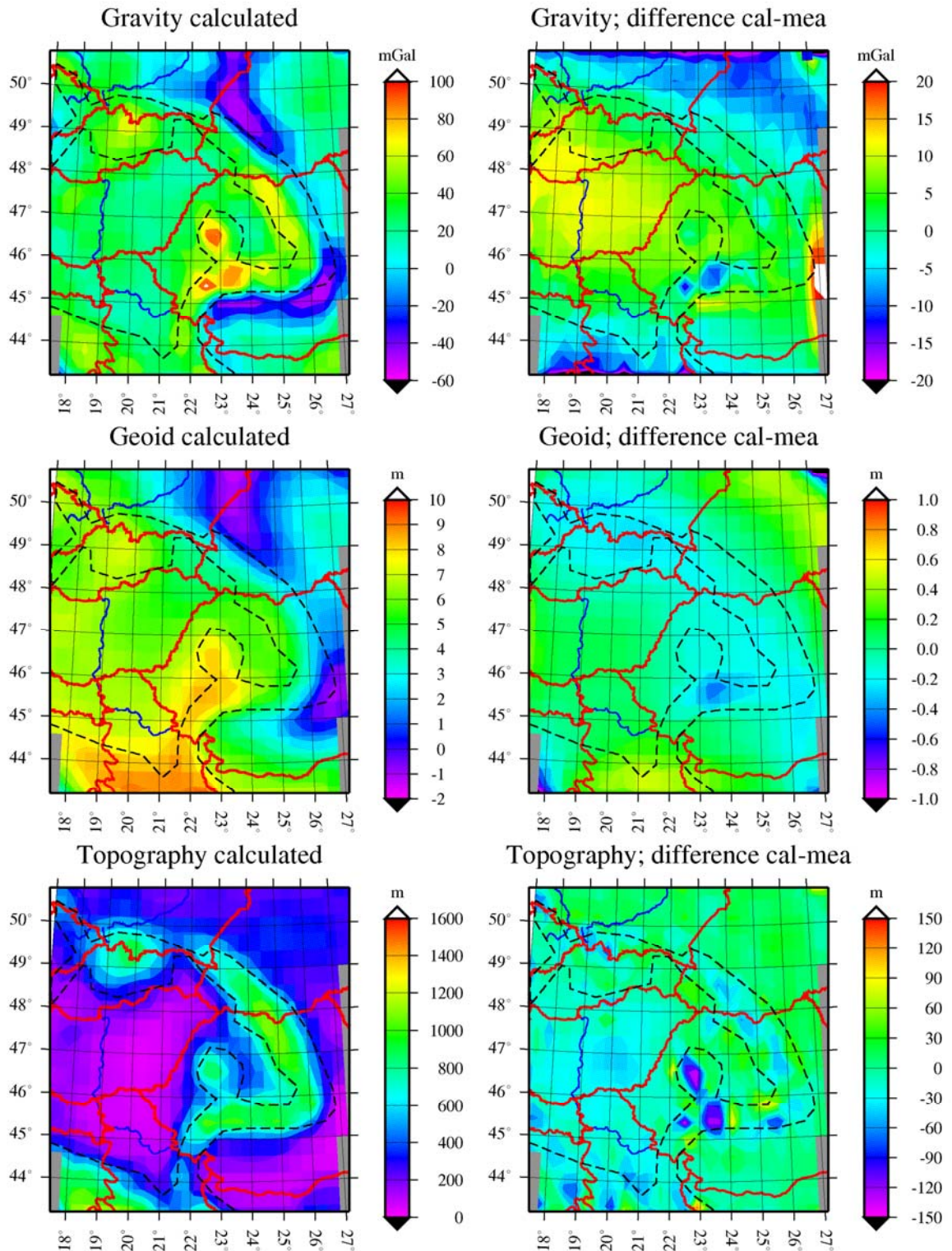
Fig. 38   Plot of difference between calculated and measured data. Csicsay (2010) Moho *a priori* data used. Black dashed line indicates the position of mountain topography (Carpathian arc, Apuseni Mountains and Dinarides).

On the other hand, the results that we got based on Csicsay (2010) data are quantitatively different. The shallowest LAB is observed in the Apuseni Mountains area (less than *50 km*) and in the Southern Carpathians (even less than *40 km*). The Pannonian

Basin reaches values about *60 km* in the whole area. Its adjacent Transylvanian Basin has a thicker central part (*110 km*) and outwards the thickness decreases up to about *80 km*. The deepest LAB can be found in the Eastern Carpathians (more than *220 km*), in the Vrancea and the Getic Basin (more than *210 km*). The rest of the Carpathian arc has a LAB depth of about *160 km*. The Moesian Platform shows values between *60* and *100 km.* The area of the Pannonian Basin and the Moesian Platform is clearly split by a belt with thicker lithosphere.

Crustal densities in both cases have an increasing trend from the Pannonian Basin (less than *2760 kg/m^3*) towards the platform. The platform areas are usually very deeply eroded and because of that, crustal densities are larger. In the Janik model we obtained densities between *2870* and *2910 kg/m^3*. In the Csicsay model we got even larger densities and in some parts can reach extreme values of *2980 kg/m^3*. In the Carpathian foredeep, the densities are smaller, in the range of *2800–2860 kg/m^3*. Here, the crustal densities are strongly influenced by the thick layer of Neogene sediments with smaller densities. On the other hand, higher densities can be found in the higher topography areas of the Carpathians (*2900–2930 kg/m^3*). We obtained very controversial results in the Moesian Platform, where in the Janik-based model we have relatively low values of crustal density (*2790–2850 kg/m^3*) and in the Csicsay–based model we got significantly higher values of the crustal densities in the range of *2900–2940 kg/m^3* in some parts even bigger *2980 kg/m^3*.

Fig. 39 shows the differences between the data misfits of the two models with *a priori* information (Fig. 37 D, E, F and Fig. 38 D, E, F). For gravity and topography, we observe a considerable scatter of these differences in most of the area. Geoid data show some scatter mainly in the Southern Carpathians and Getic Basin. In general, the most problematic area is located in the Southern Carpathians and the Getic Basin.
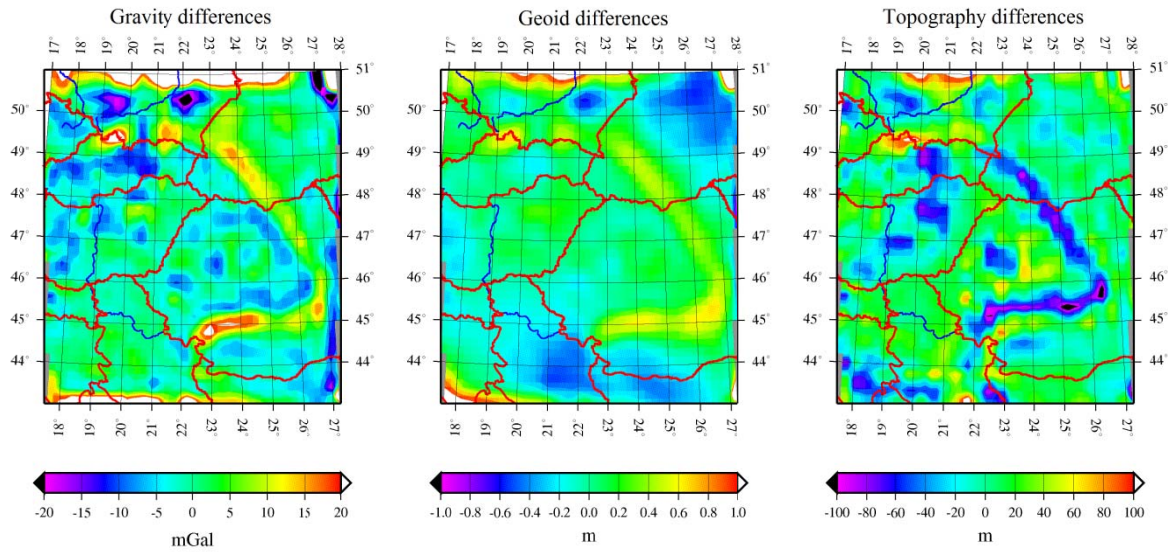
Fig. 39   Maps of the differences between the data misfits of the two models with *a priori* information (Fig. 37 D, E, F and Fig. 38 D, E, F).

6.3.3   Discussion of the 3D inversion models

The Carpathian–Pannonian Basin region was subject of extensive scientific research for the last decades. However, some parts are very well known, others are still enigmatic. Also the diversity of scientific approaches results in a diversity of results. This diversity also brings up issues for interpretation. Here, we add our piece to the puzzle. The 3D inversion is a very new and fast method to establish a model of the lithosphere and the crustal density distribution. Since there are options for stabilizing the inversion process such as smoothing, damping and using *a priori* information (Moho depth), we used them all to provides the best model. As we had two different input data sets and also the option to create the 3D inversion model based only on 1D input model we did 3 different calculations based on 3 different input data sets. The starting model for all of the three models was the same output of the 1D modelling based on the Fullea *et al.* (2006) algorithm.

At first sight it can be clearly seen that the maps of the Moho and the LAB depth are similar in terms of the tectonic features. The shallowest Moho and LAB depths are found in the Pannonian Basin and larger depths in the East European Platform and even more underneath the Carpathian arc where the maximum depths are reached in the Eastern and the Southern Carpathians. Also in the map of the crustal densities, similar features can found. Low densities were obtained in the Pannonian Basin and in the Carpathian foredeep, but these two similar features have probably two different explanations. The

previous studies in the Pannonian Basin show lower crustal densities which can be a consequence of thinner, younger crust and also considerable thicknesses of sedimentary cover. On the other hand, in the foredeep such low values of the densities are caused by the thick Neogene sediments which decrease the average density (Bielik *et al.*, 2004). The platform areas and higher mountainous areas show higher densities that are caused by the absence of a significant sedimentary cover.

The thinnest crust is modelled when using the Csicsay *a priori* data. Nevertheless the program was very limited (because of the *a priori* input data covering the whole study region), therefore the Moho map is very similar to the result of Csicsay (2010). Such a thin crust is also expected by other authors (Bielik *et al.*, 2004; Beránek and Zátopek, 1981; Guterch *et al.*, 1984, 1986; Čekunov *et al.*, 1988; Čekunov, 1993; Posgay *et al.*, 1995; Tomek *et al.*, 1987, 1989; Tomek and Hall, 1993; Horváth, 1993; Lenkey, 1999; Janik *et al.*, 2011). The most surprising area is the SE part of the Pannonian Basin, where we got very thin crust for the 1D model and also some indication of thin crust for the model based on Janik *et al.* (2011). The Transylvanian Basin is characterised by values around *34 km* for all three models and this result is also in very good agreement with the previous works (Bielik *et al.*, 2004; Ioane and Ion, 2005; Csicsay, 2010; Cloetingh *et al.*, 2005; Hauser 2007). The Southern and Eastern Carpathians show similar anomalies in all of our models; however in this case, we obtained more similarities between Csicsay Moho and no–*a priori* data than for the Janik model. Especially in the Vrancea zone we got values around *45 km* which is in the range of values of *41 km* from Hauser *et al.* (2001) and Landes *et al.* (2004), *47 km* from Hauser *et al.* (2007), but less than *50 km* from Mocanu and Radulescu, 1994 or even *53 km* from Ioane and Ion (2005). The biggest differences among the models occurs N of the Eastern Carpathians in the East European Platform. Here, the spread of the Moho depths is significant, from *39 km* (model without *a priori* data and Janik´s model) to more than *51 km* (Csicsay, 2010). The Moesian Platform is characterised by similar Moho depths around *33 km*. Only in the model without *a priori* information it can be locally even less than *30 km*. A depth of about *33 km* is shown also on the other authors' maps. (Ioane and Ion, 2004; Bielik *et al.*, 2004; Beránek and Zátopek, 1981; Guterch *et al.*, 1984, 1986; Čekunov *et al.*, 1988; Čekunov, 1993; Posgay *et al.*, 1995; Tomek *et al.*, 1987, 1989; Tomek and Hall, 1993; Horváth, 1993; Lenkey, 1999; Csicsay, 2010; Janik *et al.*, 2011).

Lithospheric thicknesses show similar features as Moho depths. The thinnest lithosphere is again obtained in an unexpected area. The minimum begins in the southern

margin of the Transylvanian Basin and continues North of the Southern Carpathians to the Pannonian Basin. This minimum can reach very low values (less than *40 km*). In this area, such a thin lithosphere was not predicted. Usually, the published thicknesses exceed *120 km* (Babuška *et al.*, 1988; Horváth, 1993; Šefara *et al.*, 1996; Lenkey, 1999; Zeyen *et al.*, 2002; Dérerová *et al.*, 2006). The results reflect clearly the tectonic complexity of the area. Since the used algorithm is based on the local isostasy conception it reaches its limit. The Pannonian Basin is characterised by values in the range from *70* to *110 km*, in some local places it could be even less (*60 km*). We obtained this very shallow LAB using Csicsay´s *a priori* data and they coincide well with previous works (Babuška *et al.*, 1988; Horváth, 1993; Šefara *et al.*, 1996; Lenkey, 1999; Zeyen *et al.*, 2002; Dérerová *et al.*, 2006), although the ultra shallow LAB of about *40 km* (Ádám *et al.*, 1996) was not confirmed by our method. The Eastern and the Southern Carpathians and their immediate foredeep show lithospheric thickness in the range from *140* to *180 km* which confirms the previous investigations (Babuška *et al.*, 1988; Horváth, 1993; Šefara *et al.*, 1996; Lenkey, 1999; Zeyen *et al.*, 2002). However, it shows also a considerable difference with the results published by Dérerová *et al.* (2006). There exist small areas with even thicker lithosphere mainly in the Ukrainian Eastern Carpathians and the Vrancea zone. Controversary results were obtained in the Moesian Platform, all models show thin lithosphere not more than *100 km*, in average, it is only *80 km*. Nevertheless Dérerová *et al.* (2006) published a thickness of *140 km*.

Concerning the crustal densities, at first sight regions with thick sedimentary cover can be distinguished on the maps, mainly in the foredeep areas. The low densities of the sediments decrease also the average density of the crust, so these regions are characterised by values between *2780* and *2820 kg/³*. On the other hand, lower densities are found also in the Pannonian Basin region, but here besides the sedimentary cover, the ALCAPA and Tisza–Dacia microplates are characterised by lower densities of upper and lower crust (Bielik *et al.*, 2004, Dérerová *et al.*, 2006, Csicsay, 2010). Platform areas on the other hand are characterised by higher values of the densities, here we obtained the maximum values between *2890* and *2980 kg/m³*. These regions are usually very deeply eroded and also they are part of old stable platform areas that are characterised by higher density values (Csicsay, 2010). Very thick crust in the southern territories caused by the *a priori* data forced the inversion algorithm to return higher densities in this region, similar to those expected in the platform areas.

The densities offer different views on the study region. While for the lithospherical thickness and Moho depth the model based on Csicsay data seems to provide the best solution, for the densities, the best solution is provided by the model without *a priori* data. Comparing average densities of the crust obtained by the 2D modelling and 3D inversion it can be seen that this model gives geologically meaningful densities in almost all parts of the model. On the contrary, the models with *a priori* data show somehow unrealistic densities in certain areas. This can be observed mainly in the Pannonian Basin, where both models with *a priori* data show very low crustal densities. Moreover, the model based on Csicsay data has problems to realistically explain the densities in the East European Platform and Moesian Platform areas, where very high values were obtained. On the other hand, all models show unrealistic average densities in the Southern Carpathians and the adjacent Getic depression.

We present here four models based on the 3D inversion approach. These models differ from each other by the input *a priori* data or used parameters of smoothing and/or damping in inversion process. Every model can explain the measured data with a similar precision. In the Carpathian–Pannonian Basin region an extensive research of the crust has been done in the last decades. In this thesis we took into account most of them, however in the 3D inversion we calculated our models based on the most recent ones and most complex work in our opinion. The models without *a priori* data are very useful in the areas where no *a priori* data such as crustal thicknesses or crustal densities exist. However, these models are based on the integrated modelling of potential fields with their inherent non-unique solutions and we have to consider them as very first models and further research has to be done, or some *a priori* data have to be taken into account. Despite its limitations, the model without smoothing gives the most acceptable results in the Carpathians and the north–eastern part of the area among all of the models. The result of the lithospheric thickness in the mentioned area is also closer to the results obtained by Dérerová *et al.* (2006). As a second step, we built another model based on high–quality seismic Moho data (Janik *et al.*, 2009). However, these data are not distributed within the whole area but only in its north–western quarter. The rest of the study area is without *a priori* data. It must be said that the rest of the area does not meet the common expectations about the area in some parts. The most doubtful one is the Vrancea zone, where the lithosphere is thinner than it would be expected. Regarding the still active subduction process one can suppose that the lithosphere here should be thicker. Also the Carpathian arc seems to have thinner

lithosphere than expected. These are the results which can throw a shadow of doubt on the method. The last model seems to be the best, except the Trans European Suture Zone, where the unexpected structures are found. Although this model is based on the Moho constructed by Csicsay (2010), it can fulfil for the most areas our expectations based on seismic models. It shows very thin crust and lithosphere of the Pannonian Basin, on the other hand, it shows thicker crust of the Vrancea zone, which is in good agreement with the previous works. Since his model is not based only on good quality seismic data but also on the gravity modelling without seismic constraints, some of the areas are still doubtful. It is mainly the area of the Trans European Suture Zone. However very similar results for the LAB were obtained by Dérerová *et al.* (2006). The most controversial result was obtained for the Southern Carpathians, where the programme calculates extremely thin lithosphere, which is not expected but on the other it has not been studied yet. One of our 2D transects (Fig. 28) crossing this area does not show such an extremely thin lithosphere but it must be said also that we were not successful in explaining all of the data

6.4   *3D lithospherical modelling (LitMod3D)*

The last task of my PhD studies was to establish a 3D lithospheric model of the Carpathian–Pannonian Basin region based on the 3D geophysical modelling (LitMod3D). Very soon after the recognition of the very time consuming work we decided to make a study area smaller. Our results from the previous methods and the studied papers show that the area of the Transylvanian Basin is worth of further investigation. During the interpretation of the data occurred some problems that made work slower and also the work with the software was really hard and slow. Since the program was not in the final version, it had still some bugs to fix. At the present time this part of the work stays unfinished.

LitMod3D was developed to perform combined geophysical–petrological modelling of the lithosphere and sublithospheric upper mantle. The main advantage of the modelling program is that is built within an internally consistent thermodynamic geophysical framework, where all relevant properties are functions of temperature, pressure, and composition which is not usual when compared with known software packages of today. The program outputs temperature, pressure, surface heat flow, density (bulk and single phase), seismic wave velocities, geoid and gravity anomalies, elevation, and lithospheric strength for any given model by simultaneously solving the heat transfer, thermodynamic, rheological, geopotential, and isostasy (local and flexural) equations. These outputs can be used to obtain thermal and compositional models of the lithosphere and sublithospheric upper mantle that simultaneously fit all available geophysical and petrological observables (Fullea *et al.*, 2009). LitMod3D is a collection of Fortran subroutines and shell scripts organized into a forward calculation execution file module (LitMod3D.exe) and an interactive interface execution file module (LitEdit.exe) used to visualize data and modify the model. The original program has been compiled for Linux distribution, however a Windows version exists as well which was being debugged with my help during the final period of my thesis. The most important problem was the LitEdit.exe – the interactive interface module. It contained a lot of more or less severe errors that made the work weary. The most serious bugs were related to the process of inserting and modifying new layers. Finally, we were able to make the programme run correctly, without undesirable effects. Today, the programme is distributed within a large community of interested Windows version users. The debugging process took me a lot of

time, so the work has stayed unfinished, therefore here I just present only a preliminary result of the lithospheric model of the Transylvanian Basin and its surroundings.

Although the program offers improved modelling, it has also some weak sides. The main advantage and its disadvantage at the same time is basically the fact that the program was built by specialist in geophysics with extended knowledge in computer programming and I think that the present version of the program is still not the final one. The main problem of the program from my point of view, as it was mentioned further up, is the interface module (LitEdit.exe) which is not very intuitive and user–friendly. Changing parameters of the layers and defining the geometry of the interfaces is a complicated and rather unstable process. Modifying interfaces and especially defining new ones creates often fake features and it is quite tricky to fix these spots. It can be concluded that the more layers are needed to explain the data the more difficult is the work with the program. Another issue of the program is the time of the thermal calculation. Although the thermal calculation does not have to be running every single time of the calculation (after *4–5* changes if it were small crustal changes), on my computer the calculation takes ca. 1 hour which makes the modelling process last long.

The Transylvanian Basin is located in the eastern part of the Carpathian–Pannonian Basin region surrounded by the Eastern Carpathians from the North and the East, the Southern Carpathians from the South and the Apuseni Mountains from the West. The area is interesting because of little previous detailed investigation done here in terms of the lithospheric structures. Moreover, our results from the previous studies have shown some interesting places where we could not explain all the data (topography mainly). The investigation area forms a rectangle with corners (*21°/28°E – 44°/48°N*). Although I tried hard to find a best model (best fit of the measured and calculated data), I failed. Therefore I will present only a preliminary result (Fig. 40, Fig. 41, Fig. 42, Fig. 43, Fig. 44, Fig. 45, Fig. 46). The starting model contains seven layers which represent the main layers of the region within lithosphere. I did not used petrological parameters of layers so far. All parameter that I used in the starting model are in the Tab. 9. The process of creation of the model is similar to that of Cages (trial–and–error). The local isostasy concept is used for topography calculation. We assume that the lithosphere of the region is divided into two parts; one belongs to the Tisza–Dacia microplate and the second one belongs to the East European Platform (the Moesian Platform included).

Body	Density (kg/m³)	Thermal Conductivity (W/m K)	Heat Production Rate (µW/m³)
Tisza-Dacia sediments	2400	2,5	1
Tisza-Dacia upper crust	2750	2,5	2
Platform sediments	2400	2,5	1
Platform upper crust	2770	2,5	2
Tisza-Dacia lower crust	2950	2	0,2
Platform lower crust	2970	2	0,2
Mantle lithosphere	3200	3,4	0,02

Tab. 9   Densities and thermal properties of the different bodies used in the 3D model.
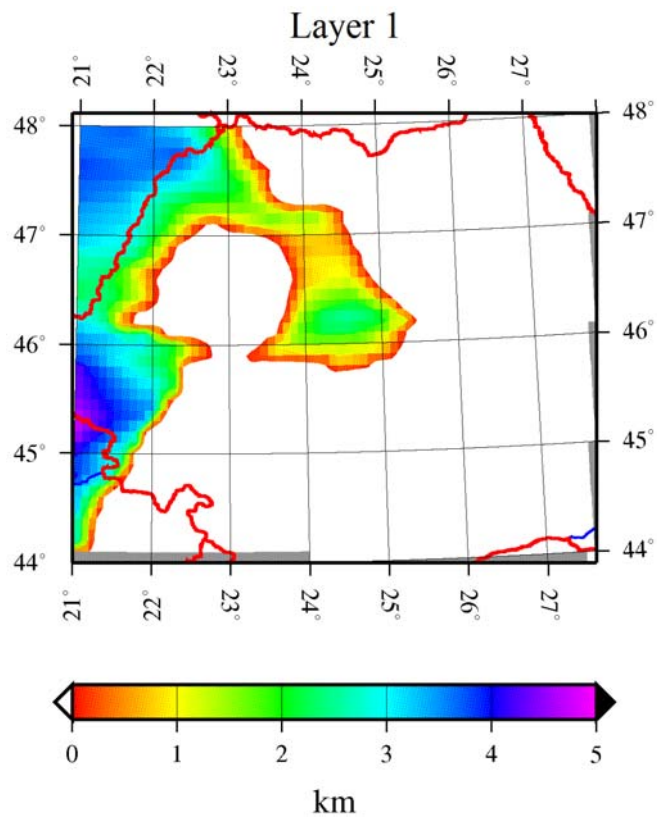
Fig. 40   Layer 1 represents the Tisza–Dacia microplate sediments.
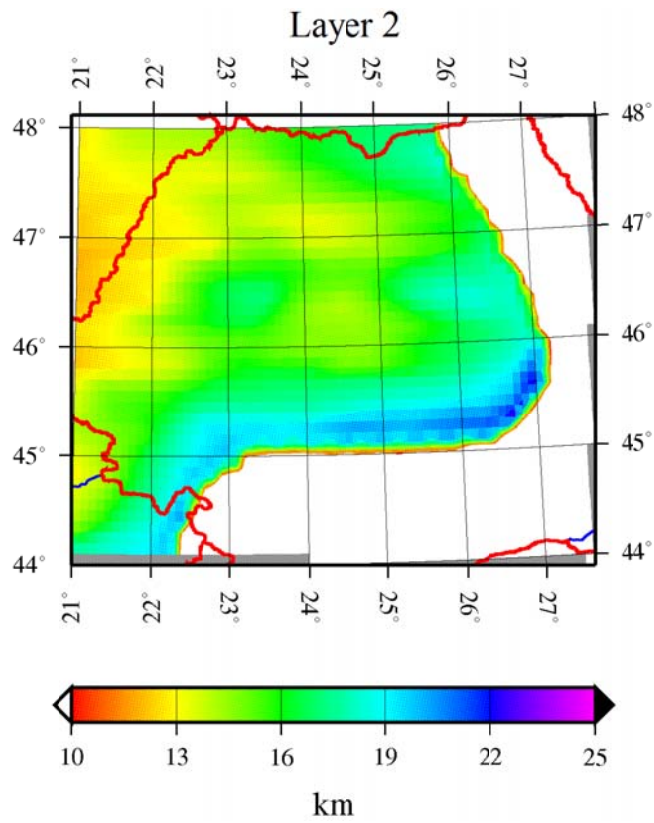
Fig. 41   Layer 2 represents the Tisza–Dacia microplate upper crust.
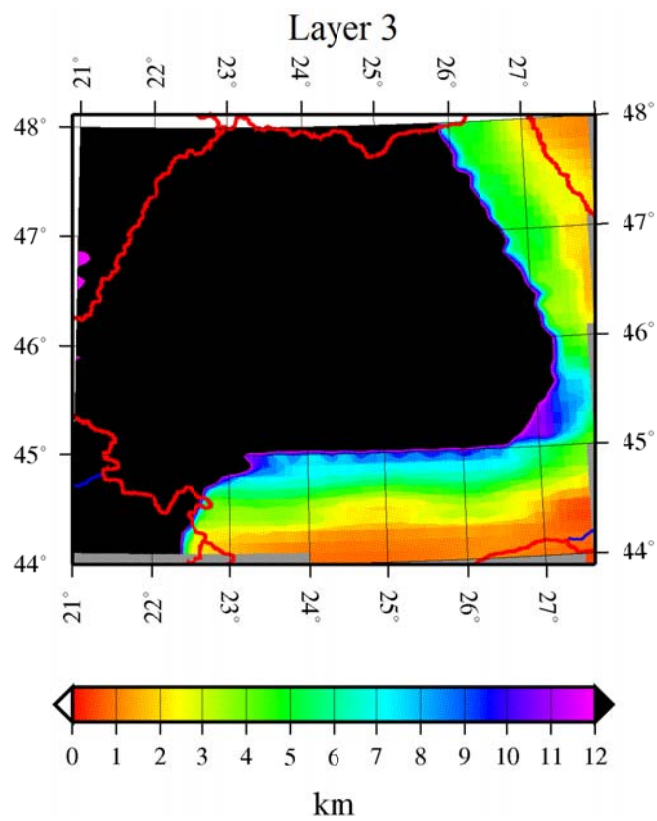
Fig. 42   Layer 3 represents the East European and Moesian Platform sediments.
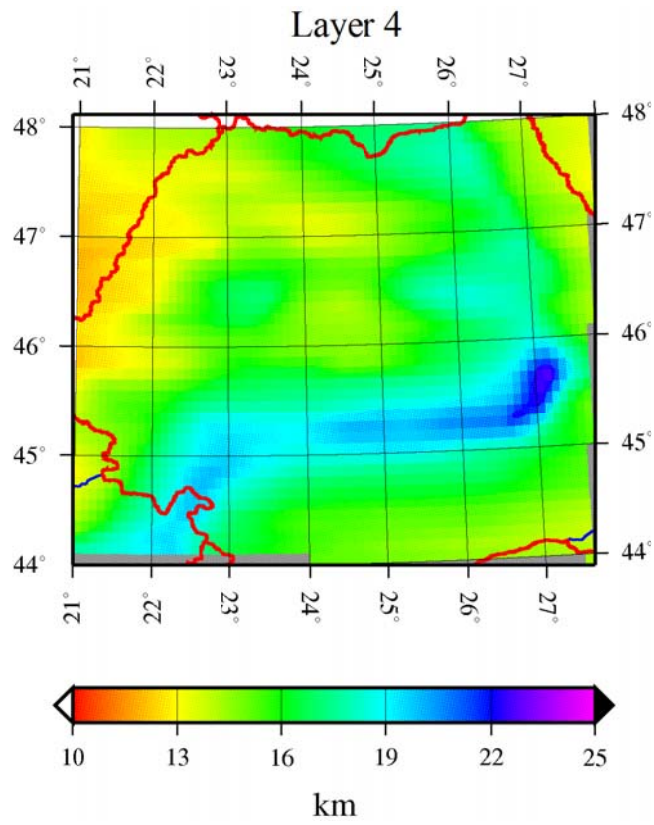
Fig. 43   Layer 4 represents the upper crust for the whole study area.
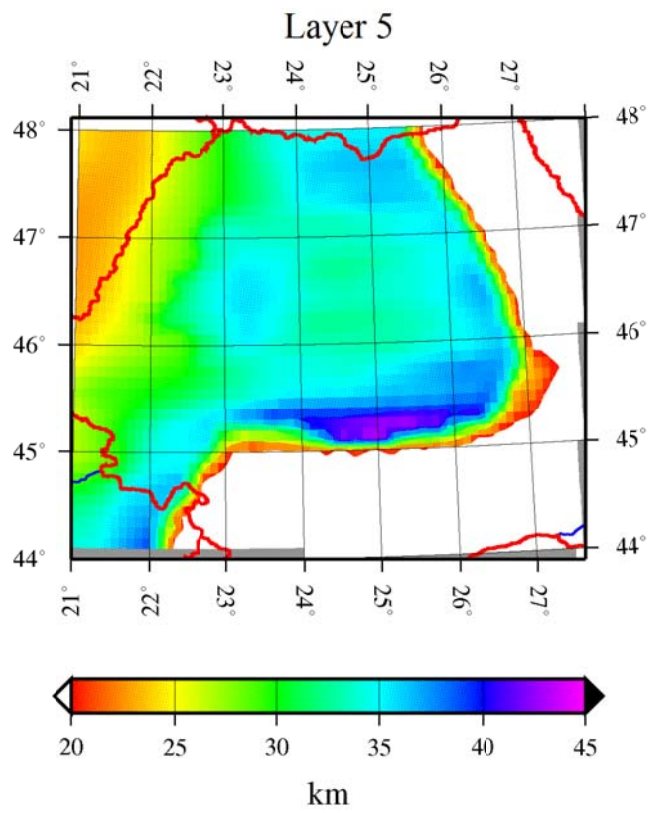
Fig. 44   Layer 5 represents the Tisza–Dacia microplate lower crust.
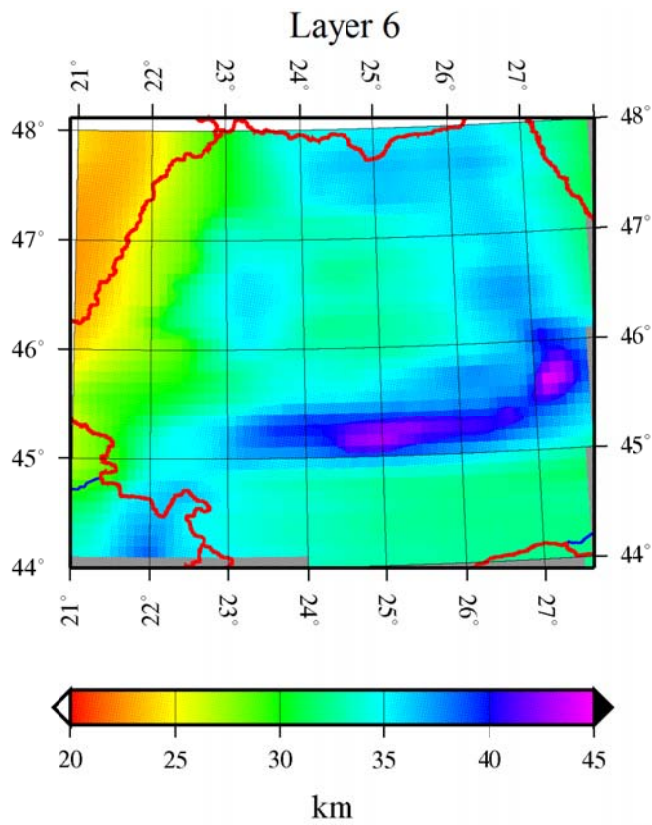
Fig. 45   Layer 6 represents the East European and Moesian Platform lower crust.
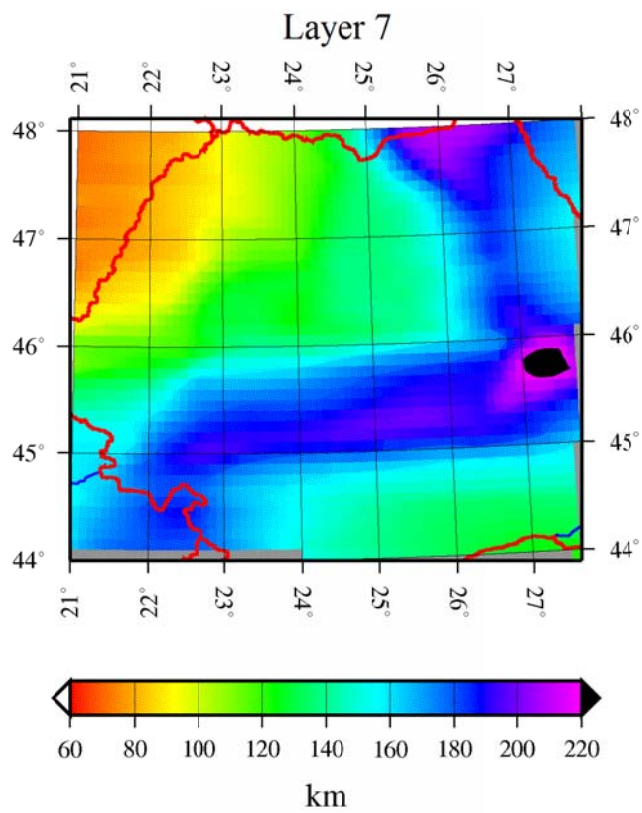
Fig. 46   Layer 7 represents thickness of lithosphere of the whole region.

Here I show also the result of this model (Fig. 47), it can be seen that it is still far from the final version. More trial and error work has to be done.
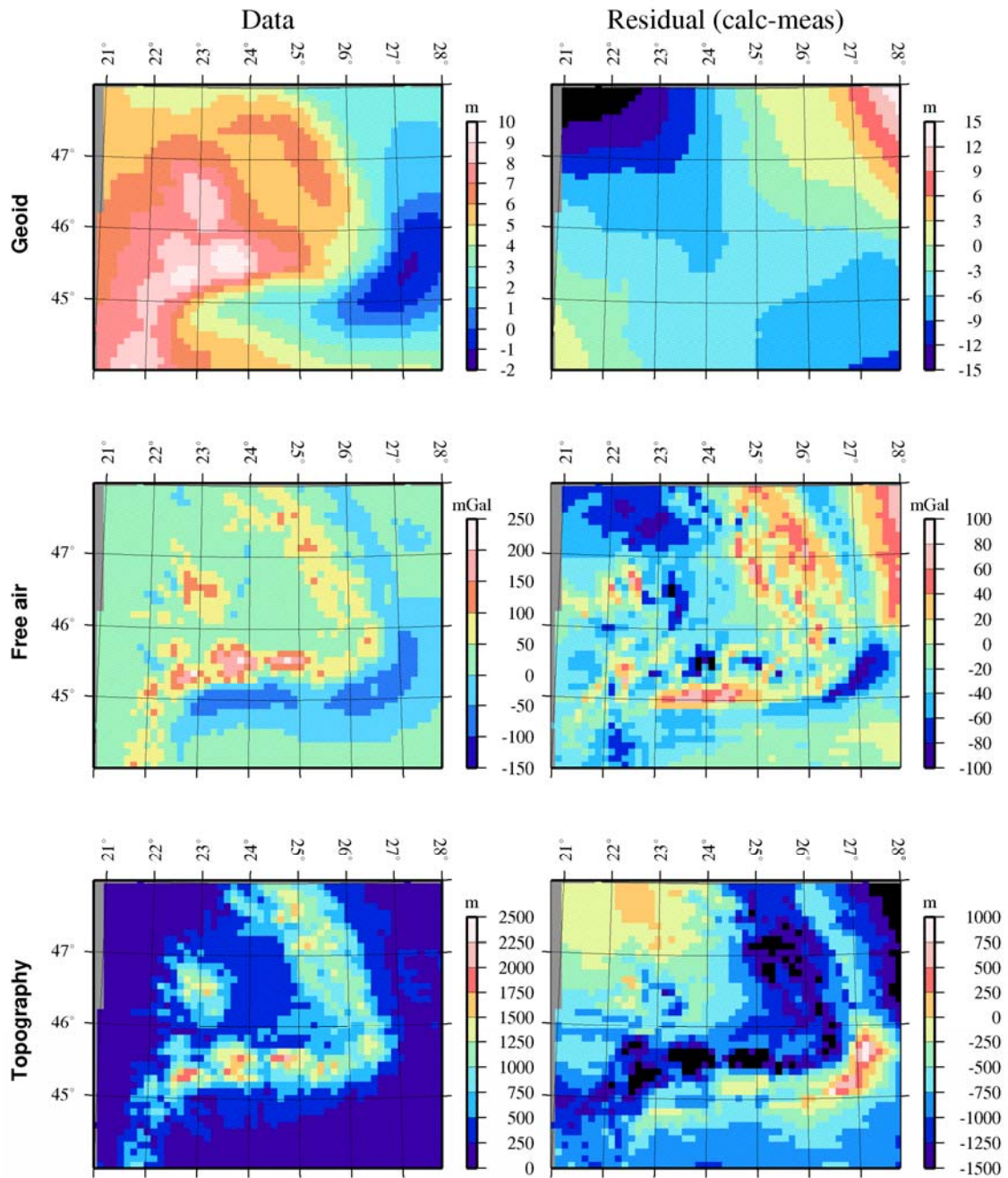
Fig. 47   Plot of the measured data (left column) and the difference "calculated minus measured" data (right column).

7 CONCLUSION

The Carpathian–Pannonian Basin region provides a very good occasion for studying its complex tectonical activities not only historical but also present ones. The complex geodynamic history reflects the complicated structure of its lithosphere. Based on critical analysis of previous results and scientific works, we have tried to bring new knowledge and shed new light on the lithosphere structure in this interesting region. Our research was based mainly on integrated geophysical interpretation of free air, geoid, surface heat flow and topography data. We created four lithospherical scale 2D geophysical integrated models, a 1D model of the Moho discontinuity and the LAB and four 3D inversion models based on different input datasets. The model using LitMod3D got only to a preliminary stage and therefore, this task is still unfinished.

Three different geophysical interpretation approaches carried out in this study allow us to propose a new overlook over the Carpathian–Pannonian Basin region. Joint modelling of surface heat flow, gravimetric and topographic data, using geological and crustal seismic data as constraints, allowed us to establish a revised model of the lithospheric structure of the Carpathian–Pannonian Basin region and parts of their surrounding tectonic units. The final transects as well as 1D and 3D models show strong variations across the studied area. It can be observed on all our results that the lithospheric thickness increases from the Western Carpathians to the Eastern Carpathians along the strike. In comparison with previous results (Horváth, 1993; Lenkey, 1999), our model reveals in general smaller differences between the thicknesses of the lithosphere under the North European Platform and the Pannonian Basin. The large published lithospheric thicknesses north of the Western Carpathians (Horváth, 1993; Lenkey, 1999), in combination with a relatively thin crust *(<40 km)*, would imply a too high gravity anomaly or a topography below sea level. The programmes calculate the topography based on the assumption of local isostasy which is an important restriction and has to be discussed. Part of the topography may be supported by elastic constraints if equivalent elastic plate thicknesses (EET) are too large. There are two different approaches to resolve the problem. In 2D modelling, if we could not find a model explaining all data sets together, we gave preference to a good fit of gravity and geoid data and left topography unadjusted. In 1D and 3D inversion, the programme is automatically trying to keep the differences between measured and calculated data as low as possible. Depending on the *a priori* data and

chosen internal options, the programme can change the thicknesses or densities to obtain as good a result/fit as it can. A few authors have analysed the effective elastic thicknesses of the different tectonic units of our region. Lankreijer *et al.* (1999) proposed very low values for the Polish Platform (*5–17 km*) and the Pannonian Basin (*5–10 km*). For the wavelengths we are concerned with (larger than *100–200 km*), the elastic effects should then be small (e.g. Turcotte and Schubert, 1982). However, locally the elastic support and deformation may be important. This concerns a few places in our transects/models, especially the area around the Southern and Eastern Carpathians, where subduction–related plate bending may be the cause for a rather bad fit between modelled and measured data at wavelengths around *50 km*. These blocks are probably not in isostatic equilibrium and their topography cannot be modelled correctly with our algorithm.

The parameter uncertainties for 3D inversion are in the order of several *km* for the Moho depth, several tens of *km* for the LAB depth and several kg/m^3 for average crustal densities (Motavalli-Anbaran *et al.*, 2013). The uncertainty also depends on the amount of the used *a priori* information. *A priori* information when they are not spread within the whole area sometimes introduce short wavelength variations in the model parameters. This might happen when the *a priori* data are very different from what the programme „expects", when there is a big jump in the *a priori* data and the calculated one. This is the reason why the combination with slight smoothing is also necessary. However, the application of smoothing might cause loss of the short and intermediate wavelengths of Moho depth or density variations in complicated areas.

Somehow different estimation of the uncertainty can be evaluated in the case of the 2D programme. Since the programme is based on trial–and–error modelling, it is difficult to give a quantitative uncertainty estimate. However, based on the many trials, we estimate the uncertainty on lithosphere thickness to be *10–15%*. The thermal parameters have only very little effect on the final results. In areas where the Moho depth is well known from seismic data, this uncertainty is somewhat smaller; in areas with a narrow zone of strong thickening, it may be somewhat bigger, since at large depth, density variations have less effect on the observables. Changes in crustal thickness can be partially compensated by changes of LAB depth in the same direction (thicker crust needs also thicker lithosphere). As a rule of thumb, *1 km* thickening of the crust can be compensated by *10 km* deepening of the LAB. However, this compensation fails for too large modifications. Experience shows that crustal thickness variations of more than *3–4 km*

cannot be compensated by LAB variation due to the different depth dependence of the three different observables.

Although our results differ locally significantly quantitatively and qualitatively between each other, they show in general similar features. Lithospheric thickness increases from the eastern segment of the Western Carpathians, and reaches a maximum value in the Eastern Carpathians and in the Ukrainian and Romanian foreland. This thickening is interpreted as remnants of a slab, which started to break off in the Miocene. These results are in good agreement with the results of seismic tomography from Spakman (1990), Spakman *et al.* (1993), Goes *et al.* (1999), and Wortel and Spakman (2000). They also suggest remnants of deep subduction and slab detachment below the Carpathian–Pannonian Basin region. They showed that the slab seems to be detached from the European plate (probably except for the seismogenic Vrancea zone). A flat–lying, high–velocity anomaly at the bottom of the upper mantle not only beneath the Carpathian–Pannonian Basin region but as well beneath the whole Mediterranean area has been interpreted as subducted lithosphere that sunk into the deeper mantle as a result of rollback and slab detachment along strike of the Carpathian arc. This important roll–back could also explain why crustal thickening is not observed above the slab or even behind the subduction, but in front of it. The increasing thickness of the lithospheric slab from the Western Carpathians to the Eastern Carpathians supports the suggestion that the slab break-off started in the NW and propagated towards the SE, the seismogenic Vrancea zone being inferred as the final expression of the progressive subduction, slab roll–back and plate boundary retreat that were responsible for the evolution of the arc (Kázmér *et al.*, 2003; Tomek and PANCARDI colleagues, 1996). The area of the Southern Carpathians brings some controversial results. On the one hand we got from 2D modelling crustal and lithospherical thickening underneath the area on the other hand we got very thin lithosphere from the 3D inversion. This might be explained by the effort of the programme to keep a reasonably good fit of all of the input data sets. This area is problematic also in 2D modelling and since 2D modelling is based on trial and error we could chose which data set needs to be well explained. We gave the preference to gravity and geoid data as it was explained further up. Since the area is not in isostatic equilibrium, we suggest that the result in 2D is more trustworthy. In the area of the Southern Carpathians, our 2D models show lithospheric and crustal thickening. We suggest that the Moesian Platform is bend and underthrusted beneath the Southern Carpathians. This could be the result of the

clockwise moving (dextral wrenching in the sense of Matenco, 1997) of the lighter and younger Tisza–Dacia microplate against the denser, older and static Moesian Platform during the Neogene. Although some authors (e.g. Sandulescu, 1994; Matenco, 1997; Nakov, 2008) proposed this scenario before, we give geophysical evidence of it for the first time. These results are supported by the existence of the large gravity low along the Southern Carpathians (Bielik *et al.*, 2006), which can be explained by the thick foredeep sediments and the elastic bending of the down–going Moesian plate. (Matenco, 1997). On its southern side, the Moesian Platform is also underthrusted underneath the Balkanides and Rhodopes which are thrusted over it. The result is in good accordance with previous work (e.g. Nakov, 2008; Schmid *et al.*, 2008). The Pannonian Basin lithosphere, based on our modelling, is thicker than usually proposed by other authors. The models that we created do not support a thinning to less than about *70 km* and we did not find any evidence for regional extreme thinning of the lithosphere to only *40 km* (Ádám, 1996; Ádám and Wesztergom, 2001; Horváth, 1993). It may exist, however, in some local features under a few narrow subbasins. However, the regional difference of *10–20 km*, although not far from the estimated uncertainties of our models, may be significant. There are a few different hypotheses which can be put forward to explain this difference. The simplest one would be that seismic, magnetotelluric and thermal analyses do not see the same variations of physical properties and that therefore different methods give the lithosphere–asthenosphere boundary at different temperatures (Dérerová *et al.*, 2006). On the other hand, it is claimed that the alkaline volcanism trace elements show a less depleted uppermost mantle than normal (e.g. Rosenbaum *et al.*, 1997). The models show mainly that the lower lithosphere has to be denser than a normal lithosphere of *60 km* thickness. Here, we interpret this higher density by lower temperatures; however, it could be also due to less depleted, possibly plume–related material. Nevertheless, in order for this argument to be valid, the less depleted material should not form the asthenosphere, which would result in too high buoyancy of the lithosphere and therefore too high topography. Finally, the fact that we used a steady state model may result in a too thick lithosphere: if a recent heating of the lowermost lithosphere happened, the average lithosphere would still be cooler and denser than it were with the same thickness in steady state. Therefore, our steady state model would result in a too thick lithosphere for a steady–state model to compensate for this relatively high average density, which means that the lateral variations of LAB depth we give here have to be considered as minimum variations.

The model based on 3D inversion without *a priori* data shows interesting features also at the contact of the SE edge of the Pannonian Basin, the Southern Carpathians and the Dinarides. Here, strong thinning of the lithosphere can be observed. In the model with Csicsay (2010) *a priori* data, where this strong thinning does not exist, the area should have a higher crustal density, since the *a priori* (gravity–based) Moho is relatively thick. Neither the lithospheric thinning, nor the high crustal densities were expected here. Although detailed studies of lithosphere in this area are rare petrological studies indicate that the Tertiary ultrapotassic volcanism of the Serbian province is related to a post-collisional tectonic regime that followed the closure of the Tethyan Vardar Ocean by Late Cretaceous subduction beneath the southern European continental margin. No mantle plume evidence was put forward (Prelević *et al.*, 2005). The regional studies (Babuška *et al.*, 1988; Horváth, 1993; Lenkey, 1999; Zeyen *et al.*, 2002; Bielik *et al.*, 2004; Dérerová *et al.*, 2006;) also do not assume lithospheric thinning. It would be very convenient to calculate a 2D transect also across this area to confirm or deny this lithospheric thinning. Also seismic data would be needed in order to check the crustal thickening claimed by Csicsay (2010).

Although a model based on the 3D integrated modelling (LitMod3D) was one of my objectives, it was finally not possible to achieve this task in the imparted times, since we had to spend too much time on debugging and testing the programme. In my opinion the programme LitEdit which is an interface programme of LitMod3D is still a beta version, it should be more user friendly because the process of entering layer parameters demands much patience of the user. On the other hand I think that once the programme is finalized, it becomes a fantastic and powerful tool for the geophysical survey of the lithosphere.

8   PROSPECTIVE

The Carpathian–Pannonian Basin region has been shown to be an area worth of further investigation. Although some interesting hypothesis about the tectonic evolution have been confirmed, there are also some questions that are still waiting for bigger scientific interest. Also the knowledge that we have today should be subject of further scientific interest, critics and improvement.

1D automatic modelling has shown up as a handy tool, because of its simplicity and quickness. It gives a very fast result and a very preliminary view on a study region, which may contribute to further or later interpretative work. Also it can be used as a starting model for 3D inversion better than starting calculation with flat layers.

2D integrated geophysical modelling defends its place in the field of geophysical investigation of lithospherical structures. Despite of its usefulness, some modification might be useful such as integration of the primary and secondary seismic wave velocities calculations, or a possibility to insert a picture file to the background of the graphical interface. This might simplify importing the *a priori* data. The advantage is a relatively fast trial-end-error process that is necessary for comfortable work.

Although 3D inversion works very well today it can still be improved. Usually the sedimentary cover is quite well known in many areas around the world. Incorporating this information to the programme might improve largely the lithospheric model. Also the possibility to distinguish between upper and lower crust can have a significant impact on the result in a positive sense. Also it misses the possibility to split the crust into more separated bodies which might represent different tectonical structures like microplates. After a few changes and adding this programme would become a very powerful tool in the lithosphere investigation field and can produce realistic models.

In our study, we revealed some areas where it is difficult to explain geophysical data by the geological reality. It is mainly the area of the Southern Carpathians and its adjacent Getic depression and also some issues can be found in the south–eastern part of the Pannonian Basin. It is clear that additional research of these areas should be followed. Probably the easiest way is to lead other 2D transects through these areas, but the best option is the investigation using LitMod3D which can provide better and more realistic

solutions thanks to its unique properties. On the other hand the programme is still encountering problems, which might discourage a user from working with it.

9 BIBLIOGRAPHY

Ádám, A. 1976. The Transdanubian crustal conductivity anomaly, Acta Geod. Geophys. Mont. Hung., 12, 73 – 79.

Ádám, A., 1996. Regional magnetotelluric (MT) anisotropy in the Pannonian basin (Hungary). Acta Geodaetica et Geophysica Hungarica 31, 191–216.

Ádám, A. a Bielik, M., 1998. The crustal and upper-mantle geophysical signature of narrow continental rifts in the Pannonian basin. Geophysical Journal International, ISSN 0956-540X, Vol. 134, No. 1, s. 157 – 171.

Ádám, A., Wesztergom, V., 2001. An attempt to map the depth of the electrical asthenosphere by deep magnetotelluric measurements in the Pannonian Basin (Hungary). Acta Geologica Hungarica 44 (2–3), 167–192.

Afonso, J. C., Ranalli, G., Fernàndez, M., 2005. Thermal expansivity and elastic properties of the lithospheric mantle: results from mineral physics of composites, Phys. Earth Planet. Int., 149(3-4), 279-306.

Afonso, J.C., Fernàndez, M., Ranalli, G., Griffin, W.L., Connolly, J.A.D., 2008. Integrated geophysical–petrological modeling of the lithosphere and sublithospheric upper mantle: Methodology and applications. Geochemistry Geophysics Geosystems 9 (Q05008). doi:10.1029/2007GC001834.

Alasonati Tašárová, Z., Afonso, J.C., Bielik, M., Götze, H.-J., Hók, J., 2009. The lithospheric structure of the Western Carpathian-Pannonian Basin region based on the CELEBRATION 2000 seismic experiment and gravity modeling. Tectonophysics, 475, 454–469.

Andreescu, M., Nielsen, S.B., Polonic, G., Demetrescu, C., 2002. Thermal budget of the Transylvanian lithosphere. Reasons for a low surface heat-flux anomaly in a Neogene intra-Carpathian basin. Geophys. J. Int., 150(2), 494–505.

Artemieva, I.M., Thybo, H., Kaban, M.K., 2006. Deep Europe today. Geophysical synthesis of the upper mantle structure and lithospheric processes over 3.5 Ga. In: Gee, D.G., Stephenson, R.A. (Eds.), European Lithosphere Dynamics. Geological Society, Memoirs, London. , pp. 11–41.

Babuška, V., Plomerová, J, and Šílený, J., 1987. Structural model of the subcrustal lithosphere in central Europe, in Composition, Structure and Evolution of the Lithosphere-Asthenosphere System, Geodyn. Ser., vol. 16, edited by K. Fuchs and C. Froidevaux, pp. 239 – 251, AGU, Washington, D. C.

Babuška, V., Plomerová, J., Pajdušák, P., 1988. Lithosphere–asthenosphere in central Europe: Models derived from P residuals. In: Proc. 4th EGT Workshop: The Upper Mantle, Commission of the European Communities, European Science Foundation, Utrecht, Netherlands, pp. 37–48.

Bada, G., 1999. Cenozoic stress field evolution in the Pannonian basin and surrounding orogens. Phd thesis. Netherlands Research Scool of Sedimentary Geology publication No. 990101, Amsterdam: Vrije Universiteit Amsterdam, 1999. s. 215. ISBN 90-9012374-1.

Balintoni, I., 1994. Structure of the Apuseni Mountains. Romanian Journal of Tectonics and Regional Geology 75 (Suppl. 2), 51–57 (Bucharest).

Balla, Z., 1987. Tertiary paleomagnetic data for the Carpatho-Pannonian region in the light of Miocene rotation kinematics. Tectonophysics 139, 67–98.

Bally, A.W., Snelson, S., 1980. Realms of subsidence. In: Miall A.D. (Ed.), Facts and principles of world petroleum occurrence. Canadian Society Petrology Geology Membranes 6, pp. 9–94.

Behm, M., Brűckl, E., Chwatal,W., Thybo, H., 2007. Application of stacking and inversion techniques to three-dimensional wide-angle reflection and refraction seismic data of the Eastern Alps, Geophys. J. Int., 170, 275–298, doi:10.1111/j.1365-246X.2007.03393.x.

Beránek B., Zátopek A., 1981a. Earth's crust structure in Czechoslovakia and in Central Europe by methods of explosion seismology. In: Zátopek A. (Ed.), Geophysical syntheses in Czechoslovakia. VEDA, 243-270.

Beránek B., Zátopek A., 1981b. Preliminary results of geophysical synthesis in Czechoslovakia and central Europe based on explosion seismology until 1990. In: Zátopek A. (Ed.), Geophysical syntheses in Czechoslovakia. VEDA, 243-270.

Bergerat, F., Vangelov, D., Dimov, D., 2010. Brittle deformation, palaeostress field reconstruction and tectonic evolution of the Eastern Balkanides (Bulgaria) during Mesozoic and Cenozoic times. Geological Society London Special Publications 340, 77–111.

Bertotti, G., Matenco, L., Cloetingh, S., 2003. Vertical movements in and around the south–east Carpathian foredeep: lithospheric memory and stress field control. Terra Nova 15, 299 – 305.

Bielik, M., 1988. A preliminary stripped gravity map of the Pannonian Basin. Phys. Earth Planet. Inter. 51, 185–189.

Bielik, M., Fusán, O., Burda, M., Hubner, M., Vyskocil, V., 1990. Density models of the Western Carpathians. Contributions of the Geophysical Institute of Slovakian Academy of Sciences 20, 103–113.

Bielik, M., 2004. The Western Carpathians interaction of Hercynian and Alpine processes. Tectonophysics. 393, 63 – 86.

Bielik, M., Makarenko, I., Starostenko, V., Legostaeva, O., Dérerová, J., Šefara, J., Pašteka, R., 2005. New 3D gravity modelling in the Carpathian–Pannonian region. Contributions to Geophysics and Geodesy 35 (1), 65–78.

Bielik, M., Kloska, K., Meurers, B., Svankara, J., Wybraniec, S., Fancsik, T., Grad, M., Grand, T., Guterch, A., Katona, M., Krolikowski, C., Mikuška, J., Pašteka, R., Petecki, Z., Polechonska, O., Ruess, D., Szalaiova, V., Šefara, J., Vozár, J., 2006. Gravity anomaly map of the CELEBRATION, 2000 region. Geologica Carpathica 57 (3), 145–156.

Bielik, M., Krajňák, M., Makarenko, I., Legostaeva, O., Starostenko, V. I., Bošanský, M., Grinč, M., and Hók, J., 2013. Pre-Tertiary basement structure of the Turiec Basin: 3D density modelling. *Geologica Carpathica*,(in print)

Bonjer, K.-P., Oncescu, M.C., Rizescu, M., Encescu, D., Driad, L., Radulian, M., Ionescu, C., Moldoveanu, T., 2000. Source- and site-parameters of the April 28, 1999

intermediate depth Vrancea earthquake: first results from the new K2 network in Romania. XXVII Gen. Ass. Europ. Seism. Comm., Lisbon, 111.

Bowin, C., 1991. The Earth's gravity field and plate tectonics. Tectonophysics 187, 69–89.

Boykova, A., 1999. Moho discontinuity in central Balkan Peninsula in the light of the geostatistical structural analysis. Physics of the Earth and Planetary Interiors 114, 49–58.

Bucha, V., Blížkovský , M., 1994. Crustal Structure of the Bohemian Massif and the Western Carpathians. Springer Verlag, Berlin, 355 pp. CELEBRATION 2000 Working Group, 2000. Contrasts of lithospheric structures in the TESZ (from NW to SE Poland) along TTZ and CEL03 seismic profiles. Geologica Carpathica 53, CD-ROM.

Brun, J.-P., Sokoutis, D., 2007. Kinematics of the Southern Rhodope Core Complex(Northern Greece). Int. J. Earth Sci. 96, 1079 – 1099.

Burchfiel, B.C., Nakov, R., Tzankov, T., 2003. Evidence from the Mesta half-graben, SW Bulgaria, for the Late Eocene beginning of Aegean extension in the Central Balkan Peninsula. Tectonophysics 375, 61 – 76.

Čekunov, A. V. (Ed), 1993. Litosféra Centraľnoj i Vostočnoj Evropy: Geotraversy III, VII, IX. In: Bielik, M., 2001. GRAVIMETRIA – integrálna súčasť geofyzikálnej interpretácie litosféry v karpatsko-panónskom regióne: Nové trendy v analýza tiažového poľa. Doktorská dizertácia. Bratislava: MS – GFÚ SAV, 2001. 113 s.

Čekunov, A. V., Ádám, A. A., Blížkovský, M., Bormann, P., Guterch, A., Dačev, CH., Kornea, I., Kutas, R. J., Magnickij, V. A., Sollogub, V. B., Chain, V. E., Sollogub, N. V., Starostenko, V. J., 1988. Litosfera Centraľnoj i Vostočnoj Evropy: Geotraversy I, II, V. In:

Čermák, V., 1994. Results of heat flow studies in Czechoslovakia. In: Bucha, V., Blížkovský , M. (Eds.), Crustal Structure of the Bohemian Massif and the West Carpathians. Springer Verlag, Berlin, pp. 5–118.

Chambers, K., Woodhouse, J. H., Deuss H., 2005. Topography of the 410-km discontinuity from PP and SS precursors, Earth Planet. Sci. Lett., 235, 610–622, doi:10.1016/ j.epsl.2005.05.014.

Christensen, N.I. and Mooney, W.D., 1995. Seismic velocity structure and composition of the continental crust: A global view. Journal of Geophysical Research, *ISSN 0148-0227, Vol.* 100, No. B7, 9761 – 9788.

Ciulavu, D., Dinu, C., Szakacs, A., and Dordea, D., 2000. Neogene kinematics of the Transylvanian Basin (Romania), American Association of Petroleum Geologists Bulletin, v. 84, no. 10, p. 1589–1615.

Cloetingh, S., Burov, E., Beekman, F., Andeweg, B., Andriessen, P.A.M., Garcia Castellanos, D., de Vicente, G., Vegas, R., 2002. Lithospheric folding in Iberia. Tectonics 21, 1–26.

Cloetingh, S.A.P.L., Burov, E., Matenco, L., Toussaint, G., Bertotti, G., Andriessen, P.A.M., Wortel, M.J.R., Spakman, W., 2004. Thermo-mechanical controls on the model of continental collision in the SE Carpathians (Romania). Earth Planet. Sci. Lett. 218, 57–76.

Cloetingh, S., Maţenco, L., Bada, G., Dinu, C., Mocanu, V., 2005. The evolution of the Carpathians–Pannonian system: interaction between neotectonics, deep structure, polyphase orogeny and sedimentary basins in a source to sink natural laboratory. Tectonophysics 410, 1–14.

Connolly, J. A. D. 2005. Computation of phase equilibria by linear programming: A tool for geodynamic modeling and its application to subduction zone decarbonation, Earth Planet. Sci. Lett., 236, 524–541, doi:10.1016/j.epsl.2005.04.033.

Constantinescu, L., and Enescu, D. 1964. Fault-plane solutions for some Roumanian earthquakes and their seismotectonic implication, J. Geophys. Res., 69, 667 – 674.

Crânganu, C., Deming, D., 1996. Heat flow and hydrocarbon generation in the Transylvanian Basin, Romania. AAPG Bulletin 10, 1641–1653.

Csato, I., Kendall, C.G.S.C., Moore, P.D., 2007. The Messinian problem in the Pannonian Basin, Eastern Hungary–insights from stratigraphic simulations. Sediment. Geol. 201, 111 – 140.

Csicsay, K., 2010. Two-dimensional and three-dimensional integrated interpretation of the gravity field based on international project CELEBRATION, 2000 data (in Slovak). Ph.D. thesis, Comenius University, Bratislava, Bratislava, 154 pp.

Csicsay, K., Bielik, M., Mojzeš, A., Speváková, E., Kytková, B., Grinč, M., 2012. Linearization of the Sobolev and Babeyko´s formulae for transformation of P-wave velocity to density in the Carpathian-Pannonian Basin region, Contributions to Geophysics and Geodesy. Vol. 42, no. 1, p. 1- 13.

Csontos, L., Nagymarosy, A., Horváth, F., Kováč, M., 1992. Tertiary evolution of the Intra-Carpathian area: a model. Tectonophysics 208, 221–241.

Csontos, L., 1995. Tertiary tectonic evolution of the intra-Carpathian area: A review, Acta Vulcanol., 7, 1 – 13.

Csontos, L., Nagymarosy, A., 1998. The Mid-Hungarian line: a zone of repeated tectonic inversions. Tectonophysics 297, 51–71.

Csontos, L., Vörös, A., 2004. Mesozoic plate-tectonic reconstruction of the Carpathian region. Palaeogeography, Palaeoclimatology, Palaeoecology 210, 1–56.

Dadlez, R., Grad, M., Guterch, A., 2005. Crustal structure below the Polish Basin: is it composed of proximal terranes derived from Baltica? Tectonophysics 411, 111 – 128.

Dallmeyer, R.D., Neubauer, F., Fritz, H., Mocanu, V., 1998. Variscan vs. Alpine tectonothermal evolution of the Southern Carpathian orogen. Constraints from $^{40}Ar/^{39}Ar$ ages. Tectonophysics 290, 111–135.

De Broucker, G., Mellin, A., Duindam, P., 1998. Tectono-Stratigraphic evolution of the Transylvanian Basin, pre-salt sequence, Romania. In: Dinu, C., Mocanu, V. (Eds.), Geological and Hydrocarbon Potential of the Romanian areas, Bucharest Geosciences Forum 1, pp. 36–70.

Decker, K., 1996. Miocene tectonics at the Alpine–Carpathian junction and the evolution of the Vienna basin. Mitt-Gesellschaft Geology Bergbaustue Österr 41, 33–44.

Demetrescu, C., Nielsen, S.B., Ene, M., Şerban, D.Z., Polonic, G., Adreescu, M., Pop, A., Balling, N., 2001. Lithosphere thermal structure and evolution of the

Transylvanian Depression — insights from new geothermal measurements and modelling results. Phyics Earth Planet Interiors 126, 249–267.

Dérerová, J., Zeyen, H., Bielik, M., Salman, K., 2006. Application of integrated geophysical modeling for determination of the continental lithospheric thermal structure in the eastern Carpathians. Tectonics 25 (3), TC3009.

Dinter, D., Royden, L., 1993. Late Cenozoic extension in northeastern Greece: Strymon Valley detachment system and Rhodope metamorphic core complex. Geol. Soc. Amer. Bull. 21, 45 – 48.

Dolapchieva, M., 1994. Review and taxonomy of data and results of the paleomagnetic investigation in Bulgaria performed by senior researcher Peter Nozharov and his team. Bulg. Geophys. J. 22, 40 – 50 (in Bulgarian with English summary).

Dupont-Nivet, G., Vasiliev, I., Langereis, C.G., Krijgsman,W., Panaiotu, C., 2005. Neogene tectonic evolution of the southern and eastern Carpathians constrained by paleomagnetism. Earth Planet. Sci. Lett. 236, 374–387.

Enescu, D., Danchiv, D., Bala, A., 1992. Lithosphere structure in Romania II. Thickness of the Earth crust. Depth-dependent propagation velocity curves for the P and S waves. Stud. Cercet. Geol. Geofiz. Geogr., Geofiz. 30, 3 –19.

Fan, G., Wallace, T.C., Zhao, D., 1998. Tomographic imaging of deep velocity structure beneath the Eastern and Southern Carpathians, Romania: implications for continental collision. Journal of Geophysical Research 103 (B2), 2705–2723.

Fodor, L., Csontos, L., Bada, G., Györfi, I., Benkovics, L., 1999. Tertiary tectonic evolution of the Pannonian Basin system and neighbouring orogens: a new synthesis of paleostress data. In: Durand, B., Jolivet, L., Horváth, F., Séranne, M. (Eds.), The Mediterranean Basins: Tertiary extension within the Alpine Orogen, Geological Society Special Publication 156, pp. 295–334.

Froitzheim, N., Plašienka, D., Schuster, R., 2008. Alpine tectonics of the Alps and Western Carpathians. In: McCann, T. (Ed.), The Geology of Central Europe, vol. 2. Mesozoic and Cenozoic. Geological Society Publishing House, London, pp. 1141–1232.

Frost, D. J. 2003. The structure and sharpness of $(Mg,Fe)_2SiO_4$ phase transformations in the transition zone, Earth Planet. Sci. Lett., 216, 313–328, doi:10.1016/S0012-821X(03)00533-8.

Frost, D. J., and Dolejš, D., 2007. Experimental determination of the effect of H_2O on the 410-km seismic discontinuity, Earth Planet. Sci. Lett., 256, 182–195, doi:10.1016/j.epsl.2007.01.023.

Fügenschuh, B., Schmid, S.M., 2005. Age and significance of core complex formation in a very curved orogen: evidence from fission track studies in the South Carpathians (Romania). Tectonophysics 404 (1–2), 33–53.

Fullea, J., Fernàndez, M., Zeyen, H., 2006. Lithospheric structure in the Atlantic–Mediterranean transition zone (southern Spain, northern Morocco): a simple approach from regional elevation and geoid data. C. R. Geoscience 338, 140–151.

Fullea, J., Fernàndez, M., Zeyen, H., Vergés, J., 2007. A rapid method to map the crustal and lithospheric thickness using elevation, geoid anomaly and thermal analysis. Application to the Gibraltar Arc System and adjacent zones. Tectonophysics 430, 97–117.

Fullea, J., Afonso, J.C., Connolly, J. A. D., Fernàndez, M., García-Castellanos, D. and Zeyen, H., 2009. LitMod3D: an interactive 3D software to model the thermal, compositional, density, rheological and seismological structure of the lithosphere and sublithospheric upper mantle. *Geochem. Geophys. Geosys*., 10, Q08019, doi:10.1029/2009GC002391.

Fullea, J. and Afonso, J.C., 2010. LitMod3D users guide Version 2.0. May 2010, http://eps.mq.edu.au/~jafonso/fotos/LitMod_userguide_last.pdf

Gesch, D.B., Verdin, K.L., Greenlee, S.K., 1999. New land surface digital elevation model covers the Earth. EOS, Transactions American Geophysical Union 80 (6), 69–70.

Gîrbacea, R., Frisch, W., 1998. Slab in the wrong place; lower lithospheric mantle delamination in the last stage of the eastern Carpathian subduction retreat. Geology 26: 611-614

Goes, S., Spakman, W., Bijwaard, H., 1999. A lower mantle source for Central European volcanism. Science 286 (5446), 1928–1931.

Grad, M., Guterch, A., Keller, G.R., Janik, T., Hegedüs, E., Vozár, J., Slaczka, A., Tiira, T., Yliniemi, J., 2006. Lithospheric structure beneath trans-Carpathian transect from Precambrian platform to Pannonian basin: CELEBRATION, 2000 seismic profile CEL05. Journal of Geophysical Research 111 (B3), B03301.

Grad, M., Guterch, A., Keller, G.R. and POLONAISE 97 and CELEBRATION 2000 Working Groups, 2007. Variations in lithospheric structure across the margin of Baltica in Central Europe and the role of the Variscan and Carpathian orogenies. Geological Society of America Memoirs, 200, 341-356, doi:10.1029/2005JB003647.

Grad, M., Tiira, T., 2009. The Moho depth map of the European Plate. Geophysical Journal International 176 (1), 79–292.

Grenerczy, G., Sella,G., Stein,S. and Kenyeres A., 2005. Tectonic implications of the GPS velocity field in the northern Adriatic region, Geophysical Research Letters, 32, L16311, doi:10.1029/2005GL022947

Grinč, M., Zeyen, H., Bielik, M., Plašienka, D., 2013. Lithospheric structure in Central Europe: Integrated geophysical modelling, Journal of Geodynamics, Vol. 66, p. 13-24.

Grinč, M. Bielik, M. Mojzeš, A. Hók, J., 2010. Results of the gravity field interpretation in the Turčianska Kotlina Basin. Contributions to Geophysics and Geodesy. Vol. 40, no. 2, p. 103- 120.

Guterch, A., Grad, M., Špičák, A., Brückl, E., Hegedüs E., Keller G. R., Thybo, H. and CELEBRATION 2000, ALP 2002, SUDETES 2003 Working Groups 2003. An overview of recent seismic refraction experiments in Central Europe. Stud. Geoph. Geod., 47 (3): 651–657.

Guterch, A., Grad, M., Materzok, R., Perchuč, E. a Toporkiewicz, S., 1986. Results of seismic crustal studies in Poland. In: Bielik, M., 2001: GRAVIMETRIA – integrálna súčasť geofyzikálnej interpretácie litosféry v karpatsko-panónskom regióne: Nové trendy v analýza tiažového poľa. Doktorská dizertácia. Bratislava: MS – GFÚ SAV, 2001. 113 s.

Guterch, A., Grad, M., Keller, G.R., 2007. Crust and Lithospheric structure—long range controlled source seismic experiments in Europe. In: Schubert, G., Romanowicz,

B., Dziewonski, A. (Eds.), Treatise on Geophysics, vol. 1. Elsevier, Amsterdam, pp. 533–558.

Haas, J., Pero, C., 2004. Mesozoic evolution of the Tisza Mega-unit, Int. J. Earth Sci., 93, 297-313, doi:10.1007/s00531-004-0384-9.

Hauser, F., Raileanu, V., Fielitz, W., Bala, A., Prodehl, C., Polonic, G., Schulze, A., 2001. VRANCEA99 – the crustal structure beneath the south-eastern Carpathians and the Moesian Platform from a seismic refraction profile in Romania. Tectonophysics 340 (3–4), 233–256.

Hauser, F., Raileanu, V., Fielitz, W., Dinu, C., Landes, M., Bala, A., Prodehl, C., 2007. Seismic crustal structure between the Transylvanian Basin and the Black Sea, Romania. Tectonophysics 430 (1–4), 1–25.

Haxby, W. F., Turcotte, D. L., 1978. On isostatic geoid anomalies, J. Geophys. Res., 83, 5473-5478.

Heiskanen, W. A., Moritz, H., 1967. Physical Geodesy, W.H.Freeman, San Francisco.

Hofmeister, A. M., 1999. Mantle values of thermal conductivity and the geotherm from phonon lifetimes. Science 283, 1699-1706.

Horner, F., Freeman, R., 1983. Palaeomagnetic evidence from Pelagic limestones for clockwise rotation of the Ionian zone, Western Greece. Tectonophysics 98, 11–27.

Horváth, F., Szalay, A., Dovényi, P., Rumpler, J., 1989. Structural and thermal evolution of the Pannonian basin. In: Maheľ, M. (Ed.), Thermal Modelling in Sedimentary Basins. Technip, Paris, pp. 339–358.

Horváth, F., 1993. Towards a mechanical model for the formation of the Pannonian Basin. Tectonophysics 226, 333–357.

Hrubcová, P., Środa, P., Špičák, A., Guterch, A., Grad, M., Keller, G.R., Brueckl, E., Thybo, H., 2005.Crustal and uppermost mantle structure of the Bohemian Massif based on CELEBRATION 2000 data. J.Geophys.Res., 110, B11305, doi:10.1029/2004JB003080.

Hrubcová, P., Środa, P., Grad, M., Geissler, W.H., Guterch, A., Vozár, J., Hegedűs, E., Sudetes Working, G., 2010. From the Variscan to the Alpine Orogeny: crustal structure of the Bohemian Massif and the Western Carpathians in the light of the SUDETES 2003 seismic data. Geophysical Journal International 183 (2), 611–633.

Hrubcová, P., Środa, P., CELEBRATION 2000 Working Group, 2008. Crustal structure at the easternmost termination of the Variscan belt based on CELEBRATION 2000 and ALP 2002 data.Tectonophysics 460, 55–75, doi:10.1016/j.tecto.2008.07.009.

Huismans, R. S., Bertotti, G., Ciulavu, D., Sanders, C. A. E., Cloetingh, S. and Dinu, C., 1997. Structural evolution of the Transylvanian Basin (Romania): a sedimentary basin in the bend zone of the Carpathians, Tectonophysics 272, 249-268

Iancu, V., Berza, T., Seghedi, A., Gheuca, I., Hann, H.-P., 2005. Alpine polyphase tectono metamorphic evolution of the South Carpathians: a new overview. Tectonophysics 410 (1–4), 337–365.

Ioane,D., Ion, D., 2005. A 3D crustal gravity modelling of the Romanian territory. J. of Balkan Geoph. Soc., Vol.8, No 4, November 2005, p.189-198

Ionescu, C., Hoeck, V., Tomek, C., Koller, F., Balintoni, I., Beşuţiu, L., 2009. New insights into the basement of the Transylvanian Depression (Romania). Lithos 108 (1–4), 172–191.

Ionesi, L., 1989. Geologia României: unitati de platforma si orogenul Nord Dobrogean (translated title: The geology of Romania: platform units and the North-Dobrogean orogen). In: Matenco, L., Bertotti, G., Cloeting, S., Dinu, C., 2003. Subsidence analysis and tectonic evolution of the external Carpathian–Moesian Platform region during Neogene times. Sediment. Geol. 156, 71–94.

Janák, M., Froitzheim, N., Georgiev, N., Nagel, T.J., Sarov, S., 2011. P–T evolution of kyanite eclogite from the Pirin Mountains (SW Bulgaria). Implications for the Rhodope UHP Metamorphic Complex. Journal of Metamorphic Geology 29 (3), 317–332.

Janik, T., Grad, M., Guterch, A., Dadlez, R., Yliniemi, J., Tiira, T., Keller, G.R., Gaczyński, E., 2005. CELEBRATION 2000 Working Group Lithospheric structure of the Trans- European Suture Zone along the TTZ & CEL03 seismic profiles (from NW to SE Poland). Tectonophysics, 411, 129–156. doi:10.1016/j.tecto.2005.09.005.

Janik, T., Grad, M., Guterch, A., CELEBRATION 2000 Working Group, 2009. Seismic structure of the lithosphere between the East European Craton and the Carpathians from the net of CELEBRATION 2000 profiles in SE Poland. Geol. Quart. 53(1), 141–158.

Janik, T., Grad, M., Guterch, A., Vozár, J., Bielik, M., Vozárova, A., Hegedus, E., Kovács, C.A., Kovács, I., Keller, G.R., 2011. Crustal structure of the Western Carpathians and Pannonian Basin: seismic models from CELEBRATION, 2000 data and geological implications. Journal of Geodynamics 52 (2), 97–113.

Jiříček, R. 1979. Tektogenetický vývoj karpatského oblúku behem oligocénu a neogénu, in Tektonické Profily Západných Karpát, edited by M. Mahel, pp. 205 – 214, GÚDŠ, Bratislava, Slovakia.

Jordanova, N., Henry, B., Jordanova, D., Ivanov, Z., Dimov, D., Bergerat, F., 2001. Paleomagnetism in northwestern Bulgaria: geological implications of widespread remagnetization. Tectonophysics 343, 79–92.

Kázmér, M., Dunkl, I., Frisch, W., Kuhlemann, J., Ozsvárt, P., 2003. The Palaeogene forearc basin of the Eastern Alps and Western Carpathians: subduction erosion and basin evolution. Journal of the Geological Society of London 160, 413–428.

Katsura, T., Yamada, H., Nishikawa, O., Song, M., Kubo, A., Shinmei, T., Yokoshi, S., Aizawa, Y., Yoshino, T., Walter, M.J., Ito, E. and Funakoshi, K., 2004. Olivine-wadsleyite transition in the system (Mg, Fe)2SiO4, J. Geophys. Res., 109, B02209, doi:10.1029/2003JB002438.

Kilényi, E., Šefara, J., 1989. Pre-Tertiary basement countour map of the Carpathian Basin beneath Austria. Czechoslovakia and Hungary. Eotvos Lorand Geophysical Institute, Budapest.

Kissel, C. and Laj, C., 1988. The tertiary geodynamical evolution of the Aegean arc: a paleomagnetic reconstruction. Tectonophysics 146, 183–201.

Kissel, C., Laj, C., Poisson, A., Görür, N., 2003. Paleomagnetic reconstruction of the Cenozoic evolution of the Eastern Mediterranean. Tectonophysics 362, 199–217.

Konečný, V., Kováč, M., Lexa, J. and Šefara, J., 2002. Neogene evolution of the Carpatho-Pannonian region: An interplay of subduction and back-arc diapiric uprise in the mantle, in Neotectonics and Seismicity of the Pannonian Basin and Surrounding Orogens. A Memoire on the Pannonian Basin, edited by F. Horváth, S. Cloetingh and G. Bada, pp. 165 – 194, Eur. Geophys. Soc., Strasbourg, France.

Koulakov, I., Zaharia, B., Enescu, B., Radulian, M., Popa, M., Parolai, S., Zschau, J., 2010. Delamination or slab detachment beneath Vrancea? New arguments from local earthquake tomography. Geochemistry, Geophysics, Geosystems 11, Q03002.

Kováč, M., Král, J., Márton, E., Plašienka, D. and Uher, P., 1994. Alpine uplift history of the central western Carpathians: Geochronological, paleomagnetic, sedimentary and structural data, Geol. Carp., 45, 83 – 96.

Kováč, M., Bielik, M., Lexa, J., Pereszlenyi, M., Šefara, J., Túnyi, I. and Vass, D., 1997. The western Carpathian intramountane basins, in Geological Evolution of the Western Carpathians, edited by P. Grecula, D. Hovorka, and M. Putiš, pp. 43 – 64, Miner. Slovaca Corp.-Geocomplex, Geofyz. Bratislava and Geol. Surv. of Slovak Republic, Bratislava.

Kováč, M., Nagymarosy, A., Oszczypko, N., Slaczka, A., Csontos, L., Marunteanu, M., Matenco, L. and Márton, M., 1998. Palinspatic reconstruction of the Carpathian-Pannonian region during the Miocene, in Geodynamic development of the Western Carpathians, edited by M. Rákus, pp. 189 – 217, Geol. Surv. Slovak Republic, Bratislava.

Kováč, M., 2000. Geodynamický, paleografický a štruktúrny vývoj karpatsko panónskeho regiónu v miocéne. Nový pohľad na neogénne panvy Slovenska Veda, Bratislava.

Krézsek, C., 2004. Salt-related gravitational gliding in Transylvanian. AAPG Regional Conference Prague 2004 Extended Abstracts (on CD), 8 pp.

Krézsek, C., Filipescu, S., 2005. Middle to Late Miocene sequence stratigraphy of the Transylvanian Basin (Romania). Tectonophysics 410 (1–4), 437–463.

Krézsek, C., and A. Bally 2006. The Transylvanian Basin (Romania) and its relation to the Carpathian fold and thrust belt: Insights in gravitational salt tectonics, Mar. Pet. Geol., 23, 405–442, doi:10.1016/j.marpetgeo.2006. 03.003.

Krohe, A., Mposkos, E., 2002. Multiple generations of extensional detachments in the Rhodope Mountains (northern Greece): evidence of episodic exhumation of highpressure rocks. In: Blundell, D.J., Neubauer, F., Von Quadt, A. (Eds.), The Timing and Location of Major Ora Depositions in an Evolving Orogen. Geol. Soc. Lond. Spec. Publ., vol. 204, pp. 151–178.

Kukkonen, I.T., Čermák, V., Hurtig, E., 1993. Vertical variation of heat flow density in the continental crust. Terra Nova 5, 389–398.

Lachenbruch, A.H., Morgan, P., 1990. Continental extension, magmatism and elevation; formal relations and rules of thumb. Tectonophysics 174, 39–62.

Landes, M., Fielitz, W., Hauser, F., Popa, M., 2004. 3-D upper crustal tomographic structure across the Vrancea seismic zone, Romania. Tectonophysics 382 (1–2), 85–102.

Lankreijer, A., Bielik, M., Cloetingh, S., Majcin, D., 1999. Rheology predictions across the Western Carpathians, Bohemian Massif and the Pannonian Basin: implications for tectonic scenarios. Tectonics 18 (6), 1139–1153.

Lazarescu, V., Cornea, L., Radulescu, F., Popescu, M., 1983. Moho surface and recent crustal movements in Romania. Geodynamic connections. Annuaire de l'Institut de Geologie et de Geophysique 63, 83–91.

Lenkey, L., 1999. Geothermics of the Pannonian Basin and its bearing on the tectonics of basin evolution. Ph.D. thesis, Free University, Amsterdam, 215 pp.

Lenkey, L., Dövényi, P., Horváth, F., and Cloetingh, S.A.P.L., 2002. Geothermics of the Pannonian basin and its bearing on the neotectonics. EGU Stephan Mueller Special Publication Series, 3, 29–40

Lillie, R.J., 1991. Evolution of gravity anomalies across collisional mountain belts: clues to the amount of continental convergence and underthrusting. Tectonics 10 (4), 672–687.

Lillie, R.J., Bielik, M., 1992. Crustal development and tectonic models of Western Carpathians from gravity interpretation. Geologica Carpathica 43 (2), 63–68.

Lillie, R.J., Bielik, M., Babuska, V., Plomerova, J., 1994. Gravity modelling of the lithosphere in the Eastern Alpine –Western Carpathian– Pannonian Basin region. Tectonophysics 231 (4), 215–235.

Lilov, P., Yanev, Y., Marchev, P., 1987. K/Ar dating of the Eastern Rhodope Paleogene magmatism. Geol. Balc. 17, 49–58.

Linzer, H.-G., 1996. Kinematics of retreating subduction along the Carpathian arc, Romania. Geology 24, 167–170.

Linzer, H.-G., Frisch, W., Zweigel, P., Girbacea, R., Hann, H.-P., Moser, F., 1998. Kinematic evolution of the Romanian Carpathians. Tectonophysics 297, 133–156.

Lőrincz, K, Horváth, F., Detzky, G., 2002: Neotectonics and its relation to the Mid-Hungarian Mobile Belt. — EGU Stephan Müller Special Publication Series 3, pp. 247–266.

Mahel', M. (Ed.), 1973. Tectonic Map of the Carpathian – Balkan Mountain System and Adjacent Areas. GÚDŠ, Bratislava, UNESCO, Paris.

Malinowski, M., Zelázniewicz, A., Grad, M.,Guterch, A.,Janik, T.,CELEBRATION 2000 Working Group, 2005.Seismic and geological structure of the crust in the transition from Baltica to Palaeozoic Europe in SE Poland–CELEBRATION2000 experiment, profile CEL02. Tectonophysics 401, 55-77.

Mareschal, J.-C., Jaupart, C., Phaneuf, C., Perry, C., 2012. Geoneutrinos and the energy budget of the Earth. Journal of Geodynamics 54, 43–54.

Martin, M., Achauer, U., Kissling, E., Mocanu, V., Musacchio, G., Radulian, M., Wenzel, F., CALIXTO working group, 2001. First results from the tomographic experiment CALIXTO '99 in Romania. 26th General Assembly of the European Geophysical Society (EGS), 25 – 30 March 2001. Geophysical Research Abstracts 3, Nice, France, p. SE1.02.

Márton, E., and Fodor, L., 1995. Combination of paleomagnetic and stress data – a case study from north Hungary, Tectonophysics, 242, 99 – 114.

Matenco, L.C., 1997. Tectonic evolution of the outer Romanian Carpathians. Constraints from kinematic analysis and flexural modeling. Ph.D. thesis, Vrije Universiteit, Amsterdam, 160 pp.

Matenco, L., Bertotti, G., Cloeting, S., Dinu, C., 2003. Subsidence analysis and tectonic evolution of the external Carpathian–Moesian Platform region during Neogene times. Sediment. Geol. 156, 71–94.

Matenco, L., and Radivojević, D., 2012. On the formation and evolution of the Pannonian Basin: Constraints derived from the structure of the junction area between the Carpathians and Dinarides, Tectonics, 31, TC6007, doi:10.1029/2012TC003206.

Matte, P., 1991. Accretionary history and crustal evolution of the Variscan belt inWetsern Europe. Tectonophysics 196, 309–337.

Mayerová, M., Novotný , M., Fejfar, M., 1994. Deep seismic sounding in Czechoslovakia. In: Bucha, V., Blížkovský , M. (Eds.), Crustal Structure of the Bohemian Massif and the West Carpathians. Academia Press – Springer Verlag, Berlin, Praha, pp. 13–20.

Menke, W., 1984. Geophysical data analysis: Discrete inverse theory. Academic Press, London, 260 pp.

Merten, S., L. Maţenco, J. P. T. Foeken, and P. A. M. Andriessen 2011. Toward understanding the post-collisional evolution of an orogen influenced by convergence at adjacent plate margins: Late Cretaceous–Tertiary thermotectonic history of the Apuseni Mountains, Tectonics, 30, TC6008, doi:10.1029/2011TC002887.

Meulenkamp, J. E., Kováč, M. and Cícha, I. 1996. On late Oligocene to Pliocene depocentre migrations and the evolution of the Carpathian-Pannonian system, Tectonophysics, 266, 301 – 317.

Minár, J., Bielik, M., Kováč, M., Plašienka, D., Barka, I., Stankoviansky, M., Zeyen, H., 2011. New morphostructural subdivision of the Western Carpathians: An approach integrating geodynamics into targeted morphometric analysis. Tectonophysics 502, Issues 1–2, 158–174 http://dx.doi.org/10.1016/j.tecto.2010.04.003

Mocanu, V., Radulescu, F., 1994. Geophysical features of the Romanian territory. Romanian Journal of Tectonics and Regional Geology 75, 17–36.

Morley, C.K., 1996. Models for relative motion of crustal blocks within the Carpathian region, based on restorations of the outer Carpathian thrust sheets. Tectonics 15, 885–904.

Morris, A., 1995. Rotational deformation during Palaeogene thrusting and basin closure in eastern central Greece: palaeomagnetic evidence from Mesozoic carbonates. Geophys. J. Int. 121, 827–847.

Motavalli-Anbaran, S.-H., Zeyen, H., Brunet, M. F., Ardestani, V.E., 2011. Crustal and lithospheric structure of the Alborz Mountains, Iran, and surrounding areas from integrated geophysical modeling, Tectonics, 30(5), TC5012.

Motavalli-Anbaran S.H., Zeyen H., Ebrahimzadeh Ardestani, V. 2013. 3D joint inversion modeling of the lithospheric density structure based on gravity, geoid and topography data: application to the Alborz Mountains (Iran) and South Caspian Basin region, Tectonophysics, 586: 192–205

Mucuta, D.M., Knapp, C.C., Knapp, J.H., 2006. Constraints from Moho geometry and crustal thickness on the geodynamic origin of the Vrancea Seismogenic Zone (Romania). Tectonophysics 420 (1–2), 23–36.

Nakov, R., 2001. Late Miocene to Recent Sedimentary Basins of Bulgaria. Geological Society of America, Boulder CO. 28 p.

Nakov, R., 2008. Neogene geodynamics of the Balkan fold-thrust belt. In: The Proceedings of the 33rd IGC International Geological Congress, Oslo, Norway, August 6th–14th, CD-ROM.

Narkiewicz, M., Grad, M., Guterch, A., Janik, T., 2011. Crustal seismic velocity structure of southern Poland: preserved memory of a pre-Devonian terrane accretion at the East European Craton margin. Geol. Mag., doi:10.1017/S001675681000049X

Nur, A., Dvorkin, J., Mavko, G. and Ben-Avraham, Z., 1993. Speculations on the origins and fate of back arc basins, Ann. Geofis., 36, 155 – 163.

Ockendon, J. R., Turcotte, D. L., 1977. On gravitational potential and field anomalies due to thin mass layers, Geophys. J. R. Astron. Soc., 48, 479-492.

Oncescu, M.C., Bonjer, K.-P., 1997. A note on the depth recurrence and strain release of large Vrancea earthquakes. Tectonophysics 272 (2– 4), 291– 302.

Oszczypko, N., 1998. The Western Carpathian foredeep – development of the foreland basin in front of the accretionary wedge and its burial history (Poland). Geologica Carpathica 49 (6), 415–431.

Oszczypko, N., 2006. Late Jurassic-Miocene evolution of the Outer Carpathian fold and thrust belt and its foredeep basin (Western Carpathians, Poland). Geological Quarterly 50 (1), 169–194.

Palotai, M., Csontos, L., 2010. Strike-slip reactivation of a Paleogene to Miocene fold and thrust belt along the central part of the Mid-Hungarian Shear Zone. Geologica Carpathica 61 (6), 483–493.

Pana, D., Erdmer, P., 1996. Kinematics of retreating subduction along the Carpathian arc, Romania. Comment. Geology 24, 862−863.

Pana, D., Morris, G.A., 1999. Slab in the wrong place: Lower lithospheric mantle delamination in the last stage of the Eastern Carpathian subduction retreat: Comment. Geology 27, 665−666.

Panaiotu, C., 1998. Paleomagnetic constrains on the geodynamic history of Romania. In:Ioane, D. (Ed.),Monograph of Southern Carpathians. Reports on Geodesy, vol. 7, pp. 205–216.

Parsons, B., Sclater, J.G., 1977. An analysis of the variations of ocean floor bathymetry and heat flow with age. J. Geophys. Res. 82, 803–827.

Patrascu, S., Panaiotu, C., Seclaman, M., Panaiotu, C.E., 1994. Timing of rotational motion of Apuseni Mountains (Romania): paleomagnetic data from Tertiary magmatic rocks. Tectonophysics 233, 163–176.

Pavlis, N.K., Holmes, S.A., Kenyon, S.C., Factor, J.K., 2008. An Earth gravitational model to degree 2160: EGM2008, General Assembly of the European Geosciences Union, Vienna, Austria, April 13–18, 2008.

Pécskay, Z., Lexa, J., Szakács, A., Kadosc-Balogh, I., Seghedi, I., Konečný, V., Kováč, M., Márton, E., Kalinčiak, M., Széky-Fux, V., Póka, T., Gyarmati, P., Edelstein, O., Rosu, E., and Žec, B. 1995. Space and time distribution of Neogene and Quarternary volcanism in the Carpatho-Pannonian Region, Acta Volcanologica, 7, 15–28.

Pharaoh, T.C., 1999. Palaeozoic terranes and their lithospheric boundaries within the Trans-European Suture Zone, TESZ, a review. Tectonophysics 314, 17–41.

Plašienka, D., Grecula, P., Putiš, M., Hovorka, D., Kováč, M., 1997. Evolution and structure of the Western Carpathians: an overview. In: Grecula, P., Hovorka, D., Putiš, M. (Eds.), Geological Evolution of the Western Carpathians. Miner. Slovaca Corporation-Geocomplex, a.s. Geofyzika Bratislava and Geological Survey of Slovak Republic, Bratislava, pp. 35–42.

Plašienka, D., 2012. Geology along transects A, B and C (14.03.2012), Bratislava, Manuscript

Pollack, H.N., Chapman, D.S., 1977. On the regional variation of heat flow, geotherms, and lithospheric thickness. Tectonophysics 38, 279–296.

Pollack, H.N., Hurter, S.J., Johnson, J.R., 1993. Heat flow from the Earth's interior: analysis of the global data set. Reviews of Geophysics 31 (3), 267–280.

Posgay, K., Bodogy, T., Hegedüs, E., Kovácsvölgyi, S., Lenkey, L., Szafián, P., Takács, E., Tímár, Z., Varga, G., 1995. Asthenospheric structure beneath a Neogene basin in SE Hungary. Tectonophics 252, 467–484.

Praus, O., Péčová, J., Petr, V., Babuška, V., Plomerová, J., 1990. Magnetotelluric and seismological determination of lithosphere–asthenosphere transition in Central Europe. Phys. Earth Planet. Inter. 60, 212– 228.

Prelević, D., Foley, S. F., Romer, L. D., Cvetković, V., and Downes, H., 2005. Tertiary ultrapotassic volcanism in Serbia: Constraints on petrogenesis and mantle source characteristics. Journal of Petrology, 46 (7), 1443–1487 doi:10.1093/petrology/egi022

Rabăgia, T., Matenco, L., 1999. Tertiary tectonic and sedimentological evolution of the South Carpathians foredeep: tectonic versus eustatic control. Marine and Petroleum Geology 16, 719–740.

Radulescu, D. P., Cornea, I., Sandulescu, M., Constantinescu, P., Radulescu, F., Pompilian, A. 1976. Structure de la croute terrestre en Roumanie - essai d'interprétation des études seismiques profunds. Anural Institutului de Geologie si Geofizica 50, 5-36

Radulescu, F., 1988. Seismic models of the crustal structure in Romania. Rev. Roum. Geol. Geophys. Geogr. Ser. Geophys. 32, 13– 17.

Răileanu, V., Diaconescu, C., Rădulescu, F., 1994. Characteristics of Romanian lithosphere from deep seismic reflection profiling. Tectonophysics 239, 165–185.

Raileanu, V, Hauser, F., Bala, F.,Fielitz, W., Prodehl, C., Dinu, C., Landes, M., 2007. Deep seismic sounding across the Vrancea region. International Symposium on Strong Vrancea Earthquakes and Risk Mitigation Oct. 4-6, 2007, Bucharest, Romania, 80 - 85

Ratschbacher, L., Merle, O., Davy, P. and Cobbold, P., 1991a. Lateral extrusion in the eastern Alps: 1. Boundary conditions and experiments scaled for gravity, Tectonics, 10, 245–256.

Ratschbacher, L., Frisch, W., Linzer, H. G. and Merle, O. 1991b. Lateral extrusion in the eastern Alps: 2. Structural analysis, Tectonics, 10, 257 – 271.

Raykova, R.B., Panza, G.F., 2006. Surface waves tomography and non-linear inversion in the southeast Carpathians. Physics of the Earth and Planetary Interiors 157 (3–4), 164–180.

Ricou, L.E., Burg, J.P., Godfriaux, I., Ivanov, Z., 1998. Rhodope and Vardar. the metamorphic and olistostromic paired belts related to the Cretaceous subduction under Europe. Geodinamica Acta 11 (6), 285–309.

Rosenbaum, J.M., Wilson, M., Downes, H., 1997. Multiple enrichment of the Carpathian–Pannonian mantle: Pb–Sr–Nd isotope and trace element constraints. Journal of Geophysical Research 102, 14947–14962.

Royden, L. H., and Horváth, F. 1988. The Pannonian Basin: A Study in Basin Evolution, AAPG Mem., 45, 375 pp.

Royden, L.H., 1993. The tectonic expression slab pull at continental convergent boundaries. Tectonics 12, 303–325.

Rudnick, R.L., Fountain, D.M., 1995. Nature and composition of the continental crust: a lower crustal perspective. Reviews of Geophysics 33 (3), 267–309.

Rumpler, J., and Horváth, F., 1988. Some representative seismic reflection lines from the Pannonian Basin and their structural interpretation, in The Pannonian Basin: A Study in Basin Evolution, edited by L. H. Royden and F. Horváth, AAPG Mem., 45, 153 – 169.

Rybach, L., 1988. Determination of heat production rate. In: Haenel, R., Rybach, L., Stegenap, L. (Eds.), Handbook of Terrestrial Heat-flow Density Determination. Kluwer Academic, Hingham, MA, pp. 125–142.

Sacchi, M. and Horváth, F., 2002: Towards a new time scale for the Upper Miocene continental series of the Pannonian Basin (Central Paratethys). EGU Stephan Mueller Special Publication Series, 3, 79 – 94.

Sachsenhofer, R.F., 1996. The Neogene Styrian Basin: an overview. Mitt-Gesellschaft Geology Bergbaustue Österr 41, 19–32.

Sanders, C. A. E., Andriessen, P. A. M. and Cloetingh, S. A. P. L., 1999. Life cycle of the East Carpathian orogen; Erosion history of a doubly vergent critical wedge assessed by fission track thermochronology, J. Geophys. Res., 104, 29,095 – 29,112,

Sanders, C., Huismans, R., van Wees, J.D., Andriessen, P., 2002. The Neogene history of the Transylvanian basin in relation to its surrounding mountains. EGU Stephan Mueller Special Publication Series 3, 121–133.

Săndulescu, M., Visarion, M., 1978. Considérations sur la structure tectonique du soubassement de la Dépression de Transylvanie. Dări de Seamă Institutul de Geologie şi Geofizică 64, 153–173 (Bucharest).

Săndulescu, M., 1988. Cenozoic tectonic history of the Carpathians. In: Royden, L., Horváth, F. (Eds.), The Pannonian Basin: a study in basin evolution. AAPG Membranes 45, pp. 17–25.

Săndulescu, M., 1994. Overview on Romanian geology. Romanian Journal of Tectonics and Regional Geology 75, 3–15.

Sandwell, D.T., Smith, W.H.F., 1997. Marine gravity anomalies from GEOSAT and ERS-1 satellite altimetry. Journal of Geophysical Research 102 (B5), 10039–10054.

Schmid, S.M., Berza, T., Diaconescu, V., Froitzheim, N., Fügenschuh, B., 1998. Orogenparallel extension in the Southern Carpathians. Tectonophysics 297, 209–228.

Schmid, S., Bernoulli, D., Fügenschuh, B., Matenco, L., Schefer, S., Schuster, R., Tischler, M., Ustaszewski, K., 2008. The Alpine-Carpathian-Dinaridic orogenic system: correlation and evolution of tectonic units. Swiss Journal of Geosciences 101, 139–183.

Schubert, G., Turcotte, D.L., Olson, P., 2001. Mantle convection in the Earth and planets, 940 pp. Cambridge University Press, U.K.

Schuller, V., W. Frisch, M. Danišík, I. Dunkl, and M. C. Melinte (2009), Upper Cretaceous Gosau deposits of the Apuseni Mountains (Romania)– Similarities and differences to the Eastern Alps, Aust. J. Earth Sci., 102, 133–145.

Schultz-Ela, D.D., 2001. Excursus on gravity gliding and gravity spreading. Journal of Structural Geology 23, 725–731.

Šefara, J., Bielik, M., Konečný , P., Bezák, V., Hurai, V., 1996. The latest stage of development of the Western Carpathian lithosphere and its interaction with asthenosphere. Geologica Carpathica 47 (6), 339–347.

Seghedi, I., Balintoni, I. and Szakacs, A. 1998. Interplay of tectonics and Neogene postcollisional magmatism in the intracarpathian region, Lithos, 45, 483 – 497, doi:10.1016/S0024-4937(98)00046-2.

Seghedi, I., Downes, H., Szakacs, A., Mason, P. R. D., Thirlwall, M. F., Rosu, E., Pecskay, Z., Márton, E. and Panaiotu, C., 2004. Neogene–Quaternary magmatism and geodynamics in the Carpathian-Pannonian region: A synthesis, Lithos, 72, 117 – 146, doi:10.1016/j.lithos.2003.08.006.

Seghedi, A., Berza, T., Iancu, V., Mărunţiu, M., Oaie, G., 2005. Neoproterozoic terranes in the Moesian basement and in the Alpine Danubian nappes of the South Carpathians. Geologica Belgica 8 (4), 4–19.

Şerban, D.Z., Nielsen, S.B., Demetrescu, C., 2001. Transylvanian heat flow in the presence of topography, paleoclimate and groundwater flow. Tectonophysics, 335, 331–344.

Sinclair, H.D., Juranov, S.G., Georgiev, G., Byrne, P., Mountney, N.P., 1997. The Balkan thrust wedge and foreland basin of eastern Bulgaria: Structural and stratigraphic development. In: Robinson, A.G. (Ed.), Regional and Petroleum Geology of the Black Sea and Surrounding Region. AAPG Memoir, vol. 68, pp. 91–114.

Sobolev, S. a Babeyko, A.Y., 1994. Modeling of mineralogical compositions,density and elastic wave velocities in anhydrous magmatic rocks. Surveys in Geophysics, ISSN 0169-3298, Vol. 15, s. 515–544.

Solomatov, V. S., and Moresi, L., 2000. Scaling of timedependent stagnant lid convection: Application to small-scale convection on the Earth and other terrestrial planets, J. Geophys. Res., 105, 21,795–21,818, doi:10.1029/2000JB900197.

Spakman, W., 1990. Tomographic images of the upper mantle below central Europe and the Mediterranean. Terra Nova 2, 542–553.

Spakman, W., van der Lee, S., van der Hilst, R., 1993. Travel-time tomography of the European-Mediterranean mantle down to 1400 km. Physics of the Earth and Planetary Interiors 79, 3–74.

Spakman, W., Wortel, M.J.R., 2000. Subduction and slab detachment in the Mediterranean-Carpathian region. Science 290, 1910–1917.

Speranza, F., Islami, I., Kissel, C., Hyseni, A., 1995. Palaeomagnetic evidence for Cenozoic clockwise rotation of the external Albanides. Earth Planet. Sci. Lett. 129, 121–134.

Sperner, B., 1996. Computer programs for the kinematic analysis of brittle deformation structures and the Tertiary tectonic evolution of the Western Carpathians. Tűbinger Geowiss. Arbeiten

Sperner, B., Lorenz, F., Bonjer, K.-P., Hettel, S., Müller, B. and Wenzel, F., 2001. Slab break-off - abrupt cut or gradual detachment? New insights from the Vrancea Region (SE Carpathians, Romania), Terra Nova, 13, 172 – 179.

Sperner, B., Ratschbacher, L. and Nemčok, M., 2002. Interplay between subduction retreat and lateral extrusion: Tectonics of the western Carpathians, Tectonics, 21(6), 1051, doi:10.1029/2001TC901028.

Sperner, B., Ioane, D. and Lillie, R. J. 2004. Slab behaviour and its surface expression: New insights from gravity modelling in the SE-Carpathians, Tectonophysics, 382, 51 – 84, doi:10.1016/j.tecto. 2003.12.008.

Sperner, B., the CRC 461 Team, 2005. Monitoring of slab detachment in the Carpathians. In: Wenzel, F. (Ed.), Challenges for Earth Sciences in the 21st Century. SpringerVerlag, Heidelberg, pp. 187–202.

Środa, P., Czuba, W., Grad, M., Guterch, A., Tokarski, A.K., Janik, T., Rauch, M., Keller, G.R., Hegedüs, E., Vozár, J., and CELEBRATION, 2000 Working Group, 2006. Crustal and upper mantle structure of the Western Carpathians from CELEBRATION, 2000 profiles CEL01 and CEL04: seismic models and geological implications. Geophysical Journal International 167 (2), 737–760.

Stefanescu, M. 1985. Geologic profile A-14, 1:200,000. Geological Institute, Bucharest

Stixrude, L., and Lithgow-Bertelloni, C., 2005. Mineralogy and elasticity of the oceanic upper mantle: Origin of the low-velocity zone, J. Geophys. Res., 110, B03204, doi:10.1029/2004JB002965.

Stulc, P., 1998. Combined effect of topography and hydrogeology on subsurface temperature–implications for aquifer permeability and heat flow. A study from the Bohemian Cretaceous basin. Tectonophysics 284, 161–174.

Šumanovac, F., 2010. Lithosphere structure at the contact of the Adriatic microplate and the Pannonian segment based on the gravity modelling. Tectonophysics 485 (1–4), 94–106.

Šumanovac, F., Jasna, O., Marek, G., 2009. Crustal structure at the contact of the Dinarides and Pannonian basin based on 2-D seismic and gravity interpretation of the Alp07 profile in the ALP 2002 experiment. Geophysical Journal International 179 (1), 615–633.

Szabó, C., Harangi, S. and Csontos, L. 1992. Review of Neogene and Quaternary volcanism of the Carpathian- Pannonian region, Tectonophysics, 208, 243 – 256.

Szafián, P., Horváth, F., Cloetingh, S., 1997. Gravity constraints on the crustal structure and slab evolution along a Transcarpathian transect. Tectonophysics 272, 233–247.

Szafián, P., Horváth, F., 2006. Crustal structure in the Carpatho-Pannonian region: insights from threedimensional gravity modelling and their geodynamic significance. International Journal of Earth Sciences, 95, 50–67. Doi:10.1007/s00531-005-0488-x

Talwani, M., Worzel, J.L., Landisman, M., 1959. Rapid gravity computations for two-dimensional bodies with application to the Mendocino submarine fracture zone. Journal of Geophysical Research 64, 49–59.

Tari, G., Báldi, T. and Báldi-Beke, M., 1993. Paleogene retro-arc flexural basin beneath the Neogene Pannonian Basin: A geodynamic model, Tectonophysics, 226, 433 – 455.

Tari, G.C., Horváth, F., Weir, G., 1995. Planispastic reconstruction of the Alpine/Carpathian/Pannonian system. In: Horváth, F., Tari, G., Bokor, Cs (Eds.), Hungary: Extensional Collapse of the Alpine Orogen and Hydrocarbon Prospects in the Basement and Basin Fill of the Western Pannonian Basin. AAPG International Conference and Exhibition 10–13 September Nice, Sixth Field Trip Notes Hungary, pp. 119–131.

Tari, G., Dicea, O., Faulkerson, J., Georgiev, G., Popv, S., Stefanescu, M., Weir, G., 1997. Cimmerian and Alpine stratigraphy and structural evolution of the Moesian Platform (Romania/Bulgaria). In: Robinson, A.G. (Ed.), Regional and Petroleum Geology of the Black Sea and Surrounding Region. AAPG Memoir, vol. 68, pp. 63–90.

Tašárová, A., Afonso, J.C., Bielik, M., Götze, H.J., Hók, J., 2009. The lithospheric structure of the Western Carpathian–Pannonian Basin region based on the CELEBRATION, 2000 seismic experiment and gravity modelling. Tectonophysics 475 (3–4), 454–469.

Tašárová Alasonati, Z., Bielik, M., Götze, H.-J., 2008. Stripped image of the gravity field of the Carpathian–Pannonian region based on the combined interpretation of the CELEBRATION, 2000 data. Geologica Carpathica 59 (3), 199–209.

Tiliţâ, M., Lenkey, L., Maţenco, L., Horváth, F., Dinu, C. (2006). Neogene evolution of Transylvanian Basin: insights derived from (2D steady-state) thermal modeling. European Geosciences Union General Assembly 2006, Vienna, Austria 2–7 April 2006, Geophysical Research Abstracts, vol. 8, 08874, SRef-ID: 1607-7962/gra/EGU06-A-08874.

Tomek, C., Dvořáková, L., Ibrmajer, J., Jiříček, R., Koráb, T., 1987. Crustal profiles of active continental collisional belt: Czecho-Slovak deep seismic reflection profiling in the Western Carpathians , Geophys. J . R. Astron. Soc., 89, 383-388.

Tomek, C., Ibrmajer, I., Koráb, T., Biely, A., Dvořáková, L., Lexa, J. and Zbořil, A., 1989. Crustal structures of the west Carpathians on deep reflection seismic line 2T (in Slovak with English summary), Mineral. Slov., 1/2, 3 – 26.

Tomek, C., and Hall, J., 1993. Subducted continental margin imaged in the Carpathians of Czechoslovakia, Geology, 21, 535 – 538.

Tomek, C., PANCARDI colleagues, 1996. PANCARDI, Dynamics of ongoing orogeny. In: Gee, D.G., Zeyen, H.J. (Eds.), EUROPROBE 1996 – Lithosphere Dynamics: Origin and Evolution of Continents. EUROPROBE Secretariat, Uppsala, pp. 15–23. Turcotte, D.L., Schubert, G., 1982. Geodynamics. J. Wiley & Sons, New York, 450 pp.

Tóth, L., Mónus, P., Zsíros, T., Kiszely, M., 2002. Seismicity in the Pannonian Region — earthquake data. In: Cloetingh, S., Horváth, F., Bada, G., Lankreijer, A. (Eds.), Neotectonics and surface processes: the Pannonian basin and Alpine/Carpathian system: EGU St. Mueller Spec. Publ. Series, vol. 3, pp. 9–28.

Turcotte, D. L., Schubert, G., 1982. Geodynamics, 450 pp., J. Wiley & Sons, New York.

Tzankov, T. Z., Angelova, D., Nakov, R., Burchfiel, B.C., Royden, L.H., 1996. The Sub-Balkan graben system of central Bulgaria. Basin Res. 8, 125–142.

Ustaszewski, K., Schmid, S.M., Fügenschuh, B., Tischler, M., Kissling, E., Spakman, W., 2008. A map-view restoration of the Alpine-Carpathian-Dinaridic system for the Early Miocene. Swiss Journal of Geosciences 101 (Suppl. 1), 273–294.

Vakarcs, G., Vail, P. R., Tari, G., Pogácsás, G., Mattick, R. E., Szabó, A.,1994. ThirdorderMiddle Miocene-Early Pliocene depositional sequences in the prograding delta complex of the Pannonian Basin. Tectonophysics 240, 81–106.

Van Hinsbergen, D.J.J., Hafkenscheid, E., Spakman, W., Meulenkamp, J.E., Wortel, M.J.R., 2005. Nappe stacking resulting from subduction of oceanic and continental lithosphere below Greece. Geology 33, 325–328.

Van Hinsbergen, D.J.J., Dupont-Nivet, G., Nakov, R., Oud, K. and Panaiotu, C., 2008. No significant post-Eocene rotation of the Moesian Platform and Rhodope (Bulgaria): implications for the kinematic evolution of the Carpathian and Aegean arcs: Earth Planet. Sci. Lett., 273

Vasiliev, I., Krijgsman, W., Stoica, M., Langereis, C. G., 2005. Mio-Pliocene magnetostratigraphy in the southern Carpathian foredeep and Mediterranean–Paratethys correlations. Terra Nova 17, 376–384.

Vilà, M., Fernández, M., Jiménez-Munt, I., 2010. Radiogenic heat production variability of some common lithological groups and its significance to lithospheric thermal modeling. Tectonophysics 490 (3–4), 152–164.

Visarion, M., Veliciu, S., 1981. Some geological and geophysical characteristics of the Transylvanian Basin. Earth Evolution Science 3–4, 212–217.

Visarion, M., Sandulescu, M., Stanica, D., Veliciu, S., 1988. Contributions à la connaissance de la structure profonde de la plateforme Moésienne en Roumanie. Stud. Teh. Econ. - Geofiz. 15, 68– 92 (in French).

Vozár, J., Ebner, F., Vozárová, A., Haas, J., Kovács, S., Sudar, M., Bielik, M., Csaba, P., 2010. Variscan and Alpine terranes of the Circum-Pannonian Region. Slovak Academy of Sciences, Geological Institute, Bratislava, Slovakia.

Vyskočil, V., Burda, M., Bielik, M., Fusán, O., 1992. Further density models of the Western Carpathians. Contributions of the Geophysical Institute of Slovakian Academy of Sciences 22, 81–91.

Watts, A.B., Platt, J.P., and Buhl, P., 1993. Tectonic evolution of the Alboran Sea Basin. Basin Res., 5:153–177.

Weidle, C., Widiyantoro, S., and CALIXTO Working Group, 2005. Improving depth resolution of teleseismic tomography by simultaneous inversion of teleseismic and global P-wave traveltime data application to the Vrancea region in Southeastern Europe. Geophysical Journal International 162 (3), 811–823.

Wenzel, F., Achauer, U., Enescu, D. *et al.*, 1998. Detailed look at final stage of plate breakoff is target of study in Romania. EOS, Trans. Am. Geophys. Un., 79 (48), 589±594.

Wenzel, F., Sperner, B., Lorenz, F., Mocanu, V., 2002. Geodynamics, tomographic images and seismicity of the Vrancea region (SE-Carpathians, Romania). EGU Stephan Mueller Special Publication Series 3, 95–104. Wollenberg, H.A., Smith, A.R., 1987. Radiogenic heat production of crustal rocks: an assessment based on geochemical data. Geophysical Research Letters 14, 295–298.

Winchester, J.A., The PACE TMRNetwork Team, 2002. Palaeozoic amalgamation of Central Europe: new results from recent geological and geophysical investigations. Tectonophysics 360, 5–21.

Winkler, W., and Slaczka, A., 1992. Sediment dispersal and provenance in the Silesian, Dukla and Magura flysch nappes (Outer Carpathians, Poland), Geol. Rundsch., 81, 371 – 382.

Wollenberg, H .A, and Smith, A.R., 1987. Radiogenic heat production of crustal rocks : An assessment based on geochemical data, Geophys. Res. Lett., 14, 295-298.

Yanev, Y., Pecskay, Z., 1997. Preliminary data on the petrology and K–Ar dating of the Oligocene volcano Briastovo, Eastern Rhodopes. Geochim. Miner. Petrol. 32, 59–66.

Yanev, Y., Innocenti, F., Manetti, P., Serri, G., 1998. Upper Eocene–Oligocene collisionrelated volcanism in Eastern Rhodopes (Bulgaria)—Western Thrace (Greece): petrogenic affinity and geodynamic significance. Acta Volcanol. 10, 279–291.

Zaranek, S. E., and Parmentier, E. M., 2004. The onset of convection in fluids with strongly temperature-dependent viscosity cooled from above with implications for planetary lithospheres, Earth Planet. Sci. Lett., 224, 371–386, doi:10.1016/j.epsl.2004.05.013.

Zeyen, H., Fernàndez, M., 1994. Integrated lithospheric modeling combining thermal, gravity and local isostasy analysis: application to the NE Spanish Geotransect. Journal of Geophysical Research 99, 18089–18102.

Zeyen, H., Dérerová, J., Bielik, M., 2002. Determination of the continental lithosphere thermal structure in the Western Carpathians: integrated modelling of surface heat flow, gravity anomalies and topography. Physics of the Earth and Planetary Interiors 134, 89–104.

Zeyen, H., Ayarza, P., Fernŕndez, M., Rimi, A., 2005. Lithospheric structure under the western African-European plate boundary: a transect across the Atlas Mountains and the Gulf of Cadiz. Tectonics 24, TC2001.

Zweigel, P., Ratschbacher, L., Frisch, W., 1998. Kinematics of an arcuate fold-thrust belt: the southern Eastern Carpathians (Romania). Tectonophysics 297, 177–207.

10 SUMMARY IN SLOVAK

*Š*truktúra litosféry v strednej Európe: integrované geofyzikálne modelovanie

ÚVOD

Geofyzikálny prieskum je neoddeliteľnou, hoci často podceňovanou, súčasťou geologického prieskumu. Zjavnou výhodou je jeho neinvazívna podstata, efektivita a efektívnosť, či už v plytkom alebo hlbokom prieskume. Jeho oponenti poukazujú naopak na potrebu *a priori* údajov a často krát kontroverznú koreláciu geofyzikálnych dát a geologickej reality. Rozvoj počítačov a vhodná kombinácia viacerých geofyzikálnych metód dnes umožňuje komplexné štúdie v oblasti geofyziky a zmierňuje túto kritiku. Geofyzika dokazuje unikátne postavenie, najmä v oblasti analýzy a výskumu hlbokých štruktúr, tektonickej stavby, ale taktiež môže byť veľmi užitočná pri riešení problémov spojenou s geodynamickou evolúciou skúmaných oblastí a regiónov. Svoje prednosti však dokáže obhájiť aj v plytkom geologickom prieskume pre potreby hydrogeológie, inžinierskej geológie alebo environmentálnej geológie.

Dizertačná práca je rozdelená do niekoľkých logických častí. V prvej časti je popísaná základná geológia oblasti a výsledky predchádzajúcich geofyzikálnych prieskumov. Druhá časť je venovaná všeobecným princípom, metodike a spracovaniu dát dvojrozmerného geofyzikálneho modelovania (2D), trojrozmernej inverzie (3D) a trojrozmerného integrovaného geofyzikálneho modelovania (3D). V tretej časti sú popísané výsledky dizertácie. Práca bola vykonávaná postupne na dvoch miestach, pretože štúdium je koncipované ako PhD. štúdium pod dvojitým dohľadom. Časť štúdia bola vedená prof. RNDr. Miroslavom Bielikom, DrSc. z Katedry aplikovanej a environmentálnej geofyziky Univerzity Komenského v Bratislave, a druhá časť prof. Hermannom Zeyenom z laboratórií IDES z Univerzity Paris-Sud XI.

Tento projekt je zameraný na výskum a rozširovanie vedomostí o hlbokých štruktúrach litosféry v karpatsko–panónskej oblasti. Mal som možnosť a potešenie, aby som predstavil a priniesol nové trendy do tradičného slovenského výskumu hlbokých litosferických štruktúr v podobe nových, moderných a progresívnych vedeckých metód integrovaného geofyzikálneho modelovania v 2D a 3D na základe algoritmov od Zeyena a Fernandeza (1994), Motavalli-Anbarana *et al*., (2013) a Fullea *et al*., 2009.

GEOLÓGIA

Študovaná oblasť zahŕňa rad veľmi odlišných litosferických blokov, ktoré boli amalgamované dohromady v hlavných európskych orogenézach. Severná časť študovanej oblasti tvorí severoeurópsku platformu, ktorá je oddelená transeurópskou suturnou zónou (napr. Pharaoh, 1999) od prekambrickej východoeurópskej platformy. Severoeurópska platforma sa skladá z koláže prekambrických a / alebo kadómskych útvarov zlúčených dohromady počas predvariských tektonických udalostí a je pokrytá množstvom sedimentárnych ložísk. V opísanom priestore, tieto útvary zahrnujú aj Małopolský masív a Český masív obkolesený nemecko-poľskými Kaledonidmi.

Počas alpínskeho vrásnenia sa mikroplatne Alcapa a Tisza-Dacia presunuli a ukotvili do starších útvarov, ktoré tvoria alpsko-karpatský oblúk. Na juhu sa karpatský oblúk otáča okolo moezijskej platformy a pokračuje do orogénnych zón Balkaníd. Južná vetva alpinského orogénu zahŕňa Južné Alpy, ktoré sú spájané s Dinaridmi, Albanidmi a Hellenidmi. Všetky tieto alpské horské pásma sa obtáčajú okolo veľkej panónskej panvy, ktorá je lemovaná sopečnými reťazcami, ktoré boli vytvorené počas zaoblúkovej extenzie počas neogénu (Csontos *et al*., 1992). Tomuto typu vulkanizmu predchádzala regionálna extenzia a s ňou súvisiaci kremičito-andesitový vulkanizmus (Kováč, 2000;. Konečný *et al*., 2002). Alpský orogénny systém ako celok vykazuje veľmi zložitú štruktúru a vývoj, ktorý sa skladá z mnohých jednotiek a blokov so zložitými vzťahmi v priestore a čase (napr. Csontos a Vörös, 2004; Schmid *et al*., 2008;. Ustaszewski *et al*., 2008).

PREDCHÁDZAJÚCI GEOFYZIKÁLNY PRIESKUM

V karpatsko-panónskej oblasti boli vypracované mnohé štúdie na základe rôznych geofyzikálnych metód.

Predchádzajúce štúdie hustotného modelovania sa sústredili najmä na vývoj kôry kontinentálnych kolíznych zón. Sú to však najmä seizmické dáta (seizmickej refrakcie, seizmická tomografia), ktoré poskytujú podrobnejšie informácie o litosferických štruktúrach. Región strednej Európy bol pokrytý hustou sieťou seizmických projektov. Tieto projekty boli vykonávané v širokej medzinárodnej spolupráci, ktorá zahŕňala 30 inštitúcií z 16 krajín Európy a Severnej Ameriky. Tieto projekty boli POLONAISE'97 CELEBRATION 2000 Álp 2002 Sudety 2003 (Guterch *et al*., 2003). Seizmické profily pokrývajú rozsiahlu oblasť tiahnucu sa od Baltského mora k Jadranskému moru.

Integrované modelovanie rôznych dát súčasne (geoid, gravitácia, tepelný tok a topografia) za pomoci rôznych geologických a seizmických údajov, umožnil už dávnejšie vytvoriť litosferický model karpatsko-panónskeho regiónu a priľahlých tektonických jednotiek (Zeyen *et al*., 2002. Dérerová *et al*., 2006). Tento model hrúbky litosféry bol založený na výsledkoch 2D integrovaného geofyzikálneho modelovania pozdĺž nových 2D profilov.

Iný prístup k modelovanie litosféry v regióne bol publikovaný Tašárovou *et al*., (2009). Autori prezentujú výsledky 3D hustotného modelovania za použitia seizmických a ďalších geofyzikálnych dát. Na ich mapách sú zobrazené hĺbky hlavných hustotných rozhraní.

Ďalší prístup štúdia štruktúr zemskej kôry bol predstavený Csicsayom (2010). Vo svojej práci predstavil hustotnú interpretáciu 2D profilov pozdĺž niektorých vybraných seizmických profilov (CELEBRATION 2000) Toto integrované modelovanie bolo založené na najčastejšie používaných vzťahov pre transformáciu seizmických rýchlostí na hustoty (Sobolev a Babeyko, 1994; Christensen a Mooney, 1995).

METODIKA

Metodika takmer každej práce sa dá rozdeliť do dvoch fáz, a to do fázy prípravnej a fázy samotnej interpretácie. Vnútorné členenie týchto fáz je následne závislé na zvolenej metóde výskumu. Táto práca sa zaoberá výskumom litosféry v karpatsko-panónskej oblasti. Za metódy výskumu boli zvolené nasledujúce; 1D automatické modelovanie, 2D integrované geofyzikálne modelovanie, 3D inverzia a 3D integrované geofyzikálne modelovanie. Všetky tieto prístupy majú svoje vlastné metodiky, ktoré sú podobné vo všeobecnej rovine.

1D modelovanie

1D modelovanie je veľmi rýchla metóda, ktorá nám umožňuje vytvoriť prvý model Moho diskontinuity a LAB (hranice litosféra-astenosféra). Tento automatický prístup modelovania bol predložený Fulleaom *et al.* (2006). Z vedeckého hľadiska sa jedná o 1D model, ktorý je zobrazený v ploche, čo nám dáva 3D pohľad na hlavné rozhrania litosféry v záujmovej oblasti.

Táto nová metóda je založená na kombinácii topografických dát a anomálií geoidu, ktorá dokáže určiť hrúbku kôry a litosféry Zeme. Dôvod pre použitie rôznych dát, je to, že každá z týchto dát je citlivá na iné fenomény litosféry. V tomto prípade sú výstupom len dve vrstvy : kôra a LAB.

2D modelovanie

V tejto práci sme použili 2D integrované modelovanie litosféry (CAGES), ktorý kombinuje súčasnú interpretáciu povrchového tepelného toku, anomálií geoidu, gravitačných a topografických dát v karpatsko-panónskej oblasti a jej okolí. Tento prístup je schopný lepšie ohraničiť zložité tektonické štruktúry študovaného územia než interpretácia každej geofyzikálnej sady dát zvlášť. Výpočet je realizovaný metódou konečných prvkov. Program najprv vypočíta distribúciu teploty v litosfére a za pomoci lineárneho prepočtu medzi teplotou a hustotou, je vypočítané rozdelenie hustoty, ktorá sa používa k výpočtu zmeny topografie, geoidu a gravitácie (Zeyen a Fernandez, 1994).

V tejto práci predstavujem štyri 2D integrované modely litosféry. Tieto modely poskytujú lepší odhad distribúcie hustoty v litosfére a hĺbky hlavných hustotných diskontinuít, ako sú hranica litosféra-astenosféra a Moho diskontinuita.

3D inverzia

Hoci 2D prístup poskytuje určité výhody, nemôže vysvetliť zložitosť trojrozmernej štruktúry študovaného regiónu. V tomto prípade je nutné použiť 3D prístup (Mottavali-Anbaran *et al*., 2013). Použitá metóda je semi-automatická, a teda je veľmi rýchla. Je založená na bayesovskom prístupe s Gaussovou funkciou rozloženia pravdepodobnosti. 3D algoritmus (GTinv3D) bol použitý pre výpočet hustoty litosféry zo spoločnej inverzie gravitácie, geoidu a topografických dát. Algoritmus poskytuje výpočet hrúbky kôry a litosféry a priemernej hustoty kôry. Inverzný proces môže byť stabilizovaný pomocou tlmenia a / alebo vyhladzovacími parametrami, taktiež použitím *a priori* informácií, ako je napr. hrúbka kôry získaná na základe seizmických dát.

LitMod3D

LitMod3D (*LIT*hospheric *MOD*elling in a *3D* geometry) mal byť použitý v tejto práci za účelom vytvorenia 3D modelu litosféry. Nakoniec však bol len dôkladne otestovaný a boli odstránené chyby, ktoré komplikovali prácu s Windows verziou programu. Tento softvér bol vyvinutý v spolupráci J. Fulleaa a J. C. Afonsa a bol navrhnutý, aby vykonával integrované geofyzikálno-petrologické modelovanie litosféry. Hlavnou výhodou je, že spája samo-konzistentným spôsobom dáta z rôznych oblasti termodynamiky, minerálnej fyziky, geochémie, petrológie a geofyziky.

LitMod3D sa skladá z dvoch modulov: modul na výpočet priamej úlohy LITMOD3D_FOR a modulu interaktívneho rozhrania LITMOD3D Intf, ktorý sa používa pre vizualizáciu a modifikáciu vstupných dát. LITMOD3D_FOR počíta prenos tepla, termodynamické a reologické rovnice, gravitačný potenciál a izostatické rovnice. Výstupy sú teplota, povrchový tepelný tok, hustota, seizmické rýchlosti, anomálie geoidu, tiažové anomálie a topografia. Program umožňuje modelovanie do hĺbky až *410 km*, s rôznymi užívateľom definovanými vrstvy. Tieto vrstvy sa vyznačujú vlastnými tepelno-fyzikálnymi vlastnosťami. (Fullea *et al*., 2009).

VÝSLEDKY

1D modelovanie

Mapa hĺbky Moho diskontinuity regiónu vykazuje výrazné zmeny v hrúbke kôry v študovanej oblasti, ktoré boli predpovedané aj na základe mnohých predchádzajúcich štúdií (Zeyen *et al*., 2002; Bielik *et al*., 2004;. Dérerová *et al*., 2006; Csicsay, 2010; Janík *et al*., 2011;. Hauser *et al*., 2001; 2007; Mocanu a Radulescu, 1994;. Baránok a Zátopek, 1981; Guterch *et al*., 1984.; 1986; Čekunov *et al*., 1988; Čekunov 1993; Posgay *et al*., 1995; Tomek *et al*., 1987; 1989; Tomek a Hall, 1993; Horváth, 1993 a ďalšie). Na mape je vidieť, že hrúbka kôry sa zvyšuje smerom von z panónskej panvy, no hrúbka kôry nie veľmi dobre koreluje s predchádzajúcimi prácami v niektorých častiach štúdie. Najhrubšia kôra sa nachádza pod karpatským oblúkom alebo v jeho bezprostrednom predpolí. Veľmi vysoké hodnoty sa vyskytujú vo Východných Karpatoch a v oblasti Vranceai (*40 km*). Na rozdiel od očakávaní, najhrubšia kôra sa nachádza v malej oblasti v Južných Karpatoch (*42 km*). Východoeurópska platforma sa vyznačuje hrubšou kôrou a dosahuje hodnoty asi *36 km*, rovnako ako v pohorí Apuseni. Na druhej strane, panónska panva a moezijska platforma majú tenšiu kôru, než okolie. Tu predpokladáme priemernú hrúbku menšiu ako *30 km*. Najtenšia kôra sa nachádza v juhovýchodnej časti panónskej panvy v kontakte s Južnými Karpatmi, kde je hrúbka len okolo *26 km*.

Hrubšie litosféra sa nachádza v severovýchodnej časti mapy v oblasti východoeurópskej platformy, Východných Karpát a Južných Karpát. Hrúbka litosféry východoeurópskej platformy je v priemere viac ako *120 km*, ale opäť je možné nájsť hrubšie oblasti v severnej časti. Ďalším miestom s veľkou hrúbkou litosféry je oblasť Vrancea. Odtiaľto hrúbka litosféry klesá smerom na západ, kde hrúbka môže byť menej ako *110 km*. Klesajúci trend pokračuje aj na juh a dosahuje tu minimálne hrúbky litosféry na južnej hranici Južných Karpát a juhovýchodnej časti panónskej panvy. Tu môžeme pozorovať hrúbky len okolo *60 km*. Tieto extrémne nízke hodnoty hrúbky litosféry neboli skôr predpokladané. Moezijska platforma sa vyznačuje hrúbkou litosféry s klesajúcim trendom od východu na západ. Na východe je hrúbka okolo *110 km* a na západe, je to len *80 km*. Hrúbka litosféry panónskej panvy sa pohybuje v rozmedzí hodnôt od *80* do *100 km.*

2D modelovanie

Dáta povrchového tepelného toku vykazujú značnú variabilitu. Vo všeobecnosti sa predpokladá, že táto variabilita je viazaná na pohyb podzemných vôd alebo je spojená s paleoklimatickými účinkami, ktoré nie sú riadne opravené (Kukkonen *et al*., 1993; Štulc, 1998). Tieto efekty nie sú zahrnuté v algoritme, čo je dôvod, prečo naše modely dosahujú minimum *50 mWm⁻²* vo východoeurópskej platforme a maximum viac ako *80 mWm⁻²* v panónskej panve. Okrem toho údaje o povrchovom tepelnom toku, ktoré sme brali do úvahy, nie sú pravidelne distribuované v študovanej oblasti, preto v našich modeloch interpretujeme len pozvoľné, hladké variácie.

Všeobecne platí, že hrúbka litosféry klesá od starších a chladnejších platfórm smerom do mladšej a horúcej panónskej panvy, pričom maximálna hrúbka je dosiahnutá vo Východných a Južných Karpatoch. Hrúbka litosféry pod karpatským oblúkom sa pohybuje v rozmedzí od *150 km* na severe po zhruba *300 km* v oblasti Vrancea. V oblastiach platforiem to je medzi *120* a *150 km* a panónskej panvy niečo okolo *70 km*. Táto hrúbka je však väčšia, než sú predtým publikované hodnoty (napr. Horváth, 1993; Lenkey, 1999), ale menšie, než aké boli publikované Dérerovou *et al.* (2006). Časť povrchového tepelného toku možno vysvetliť zvýšením rádioaktívnej produkcie tepla v panónskej vrchnej kôre a sedimentoch. Stenčenie hodnôt hrúbky litosféry medzi *40* a *60 km* by príliš zvýšilo topografiu, a teda výsledok by bol nezlučiteľný s pozorovanými dátami. Hrúbka litosféry pod pohorím Apuseni v našich modeloch dosiahol hodnôt cca *120 km* a výrazne zhrubnutie sme namodelovali v transylvánskej panve, kde lokálne dosahuje hodnôt až *200 km*.

Naše modely ukázali niektoré zaujímavé veci. Ukazuje sa, že moezijska platforma je prekrytá zo severu Južnými Karpatmi a z juhu Balkanidmi, čo už bolo skôr uvedené v niektorých starších geologických štúdiách (Bergerat *et al*., 2010; Fügenschuh a Schmid, 2005; Iancu *et al*., 2005; Rabăgia a Matenco, 1999). Toto prekrytie vedie k ohnutiu platformy, ktorá zanecháva charakteristickú stopu v pozorovateľných dátach. Ďalším výsledkom je výrazne zhrubnutie litosféry pod Východnými Karpatmi, kde v ich predhlbni sú dosiahnuté hodnoty viac ako *230 km*. Pre dobrú koreláciu medzi pozorovanou a modelovanou topografiou a anomáliami geoidu je takéto zhrubnutie nutné. Podobné zhrubnutie je možné nájsť aj vo Východných Karpatoch, ale však oveľa menšie (asi *180 km*) a taktiež pod Západnými Karpatmi (asi *150 km*).

Hrubnutie litosféry v predhlbni Západných a Východných Karpát je sprevádzané zhrubnutím kôry, s výnimkou Južných Karpatoch. Vo všetkých našich modeloch,

zhrubnutie kôry je posunuté do oblastí s najvyššou topografiou. Maximálna hrúbka kôry našich modelov mimo orogén je pod moezijskou platformou (okolo *45 km*) v niektorých oblastiach. Seizmické modely ukazujú niektoré rozporuplné výsledky v oblasti Vrancea. Mocanu a Radulescu (1994) predpokladajú zhrubnutie kôry do asi *50 km*, zatiaľ čo Hauser *et al*. (2001) a Landes *et al*. (2004) predpokladajú maximálnu hrúbku v rozmedzí od *40* do *41 km*. V našom prípade sme použili ako referenčný model od Hausera *et al*. (2007), pretože sa zdá byť najlepšie definovaný. V našom najlepšie zosúladenom modely predpokladáme najtenšiu kôru v panónskej panve (cca 26 až 27 km), čo je podobné ako predpokladá Posgay *et al*. (1995), ale asi *2 km* hrubšie ako Janík *et al*. (2011).

3D inverzia

Zostavili sme tri rôzne modely pomocou metódy 3D inverzie na základe dát topografie, tiaže a geoidu: jeden model bez *a priori* dát a dva modely s rôznymi sadami *a priori* dát, prvý vychádza z kôrových hrúbok na základe seizmických dát z projektu CELEBRATION 2000 (Janik *et al*., 2011)., a druhý je založený na modeli zverejnenom Csicsayom (2010).

Najtenšia kôra bola namodelovaná na základe *a priori* dát od Csicsaya (2010). Avšak, použitím týchto *a priori* údajov bol program výrazne obmedzený v snahe meniť hodnoty hrúbky počas inverzného procesu, preto táto mapa Moho je v podstate výsledkom publikovaným Csicsayom (2010). Takáto tenká kôra je tiež predpovedaná aj inými autormi (Bielik *et al.*, 2004; Beránek and Zátopek, 1981; Guterch *et al.*, 1984, 1986; Čekunov *et al.*, 1988; Čekunov, 1993; Posgay *et al.*, 1995; Tomek *et al.*, 1987, 1989; Tomek and Hall, 1993; Horváth, 1993; Lenkey, 1999; Janik *et al.*, 2011). Najviac prekvapujúca je JV časť panónskej panvy, kde sme dostali len veľmi tenkú kôru modelu založeného na 1D vstupnom modeli, ale taktiež v modeli založenom na *a priori* dátach od Janík *et al*. (2011) sú niektoré náznaky tenkej kôry. Transylvánska panva sa vyznačuje hodnotami okolo *34 km* v každom modeli, čo je v dobrej zhode aj s výsledkami predchádzajúcich štúdií (Bielik *et al.*, 2004; Ioane and Ion, 2005; Csicsay, 2010; Cloetingh *et al.*, 2005; Hauser, 2007). Južné a Východné Karpaty dosahujú podobné hodnoty anomálií vo všetkých modeloch, no v tomto prípade sme dosiahli podobné výsledky v modeloch založených na Csicsayových dátach a bez *a priori*. Najmä v oblasti Vrancea sme dosiahli hodnôt cca *45 km*, ktorá je v rozmedzí hodnôt *41 km* (Hauser *et al*, 2001; Landes *et al.*, 2004), *47 km* (Hauser *et al*, 2007.) *50 km* (Mocanu a Radulescu, 1994) alebo *53 km* (Ioane a Ion, 2005). Najväčší

rozdiel medzi všetkými modelmi bol dosiahnutý severne od Východných Karpát, vo východoeurópskej platforme. V tejto oblasti sme zaznamenali značný rozdiel v dosiahnutej hĺbke Moho od *39 km* (model bez *a priori* dát a Janikov model) a viac než *51 km* (Csicsay, 2010). Moezijska platforma sa vyznačuje hĺbkou Moho okolo *33 km*. Iba v mapách bez *a priori* informácií to môže byť lokálne aj menej ako *30 km*. Hĺbka Moho cca *33 km* je tiež publikovaná aj inými autormi (napr. Ioane and Ion, 2004; Bielik *et al.*, 2004; Beránek and Zátopek, 1981; Guterch *et al.*, 1984, 1986; Čekunov *et al.*, 1988; Čekunov, 1993; Posgay *et al.*, 1995; Tomek *et al.*, 1987, 1989; Tomek and Hall, 1993; Horváth, 1993; Lenkey, 1999; Csicsay, 2010; Janik *et al.*, 2011).

Litosferické hrúbky ukazujú podobné vlastnosti ako Moho hĺbky. Najtenšia litosféra je dosiahnutá v nečakanej oblasti. Minimum začína na južnom okraji transylvánskej panvy a pokračuje pozdĺž hranice medzi Južnými Karpatmi a panónskou panvou. Toto minimum môže dosiahnuť veľmi nízkych hodnôt (lokálne aj menej než *40 km*). Zvyčajne, predchádzajúce publikácie v tejto oblasti ukazujú hodnoty vyššie ako *120 km* (Babuška *et al.*, 1988; Horváth, 1993; Šefara *et al.*, 1996; Lenkey, 1999; Zeyen *et al.*, 2002; Dérerová *et al.*, 2006). Panónska panva sa vyznačuje hrúbkou litosféry v rozsahu od *70* do *110 km*, na niektorých miestach to môže byť aj menej ako *60 km*. Model s veľmi plytkou LAB sme dostali na základe modelu od Csicsaya (2010), napriek tomu sa nepotvrdila ultra-tenká litosféra (*40 km*) (Ádám *et al.*., 1996. Východné a Južné Karpaty a ich predhlbne ukazujú hrúbku litosféry v rozmedzí *140* až *180 km*, čo potvrdzuje predchádzajúce štúdie (Babuška *et al.*, 1988; Horváth, 1993; Šefara *et al.*, 1996; Lenkey, 1999; Zeyen *et al.*, 2002). Avšak, tieto ukazujú aj výrazné odlišnosti od výsledkov publikovaných Dérerovou *et al.* (2006). Sporné výsledky boli získané aj v moezijskej platforme, pričom všetky modely ukazujú tenkú litosféru v priemere okolo *80 km*, nie viac ako *100 km*. Avšak, Dérerová *et al.* (2006) publikovali hrúbku *140 km*.

Čo sa týka hustôt kôry, na prvý pohľad je možné rozlíšiť miesta s hrubými depozitmi sedimentov, je to najmä v predhlbňových oblastiach. Veľmi nízke hustoty sedimentov znižujú taktiež priemernú hustotu kôry, preto sú tieto oblasti charakterizované priemernou hustotou kôry medzi *2780* a *2820 kg/m³*. Na druhej strane nižšie hustoty sa nachádzajú aj v oblasti panónskej panvy. Avšak tu, na rozdiel od sedimentárneho pokryvu, mikroplatne ALCAPA a Tisza-Dacia sa vyznačuje nižšou hustotou vrchnej a spodnej kôry (Bielik *et al.*, 2004, Dérerová *et al.*, 2006, Csicsay, 2010). Oblasti platfórm sa naopak vyznačujú vyššími hodnotami hustoty kôry. Tu sme získali maximálne hodnoty medzi

2890 a *2980 kg/m³*. Tieto oblasti sú vo všeobecnosti hlboko erodované, navyše tieto oblasti sú oblasti starých stabilných kratónov, ktoré sa vyznačujú vyššou hustotou (Csicsay, 2010).

LitMod3D

Poslednou úlohou môjho doktorandského štúdia bolo vytvorenie 3D modelu litosféry karpatsko-panónskej oblasti na základe geofyzikálneho 3D modelovanie (LitMod3D). Veľmi rýchlo po rozpoznaní, že práca je veľmi časovo náročná sme sa rozhodli zamerať na menšiu oblasť. Naše predchádzajúce výsledky a naštudované predchádzajúce práce poukazovali na fakt, že oblasť transylvánskej panvy je hodná ďalšieho záujmu. Počas interpretácie dát sa vyskytlo mnoho problémov súvisiacich s funkčnosťou programu, ktoré spomaľovali prácu, no niektoré z nich boli natoľko závažne, že bolo nutné program opravovať. V súčasnej dobe je táto úloha nedokončená, no je nutné povedať, že program funguje spoľahlivo.

ZÁVER

Tri rôzne prístupy geofyzikálnej interpretácie boli vykonané v tejto štúdii, ktoré nám poskytujú nový pohľad na problematiku štruktúry litosféry v karpatsko-panónskej oblasti. Spoločné modelovanie povrchového tepelného toku, geoidu, tiaže a topografických dát za pomoci seizmických a geologických *a priori* dát, nám umožnilo vypracovať revidovaný model litosferických štruktúr regiónu a jeho okolitých tektonických jednotiek. Výsledné 2D profily a taktiež 1D a 3D modely poukazujú na veľké variácie v študovanej oblasti. Na všetkých našich výsledkoch je možné pozorovať väčšiu hrúbku litosféry narastajúcu z oblasti Západných Karpát do Východných Karpát. Porovnaním s predchádzajúcimi výsledkami (Horváth, 1993; Lenkey, 1999), naše vo všeobecnosti poukazujú na menšie rozdiely medzi hrúbkou litosféry pod severoeurópskou platformou a panónskou panvou. Veľká hrúbka litosféry publikovaná severne od Západných Karpát (Horváth, 1993; Lenkey, 1999), v kombinácii s relatívne tenkou kôrou (*<40 km*), by znamenalo príliš veľkú tiažovú anomáliu alebo topografiu pod úrovňou mora. Program počíta topografiu na základe hypotézy lokálnej izostázie, čo je výrazné obmedzenie. Časť topografie môžu byť podporované elastickým napätím, ak zodpovedajúca efektívna elastická hrúbka (EET) je príliš vysoká. Existujú dva odlišné prístupy ktoré prispievajú k vyriešeniu problému. V 2D modelovaní, ak nebolo možné vysvetliť všetky pozorované dáta, dali sme prednosť dobrej zhode anomálií tiaže a geoidu, topografia dostala menšiu prioritu. Pri 1D modelovaní a 3D inverzii sa program snaží automaticky udržať rozdiely medzi nameranými a vypočítanými dátami najnižšie ako je možné. Závisiac od zvolených vstupných možností, parametrov a *a priori* dát, program sa snaží meniť hustoty alebo hrúbky tak, aby bola dosiahnutá čo najtesnejšia zhoda.

Hoci naše výsledky sa lokálne líšia kvantitatívne aj kvalitatívne, čo mohlo byť spôsobené rôznymi štartovacími modelmi, ktoré boli založené na rôznych *a priori* dátach, vo všeobecnosti majú podobné vlastnosti. V každom prípade je nutné zvážiť, čo je dôveryhodné. V tejto štúdii sme mali v niektorých oblastiach k dispozícii veľmi dobré seizmické dáta pre Moho diskontinuitu. Jedná sa predovšetkým o panónsku panvu, Západné Karpaty a oblasť Vrancea. Naopak, v Južných Karpatoch a getickej panve, kde existuje len málo doplňujúcich informácií, sme dosiahli niektoré prekvapivé výsledky, alebo také, ktoré sa nedajú spoľahlivo vysvetliť. Ďalšou zaujímavou oblasťou je juhovýchodná časť panónskej panvy. Naše výsledky dosiahnuté 3D inverziou ukazujú

veľmi malú hĺbku Moho a veľmi tenkú hrúbku litosféry, čo v tejto oblasti nebolo očakávané. Bolo by vhodné a dobré, keby sa táto oblasť stala predmetom záujmu aj ďalšieho výskumu.

Je ťažké rozhodnúť, ktorý model je najlepší. Každý z nich má silné a slabé stránky. Model bez *a priori* dát je veľmi silný v oblasti Západných a Východných Karpát a najmä v oblasti Vrancea. Na druhej strane, v oblasti panónskej panvy nekorešponduje s litosferickými modelmi, ktoré boli už skôr publikované, navyše tu existujú seizmické dáta veľmi dobrej kvality. Ďalšia prekvapujúca oblasť je oblasť juhovýchodnej časti panónskej panvy. Táto oblasť je navyše pomerne dosť široká, čo nie je zrejme spôsobené elastickým efektom ohnutej dosky, tak ako to môže byť v iných oblastiach. V prípade hustoty modelov, model bez *a priori* dát podáva geologicky najprijateľnejšie výsledky, hustoty sú najrealistickejšie v porovnaní s ostatnými modelmi.

Hoci vytvorenie modelu založeného na integrovanom 3D modelovaní (LitMod3D) bol jeden z mojich cieľov, nebolo možné dokončiť túto úlohu, pretože sme museli stráviť príliš veľa času dolaďovaním a testovaním programu. Podľa môjho názoru, LitEdit je stále v beta verzii, je veľmi zložité s ním pracovať , pretože proces zadávania parametrov vrstiev vyžaduje veľa trpezlivosti užívateľa. Na druhej strane si myslím, že ako náhle bude program úplne dokončený, stane sa z neho fantastický a výkonný nástroj pre geofyzikálne štúdium litosféry.

11 SUMMARY IN FRENCH

Détermination d'un modèle lithosphérique en Europe centrale: modélisation géophysique intégrée

Introduction

L´exploration géophysique est une partie intégrante, bien que très souvent méconnu de prospection géologique. Un avantage évident est sa nature non invasive, l'efficacité et l'efficience, que ce soit en exploration peu profonde ou profonde. Ses adversaires soulignent au contraire, le besoin de données *a priori* et la corrélation souvent controversée des données géophysiques avec la réalité géologique. Avec le développement des ordinateurs, une combinaison appropriée de plusieurs méthodes géophysiques est devenue possible, ce qui permet aujourd'hui des études complètes dans les domaines de la géophysique et atténue cette critique. La géophysique s'avère une méthode unique notamment dans l'analyse et la recherche de structures profondes, du cadre tectonique, mais il peut être également très utile pour résoudre les problèmes de l'évolution géodynamique des zones et régions étudiées. Toutefois, ses avantages peuvent aussi bien se défendre en exploration géologique peu profonde pour les besoins de l'hydrogéologie, la géologie et de la géologie de l'environnement.

La présente thèse doctorale est divisée en plusieurs parties logiques. Dans le premier je décris la géologie fondamentale de la région et je résume les résultats des levés géophysiques précédents. La deuxième partie est consacrée à des principes généraux, la méthodologie et le traitement des données de la modélisation géophysique en deux dimensions (2D), de l'inversion en trois dimensions (3D) et la modélisation géophysique en trois dimensions (3D). La troisième partie est consacrée aux résultats obtenus. Le travail a été effectué successivement sur deux sites, parce que l'étude est conçue comme un doctorat en cotutelle. Une partie de l'étude a été dirigée par le prof. RNDr. Miroslav Bielik, DrSc. au département de géophysique appliquée et de l'environnement à l'Université de

Comenius à Bratislava, et la deuxième partie par le prof. Hermann Zeyen du laboratoire IDES à l'Université Paris-Sud XI.

Ce projet est orienté sur la recherche et l'élargissement de la connaissance de la structure lithosphérique profonde de la région des Carpates et du bassin pannonien. J'ai eu la chance et le plaisir d'introduire dans la recherche slovaque traditionnelle des structures profondes les nouvelles méthodes scientifiques de modélisation géophysique intégrée en 2D et de 3D basées sur les algorithmes de Zeyen et Fernandez (1994), Motavalli-Anbaran *et al.* (2013) and Fullea *et al*., 2009.

Géologie

La zone d'étude comprend une série de blocs lithosphériques fortement variables qui ont été fusionnés dans les grandes orogenèses européennes du cadomien à l'alpin. La partie nord de la zone d'étude est formée par la plateforme nord-européenne, qui est séparée par la zone de suture transeuropéenne en la plateforme est-européenne précambrienne dans l'est et la plateforme ouest-européenne paléozoïque dans l'Ouest. La plateforme est-européenne est constituée d'un collage de terranes du Gondwana du précambrien et/ou du cadomien fusionnés lors d'événements tectoniques pré-varisques puis recouverts par des dépôts sédimentaires épais. Dans la zone décrite, ces terranes comprennent également le Massif Malopolska et le Massif de Bohême entourant les calédonides germano-polonaises.

Au cours de l'orogenèse alpine, les terranes d'Alacapa et Tisza-Dacia etaient amarrés aux plus âgés, formant l'immense arc orogénique des Alpes orientales et des Carpates. Vers le sud, l'Arc des Carpates tourne autour de la Plateforme Moésienne et se poursuit dans de larges zones orogéniques des Balkanides. La branche sud de l'orogène alpin inclut les Alpes méridionales qui sont liés aux Dinarides, Albanides et Hellénides vers le sud. Toutes ces chaînes de montagnes alpines contournent le grand bassin de Pannonie qui est bordé par des chaînes volcaniques, qui ont été formées par extension arrière-arc au Néogène (Csontos *et al.*, 1992). Dans l'ensemble, le système orogénique alpin de la zone montre une évolution très complexe et aussi une structure compliquée, composée de nombreuses unités et des blocs avec des relations complexes dans l'espace et le temps (Csontos and Vörös, 2004; Schmid *et al.*, 2008; Ustaszewski *et al.*, 2008).

Exploration géophysique précédente

Beaucoup d'études se sont faites dans la région des Carpates et du bassin pannonien basées sur de nombreuses méthodes géophysiques différentes.

Des études antérieures de modélisation de la densité ont été axées principalement sur le développement des zones de collision continentale. Ce sont cependant les données sismiques (sismique réfraction, tomographie sismique) qui fournissent des informations plus détaillées sur les structures lithosphériques. La région de l'Europe centrale a été couverte d'un réseau dense de projets sismiques. Ces projets ont été réalisés dans une vaste coopération internationale, qui comprenait 30 établissements de 16 pays partout en Europe et en Amérique du Nord. Ces projets étaient POLONAISE'97, CÉLÉBRATION 2000, Alp 2002, SUDETES 2003 (Guterch *et al.*, 2003). Les profils sismiques couvrent une vaste zone qui s'étend de la mèr Baltique jusqu'à la mer Adriatique.

La modélisation conjointe de données de geoïde, gravitation, le flux de chaleur et la topographie à l'aide de données géologiques et sismiques, permettait au début des années 2000 de créer un modèle d'épaisseur lithosphérique de la région de Carpates–bassin pannonien et des unités tectoniques adjacentes (Zeyen *et al.*, 2002; Dérerová *et al.*, 2006). Ce modèle d'épaisseur lithosphérique se basait sur les résultats de la modélisation geophysique 2D intégrée basée sur neuf profils.

Une autre approche de modélisation lithosphérique dans la région a été publiée par Tašarová *et al.* (2009). Ces auteurs présentent le résultat d'une modélisation 3D de l'anomalie de Bouguer contrainte par des modèles sismiques et d'autres données géophysiques. Sur ses cartes ils represent la profondeur des limites principales de densité.

Une autre approche utilisée dans l'étude de la structure de la croûte a été réalisée par Csicsay (2010). Il a réalisé la modélisation de la densité le long des quelques profils sismiques (CELEBRATION 2000) et a effectué une modélisation gravimétrique 2D intégrée, qui utilisait des résultats de la modélisation de réfraction sismique. Cette modélisation intégrée était fondée sur les formules les plus utilisées pour la transformation de vitesses sismiques en densité, celles de Sobolev et Babeyko (1994) et celles de Christensen et Mooney (1995).

Méthodologie

La méthodologie de presque tous les travaux de géophysique peut être divisée en deux phases, la phase de préparation des données et la phase d'interprétation elle-même. La structure interne de ces étapes est alors dépendante de la méthode de recherche choisie. Cette thèse traite la recherche de la lithosphère de la région Carpates–Bassin pannonien. La méthode de recherche choisie est la modélisation automatique 1D, la modélisation géophysique 2D intégrée, l'inversion 3D et la modélisation géophysique 3D intégrée. Toutes ces approches ont leur propre méthodologie, qui sont en termes très généraux similaires.

Modélisation 1D

La modélisation uni-dimensionnelle est une méthode très rapide qui nous permet d'établir le premier modèle du Moho et de la LAB (limite lithosphère-asthénosphère) et un aperçu la lithosphère. Cette approche automatique de modélisation a été présentée par Fullea *et al.* (2006). Du point de vue scientifique, c'est une modélisation 1D, mais d'autre part, elle nous donne un regard quasi-3D des limites principales qui nous intéressent dans la zone étudiée.

Cette nouvelle méthode est basée sur la combinaison de données d'élévation et des anomalies du géoïde pour déterminer l'épaisseur de la croûte et la lithosphère de la Terre. La raison pour utiliser de données différentes, est que chacun de ces ensembles de données est sensible à différents phénomènes lithosphériques. La topographie est sensible à la variation de la densité moyenne à l'intérieur de la colonne lithosphérique, tandis que l'anomalie du géoïde dépend de la distribution en profondeur des variations de densité et est proportionnelle au moment dipolaire de la densité (Turcotte et Schubert, 1982). Dans ce cas, seuls deux couches sont considérés: croûte de manteau et la lithosphère.

Modélisation 2D

Nous appliquons la modélisation de la lithosphère intégrée en deux dimensions (logiciel Cages) qui combine l'interprétation du flux de chaleur de surface, du géoïde, de la gravité et des données topographiques de la région des Carpates-bassin pannonien et des régions avoisinantes. Cette approche est capable de contraindre les structures

lithosphériques compliquées de la région étudiée mieux que l'interprétation de chaque données geophysique par elle même. Le calcul est effectué en utilisant la technique des éléments finis, pour relier les différentes équations physiques. Le programme calcule d'abord la distribution de la température dans la lithosphère et via une relation linéaire entre températures et densités, la distribution des densité est calculée qui sert à calculer les variations de topographie, du géoïde et de la gravité. En plus, avec des paramètres rhéologiques données, la répartition de la rigidité de la lithosphèrepeut être calculée (Zeyen et Fernandez, 1994). Nous présentons dans cette thèses quatre modèles 2D intégrés de la lithosphère. Les modèles fournissent des estimations améliorées de la distribution de densité dans la lithosphère et de la profondeur de grandes discontinuités de densité telles que la discontinuité Moho et de la limite lithosphère-asthénosphère.

Inversion 3D

Bien que, l'approche 2D precedement présentée ait des advatages, elle ne peut expliquer la complexité de la structure trois dimensionnelle de la région d'étude. Dans ce cas l'approche 3D est nécessaire (Mottavali-Anbaran *et al.*, 2013). La méthode utilisée est semi-automatique et très rapide. Elle est basé sur une approche bayésienne avec des fonctions de densité de probabilité gaussiennes. Dans un premier temps, nous avons utilisé l'algorithme 3D (GTinv3D) pour obtenir la structure de la densité de la lithosphère à partir de l'inversion conjointe de la gravité, du géoïde et des données topographiques. L'algorithme fournit l'épaisseur de la croûte et de la lithosphère ainsi que la densité moyenne de la croûte. Le processus d'inversion peut être stabilisé à l'aide d'amortissement et d'un paramètre de lissage ainsi que par l'utilisation de l'information a priori comme l'épaisseurs de la croûte basées sur des profils sismiques.

LitMod3D

LitMod3D (*LIT*hospheric *MOD*elling in a *3D* geometry) a été utilisé dans ce travail pour reconstitution d'un modèle 3D, bien que finalement, pas plus d'un débogage approfondi de la version de Windows a été possible. Ce logiciel a été développé par J. Fullea et J. C. Afonso pour effectuer une modélisation géophysique-petrologique intégrée de la lithosphère. L'avantage principal est qu'il combine des données de la

thermodynamique, la physique des minéraux, la géochimie, la pétrologie, et la géophysique de la Terre.

LitMod3D est composé de deux modules: un module de calcul directe - LITMOD3D_FOR et un module d'interface interactif - LITMOD3D INTF qui est utilisé pour la visualisation et la modification des données et du modèle 3D. LITMOD3D_FOR calcule le transfert de chaleur, et les équations thermodynamiques et rhéologiques, les équations des champs potentiels et des équilibres isostatiques (isostasie locale et régionale) pour toute la lithosphères et le manteau supérieur sublithospherique. Les sorties sont la température, le flux de chaleur de surface, la densité, la vitesse sismique, la topographie et les anomalies du géoïde et de la gravité. Le programme permet la modélisation jusqu'à une profondeur de *410 km*, avec différentes couches définies par l'utilisateur. Ces couches sont caractérisées par leurs propriétés thermodynamiques (Fullea et al., 2009).

Résultats

Modélisation 1D

La carte de la profondeur du Moho montre d'importantes variations des épaisseurs de la croûte au sein de la zone étudiée, ce qui peut être prévu sur la base de nombreuses études précédentes de la région (Zeyen *et al.*, 2002; Bielik *et al.*, 2004; Dérerová *et al.*, 2006; Csicsay, 2010; Janik *et al.*, 2011; Hauser *et al.*, 2001; 2007; Mocanu and Radulescu, 1994; Beránek and Zátopek, 1981; Guterch *et al.*, 1984; 1986; Čekunov *et al.*, 1988; Čekunov, 1993; Posgay *et al.*, 1995; Tomek *et al.*, 1987, 1989; Tomek and Hall, 1993; Horváth, 1993; et d'autres). On peut constater que l'épaisseur de la croûte augmente du bassin pannonien vers l'E et le NE mais l'épaisseur de la croûte ne cadre pas bien avec les travaux précédents dans certaines parties de la zone étudiée. La croûte la plus épaisse se trouve sous l'arc des Carpates ou sous son avant-pays immédiat. Des valeurs très élevées se trouvent dans les Carpates de l'Est et de la zone de Vrancea (*40 km*). Au contraire des attentes, la croûte la plus épaisse se trouve dans la petite zone au sud des Carpates (*42 km*). La platforme de l'Europe de l'Est se caractérise par une croûte épaisse d'environ *36 km* comme on la trouve aussi sous les monts d'Apuseni. D'autre part, le bassin pannonien et la plateforme moésienne ont une croûte plus mince que la zone environnante. Ici, nous avons obtenu une épaisseur moyenne de moins de *30 km*. La croûte la plus mince se trouvé dans la partie SE du bassin pannonien dans le contact avec les Carpates du Sud où la profondeur est seulement *26 km*.

La lithosphère la plus épaisse est placée dans la partie NE de la carte sous la plateforme est-européenne, les Carpates de l'Est et les Carpates du Sud. L'épaisseur de la lithosphère de la plateforme est-européenne est en moyenne plus que *120 km* mais là aussi on peut trouver des endroits plus épais dans la partie nord de cette région. Une autre place avec une lithosphère aussi épaisse est la zone de Vrancea. De là, l'épaisseur de la lithosphère baisse vers l'ouest, où l'épaisseur est de moins de *110 km*. La tendance à la baisse se poursuit à partir de là aussi vers le sud et atteint un minimum d'épaisseur lithosphérique à la frontière sud des Carpates du Sud et la partie SE du bassin pannonien. Ici, elle est seulement *60 km*. Ces valeurs extrêmement basses de l'épaisseur lithosphérique n'ont pas été présentés auparavant. La plateforme moésienne se caractérise par une épaisseur lithosphérique avec une tendance à la baisse de l'est vers l'ouest. Dans l'est,

l'épaisseur est d'environ *110 km* et à l'ouest, elle est seulement *80 km*. L'épaisseur de la lithosphére Pannonienne varie de *80* à *100 km.*

Modélisation 2D

Les données de flux de chaleur indiquent un grand degré de dispersion. En général, ces variations sont liées à la circulation d'eau souterraine ou d'effets paléoclimatiques pas proprement corrigés (Kukkonen et al, 1993;. Stulc, 1998). Ces effets ne sont pas inclus dans l'algorithme utilisé, c'est pourquoi notre modèle se traduit par une variation lisse avec un minimum de *50 mW.m^{-2}* dans la plateforme est-européenne et un maximum de plus de *80 mW.m^{-2}* dans le bassin pannonien. En outre, les données de flux de chaleur que nous avons pris en compte ne sont pas bien répartis dans la zone étudiée. Pour nos modèles régionaux, nous n'interprétons que des variations lisses.

En général, l'épaisseur de la lithosphère diminue à partir des plateformes plus anciennes et plus froides vers le bassin pannonien plus jeune et plus chaud avec une épaisseur maximale dans les Carpates orientales et septentrionales. L'épaisseur de la lithosphère sous l'arc des Carpates varie entre *150 km* au Nord à environ *300 km* dans la zone de Vrancea. Dans les domaines de plateforme, elle est entre *120* à *150 km* et dans le bassin pannonien est d'environ *70 km*. Cette épaisseur est plus grande que publiée précédement (par exemple, Horváth, 1993; Lenkey, 1999), mais plus petite que les résultats de Dérerová *et al.* (2006). Ainsi, une partie du flux de chaleur de surface peut s'expliquer par une augmentation de la production de chaleur radioactive dans la croûte supérieure sous le bassin et dans les sédiments. En réduisant l'épaisseur lithosphérique aux valeurs entre *40* et *60 km* on éleverait trop la topographie modélisée et ainsi les données calculées seraient incompatibles avec celles observées. L'épaisseur de la lithosphère sous les monts d'Apuseni atteint dans les modèles une profondeur d'environ *120 km* et s'épaissit fortement sous le bassin de Transylvanie pour atteindre localement des valeurs de près de *200 km.*

Notre modèle apporte quelques caractéristiques intéressantes. Il montre que la plateforme moésienne est chevauchée du nord par les Carpates du Sud et du sud par les Balkanides, ce qui avait été déjà indiqué plus tôt par des études géologiques (Bergerat et al, 2010; Fügenschuh et Schmid, 2005; Iancu *et al.*, 2005; Rabăgia et Matenco, 1999). Ce chevauchement induit une flexion de la Plateforme qui donne une signature caractéristique

dans les observables. Un autre résultat est le fort épaississement lithosphérique sous les Carpates de l'Est et leur avant-pays qui atteint les valeurs de plus de *230 km*. Pour une bonne corrélation entre la topographie observée et modélisée et les anomalies du géoïde cet épaississement est nécessaire. L'épaississement peut également être trouvé dans les Carpates de l'Est, mais beaucoup moins important (environ *180 km*) et en dessous Carpates de l'Ouest (environ *150 km*).

L'épaississement de la lithosphère dans l'Ouest et l'avant-pays des Carpates de l'Est est accompagné d'épaississement de la croûte, sauf dans les Carpates du Sud. Dans tous les transects, l'épaississement de la croûte est décalé vers les domaines de la topographie la plus élevée. L'épaisseur maximale de la croûte dans nos modèles en dehors des orogènes se trouve sous la plateforme Moésienne avec une épaisseur d'environ *45 km* dans certaines régions. Les modèles basés sur les données sismiques sont contradictoires dans la région de Vrancea. Mocanu et Radulescu (1994) indiquent un épaississement de la croûte à près de *50 km*, tandis que Hauser *et al.* (2001) et Landes *et al.* (2004) donnent une épaisseur maximale de *40* à *41 km*. Pour notre interprétation, nous avons utilisé le modèle de Hauser *et al.* (2007) comme référence, car il semble être le mieux contraint. Afin de s'adapter à des anomalies à l'air libre et les données géoïde, nous avons dû modéliser un épaississement local sous la chaîne de montagne jusqu'à une épaisseur intermédiaire de *40 km*. Dans notre meilleur modèle, nous avons trouvé la croûte la plus fine dans le bassin pannonien à environ *26-27 km*, ce qui est similaire à Posgay *et al.* (1995), mais environ *2 km* plus épais que Janik *et al.* (2011).

Inversion 3D

Nous avons construit trois différents modèles avec la méthode d'inversion 3D des données de topographie, géoïde et gravité : Un modèle sans données a priori et deux modèles avec deux séries de données a priori différentes, l'un basé sur des données d'épaisseur de croûte sismiques (Janik *et al.*, 2011).et l'autre basé sur le modèle régional d'épaisseur de croûte publié par Csicsay (2010).

La croûte la plus mince a été obtenue sur la base des données a priori de Csicsay (2010). Néanmoins, comme les données a priori limitent fortement la variabilité des paramètres correspondants pendant le processus d'inversion, la carte du Moho est essentiellement le résultat de Csicsay (2010). Cette croûte mince est également prévue par

d'utres auteurs (Bielik et al, 2004;. Beranek et Zatopek, 1981; Guterch et al, 1984, 1986;. Čekunov et al, 1988;. Čekunov, 1993;. Posgay et al, . 1995; Tomek et al, 1987, 1989;. Tomek et Hall, 1993; Horváth, 1993; Lenkey, 1999; Janik et al, 2011). La zone la plus surprenante est la partie SE du bassin pannonien, où nous avons obtenu une croûte très mince avec le modèle basé sur la modélisation 1D, mais il y a aussi quelques indications d'une croûte mince dans le modèle basé sur Janik *et al.* (2011). Le bassin de Transylvanie se caractérise par des valeurs d'environ *34 km* sur chaque modèle et ce résultat est également en très bonne corrélation avec des travaux précédants (Bielik et al, 2004;. Ioane et Ion, 2005; Csicsay 2010;. Cloetingh et al, 2005; Hauser 2007). Le Sud et l'Est des Carpates présentent des valeurs d'anomalies similaires mais ici, les résultats sont plus similaires entre le modèle basé sur Csicsay et celui sans données a priori. Surtout dans la zone de Vrancea nous avons des valeurs d'environ de *45 km* ce qui est dans la gamme des valeurs de 41 km (Hauser et al, 2001; Landes et al, 2004), *47 km* (Hauser et al, 2007.) et *50 km* (Mocanu et Radulescu, 1994) voire *53 km* (Ioane et Ion, 2005). Le plus grand desajustement survient au Nord des Carpates de l'Est dans la plateforme est-européene. Dans cette région, nous observons une importante augmentation de la profondeur du Moho, passant de *39 km* à plus de *51 km* (Csicsay, 2010). La plateforme Moésienne est caractérisée par des profondeurs du Moho d'environs *33 km*. Dans les cartes sans information a priori cette profondeur peut localement même être inférieure à *30 km*. Une profondeur d'environ de *33 km* est prévue aussi par d'autres auteurs (e.g. Ioane et Ion, 2004; Boykova, 1999).

Les épaisseurs lithosphériques montrent des caractéristiques similaires à celles du Moho. La lithosphère la plus mince est visible dans une zone imprévue, commençant dans la marge sud du bassin de Transylvanie et suivant la limite entre les Carpates du Sud et le bassin pannonien. Ce minimum peut atteindre des valeurs très faibles (localement moins de *60 km*, pour un modèle même moins de *40 km*, même si ce résultat est certainement dû aux effets de flexure dont les logiciels utilisés ne tiennent pas compte). Habituellement, les publications indiquent dans cette zone des valeurs excédant *120 km* (Babuška *et al*., 1988;. Horváth, 1993; Šefara *et al*., 1996;. Lenkey, 1999; Zeyen *et al*., 2002; Dérerová *et al*., 2006). Le bassin pannonien est caractérisé par des épaisseurs lithosphériques dans la gamme de *70* à *110 km*, qui localement peuvent être moins de *60 km*. Nous avons obtenu cette LAB très mince en utilisant les données de Csicsay comme informations a priori. Néanmoins, une lithosphère ultra-mince d'environ *40 km* (Ádám *et al*., 1996) n'a pas été

confirmée par notre méthode. Les Carpates de l'Est et du Sud et ses avant-pays immédiats montrent une épaisseur lithosphérique dans la gamme de *140* à *180 km* ce qui confirme de srésultats précédents (Babuška *et al.*, 1988;. Horváth, 1993; Šefara *et al.*, 1996;. Lenkey, 1999; Zeyen *et al.*, 2002). Cependant ces épaisseurs sont considérablement différentes des résultats obtenus par Dérerová *et al.* (2006). Il y a aussi de petites zones avec une lithosphère encore plus épaisse, principalement dans les Carpates orientales ukrainiennes et dans la zone de Vrancea. Des résultats controverses ont été obtenus aussi dans la plateforme moésienne : tous les modèles montrent une lithosphère mincede *80 km* en moyenne, ne dépassant pas *100 km*. Cependant, Dérerová *et al.* (2006) présentent une épaisseur de *140 km*.

Dans les cartes de l'épaisseur de la croûte, les régions avec une couverture sédimentaire épaisse peuvent être distinguées à première vue. Elles se trouvent surtout dans les domaines de l'avant-pays. Les densités très basses des sédiments diminuent également la densité moyenne de la croûte. Ces régions sont caractérisées par des densités crustales moyennes comprises entre *2780* et *2820 kg/m³*. D'autre part des densités plus faibles se trouvent également dans la région du bassin pannonien. Cependant, ici, à part la couverture sédimentaire, les microplques Alcapa et Tisza-Dacia sont aussi caractérisées par des densités plus faibles de la croûte supérieure et inférieure (Bielik *et al.*, 2004; Dérerová *et al.*, 2006; Csicsay, 2010). Les zones de plateformes sont caractérisées par des valeurs élevées de la densité crustale. Ici, nous avons obtenu les valeurs maximales entre *2890* et *2980 kg/m³*. Ces régions sont généralement très profondément érodées et font partie d'anciennes zones de craton stable qui se caractérisent par des valeurs de densité plus élevées (Csicsay, 2010).

LitMod3D

La dernière tâche de mes études de doctorat était de créer un modèle 3D lithosphérique de la région du bassin des Carpates-Pannonie basé sur la modélisation géophysique 3D (LitMod3D). Nous avons décidé de nous concentrer sur une zone d'étude réduite à la moitié sud du système carpato-pannonien. Nos résultats par rapport aux méthodes précédentes et les documents étudiés montrent que la zone du bassin de Transylvanie est digne d'une enquête plus approfondie. Pendant l'interprétation des données quelques problèmes de programmation et d'untilisation surtout de l'interface graphique se sont découverts qui ont fait le travail plus lent et nous ont forcé de faire un

debugging approfondi du logiciel. À l'heure actuelle, la modélisation géophysique-pétrologique en 3D reste donc inachevée.

CONCLUSION

Trois approches d'interprétation géophysique différentes ont été réalisées dans cette étude. Le travail nous permet d'apporter de nouvelles données sur la structure lithosphérique de la région des Carpates et du bassin pannonien. La modélisation conjointe du flux de chaleur de surface, du géoïde, de la gravité et des données topographiques, en utilisant des données sismiques, géologiques comme contraintes, nous a permis d'établir un modèle révisé de la structure lithosphérique de cette région et de ses unités tectoniques avoisinantes. Les transects 2D ainsi que les modèles 1D et 3D montrent de fortes variations dans la zone étudiée. On peut observer sur l'ensemble de nos résultats une augmentation de l'épaisseur de la lithosphère des Carpates de l'Ouest vers les Carpates de l'Est. Une comparaison entre nos résultats et ceux publiés précédamment (Horváth, 1993; Lenkey, 1999) révèle des petites différences générales entre les épaisseurs de la lithosphère sous la plateforme européenne du nord et le bassin pannonien. La grande épaisseur lithosphérique publiée au nord des Carpates de l'Ouest (Horváth, 1993; Lenkey, 1999), en combinaison avec une croûte relativement mince (*<40 km*), impliquerait une anomalie trop élevé de gravité ou une topographie en dessous du niveau de la mer. Le programme calcule la topographie fondée sur l'hypothèse d'isostasie locale, ce qui constitue une restriction importante. Une partie de la topographie peut être supporté par des contraintes élastiques si la plaque élastique a épaisseur équivalente (EET) trop grande. Il y a deux approches différentes pour résoudre le problème. Dans la modélisation 2D, si nous ne pouvions pas trouver un modèle expliquant tous les données en même temps, nous avons donné la préférence à un bon ajustement des données de gravité et de géoïde et la topographie a été moins bien ajustée. Dans les inversions 1D et 3D, le programme essaie automatiquement de garder les différences entre les données mesurées et calculées aussi bas que possible. Selon les données *a priori* et les options internes choisies, le programme donnera des résultats différents.

Bien que nos résultats diffèrent, ils présentent en général des caractéristiques similaires. Les modèles montrent localement d'importantes différences quantitatives et qualitatives qui pourraient être causés par les différents modèles de départ qui sont basés sur différentes données *a priori*. En tout cas, il faut considérer ce qui est digne de confiance. Dans cette étude, nous avons eu à notre disposition dans certaines zones de très bonnes données sismiques pour le Moho. Il s'agit là surtout du bassin de Pannonie avec les

Carpates Occidentales et la zone de Vrancea. Par contre, dans les Carpates du Sud et le bassin gétique où il n'y a guère de données supplémentaires, nous avons obtenu certains résultats surprenants ou pas bien expliqués. Un autre domaine intéressant est le bassin de Pannonie du Sud-Est. Nos résultats d'inversion 3D montrent une faible profondeur de Moho et une épaisseur de la lithosphère très mince ce qui n'était pas prévu ici. Il serait bien que ces régions seraient l'objet de recherches suplémentaires.

Il est difficile de résoudre quel modèle est le meilleur. Chacun d'entre eux a des côtés forts et faibles. Le modèle sans données *a priori* est très fort dans la région des Carpates Occidentale et Orientale, et surtout dans la zone de Vrancea. D'un autre côté, il ne correspond pas aux modèles lithosphériques publiés antérieurement dans le bassin de Pannonie, dans lequel les données sismiques de bonne qualité existent. De plus, il montre des caractéristiques surprenantes dans la partie sud-est du bassin de Pannonie. Si dans d'autres régions, la flexion élastique de la lithosphère peut avoir un effet indésirable sur les résultats, dans cette région assez large nous ne pouvons pas évoquer cet effet pour expliquer l'amincissement lithosphérique obtenu. Dans le cas des modèles de la densité, le modèle sans données *a priori* donne des résultats géologiquement acceptables, les densités étant plus realistes que dans les autres modèles.

Bien qu'un modèle basé sur la modélisation 3D intégrée (LitMod3D) était l'un de mes objectifs, il n'était pas possible de terminer cette tâche, puisque nous avons dû passer trop de temps à déboguer et tester le programme. À mon avis, le programme LitEdit est toujours une version bêta, il devrait être plus facile à utiliser, car le processus d'entrer des paramètres d'une couche exige beaucoup de patience de l'utilisateur. D'autre part, je pense que une fois le programme sera finalisé, il devient un engin fantastique et puissant pour l'étude géophysique de la lithosphère.